



Peroxide Reactions of Environmental Relevance in Aqueous Solution

MELOD MOHAMED Ali UNIS

PhD

2010

Peroxide Reactions of Environmental Relevance in Aqueous Solution

MELOD MOHAMED Ali UNIS

PhD

2010

Peroxide Reactions of Environmental Relevance in Aqueous Solution

A thesis submitted in partial fulfilment
of the requirements of the
University of Northumbria at Newcastle
For the degree of
Doctor of Philosophy

Research undertaken in the School of Applied Sciences
at Northumbria University

Oct 2010

ACKNOWLEDGEMENTS

First and foremost, all praise be to God, Lord of the Universe, the most beneficent, the most merciful who has blessed me through my life with health, patience and ability to pursue and complete this work.

I would like to express utmost appreciation to my supervisors Dr. Michael Deary and Dr. Martin Davies for their guidance and cooperation throughout this work, and also special thanks to Dr Michael Deary for his patience, endless support, excellent guidance, and helpful comments throughout my PhD writing. He has always provided valuable, challenging and constructive comments which have encourage me to improve my research skills and demonstrate the work precisely. I would like to thanks Mr Gary Askwith, for his assistance during this research work.

I am particularly indebted to the people of my country Libya, who provided me with the opportunity to continue higher studies. I would like to acknowledge my gratitude to the Ministry of Education for the financial support to accomplish this study, which otherwise was impossible to be achieved. Therefore, I wish to be able to repay at least a portion of this debt to my home country.

I would like to express my gratitude to everybody else who extended the hand of backing and support to me throughout this study.

I am very grateful to all of my family in Libya especially to my brother Khalfa who have always given me endless encouragement and support to continue my study.

My greatest thanks to my beloved wife for her love, moral support, understanding, loneliness and patience for the successful completion of my PhD study. And my four kids make every day worth while, and I hopeful they see a better future.

Declaration

I declare that the work contained in this thesis has not been submitted for other award and that it is all my own work.

Name : Melod Mohamed Ali Unis

Signature :

Date :

Abstract

The main objective of this research programme was to determine the factors influencing the decolourisation of dyes at low pH by different peroxide species, both in the presence and absence of metal ion catalysts and, therefore, to find a set of optimal conditions for application to wastewater treatment processes. An additional study looked at whether peroxoborates were capable of acting as nucleophiles. The specific aims of the study were: to investigate the *in-situ* formation of peracetic acid from the equilibrium formed between hydrogen peroxide and acetic acid, and whether this can be achieved without the addition of an acid catalyst such as sulphuric acid; to study the comparative reactivity of *in-situ* generated peracetic acid and hydrogen peroxide towards a range of dyes used in industry; to investigate the catalytic potential of a range of metal ions towards the reaction between peroxides and dyes; to investigate the structural features of dyes that might influence reactivity (decolourisation); and to investigate the reactivities of other peracid-like peroxide species that can be generated from hydrogen peroxide (peroxoborates and peroxocarbonates).

The novel aspects arising from this study were: (a) The development of a new method for the *in-situ* generation of peracetic acid that gives the same equilibrium yield as established methods yet does not require the addition of an acid catalyst;(the reaction was slow, but there was minimal decomposition and so it is ideal for circumstances that allow the preparation of peracetic acid well in advance of use). (b) The first comprehensive study of the bleaching potential of peracetic acid and hydrogen peroxide towards a wide structural range of dyes both in the presence and absence of metal ions (iron, manganese, silver and copper). (c) The inference that for iron-catalysed bleaching of azo dyes by peracetic acid the catalytic mechanism involves pre-complexation of iron and dye, followed by reaction of the 'activated' complex with peracetic acid rather than a free radical mechanism that might have been expected for

such systems. (d) The evidence that, in contradiction to literature studies, peroxoborate species do not act as nucleophiles.

As an introduction to this work the reactions of peroxyacids are described in general terms. The experimental work is divided in three parts. In Chapter two, the homogeneous preparation of peracetic acid (PAA) from acetic acid (AA) and hydrogen peroxide (H_2O_2) was investigated with and without the catalysis of sulphuric acid (H_2SO_4). The formation of PAA and total peroxide content was determined by iodimetric titration. The reaction was slow in the absence of a strong acid catalyst, and was faster with a sulphuric acid catalyst. There was no loss of total peroxide over the timescales of both reactions, whether a catalyst was used or not. The equilibrium constant for peracetic acid formation at temperature of 20°C was found to be 2.04 with a catalyst, and 2.10 without catalyst. The rate constant for the hydrolysis of peracetic acid for both forward and reverse reactions increased when the sulphuric acid concentration was increased from 0.02 M to 0.32 M. Linear relationships were found between the observed rate constants and H^+ concentrations at 25°C . Moreover, it was found that the preparation of peracetic acid showed a first-order dependence with respect to peroxide concentration.

In Chapter three, the application of this preparation of peroxyacids to the degradation of different types of dyes was investigated. As we know, physical or other chemical methods for dye degradation are expensive and can generate secondary pollution. In this part of the study the reactions of dyes with hydrogen peroxide and peracetic acid in the absence and presence of different metal ions (Fe^{3+} , Cu^{2+} , Mn^{2+} and Ag^+) were investigated. The iron/peroxyacid system was found to be the most effective.

Consequently, Chapter 4 evaluates the decolourization of five azo dyes under conditions of bleaching by peracetic acid in the presence of Fe^{3+} as a catalyst. The experiment was carried out in aqueous acidic media. Dye oxidation systems are

complex because: they involve several different tautomers; there is the possibility of dye aggregation at lower dye concentrations; and the oxidant species involved can be either the undissociated peroxide acting as an electrophile, or the dissociated peroxide acting as a nucleophile. The results obtained for the reaction of azo dyes with peracetic acid without added iron, when converted to the second order rate constant for the electrophilic reaction, k_2^E gave a value of $4.5 \times 10^{-6} \text{ dm}^3 \text{ mol}^{-1} \text{ s}^{-1}$ for orange II, which is very high. This may be due to trace metal ions still being present and catalysing the reaction, possibly from impurities in the dye itself. No metal ion chelators were used in the present study because the bulk of the study was designed to elucidate the effect of metal ions concentration on reaction rate. For the catalysed reactions a significantly increased rate of absorbance decrease with increasing iron concentration was observed. Saturation of iron was also demonstrated at high iron concentrations, suggesting the formation of an iron (III)-dye complex which then reacted with peracetic acid. The maximum rate of reaction was observed at an iron concentration of 0.012 M, and the results showed a reactivity order of Ponceau 4R > Amaranth > (Orange II & Carmosine) > Black PN; Orange 1 was unreactive under these conditions. Also one of the key objectives of this chapter was to determine the optimum conditions for dye degradation in terms of pH and oxidant and catalyst concentrations. The optimum conditions for maximum degradation occurred at the highest pH of 3.0 and at about $1 \times 10^{-3} \text{ M}$ iron. Evidence of the possible involvement of radicals in our studies comes from the observation of a lag phase followed by a more rapid bleaching phase in the oxidation of azo dyes by peracetic acid at the lowest iron concentrations (another possibility is that at these iron concentrations the reactive iron complex forms at a much slower rate). However, this process is slow by comparison with the rate of oxidation at higher iron concentrations that do not exhibit this lag phase; consequently, if free radical mechanisms are suggested then they are not significant compared to the proposed formation of a reactive iron-dye complex.

The work contained in final experimental Chapter aimed to clarify whether or not any of the peroxyborate species displayed nucleophilic characteristics and thus accelerated the rate of the reaction of hydrogen peroxide with p-nitrophenyl acetate. The pH range of 6.0 to 8.0 is critical in terms of the distribution of peroxide species for a hydrogen peroxide / boric acid system. The trigonal peroxoboric acid, $B(OH)_2OOH$, is the only significant peroxoborate species below pH 6.5. However, above this pH, increased concentrations of the monoperoxoborate anion, $B(OH)_3OOH$, the peroxodiborate anion, $(HO)_3BOOB(OH)_3^{2-}$, and the diperoxodiborate anion $(HO)_2B(OO)_2B(OH)_2^{2-}$, are formed, with diperoxoborate, $B(OH)_2(OOH)^{2-}$ forming at higher hydrogen peroxide concentrations. Therefore this is the ideal pH range in which to elucidate any effects of borate on the reaction of hydrogen peroxide and PNPA. The observed second order rate constants (k_{2obs}) for the reaction between p-nitrophenyl acetate and hydrogen peroxide, and the corresponding second order rate constants, k_2 , for the reaction of the perhydroxyl anion with p-nitrophenyl acetate was determined by equation:

$$k_2 = k_{2obs} \times \frac{(K_a + [H^+])}{K_a}$$

In borate buffer the k_2 values were significantly reduced compared to other buffers; this reduction was consistent with the hydrogen peroxide complexing with borate to form a range of non-reactive (towards carbonyl groups) peroxoborate species, thus also reducing the equilibrium concentration of the perhydroxyl anion. There was no evidence for peroxoborate species that could act as nucleophiles, in contradiction of literature claims.

Values of k_2 in the case of phosphate buffer compared reasonably well with values in the literature of 3140 and 3520 $dm^3 mol^{-1} s^{-1}$ obtained at pH 6.8 in ionic strengths of 0.02 $dm^3 mol^{-1}$ and 0.1 $dm^3 mol^{-1}$ respectively. In carbonate buffer the literature value is 3785 $dm^3 mol^{-1} s^{-1}$ at pH 10, ionic strength 0.1 M, in borate buffer.

Table of contents

Chapter 1. Introduction	1
1.1. Peroxyacids	1
1.1.1. The chemistry of peroxyacids.....	1
1.1.2. The systematic name	1
1.1.3. Dissociation of Peroxyacids.....	2
1.1.4. Peroxyacid decomposition.....	3
1.1.5. The Preparation of peroxyacids.....	5
1.1.6. The electrophilicity of peroxyacid.....	7
1.1.7. Oxidation Capacity of Selected Sanitizers	10
1.1.8. Peroxide determination techniques	10
1.2. Dyes	15
1.2.1. Colour in dyes	16
1.2.2. The molecular excitation model of dye and aggregation of dye in solution	17
1.2.3. Classification of dyes.....	17
1.2.4. Isomerism in azo dyes.....	24
1.2.5. Toxicity of dyes	25
1.2.6. Decolouration	27
1.2.7. Advanced oxidation process (AOPs)	31
1.2.8. Peracetic acid.....	37
1.2.9. Disadvantages of advanced oxidation process.....	38
1.2.10. Biological degradation	38
1.2.11. Advantages and disadvantages of dye removal methods.....	39
1.3. Aims of this project.....	41
Chapter 2. Formation of peracetic acid from acetic acid and hydrogen peroxide.....	43
2.1. Introduction	43
2.2. Uncatalysed formation of peracetic acid from hydrogen peroxide and acetic acid	
.....	45
2.2.1. Materials	45
2.2.2. Peracetic acid solutions.....	45
2.2.3. Procedure and methods	45
2.2.4. Results and Discussion	46
2.3. Catalysed formation of peracetic acid from hydrogen peroxide and acetic acid in	
the presence of 0.1 M sulphuric acid.....	53
2.3.1. Materials	53
2.3.2. Reaction solution.....	53
2.3.3. Procedure and methods	53
2.3.4. Results and Discussion	54
2.4. Hydrolysis of peracetic acid.....	57
2.4.1. Peracetic acid solutions.....	57
2.4.2. Method for monitoring peracetic acid hydrolysis	57
2.4.3. Results	58
2.4.4. Determination of kinetic constants.....	58
2.5. Overall discussion.....	63
2.5.1. The reaction mechanism	63
2.6. General conclusion	69
Chapter 3. Dye Bleaching Studies	72
3.1. Introduction	72
3.2. Experimental work	73
3.2.1. Materials	73
3.2.2. Dyestuffs	73
3.2.3. Preparation of Solutions	74
3.2.4. Spectrophotometric Measurements.....	75

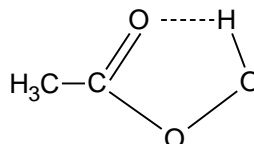
3.3. Results and Discussion.....	83
3.3.1. Summary of dye bleaching results.....	88
3.2.6. Mechanisms of dye oxidation	89
3.4. Conclusion	94
Chapter 4. Iron catalysed oxidation of azo dyes by peracetic acid	132
4.1. Introduction	132
4.2 . Experimental.....	133
4.2.1. Materials	133
4.2.2. Reaction stoichiometry	133
4.2.3. Kinetic measurements and percentage dye degradation	134
4.3.Results.....	136
4.3.1. Ponceau 4r dye	136
4.3.2. Other azo dyes.....	149
4.4. Discussion	159
4.4.1. Uncatalysed reaction.....	162
4.4.2. Catalysed reaction	163
4.4.3. Effect of pH on K.....	166
4.4.4. Factors affecting dye degradation	169
4.5. Conclusions	172
Chapter 5. Reaction of hydrogen peroxide with p-nitrophenyl acetate (PNPA) in the presence of different buffers	175
5.1. introduction	175
5.2. Experimental.....	179
5.2.1. Materials	179
5.2.3. Kinetic measurements.....	179
5.3. Results.....	182
5.4. Discussion	200
5.4.1. General	200
5.4.2. Second order rate constants	201
5.5. Conclusions and Further work.....	207
Chapter 6. Conclusions and recommendations for	209
further research	209
6.1. Novel aspects arising from the study.....	209
6.2. Main conclusions	209
6.3. Recommendations for further research	213
References	215
Appendix.....	222

Chapter 1. Introduction

1.1. Peroxyacids

1.1.1. The chemistry of peroxyacids

Organic peroxyacids are one of the most useful classes of organic peroxides due to the wide range of specific oxidation reactions that they can perform. Organic peroxyacids, or peracids, are derivatives of hydrogen peroxide in which one of the hydrogen atoms is replaced by an acyl or aroyl group. Monoperoxy acids contain one peroxy carboxyl ($-\text{CO}_3\text{H}$) group; diperoxy acids contain two. No examples of tri- or higher peroxy acids are known.



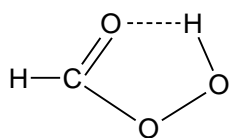
Structure [1.1]. peroxyacetic acid

Both dipole moment measurements of aliphatic peroxyacids¹, and infra red spectral evidence², suggests that peroxyacids have, to a greater or lesser extent, a skew conformation about the O - O bond, similar to that of hydrogen peroxide.

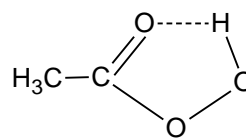
The UV spectra of peroxyacids are similar to those of hydrogen peroxide, which means they exhibit a continuously increasing absorption as the wavelength decreases. In 1962 Symons concluded that for hydrogen peroxide the transitions may involve oxygen lone pair electrons, or electrons in weakly "pi" antibonding orbitals³.

1.1.2. The systematic name

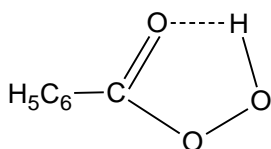
The word peracid has been in common use for a long time and is still frequently used. However, the systematic name, peroxy, which clearly indicates the presence of peroxide oxygen in the molecule, and avoids ambiguity in certain cases, is preferred. Some typical peroxyacids are shown in Structure 1.2.



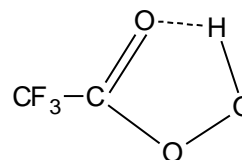
Peroxyformic acid (performic acid)



Peroxyacetic acid (peracetic acid)



Peroxybenzoic acid (perbenzoic acid)



**Peroxytrifluoroacetic acid
(Trifluoroperacetic acid)**

Structure 1. 2: Some typical examples of organic peroxy acids

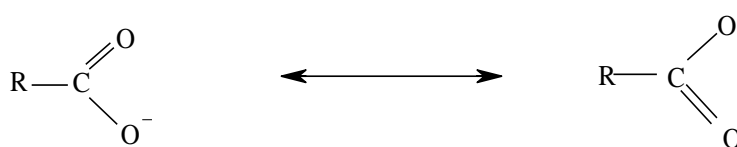
1.1.3. Dissociation of Peroxyacids.

Parent acids are generally stronger acids than the peroxyacid. Some examples listed below show the pK_a of parent acids and their respective peracids.

Table 1.1:- shows the peroxyacid with pK_a ⁴.

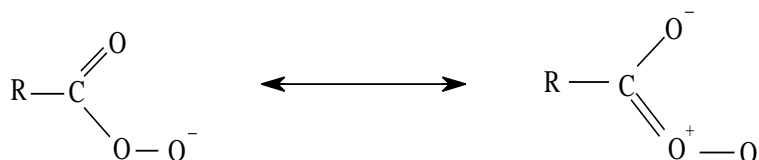
	pK_a		pK_a
Formic acid	3.8	Performic acid	7.1
Acetic acid	4.7	Peracetic acid	8.2
Propionic acid	4.9	Perpropionic acid	8.1
Sulphuric acid	1.9	Peroxomonosulphuric acid	3-4(est.)

For example, peracetic acid, which is used extensively in this work, has a pK_a of 8.2, whereas acetic acid has a pK_a of 4.7. There are two explanations for this. Firstly that intramolecular hydrogen bonding stabilises the neutral molecule relative to the anion form⁵ such as in Structure 1.1 above. The second explanation is that the parent carboxylic acid has an anion form stabilised by a delocalised electronic configuration⁶. (Scheme 1.1)



Scheme 1.1.

Compared to the parent acid, however, canonical resonance forms would be much less likely to contribute to the peroxyanion ground state⁶ (Scheme 1.2)



Scheme 1.2.

In addition, methyl substitutions in alkyl hydroperoxides and aryl substituents in Peroxybenzoic acids affect the pKa values less than in the parent alcohols and benzoic acids respectively. This is due to the fact that polar and electronic effects are weakened in passing through the O – O bond to affect the strength of the terminal O – H bond⁷ since the O – O link is one atom longer and electronically saturated this weakening of the electronic effect is not unexpected. Similar weakening is observed in organic systems by insertion of a methylene group between the substituent and reaction site.

It should be noted that the dissociation constants of peroxomonosulphuric acid⁸ and peroxomonophosphoric acid⁹ have been measured spectrophotometrically utilizing the increase in extinction in the ultra violet region on ionization of the peroxidic proton. However, due to the decomposition of the peroxyacid during the titration this method cannot be used to measure dissociation constants to a high degree of accuracy.

1.1.4. Peroxyacid decomposition

1.1.4.1. Auto decomposition

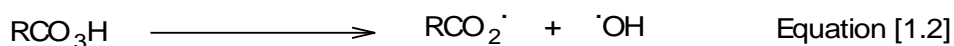
Organic peracids decompose spontaneously by auto decomposition to produce parent acids and oxygen. The rate of decomposition, v , is maximised at the pKa¹⁰, as can be seen in Equation, 1.1.



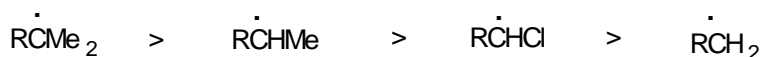
1.1.4.2. Effect of thermolysis and photolysis

The thermal decomposition of peroxyacetic acid has been studied in both the vapour phase¹¹, and in aromatic solvents¹². Under these conditions the decomposition is mainly homolytic and the dissociation energy of the O-O bond has been reported from activation energies to be 30 to 34 k cal mol⁻¹.

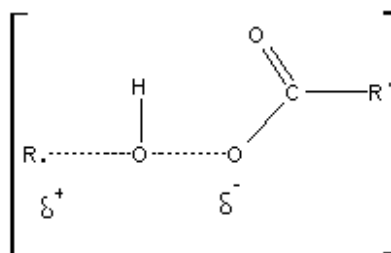
Lefort et al¹³ have demonstrated systematically the radical decomposition of peroxyacids by thermolysis, and Ando¹⁴ has summarised decomposition according to Equations 1.2 to 1.4.



The decarboxylation shown in Equation [1.3] on the aliphatic carboxy radicals is very fast, followed by radical substitution on the peroxy oxygen of the peracetic acid in the Equation 1.4, it is interesting that more nucleophilic radicals react faster with the peroxy oxygen of peracetic acid, for example the relative reactivities on Equation 1.4, being in the decreasing order tertiary > secondary > primary carbon radicals as show in example below¹⁴



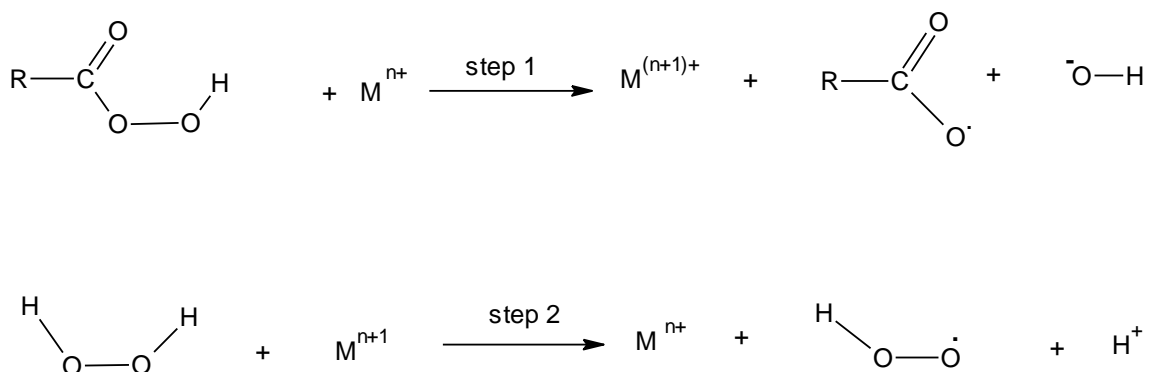
These relative reactivities of radicals with peracetic acid are correlated with their ionisation potentials; the trends for which are explained by the following polar effect in Structure 1.3.



Structure 1.3.

1.1.4.3. Metal ion interactions

Decomposition of peroxyacids has been shown to take place in aqueous solution via a free radical pathway when catalysed by metal ions of variable valence¹⁵. Scheme 1.3 below shows that metal ions are able to catalyse the decomposition of hydrogen peroxide where M is the metal ion of variable valence.



Scheme [1.3]:- Peroxide synergism in redox cycling with metal ions

Ethylenediaminetetraacetic acid (EDTA) has been shown to drastically reduce the metal catalysed decomposition of peroxyacids and hydrogen peroxide^{15, 16}, presumably by sequestering the trace metal ions, and has been used in a number of studies to reduce metal catalysed reaction.

1.1.5. The Preparation of peroxyacids

Numerous methods are known for the preparation of peroxyacids, some are general while others are specific for certain peroxyacids only. These preparations are summarised in Table (1.2).

Table 1.2:- Summary of types of reaction that have been reported for preparing peroxyacids.

	Reference
$\text{RCO}_2\text{H} + \text{H}_2\text{O}_2 \text{ (30 to 98\%)} \xrightleftharpoons{\text{H}^+} \text{RCO}_3\text{H} + \text{H}_2\text{O}$	17-19
$\text{RCHO} + \text{O}_2 \xrightarrow{\text{free radical chain reaction}} \text{RCO}_3\text{H}$	20-22
$\text{RCO}_3\text{COR} \xrightarrow{\text{Hydrolysis}} \text{RCO}_3\text{H} + \text{RCO}_2\text{H}$	23, 24
$\text{RCO}_2\text{COR} + \text{H}_2\text{O}_2 \longrightarrow \text{RCO}_3\text{H} + \text{RCO}_2\text{H}$	17, 25, 26
$\text{RCOCl} + \text{H}_2\text{O}_2 \xrightarrow{\text{base}} \text{RCO}_3\text{H} + \text{HCl}$	17, 27, 28
$\text{B (OCOR)}_3 + 3\text{H}_2\text{O}_2 \longrightarrow 3\text{RCO}_3\text{H} + \text{H}_3\text{BO}_3$	17, 29

From Table 1.2 we can see that reaction 1 is reversible, and the conversion and yields of peroxy acids are highest when the water content is at a minimum. This is accomplished either by the use of more concentrated hydrogen peroxide³⁰, or the use of excess aliphatic acid.

Peroxyacetic acid it is one the oldest known peroxy acids and was first prepared in 1864 by mixed diacetyl peroxide by Brodie³¹, but it was not isolated and characterised until much later in the classical work of D'Ans and co-workers¹⁷. This is the most important and widely used peroxyacid and, therefore the number of publications and patents describing its properties, preparation and reactions, is considerable.

In the early 1900s the first dilute aqueous solutions of peroxyacetic acid were obtained by the mild hydrolysis of diacetyl peroxide or of benzoylacetyl peroxide³² using several methods, for example: reaction of diacetyl peroxide with dilute aqueous hydrogen peroxide;³³ or by the reaction of diacetyl peroxide with in alkaline conditions followed by acidification. In 1945 the reaction of acetic anhydride with an inorganic peroxide or with a dilute solution of hydrogen peroxide was reported to result in dilute solutions of peroxyacetic acid and its salt³⁴.

1.1.5.1. Direct Preparation of peracetic acid from acetic acid

Reaction 1, Table 1.2 shows the direct acid catalyzed reaction of 30 to 98% hydrogen peroxide with acetic acid to form peroxyacetic acid; this method was the most important and widely used to prepare peroxyacetic acid. The acid catalyzed formation and hydrolysis of peroxy acetic acid is bimolecular and involves acyl-oxygen cleavage³⁵, the specific reaction rate constant for the formation of peroxyacetic acid from acetic acid and hydrogen peroxide is reported to be $7.4 \times 10^{-6} \text{ dm}^3 \text{ mol}^{-1} \text{ s}^{-1}$ at 25°C ³⁶, in the presence of 2% by weight of sulphuric acid.

Pungor and co-workers³⁷ have published the rate constants at higher reaction temperatures and at varying hydrogen peroxide concentration and water. Sulphuric acid has also been used as a solvent reaction medium for preparing peroxyacetic acid³⁸⁻⁴⁰. However, no main advantage is seen in the use of large quantities of sulphuric acid with carboxylic acids, which are easily miscible with hydrogen peroxide.

The equilibrium constant for the preparation of peroxyacetic acid from acetic acid and hydrogen peroxide is somewhat uncertain. Values ranging from approximately 3^{41} to 7^{17} have been reported in the temperature range 0 to 25°C . The three main factors determining the equilibrium constant for peroxyacetic acid formation are: sulphuric acid and hydrogen peroxide concentration and temperature^{42,43}. As anhydrous conditions are approached, the equilibrium constant is reported to increase to approximately 4.5 at 25°C ⁴³. The variation in values has been attributed to analytical difficulties and decomposition with loss of active oxygen. In 1965 Sawaki and Ogata⁴⁴ showed that the increase in the concentration of sulphuric acid leads to increase in equilibrium constant (K).

1.1.6. The electrophilicity of peroxyacid.

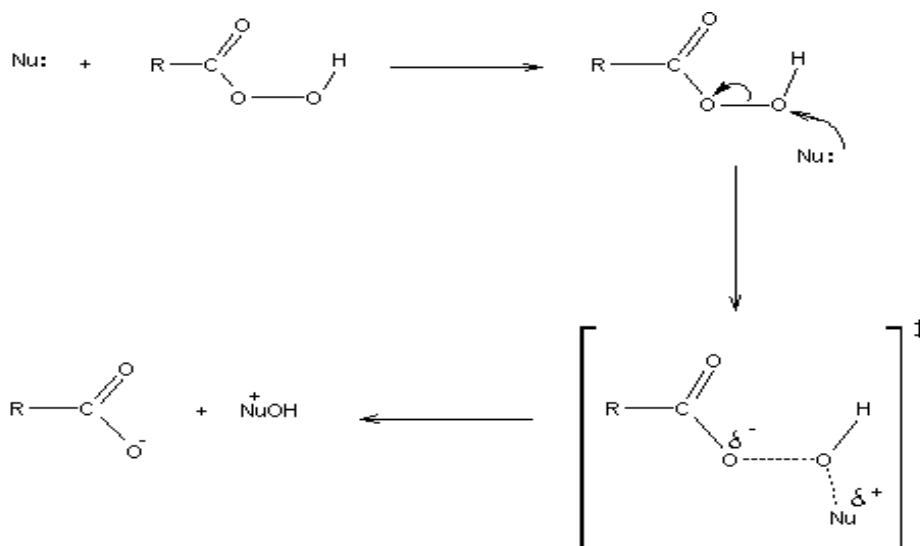
Peroxyacids are ambident electrophiles and nucleophilic attack either takes place at the outer peroxide oxygen or at carbonyl carbon. This is discussed in the following sub-sections.

1.1.6.1. The outer peroxidic oxygen

The outer peroxidic oxygen has non bonded electrons and reacts faster with polarisable soft nucleophiles; for example it reacts much faster with iodide than chloride.⁴⁵ The electrophilic oxidation of azobenzene by peroxobenzoic acid in benzene

produces azoxybenzene. The second order rate constant is $2.31 \times 10^{-4} \text{ dm}^3 \text{ mol}^{-1} \text{ sec}^{-1}$; the rate increases with electron donating substituents on the azobenzene⁴⁶.

As many reducing agents are nucleophiles, oxidation may take place by displacement mechanism on the oxygen; in 1962 Edwards⁴⁷ proposed a simple model for the transition state, as shown in Scheme 1: 4.



Scheme 1.4:- A simple model for transition state

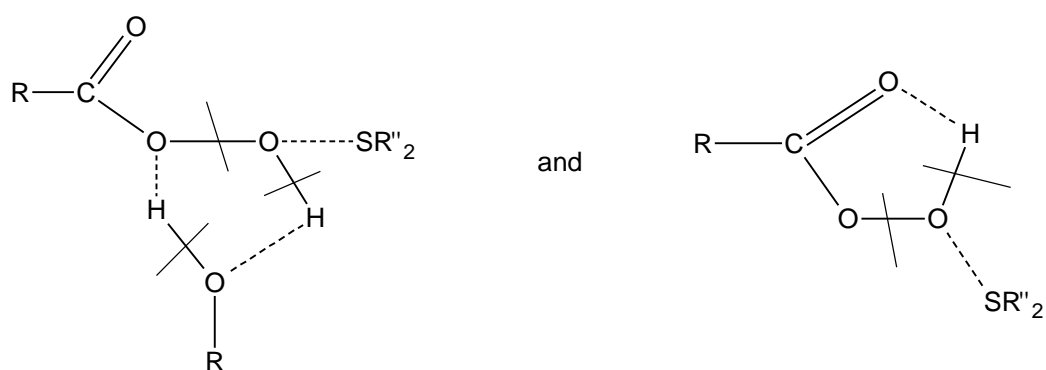
From this model there are many predications are possible such as:

- The entropy of activation should be negative.
- Less basic leaving groups RCOO^- , should result in an increase in the rate.
- Since there are unshared electron pair on the oxygen atoms various types of acid catalysis should be apparent.

The above properties have been shown in acidic solutions, for example in the oxidation of chloride and bromide ions by peroxyacetic and peroxomonosulphuric acids⁴⁵ and also of iodide by substituted peroxobenzoic acids⁴⁸. The slopes of the plots of the log of the second order rate constant against the pKa of the parent acid are -0.5, showing the electron withdrawing groups increase the rate. The magnitude of the effect is consistent with results produced for other hydroperoxides and halide ions⁴⁷.

In reactions such as the oxidation of olefins to epoxides and sulphides to sulfoxides, the scheme suggested by Edwards above is less satisfactory energetically than in the case of halides or other negatively charged nucleophiles since it involves charge separation in going from reactants to products.

In 1970 Edwards⁴⁹ proposed that these reactions are influenced by solvation of the ground state of both the substrate and peroxyacids, and also the transition state. He proposed structures, (Scheme 1.5), for the transition state in both protic and aprotic solvents which involve the bypassing of charge separation. The dotted lines represent new bonds being formed, and the solid lines indicate the bonds that will break.

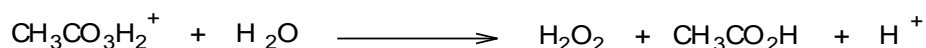
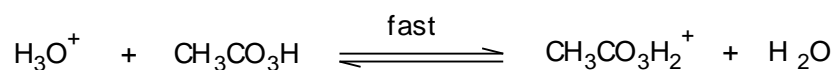


Scheme [1.5]:- the transition state in both protic and aprotic solvents.

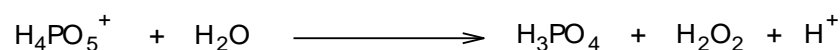
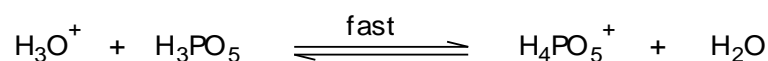
There are many studies that show the transition state is similar to those suggested by Edwards, for example the oxidation of sulphines to ketones⁵⁰ and acetylenes⁵¹.

1.1.6.2. The carbonyl carbon in peroxyacids

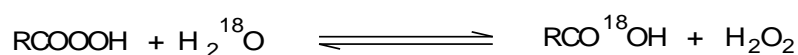
The carbonyl carbon is relatively hard since it has some positively charged character. It reacts with hard charged nonpolarisable bases such as hydroxide. In 1956 Bunton³⁵ studied the hydrolysis of peroxyacetic acid and found it to be acid catalysed, i.e. the transition state consisted of nucleophilic attack of water on the conjugate acid of the peroxyacetic acid.



A similar conclusion for the hydrolysis of peroxomonophosphoric acid has been reported by Battaglia and Edwards⁹; they also suggested the possibility of a non acid catalysed pathway but under the conditions necessary to measure this the decomposition of the peroxyacid was the predominant reaction.



In 1956 Bunton *et al* produced conclusive evidence using H_2^{18}O as a solvent that hydrolysis involves cleavage of the carbon-oxygen bond; this means that the acyl group and oxygen atom are cleaved in both of the formation and hydrolysis of peroxyacids



1.1.7 .Oxidation Capacity of Selected Sanitizers

Peracetic acid is a stronger oxidiser and has a higher oxidation potential than chlorine dioxide and sodium hypochlorite but less than ozone. Table 1.3 shows the oxidation capacity of peracids.

Table 1.3: The oxidation capacity of oxidizers.

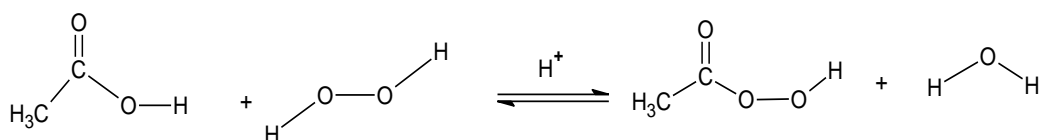
Sanitizer	electron volt
Ozone	2.07
Peracetic Acid	1.81
Chlorine dioxide	1.57
Sodium hypochlorite (chlorine bleach)	1.36

Source : Enviro Tech Chemicals, Inc

1.1.8. Peroxide determination techniques

Hydrogen peroxide is always present in peracetic acid solution; this is because the peracetic acid is technically synthesised by mixing concentrated solutions of acetic acid and hydrogen peroxide in the presence of a sulphuric acid catalyst. The quantitative determination of peracids is difficult, because aqueous peracid solutions always contain hydrogen peroxide, which shows similar reactivity, i.e., hydrogen peroxide and peracids are both reactive oxidising agents and have similar reactivities with many reagents used in peroxide determination, making resolution of a mixture of these peroxides difficult.

Various methods have been reported for the determination of peracetic acid in acidic solution, the most widely used methods for analyzing solutions containing peracetic acid and hydrogen peroxide are: the titration method of by D'Ans and Frey⁵² and its modification by Greenspan and Mckellar⁵³ and Sully and Williams⁵⁴; conductivity measurements; photometry⁵⁵⁻⁵⁸; spectrophotometry⁵⁹⁻⁶¹; gas and liquid chromatography determinations⁶²⁻⁶⁵; and electrochemical sensors measurements⁶⁶⁻⁶⁹.

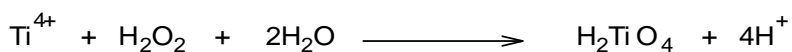


Scheme [1.6]:- Acid- catalysed equilibrium

D'Ans and Frey⁵² have described methods for analysing solutions containing peracetic acid and hydrogen peroxide. In this method the hydrogen peroxide is first titrated with permanganate and then potassium iodide is added to determine the peracetic acid by titrating the liberated iodine with thiosulphate.

In 1948 Greenspan and Mackellar⁵³ utilised a similar method to determine peracetic acid in the presence of hydrogen peroxide, by first titrating the hydrogen peroxide with ceric sulphate(IV) (ammonium tetra sulfatocerate), followed by an iodometric determination of the residual peracetic acid present. This method was also utilised by Sully and Williams.⁵⁴ To avoid significant equilibration of the peroxide in the acidic conditions the titrations must be carried out rapidly with temperatures below 10°C.⁵⁴ Liberated iodine is titrated with 0.1N sodium thiosulphate, and this is repeated several times in about 10 minutes. Titre is plotted against time, and the slope extrapolated back to zero time, which corresponds to the time for the peracetic acid alone. This method has been widely used to resolve solutions containing peracetic acid and hydrogen peroxide and the reliability of this method is very good when the concentrations of the two peroxy species are comparable.

In 1943 Eisenberg described a colorimetric method for the determination hydrogen peroxide concentrations as low as $5.29 \times 10^{-5} \text{ mol dm}^{-3}$.⁷⁰ The method utilised the yellow coloured complex that is formed between the titanium (IV) ion and hydrogen peroxide in acidic conditions which has a maximum absorption at 400nm (see the reaction below).



The titanium complex of titanium is often written as TiO_2^{2+} ⁷¹ and is selective for hydrogen peroxide at room temperature; but at high temperature the colour development is proportional to the total peroxide concentration in solution⁷². Ogleby and Williams⁷² applied this property to measure the concentration of a mixed solution from peracetic acid and hydrogen peroxide (approximately 15% PAA, 14% H_2O_2). The solution was divided into two samples, one heated to (90-95°C) and second one remaining at room temperature. The titanium (IV) oxide assay reagent is then added simultaneously and the colour development in the two samples compared, allowing the calculation of the respective percentages of the two peroxides. The colour developed in the unheated solution is proportional to the hydrogen peroxide content of the sample but the colour developed in the heated solution is proportional to the total peroxide content in the sample. The difference is proportional to the peracetic acid content of the sample. This method is capable of measuring peracetic acid in the range 1-500mg l⁻¹. In practice, in fully automated systems, sodium molybdate, which reacts with peroxides in a similar way, has replaced titanium (IV) oxalate which is unstable especially at high temperatures.

In 1959 Saltzman and Gilbert⁶⁰ developed the basic technique of kinetic colorimetry for the determination of microgram quantities of peroxides by distinguishing between hydrogen peroxide and peracetic acid using neutral potassium iodide reagent, this technique was applied to resolve mixtures of peroxides obtained from atmospheric samples^{60, 73, 74}.

In 1983 Frew et al⁵⁷ studied the development of quantitative spectrophotometric methods for the determination of solutions of mixed hydrogen peroxide and organic hydroperoxide species in the concentration ranges as low as 1 - 10µM. This method was based on four different assays: (1) formation of phenolphthalein or triiodide, (2) catalytic dye bleaching, (3) coupled oxidation of NADPH, and (4) horseradish peroxidase-coupled oxidations. The main objective of this study was to obtain a method that was highly sensitive to total peroxides, rather than an assay that was selective towards different peroxide species.

Davies and Deary⁵⁹ in 1988 developed a method for the determination of peracetic acid in the presence of up to a 1000-fold excess of hydrogen peroxide using a spectrophotometric method. This method is similar to the titrimetric method of Sully and Williams, and involves a similar extrapolation of the absorbance change caused by the

initial rate of the reaction between hydrogen peroxide and iodide back to zero time to give a value due to reaction of the peracid and iodide alone. This method has been used in the study of the formation of peracetic acid during the perhydrolysis of p-nitrophenyl acetate.

Krussmann and Bohnen⁵⁵ used the oxidation of iodide to the coloured triiodide ion to detect peracids, however, as the presence of hydrogen peroxide would lead to false positive results, it is decomposed by the catalase before to the reaction with iodide, therefore requiring an additional reaction step.

Harms and Karst⁷⁵, developed a very simple flow injection analysis (FIA) method to determine peracetic acid. This method was based on a selective reaction between the peracid and 2,20-azino-bis (3-ethylbenzothiazoline)-6-sulphate) (ABTS), which forms a green coloured radical cation (ABTS^{•+}). The advantages of this method were the simple experimental setup and the high selectivity.

In 1984 Di Furia et al⁶² developed a new method for the determination of small amounts of peracetic acid in the presence of large excess of hydrogen peroxide using a gas – liquid chromatographic method. The procedure for this method was based on the fact that the oxidation of an organic sulphide to the corresponding sulphoxide is very slow with hydrogen peroxide but very fast with peracetic acid. On this basis, a known excess of sulphide is added to the solution of peracid and hydrogen peroxide, with the reduction of the peracid taking place within a few seconds whereas hydrogen peroxide is not consumed. Then by gas- liquid chromatographic measurement, the concentration of the peracid is derived from the remaining sulphide concentration. This method has been applied to the determination of 0.002M peracid concentrations (m-chloroperbenzoic acid) in the presence of up to one hundred – fold excess of hydrogen peroxide.

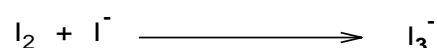
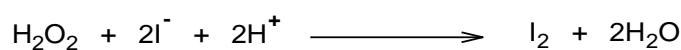
Pinkernell *et al* developed a similar chromatographic method to determine the separate concentrations of peracetic acid and hydrogen peroxide. The first step used peracetic acid to oxidise methyl-p-tolylsulfide (MTS) to the corresponding sulphoxide (MTSO). In the second step hydrogen peroxide oxidises triphenyl phosphine (TPP) to the corresponding phosphine oxide (TPPO). These four compounds can then easily be separated by liquid chromatography (LC) with UV detection. The reagents are used as the base for the development of a direct simultaneous method for the LC determination of peracetic acid and hydrogen peroxide. The derivatization of peracetic acid by MTS takes place in a pH range between 2 and 6, but for hydrogen peroxide the pH required

is between 2 and 10.5, so pH adjustment is required, which may create problems such as the equilibria involving peracetic acid and hydrogen peroxide being influenced⁷⁶ and changes in sample composition.

In an elaboration / modification, Effkemann in 1998⁷⁷ developed the methylphenylsulfoxide (MPSO) / TPP method as the ideal method for the simultaneous determination of hydrogen peroxide and peracetic acid in alkaline media without pH change prior to analysis.

Higashi *et al*⁷⁸ developed a rapid and highly selective far-ultraviolet (FUV) spectroscopic method for the simultaneous determination of peracetic acid (PAA), hydrogen peroxide, and acetic acid (AA). This simple method does not require any reagents, catalysts, or other complicated procedures for analysis.

Another technique recently used to resolve the concentrations of hydrogen peroxide and peracetic acid involved the use of coupled charge device (CCD) technologies⁷⁹. This method was based on the separation of peracetic acid and hydrogen peroxide on a reverse phase HPLC system followed by post-column reaction with a concentrated solution of potassium iodide with ammonium molybdate as catalyst, as shown in the following reactions.



The high molar absorptivity of I_3^- ($26500 \text{ M}^{-1}\text{cm}^{-1}$) gave a detection limit at 352nm of the order of 10^{-6} M levels.

Virtually all of the methods discussed above have some limitations. Titration methods, for example, are not appropriate for measuring very small amounts of peracetic acid in solutions containing a large excess of hydrogen peroxide due to the significant reaction of hydrogen peroxide with iodide under these conditions (a back-calculation method is required to overcome this). Photometric, spectrophotometric and conductivity measurements methods require calibration using the rather unstable peracetic acid as standard solution. Another problem, as for titrations, is the considerable reactivity toward hydrogen peroxide. Chromatographic methods, on the other hand, do have a

low detection limit, rely on reactions that have negligible reactivity toward hydrogen peroxide and can therefore analyze peracetic acid in the presence of a large excess of hydrogen peroxide in both acidic and alkaline⁶³ media. However, the problem is the time-consuming nature of the method, mainly because of the requirement for an extraction step with chloroform, together with the time taken to obtain the chromatogram.

Whilst there are drawbacks to the use of the titration method, as discussed above, this method is convenient and quick and was, therefore, the method of peracetic acid measurement employed throughout the course of this. The formation of peracetic acid and total peroxide content is determined by iodometric titration, where the peracetic acid reacts with iodide ion faster than hydrogen peroxide. The reaction is carried out in the presence of starch. The initial release of I_2 due to the peracid is measured by thiosulphate titration then ammonium molybdate catalyst is added and the I_2 released due to hydrogen peroxide is further titrated with thiosulphate. The difference between the total titre and that for the initial reaction of peracetic acid gives the hydrogen peroxide concentration.

1.2. Dyes

The bleaching action of peracetic acid is mainly the result of epoxidation of the double bonds present in unwanted coloured compounds^{80, 81}. In Chapter Three we consider the oxidation of a range of azo, diazo, triarylmethane, quinoline xanthene, indigoid and anthraquinone dyes by hydrogen peroxide or peracetic acid in the presence of different transition metals, and examine the structural features that hinder or contribute to their destruction. The metals used are: Fe(III), Cu(II), Mn(III) and Ag(I). The selection of metal was based on the fact that the transition metals, particularly those possessing two or more valence states between which there is a suitable oxidation-reduction potential, can react with peracetic acid. The metals are also easily obtainable and relatively low in toxicity. The use of peracids as oxidative systems for dyes, with or without metals, has thus far attracted little interest despite the use of peracid as low temperature oxidants in detergency and other applications for the last two decades.

Dyes are a class of organic compound with complex aromatic molecular structures. They are a particular problem when they enter surface waters as pollutants because of their high molar absorptivities and the fact that they are often difficult to degrade, and may also be toxic. Dye manufacturing plants, textile plants, printing and paper mills discharge their effluent containing dyes into the aqueous environment. However, many

of these dyes are toxic and carcinogenic to human. The textile industry plays a major role in the economy in many countries. A very small amount of dye in the water is highly visible and can be toxic to the ecosystem life in the water. In the textile industry, large quantities of aqueous wastes and dye effluents are discharged from the dyeing process with strong persistent colour and high biological oxygen demand (BOD). Due to the complex nature of the dyes, wastewaters may become bio-resistant. It is estimated that between 1–20% of the total world production of dyes is lost during the dyeing process⁸², and is released in the textile effluents. The release of these coloured waste waters into the environment is considerable and can form dangerous by-products through oxidation, hydrolysis, or other reactions that occur in the phase of the wastewater. Clearly the degree to which dyes enter surface waters will vary in different countries depending on levels of technology and the stringency of pollution control legislation. In Europe for example, strict environmental legislation will prohibit the discharge of dyes, whereas in less developed countries, where dyeing is a significant industry, then the pollution of water by dyes may be relatively unregulated.

1.2.1. Colour in dyes

Dyes are characterised in accordance with their capacity to absorb the energy of a particular part of the electromagnetic radiation to which the human eye is sensitive⁸³. Thus, the colour of the dye is caused by absorbance of electromagnetic radiation, and structure based on the structure of benzene. As we know, benzene appears to be a colourless liquid; In fact it absorbs electromagnetic radiation just as dyes do, but it does so at about 200nm so that we do not see it. When an object absorbs some of the radiation from within that range we see the waves that remain, and the object appears coloured⁸⁴. The wavelengths just outside the visible range are considered colourless. The colour in dyes is due the presence of a chromophore in which delocalised electron systems are conjugated with a double bond; these are responsible for the absorption of electromagnetic radiation of varying wavelengths. The chromophore is a group of atoms, which controls the colour of the dye, and it is usually an electron-withdrawing group. The most important chromophores are, -C=C-, -C=O, -C=S, -N=N-, -N=O, -NO₂, -C=NH.

The auxochromes are electron- withdrawing or electron donating substituents that cause or intensify the colour of the chromophore by altering the overall energy of the electron system. To summarise the groups which are necessary for production of colour are called chromophores and the groups which improve the colour are called auxochromes; examples include: -OH, -NR₂, -NHR, -NH₃, -COOH and -SO₃H groups⁸⁵.

There are many ways in which dyes can cause problems in the water, including: concentration of dyes; visibility of dyes in water depending on their colour, extinction coefficient and on the clarity of the water, absorption of dyes and the reflection of sunlight entering the water led to the greatest concern of the environment.

1.2.2. The molecular excitation model of dye and aggregation of dye in solution

The change in the absorption spectra of many dyes with changes in concentration, temperature and ionic strength has long been attributed to the tendency of dyes to form dimers or higher aggregates in solution; there can be large difference between the absorption spectra of dye aggregates when compared with individual molecules⁸⁶ ; these differences are caused by excitation coupling between the transition dipole moment of the individual molecules⁸⁷ .

The change in the absorption spectra of dyes because of aggregation has been treated theoretically using the molecular excitation model⁸⁸. The treatment assumes intermolecular electron overlap and electron exchange to be negligible and the dimers or higher aggregates to be held together by Van der Waal's forces. The model showed that parallel will give a blue shift, whereas head to tail dimers will give a red shift.

1.2.3. Classification of dyes.

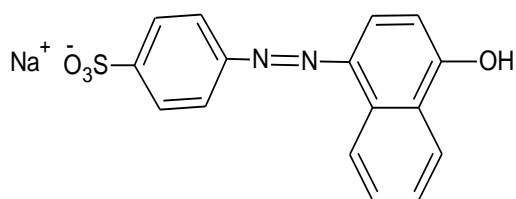
There are two classifications of dyes^{83, 89}: firstly that based on chemical structure, which is generally used by dye chemists, who use terms such as azo-dye , anthraquinone dyes or phthalocyanine dyes. The second method is mainly used by technologists and is based on the application (colouristic classification), for example reactive dyes for cotton, and dispersive dyes for polyester.

1.2.3.1. Colour index classification

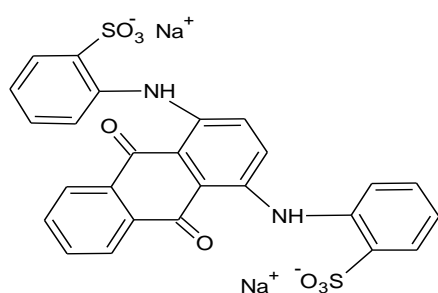
The Society of Dye and Colourists and the American Association of Textile Chemists and Colorists have classified dyes since 1924 and these are revised every three months. This classification is according to dye colour, structure and application, thus all dyes are assigned a colour index classification number and each different dye is given a C.I generic name determined by colour and application characteristics. Also many

dyes and pigments in the colour index are placed in one of the 25 structural classes according to their chemical type⁹⁰.

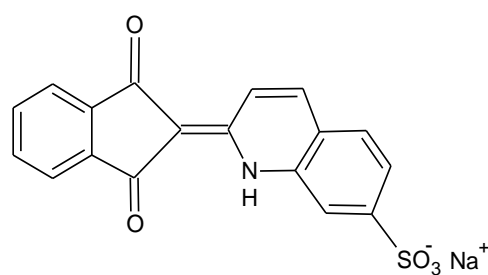
Azo dyes include mono azo dyes which have only one N=N double bond, while diazo and triazo dyes contain two and three N=N double bonds respectively. Azo dyes are subdivided into four sections and represent the largest dye class. The dyes vary structurally in terms the number of azo linkages, and the presence of phenyl and naphthyl rings and also the presence of functional groups including chloro, hydroxyl, methyl nitro and sulphonate⁹¹. Anthraquinone dyes constitute the second largest dyes in the colour index, phthalocyanine and triarylmethane dyes are also important classes. Other classes include: diarylmethane, indigoid, azine, oxazine, thiazine, xanthenes, nitro, nitroso, aminoketone and hydroxy ketone dyes. Structure 1.4 shows the most important groups of dyes. All of these structures allow “ π ” to “ π^* ” transitions in UV-visible (UV-Vis) region, with high extinction coefficients.



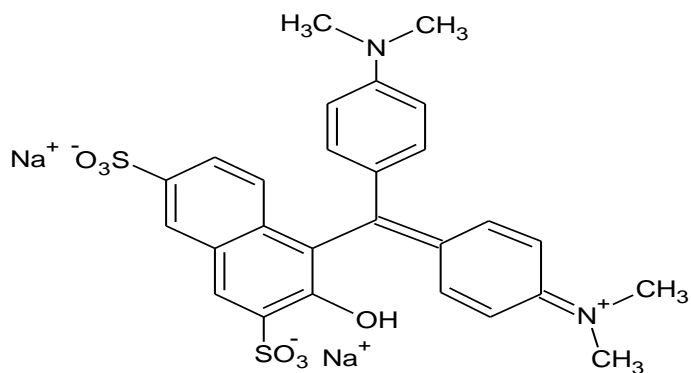
Azo dye (Orange I)



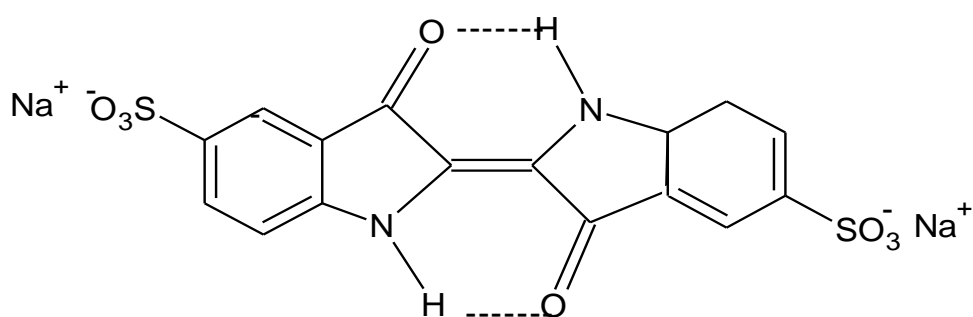
Anthraquinone (acid green 25 dye)



Quinoline (Quinoline Yellow Extra)



Triarylmethane(Green S Supra)

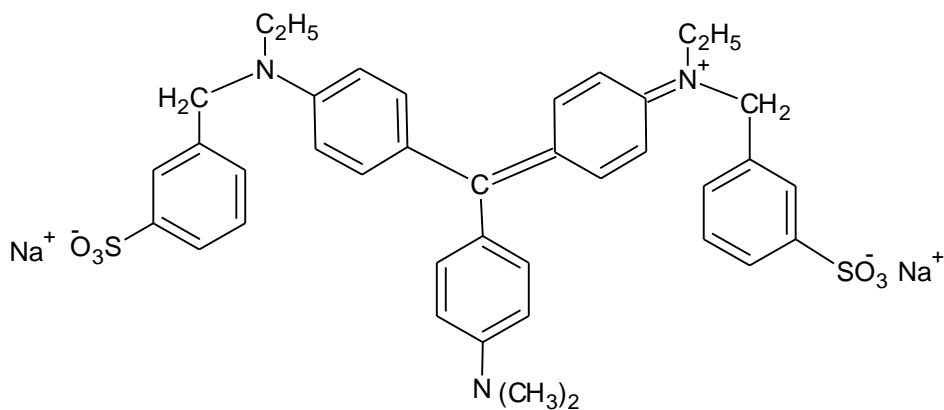


Indigo (Indigo Carmine Supra)

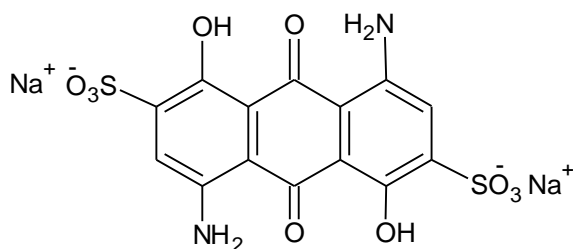
Structure 1.4: examples of dyes according to the chromophore present.

1.2.3.2. Acid dyes

Most acid dyes are azo (yellow to red) and represent the largest class of dyes in the colour Index. Acid dyes are anionic compounds and are applied to fibres such as silk, and wool. The word “acid” refers to the pH in acid dye dyebaths rather than to the presence of an acid group. Carboxyl, sulphonate or amino in the molecular structure increase their solubility in water. The chemistry of acid dyes is quite complex. Dyes are normally very large aromatic molecules consisting of many linked rings. Acid dyes having structures related to triphenylmethane predominate and many acid dyes are synthesised from chemical intermediates which form anthraquinone like structures as their final state.



Triphenylmethane dye(acid violet 49)

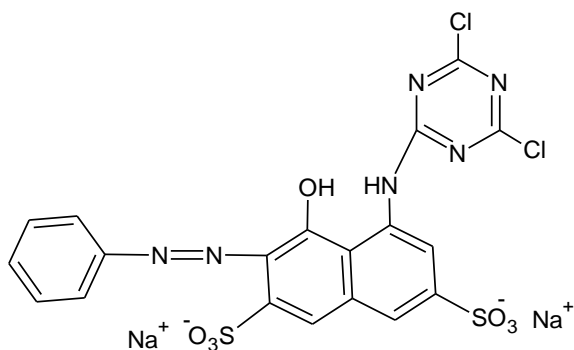


anthraquinone dye (acid blue 45)

Structure 1.5: Acid dyes

1.2.3.3. Reactive dyes

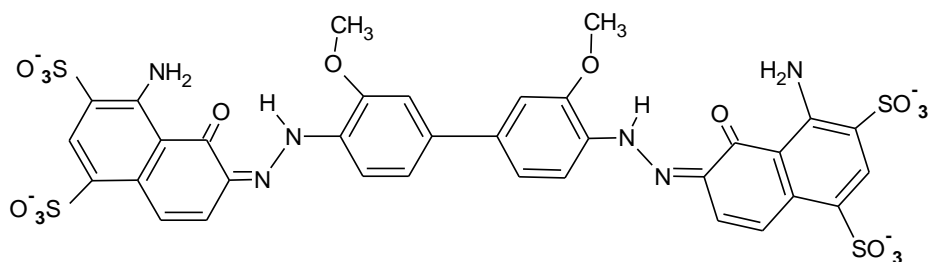
In the colour Index classification, the reactive dyes form the second largest dye class with respect to the amount of active entries; the reactive group is often a heterocyclic aromatic ring substituted with chloride or fluoride. Reactive dyes first appeared commercially in 1956. In reactive dyes a chromophore contains a substituent that is activated and allowed to directly react to the surface of the substrate. Reactive dyeing is now the most important method for the colouration of cellulosic fibres and are the most common dyes used in the textile industry due to their bright colours, good colourfastness and ease of application^{92, 93}. Reactive dyes are the principal dyes used in the cotton industry which represents more than 50% of the world's fibre usage⁹⁴. Most reactive dyes are azo dyes. Shore in 1990⁹⁰ reported that the reactive dye structures are 95% azo dyes, or metal complex azo compounds that are linked by an azo group⁹⁵. Anthraquinone and phthalocyanine reactive dyes are also used, but are toxic to many organisms and can cause direct destruction of aquatic life due to the presence of aromatic and metal chlorides⁹⁶.



Structure 1.6: Reactive Red 2.

1.2.3.4. Direct dyes

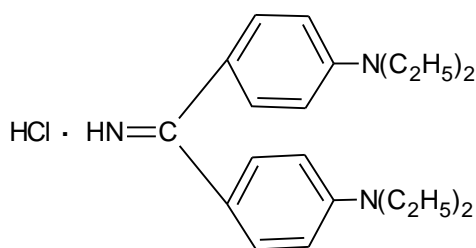
In the colour Index, the direct dyes form the second largest dye class with regard to the amount of different dyes (as opposed to active entries): approximately 1600 direct dyes are listed. Many direct dyes are azo dyes with more than one azo bond, or phthalocyanine, oxazine compounds; direct dyes are used on cotton and paper. They are also used as pH indicators and as biological stains. Direct dyes are usually negatively charged, with the coloured part of the molecule as the anion. Dyeing is normally carried out in a neutral or slightly alkaline dyebath at or near boiling point with addition of either sodium chloride or sodium sulphate. An example is shown in Structure 1.7.



Structure 1.7: Direct Blue 1

1.2.3.5. Basic dyes

In the colour index, basic dyes represent about 5% of all dyes listed. Basic dyes are water-soluble cationic dye compounds that are used for dyeing acid-group containing fibres. Basic dyes are also used in the colouration of paper. Examples include: diarylmethane, triarylmethane, anthraquinone or azo compounds. Basic dyes have amino groups, or alkylamino groups as their auxochromes and consequently have an overall positive charge. An example is shown in Structure 1.8.

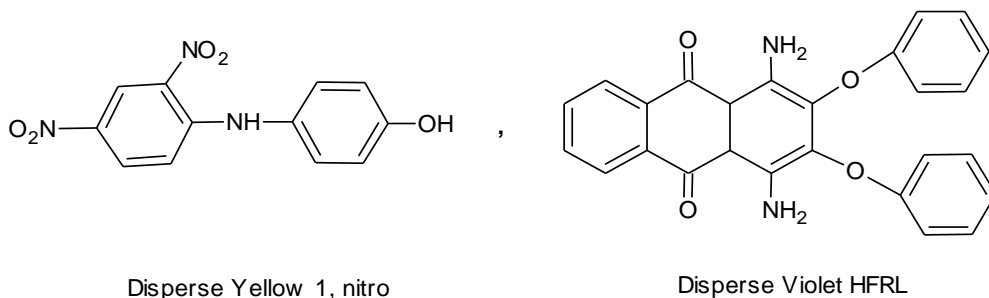


Basic Yellow 3, diphenylmethane

Structure 1.8: Basic yellow, diphenylmethane

1.2.3.6. Disperse dye

In the colour Index classification, disperse dyes form the third largest group of dyes, with approximately 1400 different compounds listed. Disperse dyes are usually small azo or nitro compounds, anthraquinones or metal complex azo compounds, and were originally developed for the dyeing of cellulose acetate, and are substantially water insoluble. Examples are shown in Structure 1.9.



Disperse Yellow 1, nitro

Disperse Violet HFRL

Structure 1.9: Disperse Yellow 1, nitro and Disperse Violet HFRL

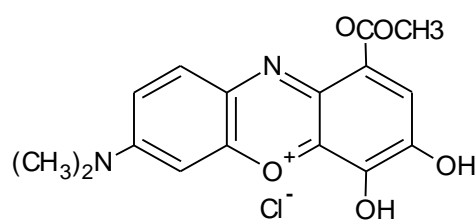
1.2.3.7. Metal complex dyes

In the colour index, metal complex dyes are usually azo compounds. These are strong complexes of one metal atom, such as copper, cobalt, nickel or chromium, and one or two dye molecules.

1.2.3.8. Mordant dyes

The use of mordant dyes is slowly decreasing. About 22% of the ~620 different mordant dyes listed in the colour index are in current production. Many mordant dyes are azo, oxazine or triarylmethane compounds. The mordant potassium dichromate is applied as an after treatment. It is important to emphasise that many mordant dyes,

especially those in the heavy metal category, can be hazardous to health and more care must be taken when used.



Mordant Violet 54, Oxazine

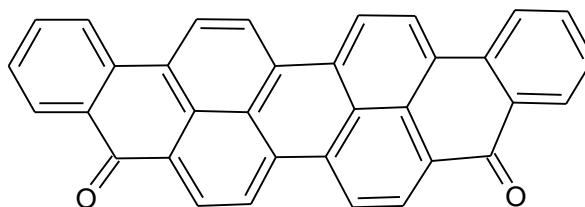
Structure 1.10 : Mordant Violet 54, Oxazine

1.2.3.9. Pigment dyes

Approximately 25% of commercial dye names listed in the colour index are pigment dyes. Pigment dyes are insoluble, non-ionic compounds or insoluble salts; this is due to their crystalline or particulate structure. The majority of pigment dyes are azo compounds or metal complexes of azo dyes.

1.2.3.10. Vat dyes

Most vat dyes are anthraquinones or indigoids; the 'vat' refers to the vats that were used for the reduction of indigo plants through fermentation. Vat dyes are water insoluble dyes. Most vat dyes are less suitable than fibre reactive dyes; indigo is an example of this dye class. Vat dyes are widely used for dyeing cellulose fibres.



Vat Blue 30

Structure 1.11: Vat Blue 30

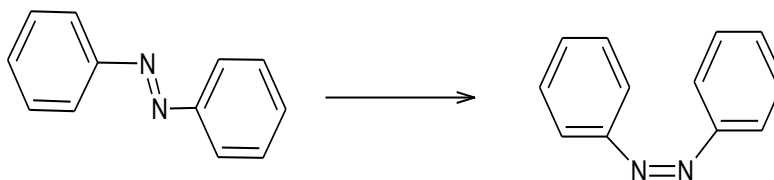
1.2.3.11. Solvent dyes

Most of the solvent dyes are diazo compounds and non-ionic dyes that are used for dyeing substrates. They are frequently called *lysochrome* dyes. The prefix *lyso* means dissolve, and *chrome* means colour. Solvent dyes are soluble in organic solvents but insoluble in water.

1.2.4. Isomerism in azo dyes

1.2.4.1. Geometrical isomerism

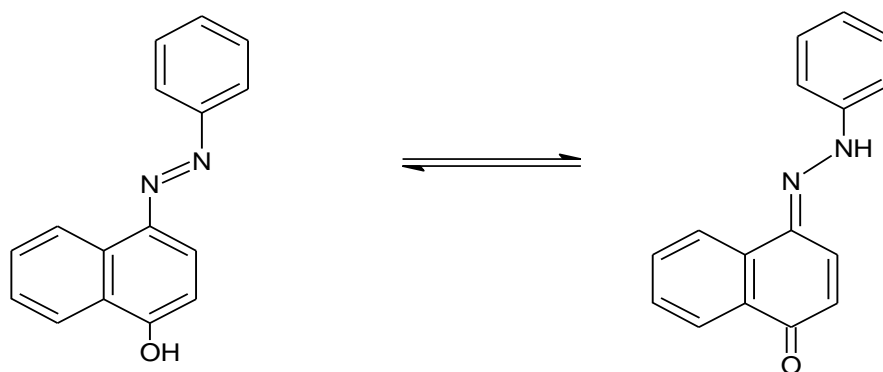
Isomerism is defined as compounds of dye with the same molecular formula but different structures.



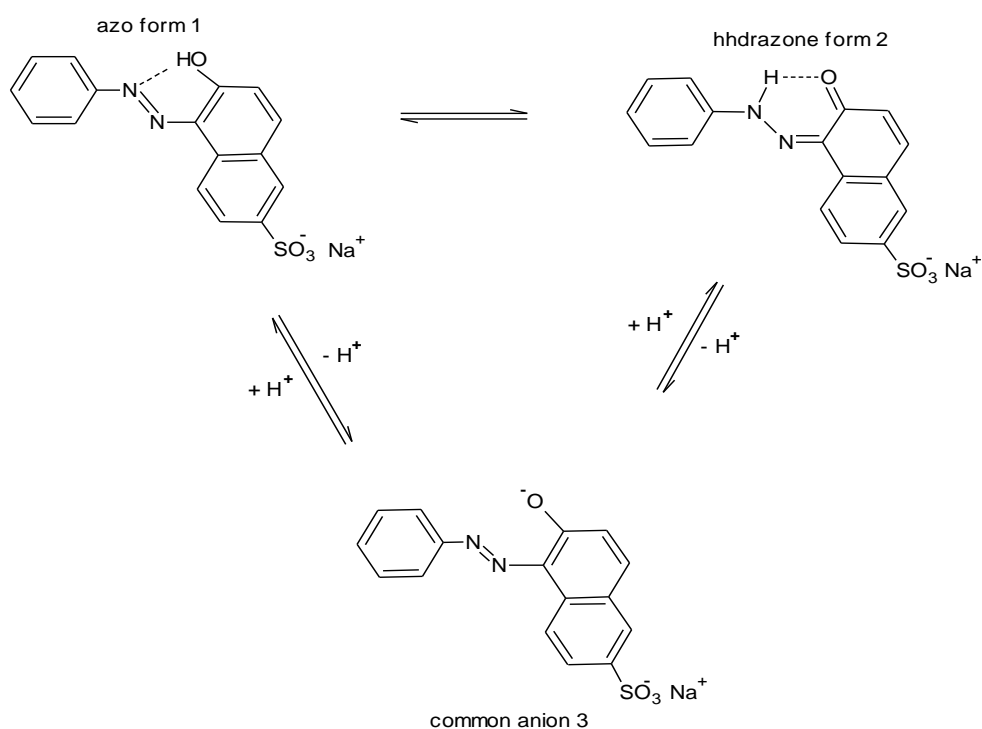
Scheme [1.7]:- isomerisms of azo dye

1.2.4.2. Tautomerism

Tautomers are structural isomers of the same chemical substance that spontaneously interconvert with each other and have different chemical properties. In the field of dyes, azo-hydrazone tautomerism such as the Schemes 1.8 and 1.9 are very important, and addition so is the formation of the common ion at high pH.



Scheme[1.8]:- Azo-dye hydrazone tautomerism

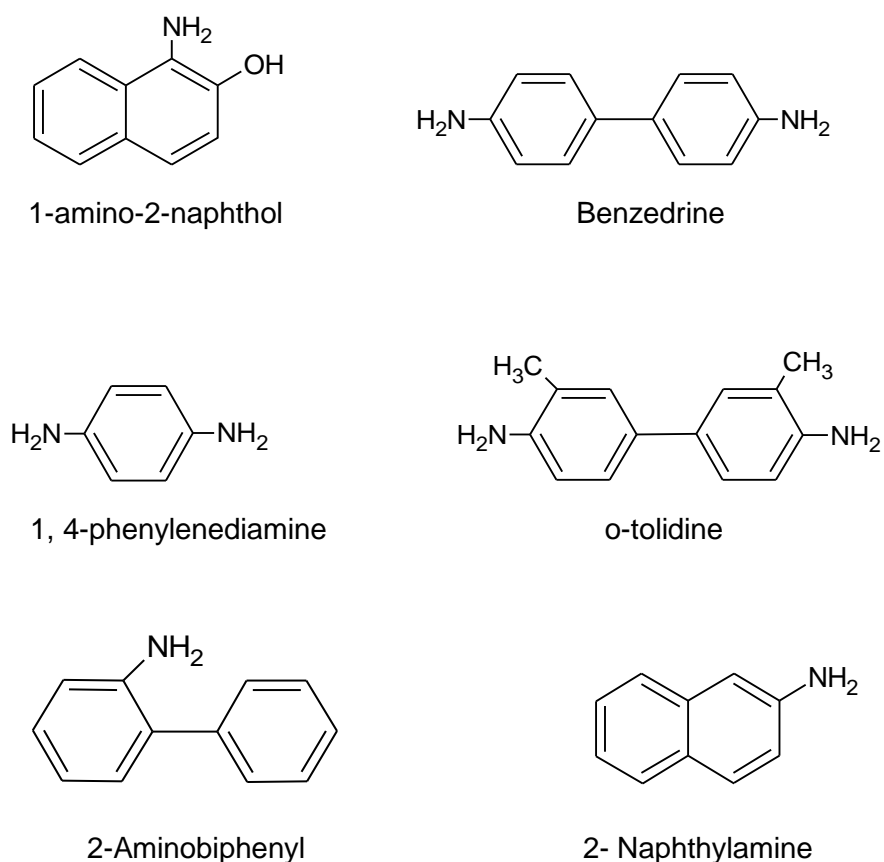


Scheme [1.9]:- Azo- hydrazone tautomerism exhibited by arylazo-2-naphthol⁹⁷

1.2.5. Toxicity of dyes

In 1895 Rehn⁹⁸ showed increased rates in bladder cancer in workers involved in dye manufacture. After that time many studies started showing the toxic potential of dyes,

specifically: mortality, genotoxicity, mutagenicity and carcinogenicity. Most of these studies focused on the effects of food colourants, azo compounds and dye manufacturing. Azo dyes are primarily composed of aromatic amines, substituted benzene and naphthalene rings. Chung and Cerniglia in 1992⁹⁹ reported that all the azo dyes containing a nitro group were found to be mutagenic; further, many of azo dyes when degraded can produce toxic products, for example 1,4-phenylenediamine, 1-amino-2-naphthol, 2-aminobiphenyl, 2-naphthylamine, benzedine (prohibited) and substituted benzidines, such as o-tolidine. These are shown in Structure 1.12¹⁰⁰.



Structure 1.12: Chemical structures of toxic products after degradation of azo dyes.

The International Agency for Research on cancer (IARC) suspects most of the amino-substituted azo dyes, fat-soluble azo dyes, benzedine azo dyes and some sulphonated azo dyes to be carcinogens. Many of these dyes were taken out of production. In addition, due to presence of heavy metals and salts in some dye and potential complexation with azo dyes, these compounds can cause high electrolyte and conductivity concentrations in the dye wastewater, leading to toxicity problems.

The toxicity of dyes depends on the nature and location of the substituents: increased toxicity is seen with nitro, methyl or methoxy group or halogen substituents atoms but lower toxicity with carboxyl or sulphonate groups.

1.2.6. Decolouration

About 70% of the Earth's surface is covered by water and there is great concern about contamination of these valuable resources. In Europe for example, the new Water Framework Directive seeks to achieve sustainable management of all water resources, ensuring that they meet a minimum quality status by a target date of 2015. Globally it is estimated that only 27% of the existing groundwater, lakes, rivers, polar ice and glaciers-can are adequately protected¹⁰¹. One of the most serious classes of pollutants of water are dyes, which are considered to be particularly dangerous organic compounds for the environment; about 20% are left in the effluent during the dyeing process: some of these cause serious human health problems as discussed above. The major source of pollution comes from the textile industry and the dye stuff manufacturing industry; these pollutants are high suspended solids, chemical oxygen demand, heat, colour, acidity, and other soluble substances, as well as having a strong colour. Most dyes used in the textile industry are reactive dyes; this is due to the bright colours produced and the ease of application. The removal of dyes from industrial effluents is an area of research receiving increasing attention as government legislation lightens on the release of pollutants.

1.2.6.1. Methods of decolouration of dyes

There are several factors that determine the technical and economic feasibility of each single dye removal technique; these include composition of the waste water, dye type and cost of required chemicals. Each different dye removal technique has its limitations and use of one individual method may not be sufficient to achieve complete decolourisation. Removal of hazardous dyes from textile effluent is essential to support the economic and environmental sustainability of the industry¹⁰². Biological methods are cheap and simple to use, but cannot be used for many wastewaters because most commercial dyes are toxic to the organisms used in the process¹⁰³. Traditional methods for treating textile dye wastewaters include: coagulation and precipitation¹⁰⁴, and adsorption processes with activated carbon¹⁰⁵, however, these processes may be costly, inefficient and often produce a high amount of secondary waste. More advanced treatment process, for example electro coagulation techniques¹⁰⁶ are considered to be potentially an effective tool for treatment of textile waste waters; similarly ultrasonic

decomposition¹⁰⁷, UV or combined oxidation processes¹⁰⁸. Other methods include: combined photochemical and biological processes¹⁰⁹, ozonation¹¹⁰⁻¹¹³, advanced chemical oxidation¹¹⁴, electrochemical oxidation^{115, 116}, Fenton's reagent¹¹⁷, ozone and Fenton's reagent¹¹⁸, and supported liquid membrane¹¹⁹⁻¹²¹. Each of these methods has its advantages and disadvantages in terms of efficiency, rapidity, formation of by-products, cost and overall environmental impact.

1.2.6.2. Chemical decolouration methods

(a) Oxidation Techniques

Chemical oxidation is the most extensively used technique for decolourization in research and industry; this is because of the diversity of chemical processes that can be effective: these techniques include oxidation reactions, photochemical oxidations and electrochemical treatment. Electrochemical technology has been applied to effectively remove acid as well as dispersed and metal complex dyes. Naumczyk, *et al*¹²¹, have suggested that electrochemical techniques for the treatment of dye waste are more efficient than other treatments.

Chemical oxidation is a very attractive technique for the purification of water contaminated with organic substances, especially with those which are too toxic for biological degradation. However, the direct reaction of organic molecules with oxygen, carried out at ambient temperatures, is usually too slow to be of practical use. Oxidation can be accelerated using high temperature as well as electric energy, but the application of these methods is not very extensive.

As environmental needs and regulations continue to become more stringent through the 2000's, destructive treatment technologies consistent with waste minimization are preferred. Oxidation technologies that are capable of achieving desired on site pollutant destruction present a commercially viable alternative to meet these increasingly demanding needs. If carried out to its ultimate stage, oxidation can completely oxidise organic compounds to carbon dioxide, water and salts. Partial oxidation can result in increased biodegradability of pollutants so that residual organic compounds can be removed through biological treatment. Many biological processes are, in fact, oxidative processes.

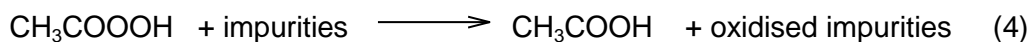
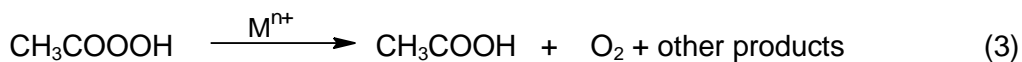
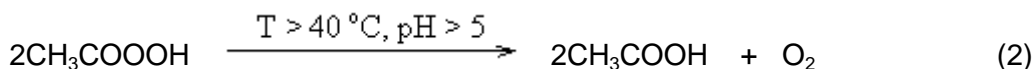
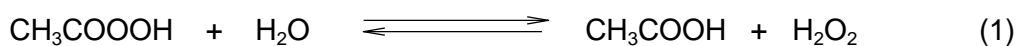
(b) Bleaching

Bleaching has been defined as the structural modification of a coloured substance to give a colourless or less intensely coloured product. The process of bleaching can take place either in solution, or on the cloth. Bleaching agents range from oxygen, ozone, peroxides, chlorine and oxides of chlorine on one hand to sulphur dioxide and bisulphite ions on the other. The first method of bleaching used by the Romans utilised sulphur dioxide fumes to bleach woollen goods, and this method was used until the emergence of cheap hydrogen peroxide; bisulphite (HSO_3^-) was the active species^{122, 123}. There are disadvantages from using sulphur dioxide bleaching, for example the substrate is reduced during bleaching and can be slowly oxidised back to its coloured form by oxygen.

Numerous changes occurred in the textile industry after bleaching powder (calcium hypochlorite) was introduced in the eighteenth century because of its ease of use and the very good bleaching performance on cellulosic fibres. Calcium hypochlorite was subsequently replaced by sodium hypochlorite which had the advantage that there were no difficulties caused by the insolubility of residual unreacted hydroxide. However there are also disadvantages from using hypochlorite, such as the formation of highly toxic chlorinated organic by-products during the bleaching process. Hydrogen peroxide is a weaker oxidising agent than hypochlorite and can be used to bleach polypeptides as well as cellulose fibres with much less risk of fibre damage. Sodium perborate ($\text{NaBO}_3 \cdot 4\text{H}_2\text{O}$) and percarbonate ($2\text{NaCO}_3 \cdot 3\text{H}_2\text{O}$) are compounds used to produce hydrogen peroxide when dissolved in water; they are used in domestic washing powders but require high pH and high temperature to be effective.

An environmentally safe alternative to hypochlorite is peracetic acid (PAA) and over the last few years, hypochlorite has been replaced by peracetic acid to some extent¹²⁴. The decomposition products of PAA are acetic acid, hydrogen peroxide, oxygen and water; furthermore peracetic acid gives higher brightness values and less fibre damage¹²⁴⁻¹²⁶ compared to hydrogen peroxide, and therefore, a satisfactory degree of whiteness can be obtained at 60 °C in 40 minutes at neutral pH without the addition of auxiliary agents, meaning lower energy and water consumption when rinsing of the fabric. The bleaching action of peracetic acid is mainly the result of epoxidation of the double bonds present in unwanted coloured compounds¹²⁷.

To optimise the use of peracetic acid in the bleaching process it is needed to consider the mechanism and conditions governing three possibilities: hydrolysis decomposition and oxidation scheme 1.10¹²⁸.



Scheme [1.10]:-Hydrolysis, decomposition and oxidation of peracetic acid (adapted from ref 128)

(c) Mechanisms of bleaching

Reductive Bleaching: - such as the action of sulphite on aromatic nitro compounds or bisulphite on carbonyl compounds which causes a decrease in the length of the conjugated system accompanied by a shift towards the ultraviolet part of the spectrum. The reaction can often be reversed by aerobic oxidation of the bleached material

Oxidative bleaching: - generally involves disruption of the conjugated system of the coloured molecule often going as far as the breakdown of the molecule into smaller fragments. The reaction can go via a free radical mechanism, or electrophilic or nucleophilic attack on the substrate.

One group of processes that is receiving a lot of attention are the advanced oxidation process (AOPs). These are currently subject to rapid evolution, especially those involving catalytic and/or photochemical systems; the successful application of AOPs depends primarily on the nature of the pollutants. Currently, only AOPs are considered to have the capacity for the complete elimination of most dye pollution. The most important of these advanced oxidation processes are briefly discussed in sections below.

1.2.7. Advanced oxidation process (AOPs)

In 1987, Glaze et al¹²⁹, defined advanced oxidation processes as “near ambient temperature and pressure water treatment processes which involve the generation of hydroxyl radicals in sufficient quantity to effect water purification”.

Since the early 1970s advanced oxidation processes (AOPs) have been used to remove both low and high concentrations of organic compounds because the alternative treatment of waste water containing organic compounds like aromatic rings such as dyes, dyestuffs, chlorophenols by methods such as physic-chemical treatment (flocculation, precipitation and absorption) are not effective;¹³⁰ nor are methods such as traditional biotreatment.^{131, 132} In the advanced oxidation processes, the organic compounds can be completely converted to carbon dioxide and water mainly by hydroxyl radicals^{133, 134}. The hydroxyl radical, which is the most powerful oxidizing agent generated, acts very rapidly with most organic compounds, through transfer of one or more electrons from an electron donor (reductant) to an electron acceptor (oxidant). During these processes chemical species are produced that have an odd number of valence electrons; these species are called radicals and because one of their electrons is unpaired these species tend to be highly unstable and thus highly reactive. The radical oxidants react with other reactants until a stable oxidation product is formed. To summarise the above, the advanced oxidation processes have two routes of oxidation: (1) the formation of strong oxidants such as •OH, and (2) the reaction of these oxidants with organic contaminants in water. Advanced oxidation processes are used to decompose many hazardous chemical compounds to acceptable levels, without producing additional hazardous by-products or sludge which require further handling. Table 1.5 shows the relative oxidation power of some oxidizing species. Hydrogen peroxide is currently considered the most appropriate reactant for use in generating hydroxyl radicals; this is discussed further in the following section.

Table 1.4: Relative oxidation power of some oxidizing species¹³⁵

Oxidizing species	Relative oxidation power
Chlorine	1.00
Hypochlorous acid	1.10
Permanganate	1.24
Hydrogen peroxide	1.31
Ozone	1.52
Atomic oxygen	1.78
Hydroxyl radical	2.05
Positively charged hole on titanium dioxide, TiO_2^+	2.35

1.2.7.1. Methods for generating •OH radicals

Methods for generating •OH radicals include photochemical and non- photochemical methods. Figure 1.1 shows the most popular techniques used recently for •OH generation as applied to the decolourization of dyes.¹³⁶ These include: oxidation with Fenton's reagent (H_2O_2 and Fe^{2+}); photo catalysis and ozonation (H_2O_2 – ozone), (H_2O_2 – UV) radiation; ozone / ultraviolet light (O_3 /UV); H_2O_2 / ozone / ultraviolet (H_2O_2 / O_3 /UV); photocatalytic oxidation (UV/ TiO_2 / H_2O_2); and H_2O_2 – peroxidise. These techniques have shown great potential for effective removal of dyes from waste water. The hydroxyl radical is a powerful oxidant and starts a cascade of oxidation reactions that can in the end lead to total mineralization of organic pollutants¹³⁷.

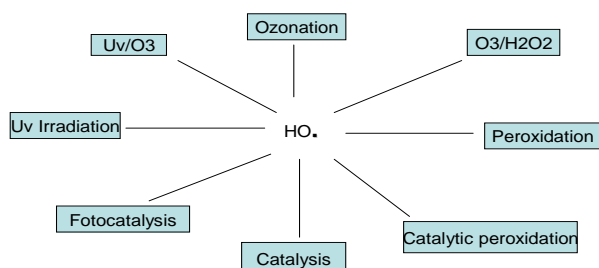
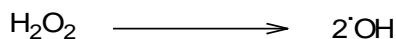


Figure 1.1: Advanced oxidation processes¹³⁶.

1.2.7.2. H₂O₂-UV radiation

Hydrogen peroxide alone is ineffective in the oxidization of the textile wastewater under both acid and alkaline conditions¹³⁸. However under UV-irradiation, H₂O₂ is photolysed to produce two •OH radicals.¹³⁹



In this way, hydrogen peroxide is activated by UV- light; however, there are many factors determining the effectiveness of the treatment by H₂O₂-UV, such as H₂O₂ concentration, the intensity of UV- irradiation, pH, and dye structure. Shen and Wang in 2002¹⁴⁰ investigated the relationship between UV-light intensity and dye decomposition in UV/H₂O₂ process the decomposition rate of dye was found to increase with increasing UV light intensity.

Shu *et al*¹⁴¹ in 1995 found that acid dyes are the easiest to decompose and that the decolouration effectiveness decreases with increasing numbers of azo groups.

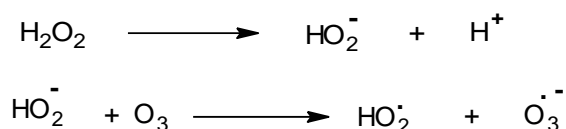
Pittroff¹⁴² reported that the decolourisation is more rapid for reactive dyes and direct, metal-complex and disperse dyes; however, that yellow and green reactive dyes are oxidised very slowly, thus requiring a longer reaction time.

1.2.7.3. Ozone and ozone/UV

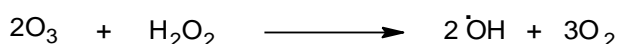
Rein in 2001¹³⁵ found that the ozonation of organic compounds does not lead to complete mineralisation and that the intermediates formed in some solutions after oxidation may be toxic or more toxic than the starting compounds. However, use of UV radiation *in addition* could lead to complete the oxidation. Hung-Yee in 1995 reported ineffective decolourisation of dyes by UV or O₃ alone but effective decolourisation of dyes when using combination of O₃ with UV (O₃/UV). Ozone photolysis at 254nm leads to formation of hydrogen peroxide as an intermediate; this then decomposes to •OH⁶⁸.

1.2.7.4. H₂O₂ -Ozone

The addition of both H₂O₂ and ozone to wastewater accelerates the decomposition of ozone and enhances formation of the hydroxyl radical⁶⁸.



The reaction continues along the indirect pathway as considered above and •OH radicals are produced¹⁴³. The combination of different reaction steps shows that two ozone molecules produce two •OH radicals:

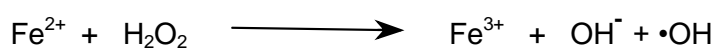


1.2.7.5. Ozone – H₂O₂ – UV-radiation (O₃/ H₂O₂/UV)

The decomposition of ozone increased by addition of hydrogen peroxide to the O₃/UV system, which results in an increased rate of •OH generation¹⁴⁴. Azbar *et al*¹³⁰ reported that the most efficient process for decolouration of dye house wastewater from polyester dyeing, was the combined system of H₂O₂/O₃/UV.

1.2.7.6. Fenton system (H₂O₂/Fe²⁺)

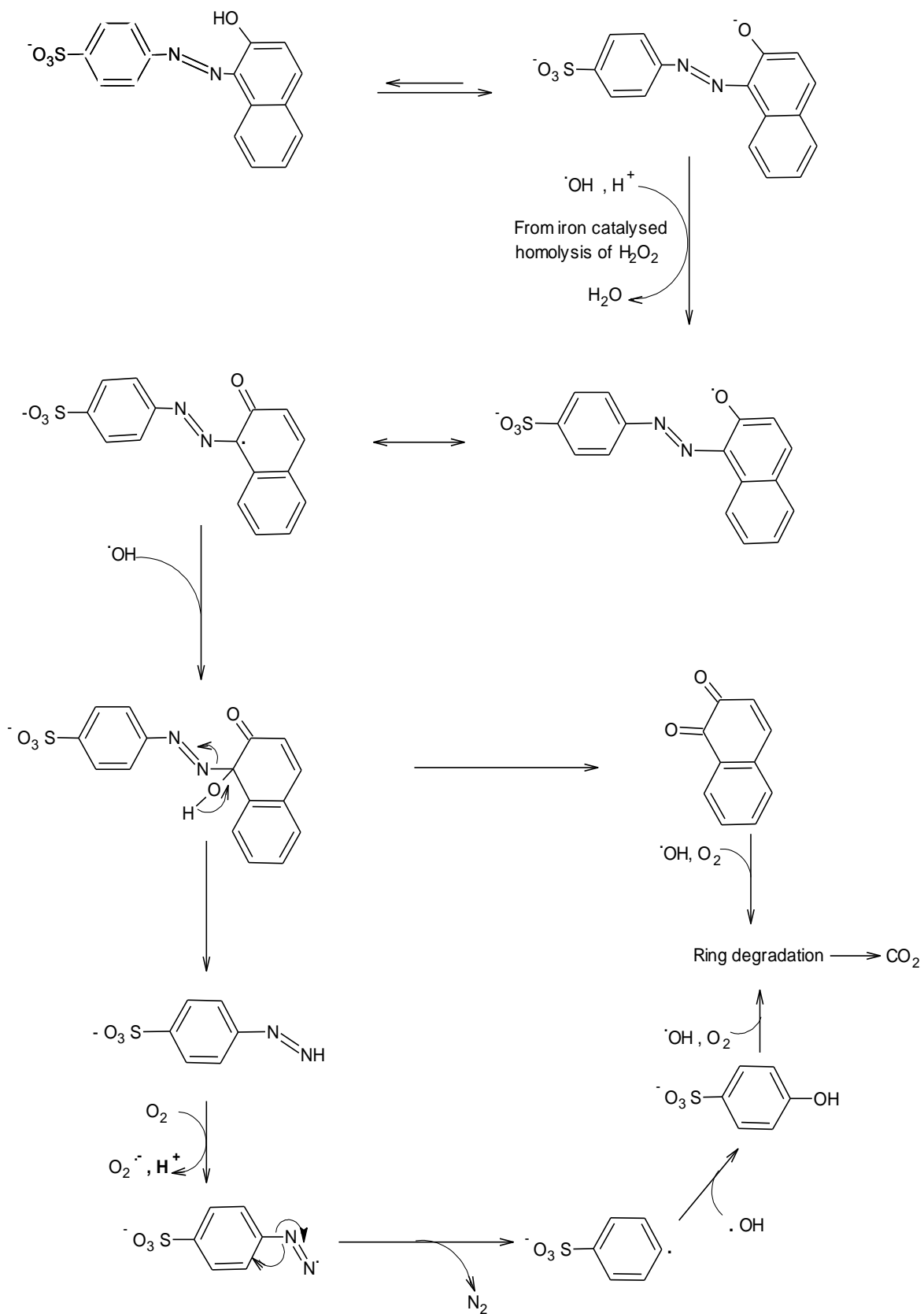
Fenton,¹⁴⁵ discovered what is now known as the Fenton process in 1884 and it was originally applied to maleic acid oxidation:



Fenton's reagent (hydrogen peroxide, activated by Fe II salts) is very applicable for the oxidation of wastewaters, this is due to the fact that the rate constant for reaction of ferrous ion with H_2O_2 is high and Fe(II) oxidises to Fe(III) very quickly even in excess amounts of H_2O_2 . The Fenton's system has the capacity to completely decolourise and partially mineralise textile industry dyes in a short reaction time, as reported by several studies.^{125, 126, 146}

The main advantages of using ($\text{Fe}^{2+}/ \text{H}_2\text{O}_2$) as an oxidant are that iron is a highly abundant and non-toxic element and H_2O_2 is simple to handle and environmentally benign.

In addition to Iron (II) salts, Fe (III) - oxalate complexes have been used as a catalyst in the photodegradation of textile dyes in water¹⁴⁷⁻¹⁴⁹. There are several published studies on the degradation of dyes with hydrogen peroxide in the presence of Fe (III) as a catalyst as shown in Scheme 1.11.



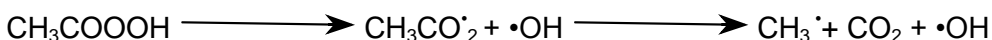
Scheme 1.71: A proposed mechanism for the degradation of Orange II by Fe^{III} and hydrogen peroxide. (adapted from¹⁵⁰, p 63)

1.2.7.7. Photocatalytic oxidation (UV/TiO₂)

One of the most widely used metal oxides in industry is titanium dioxide, both in the anatase and rutile forms, and also its use as a catalyst support or as a catalyst and photocatalyst itself. The TiO₂ photocatalyst has been one of the most widely used advanced oxidation processes in recent years; the basis of photocatalysis is the photo-excitation of a solid semiconductor by the absorption of electromagnetic radiation. Therefore with TiO₂ catalysed UV treatment, there are many dyes that can be oxidised; such is the strength of oxidation that these are not only decolourised but can be highly mineralised as well¹⁵¹.

1.2.8. Peracetic acid.

We have seen a variety of processes that can produce hydroxyl radicals, which can react with and destroy a wide range of organic contaminants. In addition to hydrogen peroxide, peracetic acid might also be a convenient source of •OH hydroxyl radicals both in the gas phase and in solution; the radicals being formed by a sequence of reactions¹¹.



The second order rate constant for oxidation of the organics with hydroxyl radicals range from 10⁸ to 10¹¹ dm³ mol⁻¹ s⁻¹ and are summarised in Table .1.6, along with those for molecular ozone

Table1.5:- Reaction rate constants (k, dm³ mol⁻¹ s⁻¹) of ozone vs. hydroxyl radical¹³⁵

Compound	O ₃	•OH
Chlorinated alkenes	10 ³ –10 ⁴	10 ⁹ –10 ¹¹
Phenols	10 ³	10 ⁹ –10 ¹⁰
N-containing organics	1–10 ²	10 ⁸ –10 ¹⁰
Aromatics	1–10 ²	10 ⁸ –10 ¹⁰
Ketones	1	10 ⁹ –10 ¹⁰
Alcohols	10 ⁻² –1	10 ⁸ –10 ⁹

1.2.9. Disadvantages of advanced oxidation process

There are disadvantages to AOPs under certain conditions. For example: ozone must be produced on site, and is expensive; the Fenton system, using hydrogen peroxide and ferrous ions produces a lot of ferric sludge, and the pH¹⁵² of the system must be strictly controlled by the addition of mineral aids such as sulphuric acid; and UV irradiation is ineffective in soil matrices or strongly absorbing solutions. Furthermore, there is a fundamental problem with AOPs in circumstances where biorefractory pollutants are mixed with easily degradable ones, or with natural organic compounds from the breakdown of living organisms. The very strength of AOPs is the production of hydroxyl radicals that are strong and indiscriminate oxidants. In mixed pollutant environments the oxidising power is wasted on chemicals that are harmless or easily degraded by natural processes. A profound weakness of the Fenton (hydrogen peroxide-ferrous) system is that a rapid burst of hydroxyl radical is produced, so that in dilute solutions of pollutants most of the oxidising power of the peroxide is dissipated in wasteful O₂ production via superoxide, HOO•, formed from the reaction of hydroxyl radicals and hydrogen peroxide.

1.2.10. Biological degradation

Biological degradation or breakdown by living organisms is the most important process for removal of organic contamination from wastewater. There are both aerobic and anaerobic processes, relying on a wide range of microorganisms, including bacteria, fungi, and algae. By utilising anaerobic-aerobic (combined) biodegradation there can be complete decolourisation of dyes and significant reduction in BOD and COD levels. The most important microorganisms are bacteria and fungi.

1.2.10.1. Bacterial

There are a variety of studies that have investigated the ability of bacteria to metabolise azo dyes¹⁵³⁻¹⁵⁵. To achieve complete degradation of azo dyes it is necessary to use both aerobic and anaerobic processes¹⁵⁶, whereby there is anaerobic reduction of the azo dyes, followed by aerobic transformation of the aromatic amines. This method there allows the treatment of dyes such as triphenylmethanes¹⁵⁷, anthraquinones¹⁵⁸ and phtalocyanines¹⁵⁹.

1.2.10.2. Fungal

The use of ligninolytic fungi is one of the possible alternatives studied for the biodegradation of dyes. Fungi have been shown to be capable of decolourising and degrading a number of dyes¹⁰⁰. White-rot fungi in particular produce enzymes such as lignin peroxidase and manganese peroxidase that degrade many aromatic compounds¹⁵⁵.

1.2.11. Advantages and disadvantages of dye removal methods.

The Table 1.7 summarises the advantages and disadvantages of some methods of dye removal from wastewater.

Table 1.6:- The advantages and disadvantages of some methods of dyes removal from wastewater. Adapted from reference¹⁶⁰.

Method	Advantages	Disadvantages
Adsorption	<ul style="list-style-type: none"> • low cost • no regeneration needed • dye-adsorbed materials can be used as substrates in solid state fermentation 	<ul style="list-style-type: none"> • some adsorbents have low surface area • possible side reactions • loss of adsorbents • performance depends on wastewater characteristics
Nanofiltration	<ul style="list-style-type: none"> • removes all dye types • high effluent quality • easy to scale-up 	<ul style="list-style-type: none"> • high investment costs • membrane fouling • effluent must be treated
Electro coagulation	<ul style="list-style-type: none"> • removes small colloidal particles • no use of coagulants • low sludge production • low cost 	<ul style="list-style-type: none"> • not effective for all dyes
Coagulation and precipitation	<ul style="list-style-type: none"> • effective for all dyes 	<ul style="list-style-type: none"> • high cost • high sludge production
Advanced chemical oxidation	<ul style="list-style-type: none"> • non-hazardous end products 	<ul style="list-style-type: none"> • high cost
Electrochemical oxidation	<ul style="list-style-type: none"> • no sludge production • breakdown compounds are non-hazardous • no chemicals used 	<ul style="list-style-type: none"> • high cost
Photo oxidation	<ul style="list-style-type: none"> • no sludge production 	<ul style="list-style-type: none"> • releases aromatic amines
Ozonation	<ul style="list-style-type: none"> • no sludge production • no alteration of volume 	<ul style="list-style-type: none"> • high cost • short half life
Supported liquid membrane	<ul style="list-style-type: none"> • minimal loss of extractants • simple to operate • low energy consumption • easy to scale up • low cost 	<ul style="list-style-type: none"> • emulsification may occur
Liquid-liquid extraction	<ul style="list-style-type: none"> • low cost • low energy consumption • variety of solvents available • easy to scale-up 	<ul style="list-style-type: none"> • emulsification may occur • effluent must be treated
Biological processes	<ul style="list-style-type: none"> • environmentally friendly • public acceptance • economically attractive 	<ul style="list-style-type: none"> • slow process • needs adequate nutrients • narrow operating temperature range

1.3. Aims of this project

The main objective of this research programme is to determine the factors influencing the decolourisation of dyes at low pH by different peroxide species, both in the presence and absence of metal ion catalysts and, therefore, to find a set of optimal conditions for application to wastewater treatment processes. An additional study looked at whether peroxoborates were capable of acting as nucleophiles.

Specific aims of the study will be:

1. To investigate the *in-situ* formation of peracetic acid from the equilibrium formed between hydrogen peroxide and acetic acid, and whether this can be achieved without the addition of an acid catalyst such as sulphuric acid.
2. To study the comparative reactivity of in-situ generated peracetic acid and hydrogen peroxide towards a range of dyes used in industry.
3. To investigate the catalytic potential of a range of metal ions towards the reaction between peroxides and dyes.
4. To investigate the structural features of dyes that might influence reactivity (decolourisation).
5. To investigate the reactivities of other peracid-like peroxide species that can be generated from hydrogen peroxide (peroxoborates and peroxocarbonates).

Chapter 2 describes the study of the formation of peracetic acid from the equilibrium between hydrogen peroxide and a large excess of glacial acetic acid, both in the presence and absence of an acid catalyst (sulphuric acid). The equilibrium and rate constants for the forward and reverse reactions are determined for both cases and are compared with literature studies.

In Chapter 3 the relative reactivities of hydrogen peroxide and peracetic acid (generated using the methods developed in Chapter 2) towards a range of dyes are studied; these include monoazo, diazo, triarylmethane, quinoline, xanthene, indigoid and anthraquinone dyes. The catalytic effects of iron, silver, manganese and copper ions on the bleaching reactions are compared.

Chapter 4 extends the broad study carried out in Chapter 3 to look in detail at the oxidation of a range of azo dyes by peracetic acid in the presence of iron (III) as a catalyst. The focus on peracetic acid and iron was because this was found to be the most effective oxidation system across the range of dyes. The focus on azo dyes

allowed the importance of structural features, such as having a hydroxyl group ortho or para to the azo linkage, to be investigated. The influence of catalyst concentration, pH, peracetic acid concentration and dye concentration on the reaction rate and overall percentage decolourisation is investigated. The results are discussed in terms of structural features of dyes, complexation between dye and iron and the likely reaction pathway, i.e. does the peracid act as an electrophile or nucleophile?

The concept of nucleophilic / electrophilic reactions of peroxide species is further explored in the final experimental chapter (Chapter 5) where the reactivity of peroxoborate species towards an ester, *p*-nitrophenyl acetate, is investigated. Above pH 6 hydrogen peroxide in equilibrium with boric acid forms a complex system of peracid-like peroxoborate species. Several of these species, for example monoperoxoborate, have been found to be better electrophiles than hydrogen peroxide (for example in the reaction with organic sulphides), the suspicion remains that there may be some peroxide species that may also be good nucleophiles. The Chapter reports on a pH dependence study for the reaction of these species with *p*-nitrophenyl acetate.

Chapter 2. Formation of peracetic acid from acetic acid and hydrogen peroxide.

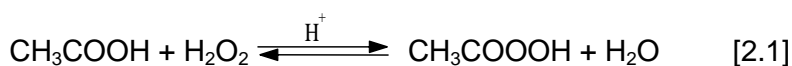
2.1. Introduction

This Chapter reports on a new method for the preparation of peracetic acid solutions from hydrogen peroxide and glacial acetic acid, but without the necessity to use sulphuric acid as a catalyst. The method gives similar peracetic acid equilibrium concentrations as the sulphuric acid catalysed method; however the reaction time is significantly longer, meaning that its application lies in situations where preparation time is not such a significant issue. The advantage of the method is that catalyst use is avoided, leading to reductions in material use. This method was used to generate the peracetic acid used in the majority of studies reported on in this thesis.

Chlorine was first used as a water disinfectant as long ago as the 1900s and was still used in the water and wastewater industries for disinfection until 1974 when Rook found several harmful disinfection by-products in chlorinated water¹⁶¹. Since then the water industry has been looking at alternative disinfectants such as hydrogen peroxide, UV, ozone and peracetic acid (PAA). PAA has similar disinfection abilities to those of chlorine and is preferred for use because it does not lead to any harmful by-products¹⁶². Also PAA is a strong oxidant with a reduction potential of 1.06v which is similar to that of traditional bleaching agents, and is used to bleach textiles and pulps¹⁶³⁻¹⁶⁶, in the epoxidation of olefins^{167, 168}, and furthermore is applied in disinfection^{169, 170}. Above all peracetic acid offers advantages such as leaving only non-toxic residues¹⁷¹, has safe decomposition products, presents no disposal problems, is easy to use, controls odours, operates over a wide temperature ranges, removes sulphides, and is effective against broad spectrum of microorganisms. Acetic acid is the end product of PAA treatment, and harmless according to the EPA¹⁷². There are no risks to the public or the environment when the active ingredient is acetic acid, which is found in all living organisms. Many people are familiar with acetic acid in its diluted form, and it is readily broken down in to carbon dioxide and water.

Various methods can be used to generate peroxyacetic acid as described in Chapter 1. For many years the two most commonly used methods for preparing peracetic acid were: (1) hydrogen peroxide with acetic acid and (2) hydrogen peroxide with acetic anhydride.

The method of preparation used in this study is described in this chapter and involves the oxidation by hydrogen peroxide of acetic acid, as in Equation (2.1).



Peracetic acid left standing for long periods of time without stabiliser will be hydrolysed to hydrogen peroxide and acetic acid. Both PAA and H_2O_2 are strong oxidizing agents and there is a risk of a decrease in activity due to self-decomposition during shipping and storage, which may be dangerous as well as reducing the amount of active ingredient. Because of this, rather than relying on the purchase of PAA, it is an attractive alternative to consider methods for the in-situ formation of this chemical. At room temperature, a typical PAA solution can lose 2% of concentration per day. Storage below 20°C in coloured, vented glass bottles minimises the heat and light decomposition reactions of PAA and avoids too much pressure in storage vessels.

As mentioned above, in addition to the reaction of hydrogen peroxide with glacial acetic acid, PAA can also be synthesised from the reaction between hydrogen peroxide and acetic anhydride as in Equation (2.2).



The reaction of acetic anhydride with hydrogen peroxide is exothermic and difficult to control, and the possible formation of diacetyl peroxide causes increased explosion hazards¹⁷³. For this reason, the reaction of acetic acid with hydrogen peroxide is commonly preferred in the preparation of PAA. This reaction is reversible and, as a result, an equilibrium mixture of reactants and products is obtained. Homogeneous acidic catalysts (e.g. sulphuric acid H_2SO_4) are usually used to facilitate the reaction to achieve equilibrium and the addition of 1% to 9% sulphuric acid is usually used^{19, 173-175} (see Equation 2.1); however we will show that its use can be avoided, providing that sufficient time is available for PAA formation.

2.1.1. Catalysed and Uncatalysed formation of peracetic acid

In this research the synthesis of peroxyacetic acid was achieved using acetic acid and hydrogen peroxide with and without sulphuric acid as an acid catalyst. The reverse reaction of peracetic acid hydrolysis was also studied.

2.2. Uncatalysed formation of peracetic acid from hydrogen peroxide and acetic acid

2.2.1. Materials

Acetic acid 100% (Analar), and hydrogen peroxide H_2O_2 (30%) were supplied by Fisher Scientific. Potassium hydrogen phthalate (KHP) $\text{COOHC}_6\text{H}_4\text{COOK}$, after drying (99.5%) and potassium iodide KI (99%) were supplied by Aldrich. Sodium thiosulphate, $\text{Na}_2\text{S}_2\text{O}_3 \cdot 5\text{H}_2\text{O}$, and ammonium heptamolybdate (AHM), $(\text{NH}_4)_6\text{Mo}_7\text{O}_{24} \cdot 4\text{H}_2\text{O}$ were supplied from BDH Chemicals Ltd England.

2.2.2. Peracetic acid solutions

Peracetic acid stock solutions were prepared by placing two ml of 1M hydrogen peroxide plus 10 ml distilled water in a 100ml volumetric flask. The flask was filled up to 100ml with glacial acetic acid and was mixed well at room temperature.

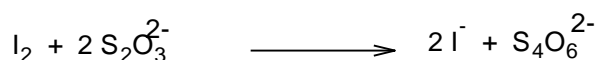
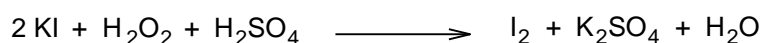
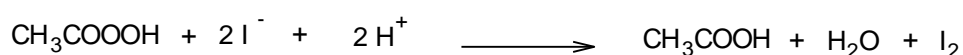
2.2.3. Procedure and methods

Peroxyacid concentrations were determined iodometrically as follows. Five ml of the sample was taken and placed in a conical flask containing 25ml KI with a concentration of $0.079 \text{ mol dm}^{-3}$ and 10ml of potassium hydrogen phthalate with a concentration of 0.24 mol dm^{-3} . Starch was added as an indicator. The reaction between iodide and peracetic acid is very fast and the liberated iodine was titrated with $0.005 \text{ mol dm}^{-3}$ sodium thiosulphate solution delivered from a 50ml burette. The titration was accurate to $\pm 0.01\text{ml}$. The titration was then continued to an end point after the addition of 1ml ammonium heptamolybdate ($3.2 \times 10^{-3} \text{ mol dm}^{-3}$), no further colour development was observed for over one minute. The volume of thiosulphate achieved after addition of ammonium heptamolybdate gave the total peroxide concentration (peracetic acid and hydrogen peroxide). The procedure was repeated over a period of 12 days until the peracetic acid had reached equilibrium.

2.2.4. Results and Discussion

The change in peracetic acid and total peroxide concentration during the reaction between acetic acid and hydrogen peroxide was determined using the procedure outlined below.

The peracetic acid concentration (C_{PAA}) was determined directly from the thiosulphate titration of iodine liberated upon mixing with potassium iodide, whereas the total peroxide concentration (C_{ox}) was determined from the initial titre plus the additional titre obtained upon the addition of ammonium heptamolybdate solution, which catalyses the very slow reaction between hydrogen peroxide and iodide. Peracetic acid and hydrogen peroxide react with potassium iodide as the reactions below and the iodine released then reacts with sodium thiosulphate.



Equation 2.3 shows the conversion of titre into concentration for both peracetic acid and total peroxide.

$$C_{PAA,ox} = (V_{\text{titr}} \times 0.005) / (V_s \times 2) \quad [2.3]$$

In Equation 2.3, V_{titr} is the volume of 0.005M sodium thiosulphate solution consumed in the titration and V_s is the volume of the sample. All values reported were the average of at least two readings.

The difference between the total peroxide concentration (C_{ox}) and peracetic acid concentrations (C_{PAA}) gives the concentration of hydrogen peroxide ($C_{H_2O_2}$), as shown in Equation (2.4).

$$C_{H_2O_2} = C_{ox} - C_{PAA} \quad [2.4]$$

Figure 2.1 shows the formation of peracetic acid, and the concentration of total peroxide, during the course of a twelve day period. The peracetic acid concentration reaches equilibrium at the end of this period, and it is also interesting to note that the total peroxide concentration remains relatively constant over the course of the reaction period, i.e. there is little or no overall decomposition of the peroxide species present.

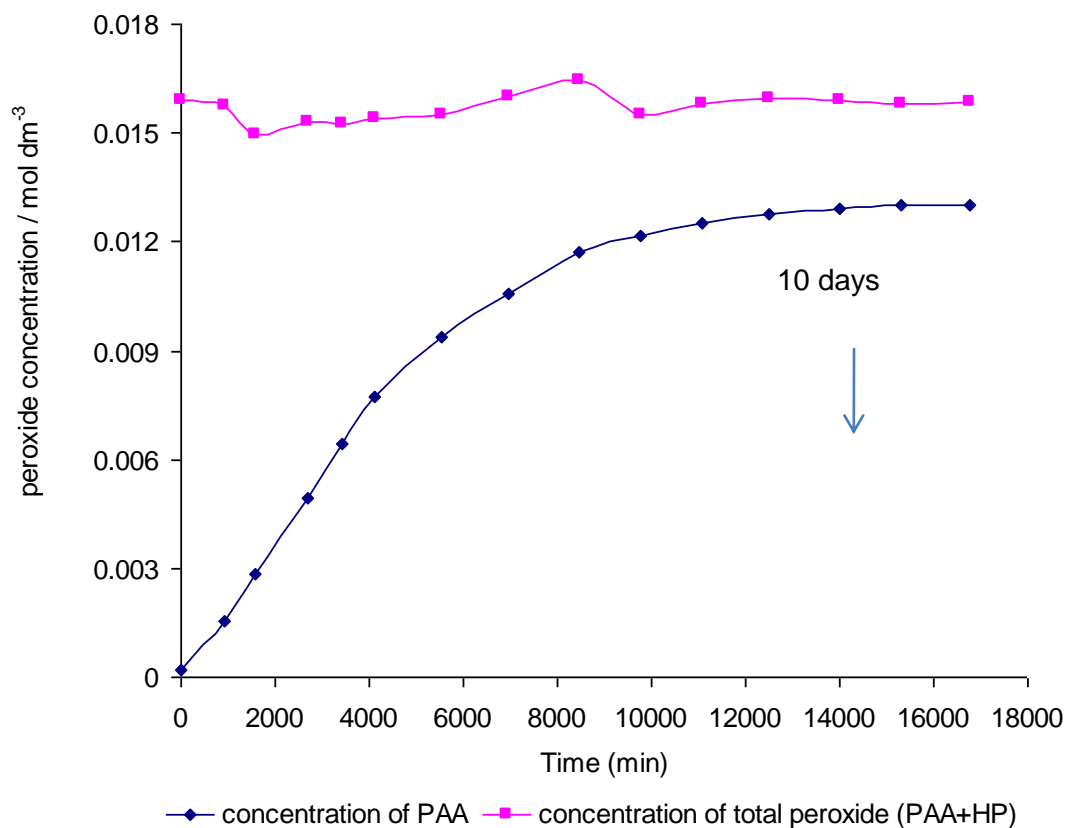


Figure 2.1: Forward formation of peracetic acid and total peroxide without sulphuric acid from hydrogen peroxide in aqueous acetic acid initial concentration 15.5 mol dm^{-3} , $[\text{H}_2\text{O}_2] = 0.02 \text{ mol dm}^{-3}$ at room temperature.

2.2.4.1. Kinetics of peracetic acid formation

The kinetics of PAA formation were obtained from a pseudo first order plot of $\ln(V_\infty - V_t)$ against time, where V_t and V_∞ are the volumes at time t and at the end of the reaction, respectively. This results in a fit with a high degree of linearity (Figure 2.2), the slope of which yields pseudo first order rate constant for the formation reaction, k_{obs} , of $3.0 \times 10^{-4} \text{ min}^{-1}$. This result agrees with that of Zhao 2007 who found that both of the forward and reverse reactions were first-order at temperatures below 323K ¹⁷⁶.

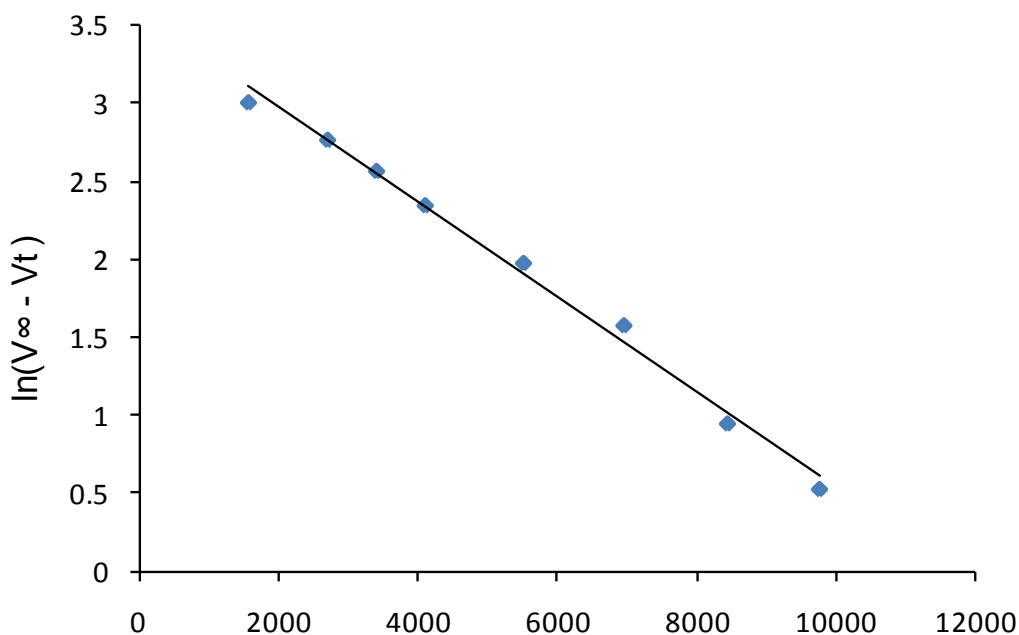
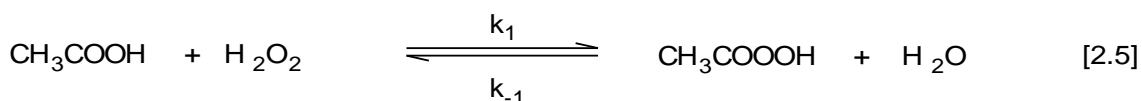


Figure 2.2:- Pseudo first order kinetic plots the data obtained from Figure 2.1

The pKa values of acetic acid and PAA at 25°C are 4.8⁴ and 8.2⁴, respectively, which means that under the conditions employed for the formation of peracetic acid in this study the dissociation of peracetic acid is negligible. Consequently, excluding any decomposition reactions (which this study has shown to be negligible), the reaction system mainly consists of two reactions, the formation and hydrolysis of PAA, as shown in Equation 2.5. Havel and Weigner⁴² have suggested that this equilibrium reaction is “impractically slow” in the absence of a strong acid catalyst, and that the uncatalysed reaction is only slightly exothermic¹⁷.



The chemical equilibrium constant (K) and the rate constant for the formation of peracetic acid from acetic acid and hydrogen peroxide have been calculated using experimentally determined values for the forward (k₁) and reverse(k₋₁) reaction rate constant, as described in the following section.

2.2.4.2. The calculation of rate constants

The rate constants can be calculated as detailed below. Firstly the respective concentrations of water and acetic acid, which both appear in Equation 2.5, must be calculated. In the reaction solution there are 12ml of water in a total of 100ml, which equates to a water concentration of $55.5 \text{ (mol dm}^{-3}) \times 12\text{ml}/100\text{ml} = 6.7 \text{ mol dm}^{-3}$.

Similarly for 88ml, of acetic acid at a density of 1.05 g cm^{-3} this gives a concentration in the reaction solution of 15.5 mol dm^{-3} .

For the equilibrium shown in the Equation 2.5, the concentration of reactants and products can be related by the following equations, in which the subscripts o and e refer to the initial and equilibrium concentrations respectively. Initial concentrations are used when the concentration can be assumed to remain constant during the course of the reaction.

$$k_1 [\text{CH}_3\text{COOH}]_0 [\text{H}_2\text{O}_2]_e = k_{-1} [\text{CH}_3\text{COOOH}]_e [\text{H}_2\text{O}]_0$$

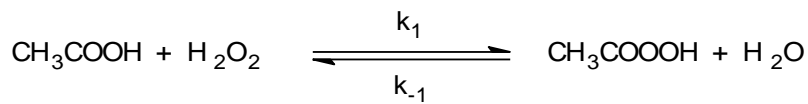
$$K_{\text{obs}} = \frac{[\text{CH}_3\text{COOOH}]_e}{[\text{H}_2\text{O}_2]_e} = \frac{k_1 [\text{CH}_3\text{COOH}]_0}{k_{-1} [\text{H}_2\text{O}]_0}$$

$$K_{\text{overall}} = \frac{[\text{CH}_3\text{COOOH}]_e [\text{H}_2\text{O}]_0}{[\text{H}_2\text{O}_2]_e [\text{CH}_3\text{COOH}]_0} = \frac{k_1}{k_{-1}}$$

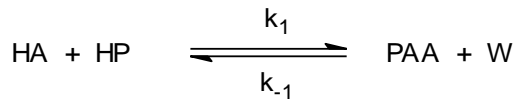
So now we can calculate the K overall from this equation:

$$K_{\text{overall}} = K_{\text{obs}} \frac{[\text{H}_2\text{O}]_0}{[\text{CH}_3\text{COOH}]_0} = \frac{k_1}{k_{-1}} \quad [2.6]$$

The second order rate constant of the reverse reaction (peracetic acid hydrolysis), k_{-1} , can be obtained as follows.



Since $\text{CH}_3\text{COOH} = \text{HA}$ and water = W are in large excess their concentration remain effectively constant in the reaction.



The experimental measurements involve concentration of the product PAA.

Hence,

$$\frac{d[\text{PAA}]}{dt} = k_1 [\text{HA}] [\text{HP}] - k_{-1} [\text{W}] [\text{PAA}]$$

Since the total peroxide concentration remains constant

$$[\text{PAA}] + [\text{HP}] = [\text{Peroxide}]_T$$

$$\frac{d[\text{PAA}]}{dt} = k_1 [\text{HA}] ([\text{Peroxide}]_T - [\text{PAA}]) - k_{-1} [\text{W}] [\text{PAA}] \quad [2.7]$$

At equilibrium $[\text{PAA}]_e = \text{constant}$

$$\frac{d[\text{PAA}]_e}{dt} = 0 = k_1 [\text{HA}] ([\text{Peroxide}]_T - [\text{PAA}]_e) - k_{-1} [\text{W}] [\text{PAA}]_e \quad [2.8]$$

Eqn [2.7] – Eqn [2.8] gives

$$\frac{d[\text{PAA}]}{dt} = (k_1 [\text{HA}] + k_{-1} [\text{W}]) ([\text{PAA}]_e - [\text{PAA}])$$

Integrate between the limits of $t = 0$ and $t = t$

$$\int_{[PAA]_o}^{[PAA]} \frac{d[PAA]}{[PAA]_e - [PAA]} = \int_0^t (k_1 [HA] + k_{-1} [W]) dt$$

$$\ln([PAA]_e - [PAA]) - \ln([PAA]_e - [PAA]_o) = -(k_1 [PAA] + k_{-1} [W]) t \quad [2.9]$$

Experimentally it is found that first order kinetics are observed with

$$\ln([PAA]_e - [PAA]_t) = -k_{obs} t \quad [2.10]$$

$$\text{Equivalent to } \ln(V_\infty - V_t) = -k_{obs} t$$

Comparing eqns (2.9) and (2.10)

$$k_{obs} = k_1 [CH_3COOH]_o + k_{-1} [H_2O]_o$$

$$k_{obs} = K_{obs} k_{-1} [H_2O]_o + k_{-1} [H_2O]_o$$

$$k_{obs} = k_{-1} [H_2O]_o (K_{obs} + 1)$$

Thus, k_{-1} can be calculated from Equation 2.11:

$$k_{-1} = \frac{k_{obs}}{(1 + K_{obs}) [H_2O]_o} \quad [2.11]$$

The second order rate constant for the formation of peracetic, k_1 , acid can similarly be obtained:

$$k_{obs} = k_1 [CH_3COOH]_o + k_{-1} [H_2O]_o$$

$$k_{obs} = k_1 [CH_3COOH]_o + \frac{k_{obs}}{1 + K_{obs}}$$

$$k_{\text{obs}} \left(1 - \frac{1}{1 + K_{\text{obs}}} \right) = k_1 [\text{CH}_3\text{COOH}]_0$$

$$k_{\text{obs}} \left(\frac{1 + K_{\text{obs}} - 1}{1 + K_{\text{obs}}} \right) = k_1 [\text{CH}_3\text{COOH}]_0$$

Thus, the equations can be expressed as below to calculate the formation of the reaction:

$$k_1 = \frac{k_{\text{obs}} K_{\text{obs}}}{(1 + K_{\text{obs}}) [\text{CH}_3\text{COOH}]_0} \quad [2.12]$$

The rate and equilibrium constants defined above have been calculated, and are shown in Table 2.1.

Table 2.1:- shows the typical rate constant for the formation of peracetic acid without added catalyst at temperature 293K

Rate / equilibrium constants	Value
$[\text{H}_2\text{O}] / \text{mol dm}^{-3}$	6.7
$[\text{CH}_3\text{COOH}]_0 / \text{mol dm}^{-3}$	15.5
K_{obs}	4.84
K_{overall}	2.105
$k_{\text{obs}} / \text{min}^{-1}$	3.0×10^{-4}
$k_1 / \text{dm}^3 \text{mol}^{-1} \text{min}^{-1}$	1.6×10^{-5}
$k_{-1} / \text{dm}^3 \text{mol}^{-1} \text{min}^{-1}$	7.66×10^{-6}

2.3. Catalysed formation of peracetic acid from hydrogen peroxide and acetic acid in the presence of 0.1 M sulphuric acid

As has already been mentioned, the formation of peracetic acid from acetic acid and hydrogen peroxide is greatly accelerated by the use of a suitable acid catalyst. D'Ans and Frey⁵² for example, aiming to prepare peracids in the pure state, used sulphuric acid to speed up what they considered to be an extremely slow reaction. Consequently in order to compare the equilibrium concentrations obtained for the uncatalysed reaction method that we have developed, the same reaction as in Section 2.2 was repeated with sulphuric acid added as a catalyst in order to speed up the reaction.

2.3.1. Materials

Sulphuric acid H_2SO_4 , Acetic acid 100% (Analar) CH_3COOH 60.05g/mol, and hydrogen peroxide H_2O_2 (30%), were supplied by Fisher Scientific. Potassium hydrogen phthalate (KHP) $\text{COOH}\text{C}_6\text{H}_4\text{COOK}$, after drying (99.5%), and potassium iodide KI (99%) were supplied by Aldrich. Sodium thiosulphate ($\text{Na}_2\text{S}_2\text{O}_3 \cdot 5\text{H}_2\text{O}$) was provided as a $0.005 \text{ mol dm}^{-3}$ solution. Ammonium heptamolybdate (AHM), $(\text{NH}_4)_6\text{Mo}_7\text{O}_{24} \cdot 4\text{H}_2\text{O}$.

2.3.2. Reaction solution

Two ml of 1 mol dm^{-3} hydrogen peroxide stock solution, plus 10 ml of a 1 mol dm^{-3} sulphuric acid solution were added to a 100ml volumetric flask and this was made up to the mark with glacial acetic acid.

2.3.3. Procedure and methods

The formation of peracetic acid is very rapid with an added catalyst such as sulphuric acid, so the same procedure in section 2.2.3 was repeated over a period of 7 hours until the peracetic acid had reached equilibrium (see Figure 2.3). The total peroxide concentration and the peracetic acid concentration were determined as described in Section 2.2.

2.3.4. Results and Discussion

2.3.4.1. Determination of kinetic constants

The experimental data for the formation of peracetic acid and total peroxide are shown in Figure 2.3. An equilibrium concentration of peracetic acid is obtained after about 400 minutes, contrasting with 17,000 minutes in the absence of sulphuric acid. As with the uncatalysed reaction, the total peroxide concentration remains relatively stable throughout the course of the reaction, indicating minimal decomposition side reactions.

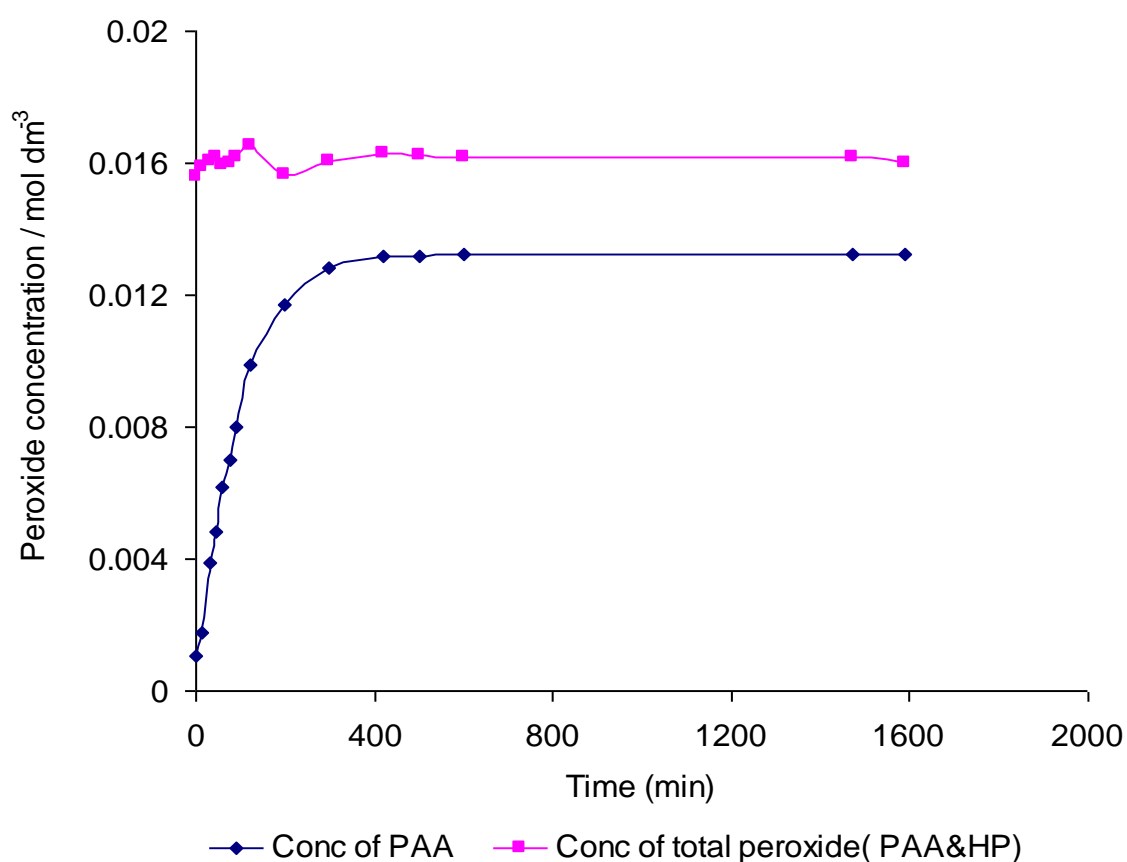
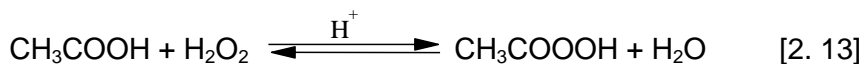


Figure 2.3:- the formation of peracetic acid and total peroxide by iodometric titration as a function of the reaction time using $0.1 \text{ mol dm}^{-3} \text{ H}_2\text{SO}_4$, as a catalyst initial concentration of $[\text{CH}_3\text{COOH}] = 15.5 \text{ mol dm}^{-3}$, $[\text{H}_2\text{O}_2] = 0.02 \text{ mol dm}^{-3}$ at room temperature.

2.3.4.2. The effect of the acidity of the media

The acid catalysed reaction can be stated as occurring according to Equation 2.13, with the hydrogen ions coming from the sulphuric acid.



As with the uncatalysed reaction, an observed pseudo first order rate constant can be calculated for the catalysed reaction by plotting $\ln(V_\infty - V_t)$ against time, where V_t and V_∞ are the volume at time t and at the end of the reaction, respectively. This data, shown in Figure 2.4, gives an excellent straight line with correlation coefficient higher than 0.99, indicating that the overall reaction is a pseudo-first-order reaction.

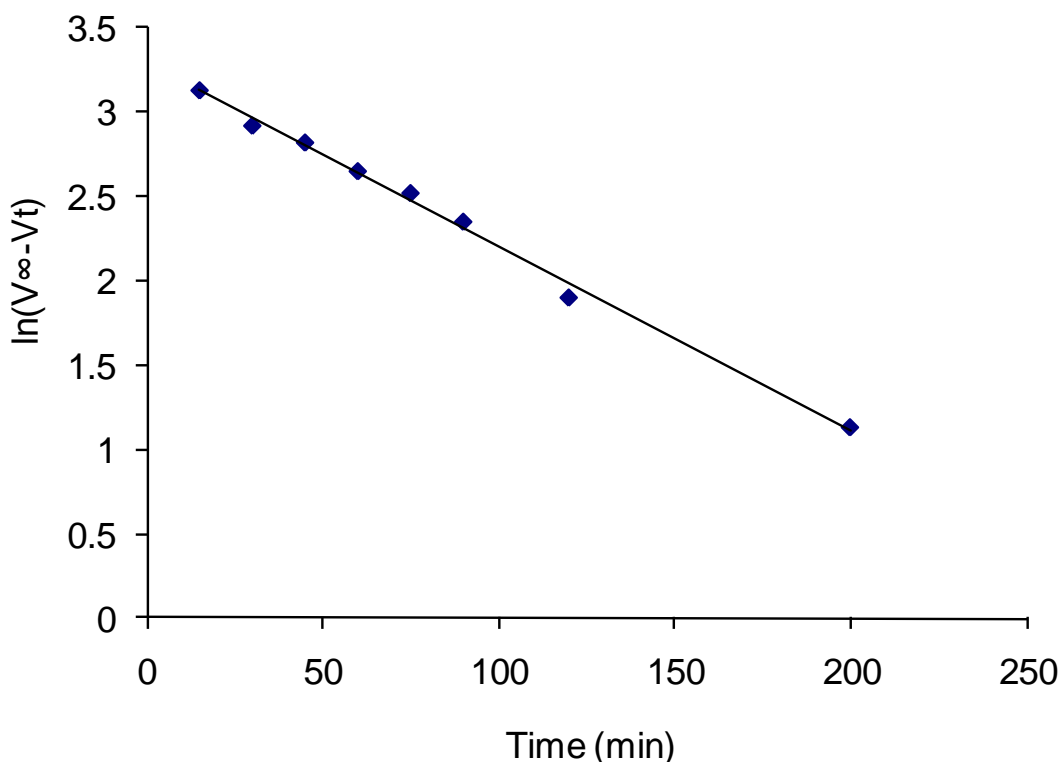


Figure 2.4:- first order kinetic plots for the data obtained from Figure 2.3.

2.3.4.3. Calculation of rate constants

According to Equation 2.13, the reaction of acetic acid with hydrogen peroxide to form peracetic acid, at equilibrium can be related by the following equation:

$$\text{At equilibrium } k_1 [\text{CH}_3\text{COOH}]_e [\text{H}_2\text{O}_2]_e = k_{-1} [\text{CH}_3\text{COOOH}]_e [\text{H}_2\text{O}]_e$$

Calculating the initial concentration of acetic acid and water as outlined in Section 2.2, and assuming the volume of hydrogen peroxide is negligible because the very small amount has been used, the rate of peracid formation can be calculated from Equations 2.6, 2.11 and 2.12. The results of the calculation are shown in Table 2.2.

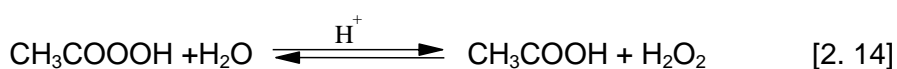
Table 2.2:- Comparison of rate and equilibrium data for the formation of peracetic acid in the presence and absence of sulphuric acid.

Parameter	No Catalyst	0.1 mol dm ⁻³ H ₂ SO ₄
[H ₂ O] / mol dm ⁻³	6.7	6.7
[CH ₃ COOH] ₀ / mol dm ⁻³	15.5	15.5
K _{obs}	4.84	4.71
K _{overall}	2.105	2.049
k _{obs} / min ⁻¹	3.0x10 ⁻⁴	1.09x10 ⁻²
k ₁ / dm ³ mol ⁻¹ min ⁻¹	1.6x10 ⁻⁵	5.83x10 ⁻⁴
k ₋₁ / dm ³ mol ⁻¹ min ⁻¹	7.6x10 ⁻⁶	2.84x10 ⁻⁴
Equilibrium concentration of PAA / mol dm ⁻³	1.32x10 ⁻²	1.32x10 ⁻²
Equilibrium concentration of H ₂ O ₂ / mol dm ⁻³	2.85x10 ⁻³	3.05x10 ⁻³

2.4. Hydrolysis of peracetic acid

As explained previously, peracetic acid can be prepared either from oxidation of acetaldehyde or the reaction of hydrogen peroxide with acetic acid. According to Equation 2.5 the reaction of peracetic acid from acetic acid and hydrogen peroxide is very slow and it can take several days.

If the reaction conditions are altered, so that we start with peracetic acid and water, and allow this reaction solution to form hydrogen peroxide and acetic acid through the process of hydrolysis then the reverse equilibrium for the formation of hydrogen peroxide can be written, as shown in Equation 2.14. This reaction is the subject of this Section.



2.4.1. Peracetic acid solutions

A peracetic acid solution was prepared by placing five ml of a 4 mol dm⁻³ hydrogen peroxide solution. The flask was filled up to 250 ml with glacial acetic acid and it was mixed very well and stored for 10 days at 298K; under these catalysed conditions, as determined in Section 2.3, an equilibrium concentration of peracetic acid will have been reached.

A series of solutions were then prepared in which peracetic acid, formed as described above, and water were mixed different concentrations of sulphuric acid in a 100ml volumetric flask.

Specifically, 2, 4, 8, 16, 24 and 32ml of 1 mol dm⁻³ sulphuric acid solution were added to 20 ml of the equilibrium peroxyacid solution in six volumetric flasks and diluted to 100ml with distilled water. The subsequent hydrolysis of peracetic acid was followed as described below.

2.4.2. Method for monitoring peracetic acid hydrolysis

The hydrolysis of peracetic acid to hydrogen peroxide and acetic acid was monitored by iodometric titration. At various intervals, five ml of the sample was poured into a conical flask containing 25ml potassium iodide (0.079 mol dm⁻³) and 10ml potassium

hydrogen phthalate (0.24 mol dm^{-3}). One drop of 1 % (w/v) iodine starch solution was added and the liberated iodine titrated with sodium thiosulphate.

2.4.3. Results

Figure 2.5 shows the hydrolysis of peracetic acid at varying sulphuric acid concentrations. The results are expressed as volume of thiosulphate titrated. Total peroxide concentration was not monitored for these runs.

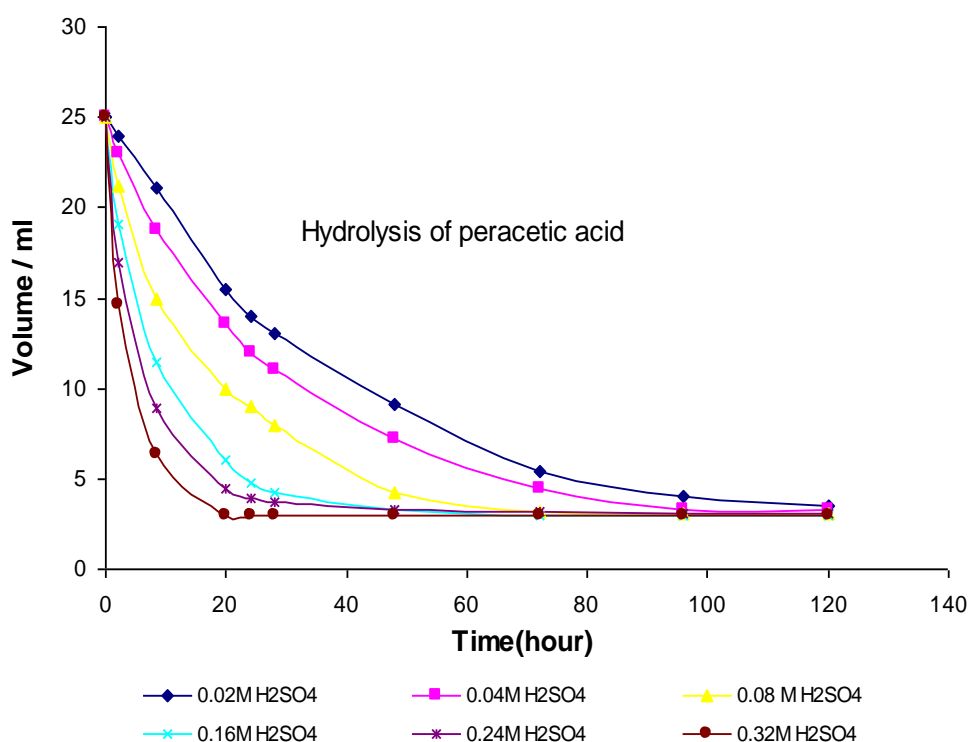
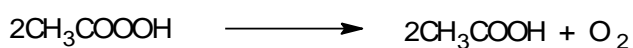


Figure 2.5:- Hydrolysis of peracetic acid at temperature 298K with different concentrations of sulphuric acid as catalyst, 0.02 mol dm^{-3} , 0.04 mol dm^{-3} , 0.08 mol dm^{-3} , 0.16 mol dm^{-3} , 0.24 mol dm^{-3} , 0.32 mol dm^{-3} .

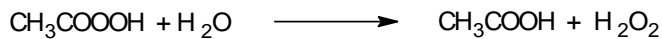
2.4.4. Determination of kinetic constants

Firstly, in looking at the decomposition of peracetic acid, there are three important reactions that should be considered, as detailed below.¹⁷⁷

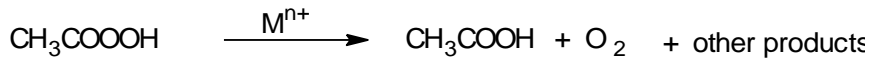
1. Spontaneous decomposition to acetic acid and oxygen:



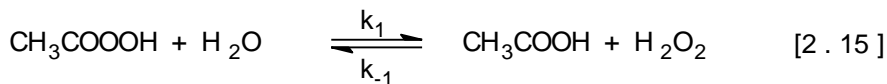
2. Hydrolysis to acetic acid and hydrogen peroxide:



3. Transition metal ions catalyzed decomposition:



Koubek and Edwards¹⁷⁸ have found that during the hydrolysis of peroxyacetic acid no gaseous products were observed, and we observed the same so it is unlikely that reactions 1 and 3 will be significant. Consequently only the forward and reverse reactions should be considered as shown in Equation 2.15 below.



At equilibrium, the concentrations of reactants and products can be related by the following equation:

$$\text{At equilibrium } k_1 [\text{H}_2\text{O}]_0 [\text{CH}_3\text{COOOH}]_e = k_{-1} [\text{H}_2\text{O}_2]_e [\text{CH}_3\text{COOH}]_0 \quad [2.16]$$

$$k_{\text{obs}} = \frac{[\text{H}_2\text{O}_2]_e}{[\text{CH}_3\text{COOOH}]_e} = \frac{k_1 [\text{H}_2\text{O}]_0}{k_{-1} [\text{CH}_3\text{COOH}]_0} \quad [2.17]$$

$$K_{\text{overall}} = \frac{[\text{H}_2\text{O}_2]_e}{[\text{CH}_3\text{COOOH}]_e} \frac{[\text{CH}_3\text{COOH}]_0}{[\text{H}_2\text{O}]_0} = \frac{k_1}{k_{-1}} \quad [2.18]$$

So now we can calculate the K overall from this equation:

$$K_{\text{overall}} = k_{\text{obs}} \frac{[\text{CH}_3\text{COOH}]_0}{[\text{H}_2\text{O}]_0} = \frac{k_1}{k_{-1}} \quad [2.19]$$

The rate of hydrolysis of peracetic acid can be obtained as:

$$k_{\text{obs}} = k_1 [\text{H}_2\text{O}]_0 - k_{-1} [\text{CH}_3\text{COOH}]_0 \quad [2.20]$$

$$k_{\text{obs}} = K_{\text{obs}} k_{-1} [\text{CH}_3\text{COOH}]_0 + k_{-1} [\text{CH}_3\text{COOH}]_0 \quad [2.21]$$

$$k_{\text{obs}} = k_{-1} [\text{CH}_3\text{COOH}]_0 (K_{\text{obs}} + 1) \quad [2.22]$$

Thus, the equations can be expressed as below to calculate the hydrolysis of the reaction:

$$k_{-1} = \frac{k_{\text{obs}}}{(1 + K_{\text{obs}})[\text{CH}_3\text{COOH}]_0} \quad [2.23]$$

The rate of formation of peracetic acid can similarly be obtained:

$$k_{\text{obs}} = k_1 [\text{H}_2\text{O}]_0 + k_{-1} [\text{CH}_3\text{COOH}]_0 \quad [2.24]$$

$$k_{\text{obs}} = k_1 [\text{H}_2\text{O}]_0 + \frac{k_{\text{obs}}}{(1 + K_{\text{obs}})} \quad [2.25]$$

$$k_{\text{obs}} \left(1 - \frac{1}{1 + K_{\text{obs}}}\right) = k_1 [\text{H}_2\text{O}]_0 \quad [2.26]$$

$$k_{\text{obs}} \left(\frac{K_{\text{obs}}}{1 + K_{\text{obs}}}\right) = k_1 [\text{H}_2\text{O}]_0 \quad [2.27]$$

Thus, the equations can be expressed as below to calculate the formation of the reaction:

$$k_1 = \frac{k_{\text{obs}} K_{\text{obs}}}{(1 + K_{\text{obs}}) [\text{H}_2\text{O}]_0} \quad [2.28]$$

Thus, from Equations 2.19, 2.23 and 2.28 the rate and the equilibrium constant have been calculated and these are shown in Table 2.3 at each different sulphuric acid concentration. From Table 2.3, we can see that the rate of hydrolysis of peracetic acid increases with increasing concentrations of sulphuric acid; the equilibrium constants are also found to increase. Table 2.3 also summarises the results at different concentrations of sulphuric acid.

Table 2.3:- Conditions on the rate constants for the kinetics of PAA at 25°C

$[H^+]_0 / \text{mol dm}^{-3}$	K_{obs}	K_{overall}	$k_1 (\text{dm}^3 \text{mol}^{-1} \text{min}^{-1})$	$k_{-1} (\text{dm}^3 \text{mol}^{-1} \text{min}^{-1})$
0.04	7.35	0.450	7.88×10^{-6}	1.59×10^{-5}
0.08	7.85	0.530	9.28×10^{-6}	1.75×10^{-5}
0.16	8.42	0.566	1.34×10^{-5}	2.37×10^{-5}
0.32	8.74	0.574	2.66×10^{-5}	4.53×10^{-5}
0.48	9.43	0.634	3.77×10^{-5}	5.94×10^{-5}
0.64	9.82	0.660	4.87×10^{-5}	7.38×10^{-5}

Plots of k_1 and k_{-1} versus sulphuric acid concentration are shown in Figures 2.6 and 2.7 respectively. A linear relationship observed between k_1 and $[H^+]$, and k_{-1} and $[H^+]$ concentration, which shows that the formation and hydrolysis of peracetic acid are both first-order reactions with respect to sulphuric acid concentration.

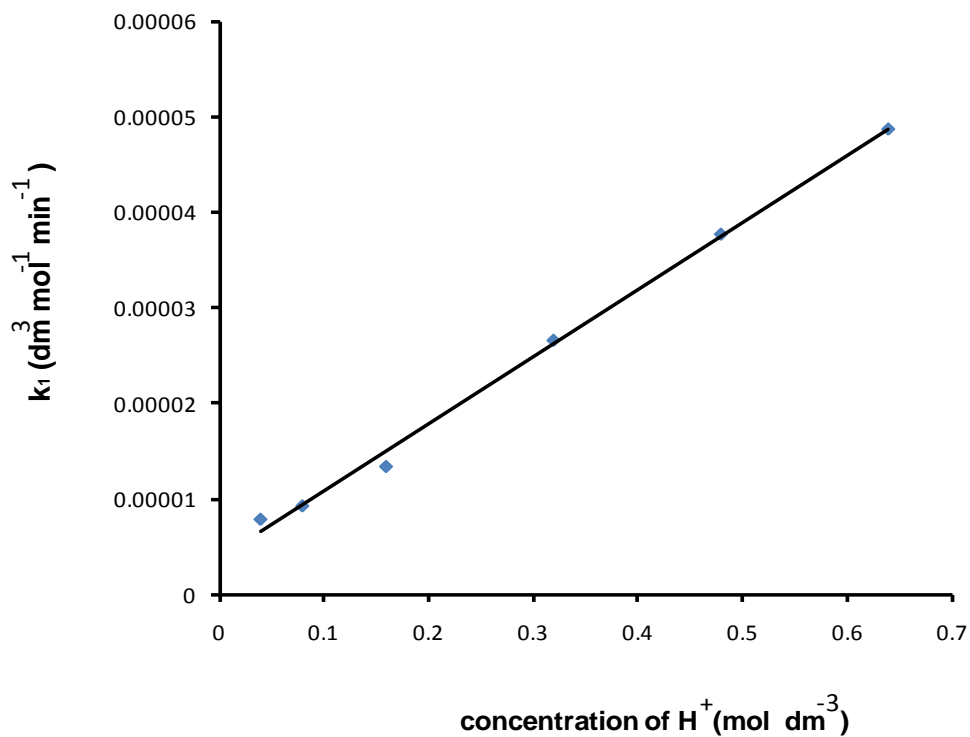


Figure 2.6:- linear plots of k_1 vs. $[H^+]$ at temperature 298K.

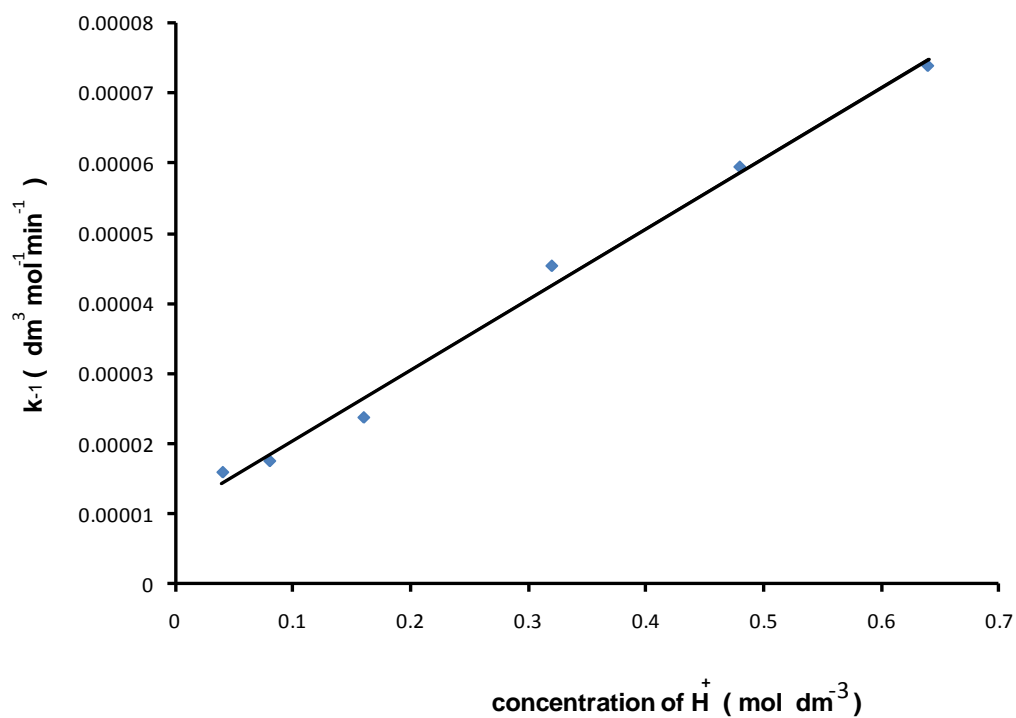


Figure 2.7:- linear plots of k_{-1} vs. $[H^+]$ at temperature 298K.

2.5. Discussion

2.5.1. Catalysed and uncatalysed formation of peracetic acid

The main objective of the work described in this chapter was to develop an alternative method for the formation of peracetic acid from glacial acetic acid and hydrogen peroxide that does not rely on the use of an acid catalyst. Such an approach would lead to a reduction in (hazardous) material use and have the additional advantage of requiring less neutralising base when used at higher pHs. Our studies have shown that a non-catalysed route is feasible and, indeed, this method has been used for many of the subsequent studies in this thesis that have required the use of peracetic acid.

As was shown in Table 2.2 the overall equilibrium constant, K_{overall} , for peracetic acid formation in the absence of sulphuric acid (2.105), is nearly the same as in the presence (2.049) and, therefore, the equilibrium concentrations of the formed peracetic acid and the residual hydrogen peroxide are virtually identical. Additionally there is no overall loss of total peroxide over the course of runs conducted either in the presence or absence of acid catalyst. The only significant difference between the two methods is that the time taken to reach equilibrium in the absence of sulphuric acid (17,000 minutes) is nearly forty times longer than in the presence of catalyst. This is in agreement with the results of Sawaki and Ogata⁴⁴ who have investigated the effect of sulphuric acid concentration on the rate of reaction as one of their experimental variables. Nevertheless, if sufficient preparation time is available in advance of experimental work then this non-catalysed method should be considered as a viable alternative for the production of peracetic acid.

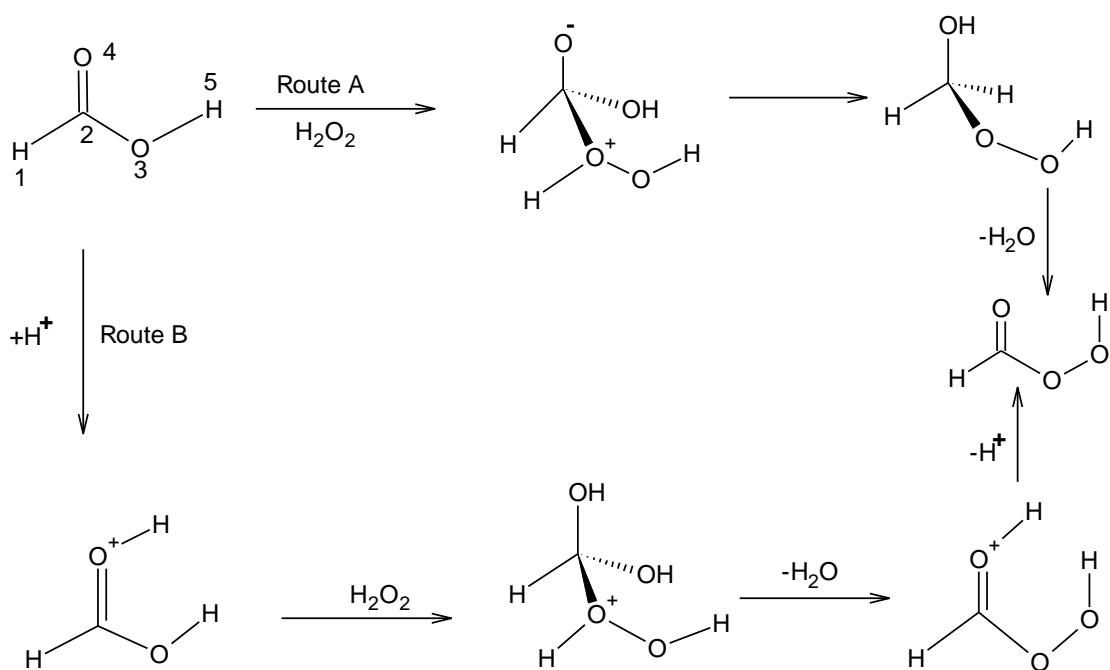
As well as investigating the feasibility of producing peracetic acid via a non-catalysed method, the experimental work in this Chapter also allowed us to investigate the kinetics and equilibria of the forward and reverse reactions for peracetic acid formation and hydrolysis, both in the presence and absence of sulphuric acid catalyst, and to make comparisons with literature values. These aspects of the study are discussed in the following sections.

2.5.2. Reaction mechanism

The mechanism for the forward and reverse reactions of acetic acid with hydrogen peroxide to produce peracetic acid has been established for many years through the isotope labelling studies of Bunton and kinetic studies carried out by Sawaki and Ogata⁴⁴). Bunton showed that the mechanism of peracid hydrolysis is similar to the

mechanism of ester hydrolysis³⁵. Using the oxygen isotope labelled $\text{CH}_3\text{C}^{18}\text{OOH}$ it was found that the reactions for the formation and hydrolysis of peracetic acid did not involve the dissociation of the O-O bond in initial hydrogen peroxide, therefore implying the formation of a tetrahedral intermediate as part of the reaction mechanism.

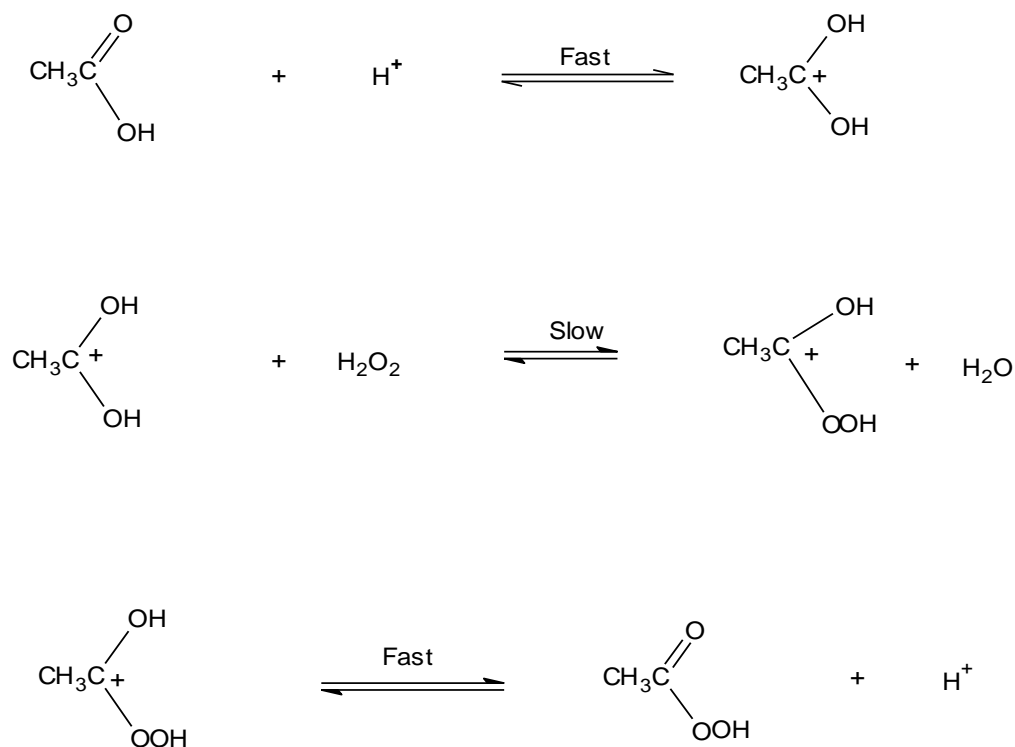
Rubio et al¹⁷⁹, using the analogous reaction of performic acid has proposed two different routes for the formation of peroxyacids that involve a tetrahedral intermediate. The first route involves formation of a tetrahedral intermediate by addition of hydrogen peroxide to the carbonyl carbon then loss of water molecule to form performic acid. In the second route, the carbonyl carbon is activated in the acid medium, with addition of hydrogen peroxide to form the tetrahedral intermediate from which the performic acid is then formed via the stepwise loss of water and a proton. The fact that acid catalysis is observed, both in the present study and in the literature, indicates that the route involving initial protonation of the performic acid is preferred.



Scheme 2.1: Reaction mechanisms for the formation of the performic acid¹⁷⁹

Different researchers have drawn various conclusions concerning the rate determining step for this reaction. Some suggest that for the forward reaction it is elimination, whilst others suggest that it is protonation of peracetic acid. Sawaki and Ogata⁴⁴ found, like us, that the equilibrium constant increases with increasing sulphuric acid concentration and explained this in terms of the elimination of free water from the reaction system by protonation. They concluded that the rate determining step was the reaction between

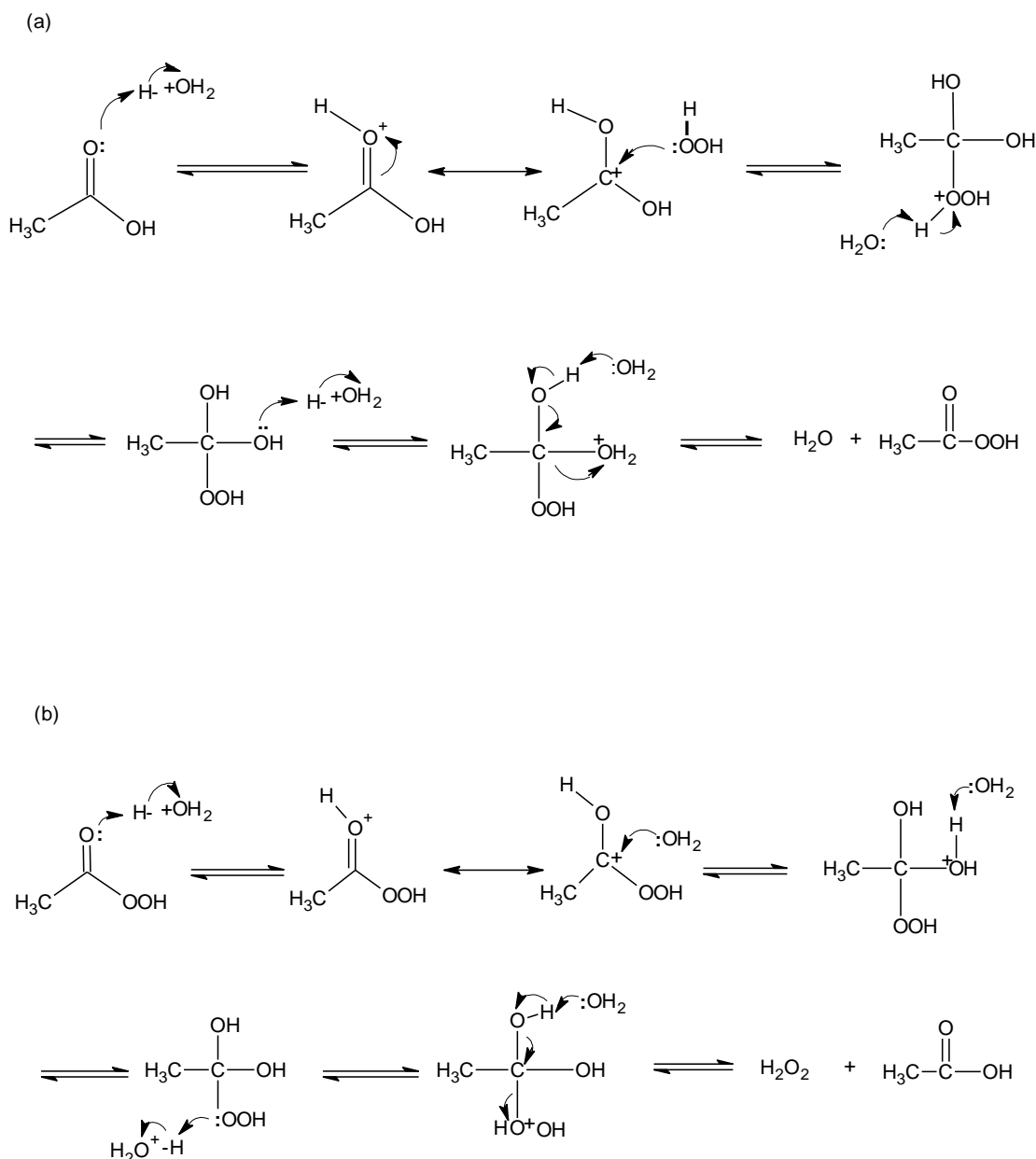
the activated carbonyl with hydrogen peroxide in the forward reaction, and between the activated carbonyl with water in the reverse reaction as in Scheme 2.2 below.



Scheme 2.2 : Reaction mechanism for the acid catalysed formation of peracetic acid

Much kinetic evidence has been produced in the literature to support this proposed reaction mechanism^{175, 180-182} and in 2007 Zhao *et al* produced a more detailed scheme for both the forward and reverse reactions, as shown below in Scheme 2.3¹⁷⁶.

In the following two sections we discuss our own results in the context of this proposed reaction mechanism.



Scheme 2.3: Reaction mechanisms of PAA synthesis and hydrolysis with acid-catalysis: (a) PAA synthesis; (b) PAA hydrolysis¹⁷⁶

2.5.3. Effect of acetic acid concentration.

The 'overall' equilibrium constant for the reaction of peracetic acid with hydrogen peroxide, K_{overall} , can be determined by either studying the formation of peracetic acid from glacial acetic acid and hydrogen peroxide, or from the hydrolysis of peracetic acid to acetic acid and hydrogen peroxide. We have investigated both processes as part of this study, both in the absence and presence of sulphuric acid catalyst. For the formation of peracetic acid, the reaction PAA is usually carried out in glacial acetic acid in

order to obtain the highest yield possible, whereas the hydrolysis of peracetic acid is best carried out in dilute aqueous solution. We therefore have a situation where the equilibrium and kinetics of this reaction have been studied under two very different solvent systems; this has important implications for the nature of the catalytic acid species, if present.

In dilute aqueous solution, as used to study the hydrolysis of peracetic acid, the protons from the sulphuric acid catalyst will be solvated in the form of H_3O^+ . However for the studies looking at the formation of peracetic acid in 88% glacial acetic acid, these protons will be less solvated, and may combine to form stronger acids than H_3O^+ for example $\text{CH}_3\text{COOH}_2^+$ and possibly H_3SO_4^+ depending on the concentration of sulphuric acid present. To account for these solvent effects, the Hammett acidity function, H_0 , is often used instead of the simple acid concentration⁴⁴; this parameter gives a measure of the equivalent protonating ability of a solvent and is determined spectrophotometrically using *o*- and *p*-nitroanilines as indicators (H_0 is a log quantity, analogous to pH and can be converted to calculate the equivalent concentration of H_3O^+ that would give the same protonating ability – often these are impossible concentrations).

The effects of the different solvents are clearly seen in the present study where the rate constant for the formation of peracetic acid in the presence of 0.1 mol dm^{-3} sulphuric acid in approximately 88% volume acetic acid ($5.83 \times 10^{-4} \text{ mol}^{-1} \text{ min}^{-1}$, see Table 2.2) is almost 20-fold higher than the corresponding value ($3.05 \times 10^{-5} \text{ mol}^{-1} \text{ min}^{-1}$, interpolated from Figure 2.7) determined from the study of the hydrolysis of peracetic acid in aqueous solution. It is important to note here, as defined in the respective set of equations in Sections 2.2.4 and 2.4.4, that for runs conducted in 88% peracetic acid, k_1 represents the rate constant for the formation of peracetic acid, whereas for runs conducted on peracetic acid hydrolysis in aqueous solution, the corresponding parameter for the formation of peracetic acid is denoted by $k_{1..}$.

This observation supports the proposed scheme in Section 2.5.2 in which for both the forward and reverse reaction there is an initial rapid protonation of the carbonyl carbon of the acetic acid (or peracetic acid for the reverse reaction) followed by a rate determining attack of the hydrogen peroxide (or water for the reverse reaction) at the carbonyl carbon. The $\text{CH}_3\text{COOH}_2^+$ moiety mentioned above, which will be formed when high concentrations of acetic acid are present, is in fact the same activated species that forms in the initial pre-equilibrium, as specified in Schemes 2.2 and 2.3. Thus in concentrated acetic acid this species already exists in high concentrations, whereas in

aqueous solution its formation is dependent on protonation of the acetic acid by H_3O^+ ; clearly the latter case will result in a much lower $\text{CH}_3\text{COOH}_2^+$ concentration with which to react with hydrogen peroxide in the rate determining step, hence the significant difference in rates.

In Sawaki and Ogata's study of the effect of volume % of acetic acid on the rate of formation of peracetic acid, k_1 , in the presence of 0.2M sulphuric acid, the rate was found to increase almost exponentially on going from 40 to 90%(v/v) acetic acid, again supporting the proposed mechanisms in Schemes 2.2 and 2.3¹⁷⁶. When the determined H_0 value was plotted against the log of the rate a linear relationship was obtained. The authors did not use a set of experimental conditions corresponding to our own study, nevertheless at 90% (v/v) and correcting for the two-fold higher sulphuric acid concentration, they obtained a k_1 value of $8.6 \times 10^{-4} \text{ mol}^{-1} \text{ min}^{-1}$ which is entirely consistent with our own value of $5.83 \times 10^{-4} \text{ mol}^{-1} \text{ min}^{-1}$ at 88% (v/v) acetic acid.

Turning to the equilibrium constant, K_{overall} , Table 2.4 compares values obtained for the formation of peracetic acid in this work (catalysed, non-catalysed, in concentrated acetic acid and in dilute solution) with those from the literature, obtained under a variety of different conditions. Sawaki and Ogata carried out the definitive study in this area, investigating the effect of both sulphuric acid and acetic acid concentration on the equilibrium constant⁴⁴. The first fifteen entries in Table 2.4 show the trends determined by these authors: with constant acetic acid concentration and increasing sulphuric acid concentration K_{overall} increases gradually up to 1.0M sulphuric acid, but then increases markedly. It is likely that in strong acetic acid, with increasing sulphuric acid concentrations there is elimination of free water from the reaction system by protonation, thus reducing the extent of the hydrolysis reaction. A plot of $\text{Log } K_{\text{overall}}$ against the Hammett acidity function, H_0 , gives a linear dependence. When increasing the acetic acid concentration whilst maintaining the sulphuric acid concentration constant, K_{overall} also increases, though this is to be expected from a consideration of the respective equilibria. The values determined by us at high acetic acid concentration are a little low compared to those determined by Sawaki and Ogata at similar concentrations⁴⁴, though compare favourably to that determined by Dul'neva and Moskvin¹⁷⁵.

For the K_{overall} values obtained from the hydrolysis reaction (entries 20 to 25 in Table 2.4) the value actually decreases with increasing sulphuric acid concentration. It should be noted that these values, have been converted from those shown in Table 2.3, which refer to the hydrolysis reaction, and therefore need to be inverted. It is not clear why

this trend should be observed, though the implication is that the hydrolysis rate is preferentially accelerated over that for the formation.

Table 2.4:- Comparison of equilibrium constants for peracetic acid formation at 293K

Entry	[CH ₃ COOH] / mol dm ⁻³	[H ₂ SO ₄] / mol dm ⁻³	K _{overall}	Reference
1	13.9	0.1	2.71	Ref ⁴⁴
2	"	0.2	2.87	Ref ⁴⁴
3	"	0.4	3.22	Ref ⁴⁴
4	"	0.6	3.53	Ref ⁴⁴
5	"	0.8	3.94	Ref ⁴⁴
6	"	1.0	4.52	Ref ⁴⁴
7	"	1.2	5.15	Ref ⁴⁴
8	"	1.5	6.02	Ref ⁴⁴
9	"	2.0	7.6	Ref ⁴⁴
10	"	3.0	12.81	Ref ⁴⁴
11	6.96	0.2	2.08	Ref ⁴⁴
12	10.45	"	2.56	Ref ⁴⁴
13	12.19	"	2.91	Ref ⁴⁴
14	13.93	"	3.05	Ref ⁴⁴
15	15.74	"	3.55	Ref ⁴⁴
16	1.329	0	0.97	Ref ¹⁶⁸
17	14.5	0.057	2.1	Ref ¹⁷⁵
18	15.4	0	2.1	This work
19	"	0.1	2.04	This work
20	3.08	0.02	2.41	This work
21	"	0.04	1.89	This work
22	"	0.08	1.77	This work
23	"	0.16	1.7	This work
24	"	0.24	1.58	This work
25	"	0.32	1.52	This work

2.5.4. Acid-base catalysis.

It is clear from both our results and those from the literature, particularly from Sawaki and Ogata's study⁴⁴, that the forward and reverse reactions are catalysed by the presence of added acid. Literature studies, for example Schemes 2.2 and 2.3, favour a mechanism by which there is a rapid protonation of acetic acid followed by rate limiting attack of the hydrogen peroxide. An analogous situation exists for the reverse reaction. In Figures 2.6 and 2.7 we show a linear relationship between [H⁺] and both k₁ and k₋₁

(note these refer to hydrolysis and formation of peracetic acid respectively, as defined in Section 2.4.4).

Such a relationship could be expected for both specific acid catalysis, in which there is rapid protonation of the substrate by H_3O^+ followed by rate limiting attack of the hydrogen peroxide, or for general acid catalysis where proton transfer is rate limiting. In the latter case it is a species other than H_3O^+ that is responsible for the protonation. It is possible to distinguish between the two forms of catalysis by varying the buffer concentration (if in a buffered system): for general acid catalysis the rate will show a dependence on buffer concentration at a constant pH whereas for specific acid catalysis the rate is only dependent on H_3O^+ . For our work it is impossible to make this distinction since at the pHs that we have used, any catalytic contributions from other species will be negligible compared to that from H_3O^+ . Nevertheless, literature evidence strongly indicates that specific acid catalysis is involved for these reactions.

2.6. General conclusion

The formation of peracetic acid from acetic acid and hydrogen peroxide has been studied kinetically both in the presence and absence of sulphuric acid, which acts as a catalyst for this reaction. The reaction is slow in the absence of sulphuric acid, taking about 12 days to achieve equilibrium, compared to only 7 hours for the sulphuric acid catalysed reaction.

Notwithstanding the slow time to reach equilibrium, our study has shown that if time is not a factor in producing the peracetic acid, then there are many advantages of not using a catalyst. The yield itself is not affected by employing a much longer equilibrium time (we have shown almost identical equilibrium constants of 2.04 and 2.1 for catalysed and uncatalysed respectively), and there is no overall loss of peroxide over the 12 days. The main advantage of not using sulphuric acid is that there is a reduced requirement for neutralisation once the peracetic acid is formed (which also reverses the reaction) and that the requirement to use an environmentally hazardous material has been eliminated, in line with current industry efforts.

Our studies have shown that the rate of hydrolysis of peracetic acid increases with increasing concentrations of sulphuric acid as catalyst. The hydrolysis of peracetic acid is first order with respect to peracetic acid concentration, water concentration and H^+

concentration, and linear relationships were found between the observed rate constants and H^+ concentration at 298K.

Chapter 3. Dye Bleaching Studies

3.1. Introduction

The oxidation of organic compounds is carried out by highly reactive hydroxyl radical species¹⁸³ produced during the reaction between hydrogen peroxide and ferrous ions. Fenton's reagent belongs to the overall class of Advanced Oxidation Processes (AOPs) and may hold interesting possibilities for the treatment of dye pollution in waste water.

Iron(II) is not the only metal capable of reacting with hydrogen peroxide; there are many other transition metals^{184, 185} that can react with hydrogen peroxide such as Cu, Ag and Fe(III) or transition metal complexes¹⁸⁶. The fact that the iron (II) or iron(III) is the sole metal used for the waste treatment is understandable because it is one of the safest transition metals from a health and safety and environmental point of view. The reaction between iron (III) and hydrogen peroxide is called a Fenton-*like* reaction. The Fenton reaction and the Fenton-like reaction can occur simultaneously in the reaction medium.

As mentioned already, iron(II) is not the only metal species able to react with hydrogen peroxide to oxidise organic compounds. In this chapter the effectiveness of a range of other transition metals such as Cu, Mn, Ag and Fe(III) in generating hydroxyl radicals from hydrogen peroxide will be investigated.

In addition, bleaching reactions of peracetic acid, which can be generated from hydrogen peroxide, will also be investigated, both in the presence and absence of Fe(III), Cu, Mn and Ag. Bleaching has been defined earlier in Chapter 1 as the structural modification of a coloured substance to give a colourless or less intensely coloured product.

This chapter will focus on the bleaching by peracetic acid and hydrogen peroxide of 18 different dyes in aqueous solution; these dyes include eight monoazo dyes, two diazo, four triarylmethane, one quinoline, one xanthene, one indigoid and one anthraquinone.

3.2. Experimental work

3.2.1. Materials

Hydrogen peroxide, H_2O_2 (Fisher, 30% aqueous solution), and acetic acid (Fisher, Anal reagent Grade) were used without further purification, ferric nitrate nonohydrate, $\text{Fe}(\text{NO}_3)_3 \cdot 9\text{H}_2\text{O}$, ammonium iron(II) sulphate, $(\text{NH}_4)_2\text{SO}_4 \cdot \text{FeSO}_4 \cdot 6\text{H}_2\text{O}$, cupric sulphate, $\text{CuSO}_4 \cdot 5\text{H}_2\text{O}$, silver sulphate, Ag_2SO_4 , manganese sulphate, $\text{MnSO}_4 \cdot 4\text{H}_2\text{O}$, (BDH, Chemicals Ltd, Poole, England) were used without further purification. Potassium hydrogen phthalate, $\text{COOHC}_6\text{H}_4\text{COOK}$, potassium iodide, KI, sodium thiosulphate $\text{Na}_2\text{S}_2\text{O}_3 \cdot 5\text{H}_2\text{O}$, and ammonium heptamolybdate (AHM), $(\text{NH}_4)_6 \text{Mo}_7 \text{O}_{24} \cdot 4\text{H}_2\text{O}$, were obtained from BDH Chemicals Ltd, England.

3.2.2. Dyestuffs

The dyes used for the bleaching studies described in this work are listed in Table 3.1; they were obtained from Pointing Limited, except amaranth from BDH chemicals Ltd Poole England, acid green 25 from Acros organics and Malachite green obtained from Aldrich. A list of their common names and their structures is shown in Table 3.3.

Table 3.1: Dyes used in degradation studies.

Commercial Dye	Colour Index Classification	Dye Class
Sunset Yellow Supra	C.I Yellow 3	Monoazo
Amaranth Supra	C.I Red 9	Monoazo
Carmosine Supra	C.I Red 3	Monoazo
Red 2G Supra	C.I Red 10	Monoazo
Tartrazine Supra	C.I Yellow 4	Monoazo
Ponceau 4R Supra	C.I Red 7	Monoazo
Orange I	C.I acid orange 20	Monoazo
Orange II	C.I acid orange 7	Monoazo
Black PN Extra	C.I Black 1	Diazo
Chocolate Brown HT Extra	C.I Brown 3	Diazo
Green S Supra	C.I Green 4	Triarylmethane
Patent Blue V Supra	C.I Blue 5	Triarylmethane
Brilliant Blue Supra	C.I Blue 2	Triarylmethane
Malachite green	C.I Basic green 4	Triphenylmethane
Quinoline Yellow Extra	C.I Yellow 13	Quinoline
Erythrosine Supra	C.I Red 14	Xanthene
Indigo Carmine Supra	C.I Blue 1	Indigoid
Acid green 25	C.I acid a green 25	anthraquinone

3.2.3. Preparation of Solutions

3.2.3.1. Preparation of Peroxide Solutions

The aim of this work was to compare the reactions of both peracetic acid and hydrogen peroxide under the same conditions. The peracetic acid was generated from the equilibrium obtained from mixing hydrogen peroxide with a large excess of glacial acetic acid; this equilibrium takes ten days to establish, as described in Chapter 2. In order to obtain comparable conditions for the hydrogen peroxide reactions, the same hydrogen peroxide / glacial acetic acid solution was used, except that it was taken immediately after mixing, so that there was negligible peracetic acid present.

3.2.3.2. Analytical solutions

Potassium hydrogen phthalate (KHP) and potassium iodide solutions were prepared from Analar grade reagents and distilled water at concentrations of 0.24 mol dm^{-3} and $0.079 \text{ mol dm}^{-3}$ respectively. Stock solutions of metal salts were made by dissolving appropriate weights in 50mls distilled water to give concentrations of 0.02M. potassium hydrogen phthalate provides a suitable low pH for the oxidation of iodide to take place, whilst not too low so that oxidation of iodide by dissolved oxygen takes place.

3.2.3.3. Dye solutions

Stock solutions of dyes (approximately $1 \times 10^{-3} \text{ mol dm}^{-3}$) were made up in distilled water in 100 ml volumetric flask; working concentrations of $5 \times 10^{-5} \text{ mol dm}^{-3}$ were prepared by 20-fold volumetric dilution.

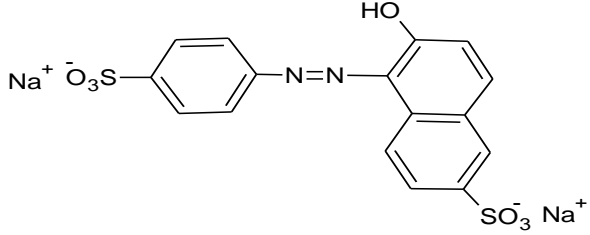
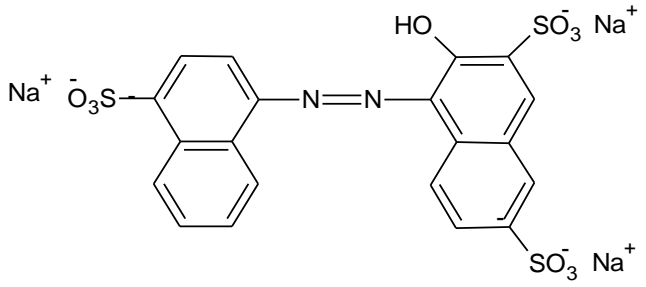
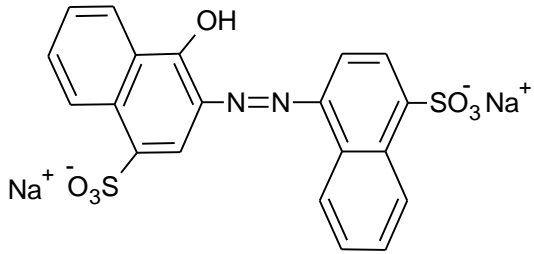
3.2.4. Spectrophotometric Measurements

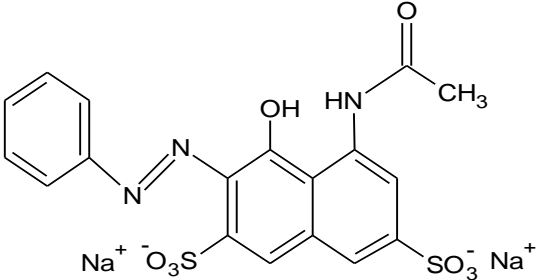
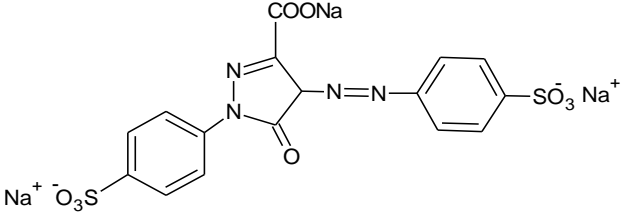
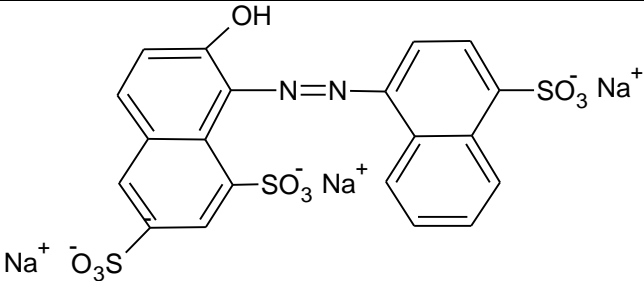
The various reactions were followed at the λ_{max} wavelength of each dye as indicated in Table 3.2. Kinetic studies were carried out in 1cm path length cuvettes using a Pharmacia Biotech Ultrospec 2000 spectrophotometer, maintained at $25^\circ\text{C} \pm 0.1^\circ\text{C}$ by a circulation of water from a thermostatically controlled bath. Typically the runs were carried out by mixing 0.7ml of dye solution with 2.1ml of metal ion solution. 0.7ml of the appropriate peroxide solution was added to start the reaction. The measurements of the initial rate of absorbance decrease of each dye were recorded for 10 minutes.

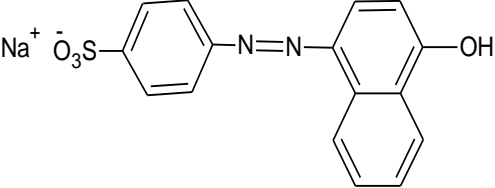
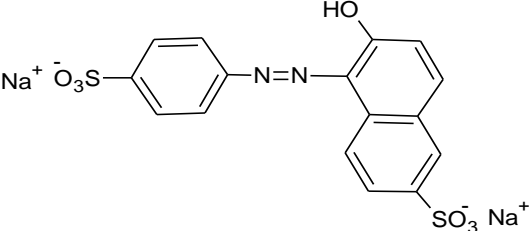
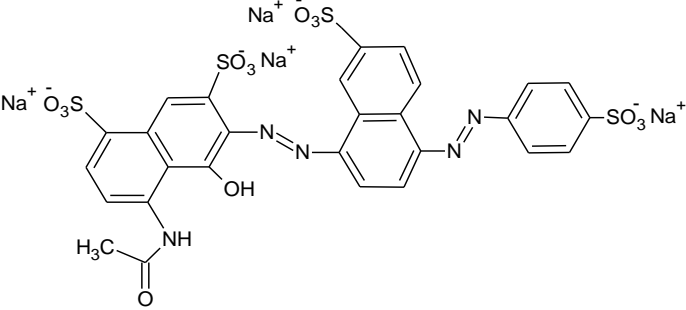
Table 3.2: λ_{\max} values of dyes used

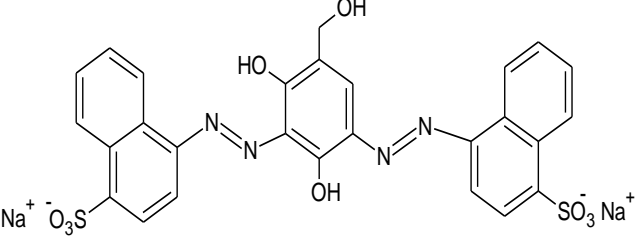
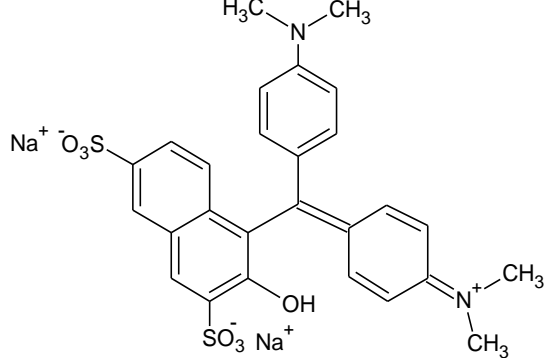
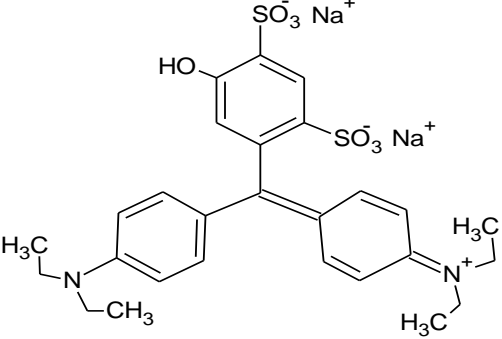
Dyes	λ_{\max} (nm)	Molar mass (g/mol)
Sunset Yellow Supra	481nm	424.35
Amaranth Supra	521nm	604.48
Carmosine Supra	514nm	456.21
Red 2G Supra	538nm	615.34
Tartrazine Supra	425nm	534.37
Ponceau 4R Supra	514nm	601.13
Orange I	476nm	328.34
Orange II	485nm	350.32
Black PN Extra	571nm	711.15
Chocolate Brown HT Extra	460nm	606.09
Green S Supra	635nm	576.6
Patent Blue V Supra	638nm	559.11
Brilliant Blue Supra	629nm	790.16
Malachite green	616nm	382.94
Quinoline Yellow Extra	415nm	477.10
Erythrosine Supra	525nm	879.87
Indigo Carmine Supra	608nm	466.36
Acid green 25	645nm	622.57

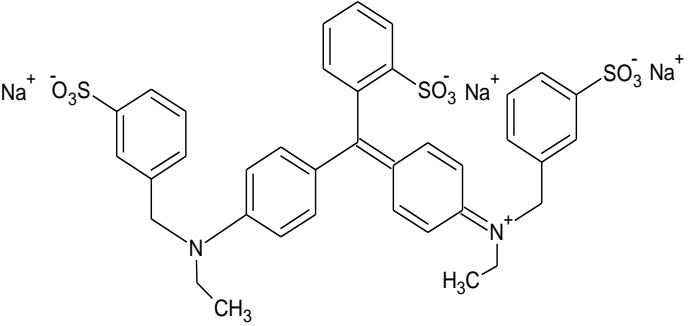
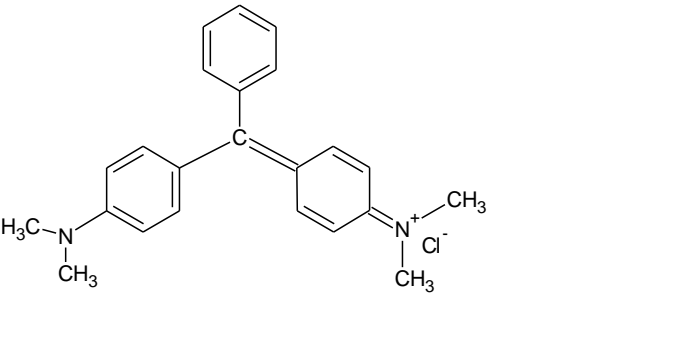
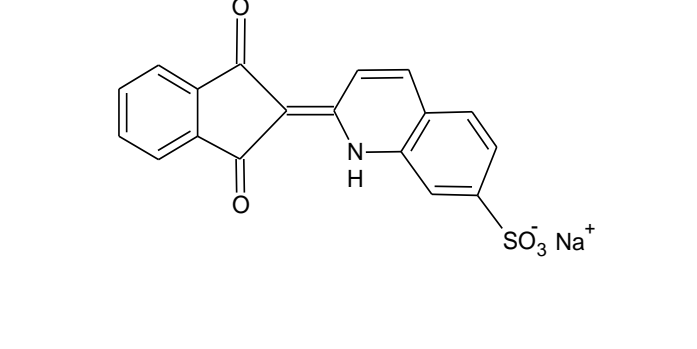
Table 3.3:- shows name of all dyes used in this studied and systematic name with chemical structure.

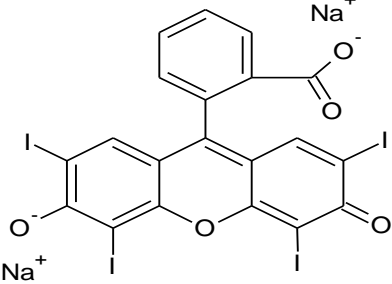
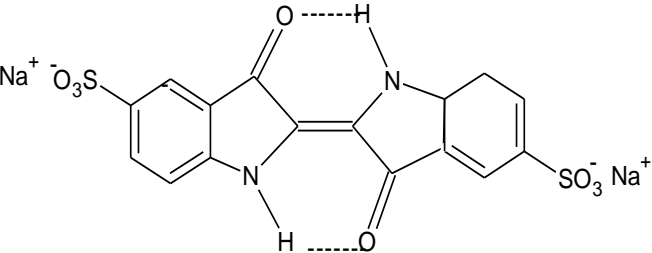
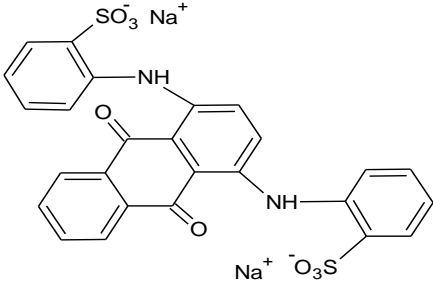
Dyes name	systematic name	Chemical formula	Chemical Structure
SunsetYellow FCF	Disodium 1-p sulphophenylazo-2-naphthol-6-sulphonate.	$C_{16}H_{10}N_2Na_2O_7S_2$	
Amaranth	Trisodium 1-(4-sulpho-1 naphthylazo) 2 Naphthol-3:6-disulphonate	$C_{20}H_{14}N_2Na_3O_{10}S_3$	
Carmosine	Disodium 2-(4- sulpho-1 naphthylazo) 1 naphthol-4-sulphonate.	$C_{20}H_{14}N_2Na_2O_7S_2$	

<p>Red 2G</p>	<p>Disodium salt of 8-actamido-1-hydroxy-2 phenylazonaphthalene-3, 6 disulphonate.</p>	<p>C₁₈H₁₃N₃Na₂O₈S₂</p>	
<p>Tartrazine</p>	<p>Trisodium 5-hydroxy-1-p sulphophenyl -4-p sulphophenylazo pyrazole-3- carboxylate.</p>	<p>C₁₆H₉N₄Na₃O₉S₂</p>	
<p>Ponceau 4R</p>	<p>Trisodium 1-(4-sulpho-1-naphthylazo) - 2-naphthol- 6,8-disulphonate acid.</p>	<p>C₂₀H₁₁N₂Na₃O₁₀S₃</p>	

<p>Orange I</p>	<p>4-(4-sulfophenylazo)-1-naphthol</p>	<p>C₁₆H₁₁N₂NaO₄S</p>	
<p>Orange II</p>	<p>1-(4-sulfophenylazo)-2-naphthol</p>	<p>C₁₆H₁₂N₂Na₂O₇S₂</p>	
<p>Black PN Extra</p>	<p>Tetra sodium 8- acetamido-2-(7-sulpho)-naphol-3:5-disulphonate</p>	<p>C₂₈H₁₇N₅Na₄O₁₄S₄</p>	

<p>Chocolate Brown H.T.</p>	<p>Disodium 2, 4-dihydroxy-3:5 di(4-sulpho-1-naphthylazo) benzyl alcohol.</p>	<p>C₂₇H₁₈N₄Na₂O₉S₂</p>	
<p>Greens S</p>	<p>Sodium di-(p- dimethyl aminophenyl)-2-hydroxy-3-disulphonaphthyl methanol anhydride.</p>	<p>C₂₇H₂₅N₂Na₂O₇S₂</p>	
<p>Patent Blue V</p>	<p>The sodium compound of [4-[alpha-(4-diethyl-aminophenyl)-5-hydroxy-2, 4-disulfo-henyl-methylidene]-2,5-cyclohexadien-1-ylidene]diethyl ammonium hydroxide inner salt.</p>	<p>C₂₇H₃₁N₂Na₂O₇S₂</p>	

<p>BRILLIANT BLUE FCF</p>	<p>Disodium a-[4-(N-Ethyl-3-Sulfonato Benzyl Amino)Phenyl]-a-[4-(N-ethyl -3-Sulfonato Benzylamino) Cyclohexa-2,5-Dienylidene] Toluene-2-Sulfonate.</p>	<p>$C_{37}H_{34}N_2Na_2O_9S_3$</p>	 <p>The structure shows a central carbon atom double-bonded to a cyclohexadiene ring. The cyclohexadiene ring has an ethylamino group (-N(CH₂CH₃)₂) at the 2-position and a toluene-2-sulfonate group (-N(CH₃)₂SO₃⁻Na⁺) at the 5-position. The central carbon is also double-bonded to a phenyl ring, which is further substituted with a 4-(N-ethyl-3-sulfonato benzylamino) group (-CH₂-N(CH₂CH₃)₂-C₆H₄-SO₃⁻Na⁺).</p>
<p>Malachite green</p>	<p>4-[(4-dimethylaminophenyl)-phenyl-methyl]-N, N-dimethyl-aniline)</p>	<p>$C_{23}H_{25}N_2Cl$</p>	 <p>The structure shows a central carbon atom double-bonded to a phenyl ring and a 4-(N,N-dimethylaminophenyl) group (-CH₂-N(CH₃)₂-C₆H₄-). The central carbon is also double-bonded to a 4-(N,N-dimethylaminophenyl) group (-CH₂-N(CH₃)₂-C₆H₄-) which is shown as a zwitterion with a positive charge on the nitrogen and a chloride counterion (Cl⁻).</p>
<p>Quinoline Yellow</p>	<p>The disodium salts of the disulphonates of 2-(2-quinodyl) indan-1,3-dione</p>	<p>$C_{18}H_9NNaO_8S_2$</p>	 <p>The structure shows a central carbon atom double-bonded to a 2-quinodyl group (a benzene ring fused to a five-membered ring with two carbonyl groups) and a 2-(2-quinodyl)indan-1,3-dione group. The 2-(2-quinodyl)indan-1,3-dione group is shown as a zwitterion with a positive charge on the nitrogen and a sulfonate counterion (SO₃⁻Na⁺).</p>

<p>Erythrosine</p>	<p>Disodium 2, 4, 5, 7-Tetraiodo fluorescein.</p>	<p>C₂₀H₆I₄Na₂O₅</p>	
<p>Indigo carmine</p>	<p>Disodium indigotine-5,5'' - disulphonate</p>	<p>C₁₆H₈N₂Na₂O₈S₂</p>	
<p>Acid green 25</p>	<p>Disodium 2, 2'-(9, 10-dioxoanthracene-1, 4-diyldiimino) bis (5-methylsulphonate)</p>	<p>C₂₈H₂₂N₂Na₂O₈S₂</p>	

3.3. Results and Discussion

For the purposes of comparison, relative initial rates of absorbance decrease, $-(dA/dt) / A_0$, were calculated for the initial linear region of the reaction; these are summarised in Tables 3.4 and 3.5, and are plotted in Figures 3.1 and 3.2. Individual plots of absorbance decrease with time for each peroxide/dye/metal ion combination are shown in Figures 3.3 to 3.20. In addition, Figures 3.3 to 3.20 also indicate that some dyes, particularly the azo dyes, form complexes with iron; this is shown through the elevated initial absorbance of the solution compared to other metal ions or solutions with no metal ions. Dyes that appear to form significant complexes with iron are indicated in Tables 3.4 and 3.5 using shaded boxes.

Table 3.4. The effect of Peracetic acid solution with or without metal ions on the relative initial rate of absorbance decrease ($-dA/dt/A_0$) / 10^{-3} min^{-1} , for a range of different dyes. Note: rates in parentheses indicate absorbance increases, and shaded boxes indicate evidence of binding between the metal ion and dye.

DYES +PAA	Fe³⁺	Ag⁺	Mn²⁺	Cu²⁺	No metal
Sunset yellow	19.6	4.39	(18.9)	4.71	4.27
Amaranth supra	185	3.79	30.6	2.02	2.9
Carmosine supra	31.9	9.9	12.6	(19.6)	(1.88)
Red 2G supra	24.3	9.69	12.7	(9.64)	(3.59)
Tartrazine supra	(34.6)	(20.6)	(8.71)	(11.3)	(32.4)
Ponceau 4R supra	30.1	15.7	17.0	(42.8)	1.5
Orange I	0.691	31.6	28.6	15.4	2.01
Orange II	68.6	25.7	(13.1)	>200**	0.00134
Black PN Extra	31.4	17	29	3.1	1.9
Chocolate Brown	11.2	12.3	10.6	20.4	4.8
Green S Supra	53.5	74.5	68.0	52.1	59.7
Patent Blue supra	78.7	1.10	9.41	(3.25)	2.41
Brilliant Blue	59.4	8.20	1.64	4.99	1.46
Malachite green	30.8	16.6	26.3	21.9	17.5
Quinoline yellow	8.11	15.1	70.5	53.5	56.3
Erythrosine supra	32.6	14.4	44.5	42.4	54.4
Indigo carmine	>400**	62.3	63.4	>400**	12.2
Acid green 25	>200**	13.9	13.1	36.4	18.5

**indicates that reaction was virtually complete by the time the first measurement was made. Rate was estimated on the assumption of 0.5 minute mixing time, and an initial absorbance estimated from absorbance profile in the absence of metal ions.

Table 3.5. The effect of hydrogen peroxide solution with or without metal ions on the relative initial rate of absorbance decrease ($-dA/dt/A_0$) / 10^{-3} min^{-1} , for a range of different dyes. Note: rates in parentheses indicate absorbance increases, and shaded boxes indicate evidence of binding between the metal ion and dye.

DYES + HP	Fe³⁺	Ag⁺	Mn²⁺	Cu²⁺	No metal
Sunset yellow	(2.69)	(12.1)	(11.6)	3.11	(0.729)
Amaranth supra	6.13	0.0238	0.201	(5.39)	8.13
Carmosine supra	(0.798)	(0.923)	0.872	(15.6)	5.19
Red 2G supra	(12.8)	(0.289)	1.75	(7.73)	(1.14)
Tartrazine supra	(20.1)	(12.3)	(7.03)	(18.9)	(36.6)
Ponceau 4R supra	0.857	1.01	(7.72)	(20.4)	(8.95)
Orange I	(0.858)	8	2.14	03.33	1.19
Orange II	0.981	0.480	(55.9)	(37.7)	0.485
Black PN Extra	4.05	(0.33)	3.7	5.0	(0.318)
Chocolate Brown	1.85	8.25	6.71	(34.7)	(0.454)
Green S Supra	18.1	(0.744)	(0.552)	0.583	(1.72)
Patent Blue supra	50	(6.92)	(7.58)	(3.91)	(3.83)
Brilliant Blue	31.9	(0.172)	(0.264)	2.78	0.872
Malachite green	23.9	4.46	7.67	7.82	5.55
Quinoline yellow	0.140	1.48	(4.13)	(1.18)	1.61
Erythrosine supra	14.6	12.9	7.14	28.4	9.9
Indigo carmine	>400**	53.8	(7.59)	886	17.2
Acid green 25	>200**	4.10	0.704	44.3	2.94

**indicates that reaction was virtually complete by the time the first measurement was made. Rate was estimated on the assumption of 0.5 minute mixing time, and an initial absorbance estimated from absorbance profile in the absence of metal ions.

Figure 3.1. The effect of hydrogen peroxide solution, with or without metal ions, on the relative initial rate of absorbance decrease $(-dA/dt / A_0) / 10^{-3}$, for a range of different dyes. Note: results for dyes that showed an absorbance increase are not included. Rates above 100 from Table 3.4 are capped at 100.

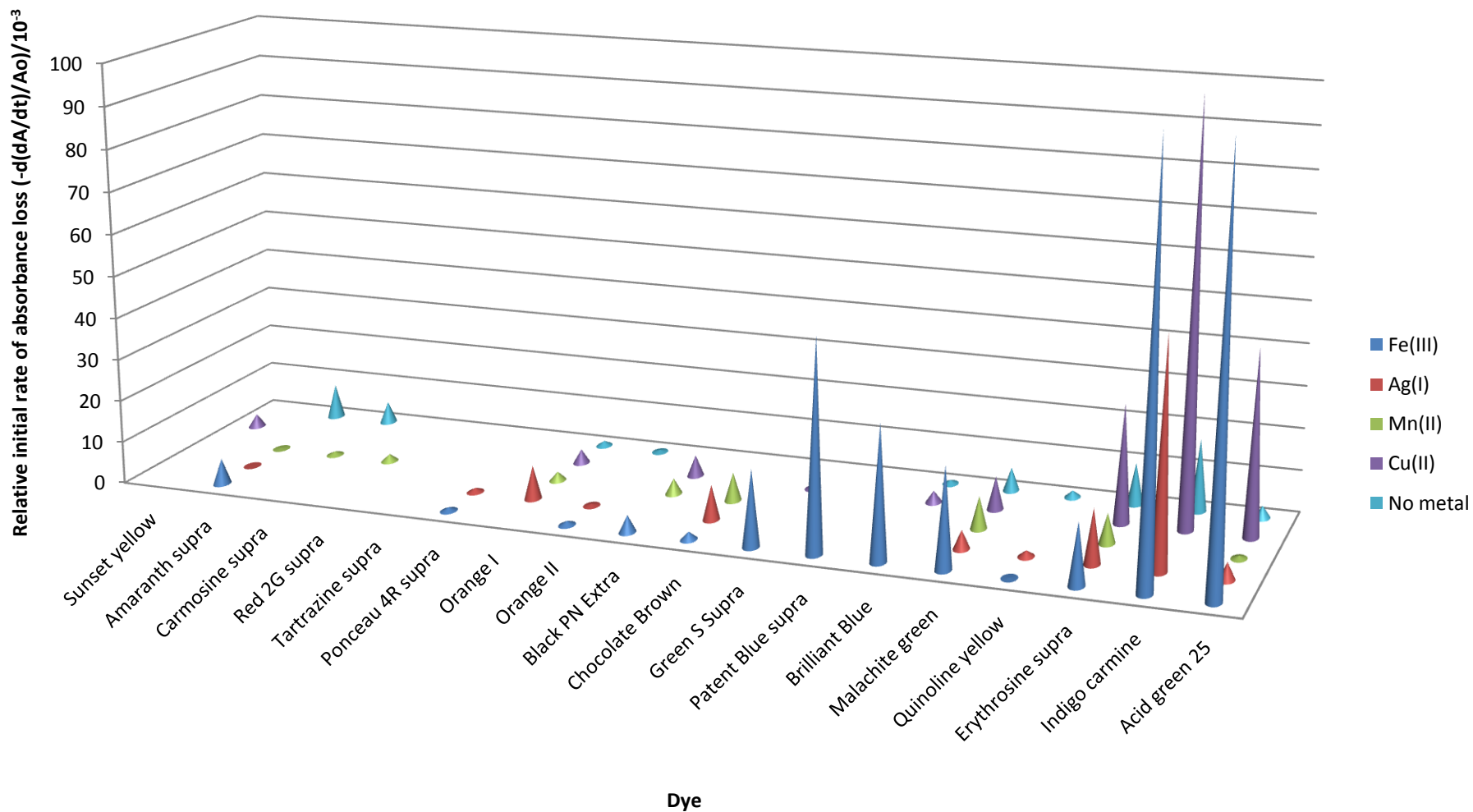
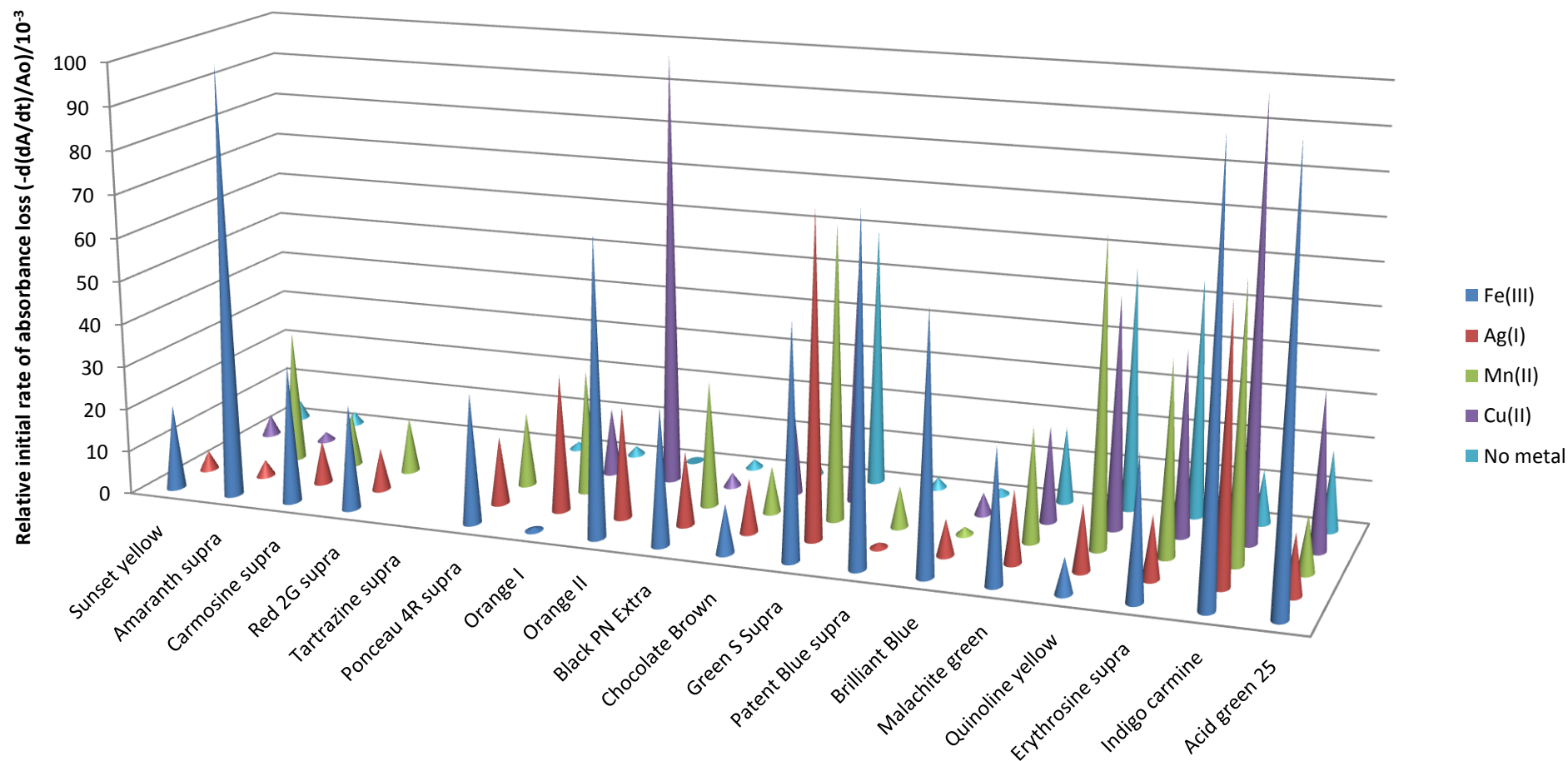


Figure 3.2. The effect of peracetic acid solution, with or without metal ions, on the relative initial rate of absorbance decrease $(-dA/dt/A_0) / 10^{-3}$, for a range of different dyes. Note: results for dyes that showed an absorbance increase are not included. Rates above 100 from Table 3.5 are capped at 100.



3.3.1. Summary of dye bleaching results

3.3.1.1. Hydrogen peroxide

A comparison of the plots for dye bleaching experiments using peracetic acid and hydrogen peroxide, with or without metal ions shows that generally the former is a much more effective oxidant.

For the reaction with hydrogen peroxide, Erythrosine Supra (xanthene) and Indigo Carmine (Indigoid) both show significant bleaching in the absence or presence of metal ions, though these reactions, particularly for Indigo Carmine, are significantly accelerated by the presence of iron and copper ions (this dye also showed an absorbance increase in the presence of manganese). Of the remaining dyes, the bleaching of the four triarylmethane dyes are all significantly enhanced by iron as a catalyst, but not by other metals. The azo dyes (mono and di), quinoline and anthraquinone dyes are relatively unreactive either in the presence or absence of metal ion catalysts.

Many of the runs resulted in absorbance increases that are probably due to the formation of bubbles in the cuvette as a result of decomposition of the hydrogen peroxide to yield oxygen.

It is also significant that all of the azo dyes, plus Green S and Quinoline Yellow appear to form complexes with iron: this was ascertained from the instantaneous increase in absorbance that occurred when mixing these dyes with iron compared to solutions with other metals and in the absence of metals.

3.3.1.2. Peracetic acid

For bleaching by peracetic acid, two triarylmethane dyes (Green S Supra and Malachite Green) as well as Quinoline Yellow (a quinoline), Acid Green 25 (an anthraquinone) and Erythrosine Supra (a xanthenes dye) show ready reactivity with or without metal ion catalysts being present (in fact the bleaching of Quinoline Yellow seems to be inhibited by the presence of iron or silver ions).

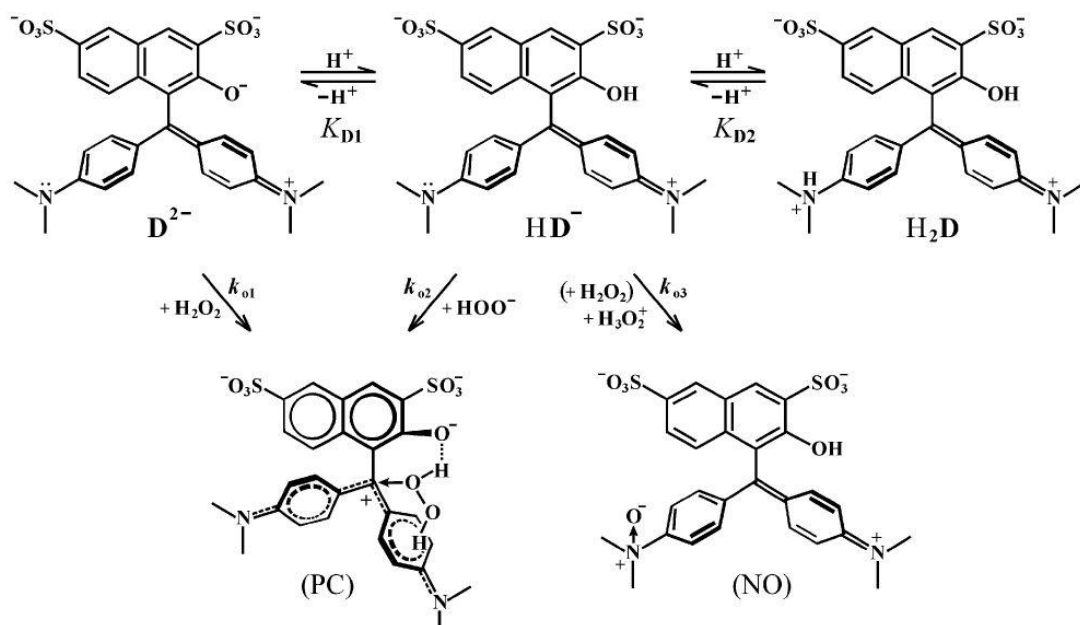
Azo dyes as a class (mono or di) are relatively unreactive towards peracetic acid in the absence of metal ion catalysts, but most do show significant bleaching in the presence of catalysts, particularly iron, but also silver; of the other metals. Copper is particularly effective in catalysing the bleaching of Orange II (all of the reaction is complete by the

time the first measurement is made). Tartrazine Supra is unreactive in the presence of all metal catalysts, whilst Orange I is unreactive in the presence of iron, but its reaction with peracetic acid is catalysed by the presence of silver, manganese and copper.

3.3.2. Mechanisms of dye oxidation

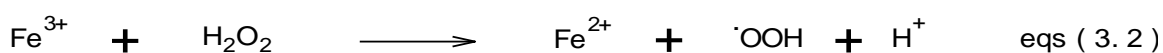
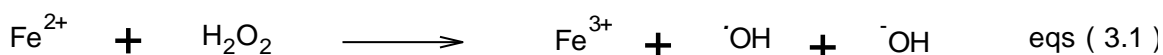
Dyes, by their very nature, are complex molecules comprising conjugated systems and auxochromes, some of which may be ionisable; meaning that for any particular dye there may be a number of distinct chemical species. The study of the oxidation of these molecules is, therefore, complex since each of the pH dependent dye species may react differently, for example the initial reaction centre may differ between species, as might the mechanism. Azo dyes, for example can be oxidised by peroxide species acting as either nucleophiles or electrophiles, depending on the pH¹⁸⁷. After the initial attack of the oxidant on the dye molecule, fragmentation usually, but not always, occurs and these fragments may react further, which in the case of powerful oxidants such as heterogeneous photocatalytic systems (e.g. UV with hydrogen peroxide and TiO₂)¹⁸⁸ may result in almost complete mineralisation. For less aggressive oxidative systems of the type studied in this research, particularly without metal ion catalysts present, bleaching may be accomplished by disruption of the conjugated system, yet significant dye fragments may still remain. In common with probably the majority of dye bleaching studies we have not attempted as part of this work to analyse the reaction products, but rather to compare relative rates of reaction of different dye classes with different peroxides in the presence and absence of metal ion catalysts; such a wide ranging comparison, particularly with peracetic acid has not been previously reported.

A good example of the potential complexity of dye oxidation studies is given by reaction of the triarylmethane dye, Green S, with hydrogen peroxide^{189, 190}. Davies and Moozyckine have determined that there are five significant species of this dye and that at low pH (1-2) the mechanism of oxidation is via N-oxidation of an amine group (resulting in disruption of the conjugated system), whereas at neutral and higher pHs attack takes place at the central carbon, which is more typical of reported oxidation pathways for arylmethane dyes. Green S has an -O⁻ group ortho to the neighbouring central carbon that can assist in intramolecular base catalysis of the reaction by forming a dye-peroxide complex which subsequently attacks the central carbon; this feature makes it more reactive than other arylmethane dyes at neutral pH. Scheme 3.1, reproduced from¹⁸⁹, shows these different reaction pathways.



Scheme 3.1: Speciation of Green S and potential reaction pathways with hydrogen peroxide (reproduced from¹⁸⁹).

In the low pH conditions used in our studies for Green S oxidation there was virtually no detectable absorbance change over the initial 10 minutes for any of the hydrogen peroxide solutions, except for that where iron was present; similar results were observed for the other three arylmethane dyes, though Malachite Green was generally more reactive than the others, even in the absence of metal ions. According to Moozyckine and Davies¹⁸⁹ at this pH the bleaching is likely to be via N-oxidation, as discussed above, and is known to be slow. The catalysis of arylmethane dye oxidation by iron could be due to the formation of hydroxyl radicals in a Fenton-like reaction as shown in Equations (3.1 and 3.2)¹⁹¹. However, we should not discount the fact that Green S, like the azo dyes, complexes with iron (from the colour intensity increase that we observed) and so it is possible that the complex in some way activates the dye to attack. Nevertheless, Patent Blue and Brilliant Blue do not form complexes with iron yet show the same enhanced reactivity, so perhaps a common radical mechanism is more likely after all.



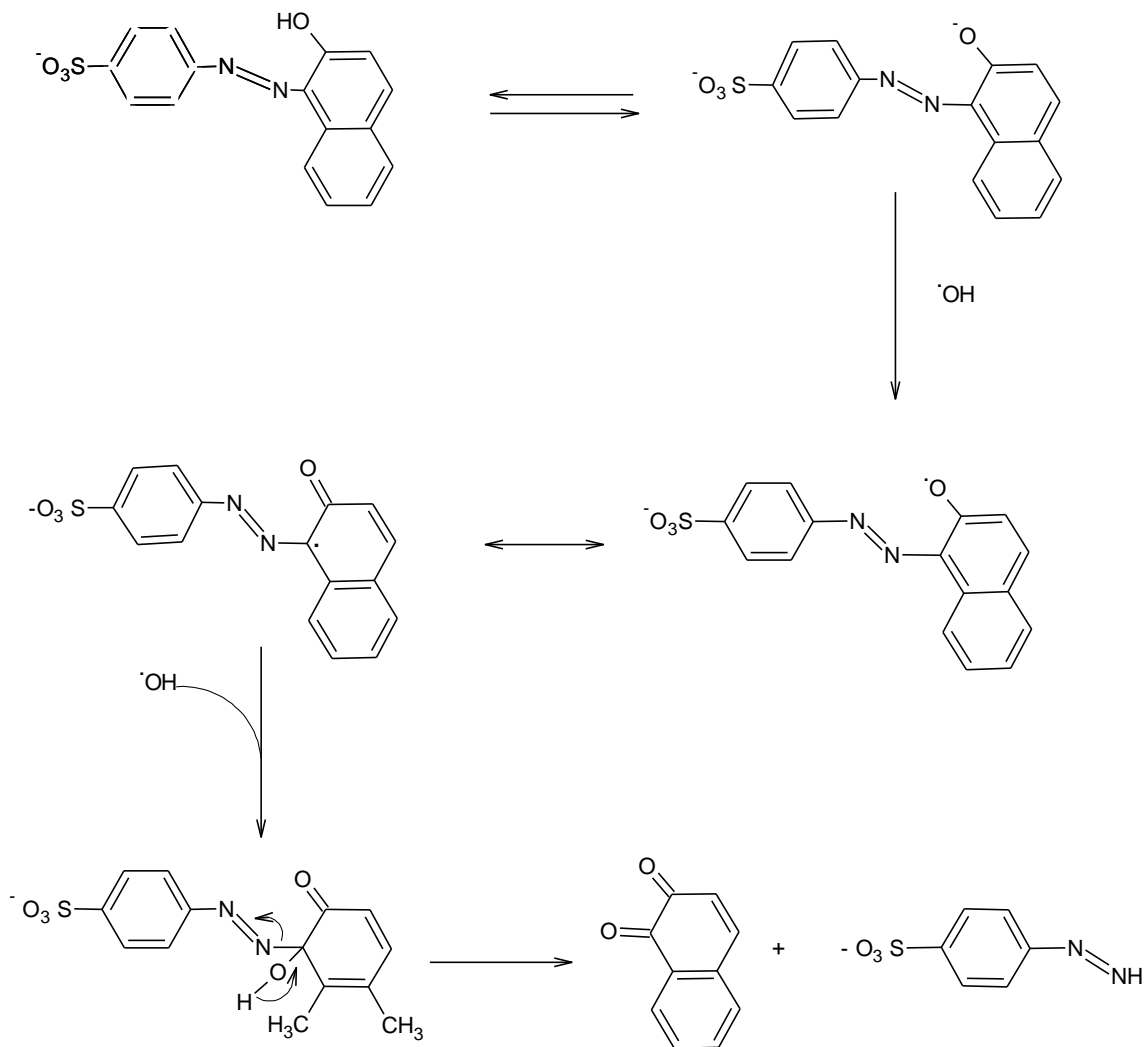
For the reaction of aryl methane dyes with peracetic acid, which has not been previously reported, Green S bleaching is found to proceed at roughly the same rate regardless of whether metal ions are present, suggesting a mechanism that does not involve radicals, nor the involvement of metals acting as Lewis acid catalysts; a possibility is the direct attack of the peracetate anion at the central carbon or N-oxidation by the undissociated peracid; Malachite Green shows similar properties, though Brilliant Blue and Patent Blue V only show appreciable reactivity in the presence of iron. It is not clear from the structures why there should be such a significant difference between these arylmethane dyes.

The largest group of dyes studied in this Chapter were the azo dyes (mono and di). Like arylmethane dyes, azo dyes can form different species depending on the pH, with azo-hydrazone tautomerism occurring at lower pHs and a common ion being formed at higher pH: the pKa value is dependent on whether the ionisable hydroxyl group is ortho or para to the azo group: for ortho-hydroxyls, such as for Orange II (11.4), the pKa values are approximately two units higher than para-hydroxyls, such as for Orange I. Oakes and Gratton have shown that the mechanism of reaction differs for hydrogen peroxide and peracetic acid, with the former involving attack of the perhydroxyl anion on the hydrazone form of the dye, whilst the undissociated peracetic acid is shown to act as an electrophile, reacting with the common ion; the reaction site is the azo linkage in both cases.

Ortho-hydroxyl substituted mono-azo dyes are the subject of a detailed study in Chapter 4; however it is worthwhile making some general comparisons for the reactions of the wider group of azo dyes studied in this Chapter. It is clear that in the reaction with hydrogen peroxide, the dyes are fairly unreactive over 10 minutes, either with or without metal ions, and certainly less reactive than for the corresponding reactions using peracetic acid as the oxidant. This is perhaps surprising since there is a large body of literature that has looked at Fenton-like and photo-Fenton reactions for peroxide oxidations of azo dyes. It is possible that the formation of bubbles may have masked any absorbance decrease, yet overall the picture is quite consistent, with minimal bleaching being observed.

Notwithstanding the results observed in this Chapter, literature studies have suggested that the overall mechanism of azo dye decolourisation in Fenton-like systems may involve two consecutive one electron transfer steps (Scheme 3.2). The first $\bullet\text{OH}$ removes an electron from the phenolate anion to produce the corresponding resonance

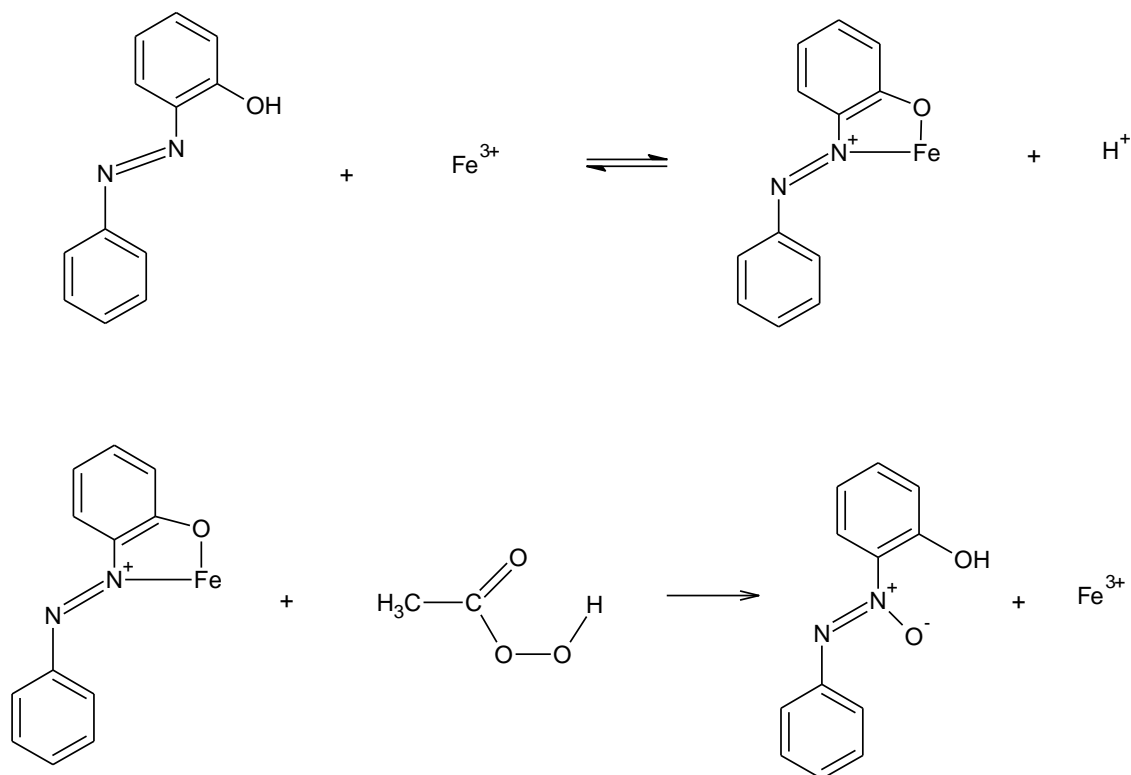
stabilised phenoxy radical. Subsequently a further $\cdot\text{OH}$ adds to the C-1 carbon of the naphthol ring, generating an unstable tetrahedral intermediate, which breaks down to produce 1,2-naphthoquinone and 4-sulfophenyldiazine in o-hydroxy –or o-amino-aryldiazo compounds.



Scheme 3.2:- A proposed mechanism for the degradation of Orange II by $\text{Fe}^{3+} / \text{H}_2\text{O}_2$ ¹⁵⁰

When using peracetic acid as the oxidant, the picture is very different: in the absence of metal ions there is negligible bleaching, yet in the presence of metals, particularly iron, there is significant bleaching of the dyes in most cases. From the hydrogen peroxide study discussed above, it seems unlikely that the bleaching is due to radical formation and so an alternative explanation is required. One possibility that is supported by the results is the formation of a dye-iron complex that activates the dye to attack by the undissociated peracetic acid; such a scheme is shown in Scheme 3.3. In this scheme, for activation to occur the hydroxyl group must be in the ortho position, as in Orange II, otherwise the bridge cannot be formed. This is supported by the results

because Orange I, which has a para-hydroxyl group, shows minimal bleaching with peracetic acid in the presence of iron (though it does bleach in the presence of the other metal ions). Additionally there is evidence from the raw absorbance plots at the end of this chapter that complexes are formed between the iron and the dye; this manifests as an increase in absorbance compared to the absence of iron.



Scheme 3.3:- reaction of ortho – substituted azo dyes with peracetic acid in the presence of iron.

There were four other dye classes studied in this chapter, all with one representative: Indigo Carmine Supra (an Indigoid), Quinoline Yellow (a Quinoline), Erythrosine Supra (a Xanthene), and Acid Green 25, (an anthraquinone).

For the indigoid dye, Indigo Carmine Supra, literature studies for catalysed reactions involving hydroxyl radical formation suggest that the initial reaction centre is the central ethylenic bond, cleaving the dye into two aromatic intermediates¹⁹². Our results for hydrogen peroxide oxidation of this dye show that the reaction is accelerated by the presence of iron, silver and particularly copper, though there is still a significant uncatalysed reaction. A similar pattern is observed for the oxidation by peracetic acid

(Figure 3.2), with the reaction rates for copper and iron catalysed solutions particularly large (the reaction is so fast that it has completed before the first reading has been taken).

Quinoline Yellow, appears not to be particularly reactive towards hydrogen peroxide nor any radicals that might be formed in the presence of metal ions. Nevertheless, it is interesting to note that the dye itself appears to complex with iron, as previously observed for azo dyes; this is clear from the raw absorbance plots shown in Figure 3.17, where in the presence of iron, both for peracetic acid and hydrogen peroxide, the absorbance is significantly increased; there is no evidence of complex formation for the other metals. There is no evidence of metal ion catalysis with either peracetic acid or hydrogen peroxide; for peracetic acid the rates are comparable both in the presence and absence of metal ions. As with Indigo Carmine the initial reaction site is likely to be the central ethylenic linkage.

The xanthene dye, Erythrosine Supra, shows no evidence of metal ion catalysis, with similar rates of reaction in the presence and absence of metal ions, for both peracetic acid and hydrogen peroxide.

Finally, for the anthraquinone dye, Acid Green 25, copper and iron are both found to significantly enhance the rate of bleaching. It is not possible to say from the available data whether the catalysis is due the metal either acting as Lewis acid catalyst, or via the production of radicals through peroxide decomposition.

3.4. Conclusion

A variety of different behaviours is observed for the different dye/peroxide/metal combinations. In some cases, such as for Green S Supra, Malachite Green, and Erythrosine Supra with peracetic acid as the oxidant the rates in the presence and absence of metal ions are similar, suggesting that radical mechanisms are not so significant compared to reaction with the peracetic acid directly. For Quinoline Yellow, which complexes with iron, the rate is actually lower in the presence of iron (and silver), and it is possible that complex is less reactive to peracetic acid. There are also several examples of dye bleaching by peracetic acid being significantly accelerated by the presence of metal ions: Patent Blue and Brilliant Blue, and most of the azo dyes. Here, radical mechanisms might be suggested, but there is also the possibility, which will be explored further in the next chapter that the complexes formed between iron and azo dyes activate the dye to attack by peracetic acid.

With hydrogen peroxide as the oxidant, many of the dyes are virtually unreactive in either the presence or absence of metal ions, though radical mechanisms are suggested for the arylmethane dyes and also for Indigo Carmine, Acid Green and Erythrosine Supra; copper and iron are particularly effective in this respect.

In the following chapter, the reaction of the mono azo dyes with peracetic acid in the presence and absence of iron as a catalyst will be studied. Iron was the most consistent catalyst, and peracetic acid was shown to be a much more effective oxidant than hydrogen peroxide. The aim of the study will be to determine the optimum experimental conditions for the bleaching of these dyes, both in terms of rate of degradation and overall percentage colour removal. Parameters studied will include pH, iron concentration, peracetic acid concentration and dye concentration. In addition, the significance of ionisable hydroxyl groups in positions on the aryl group that are either ortho or para to the azo linkage will be investigated by comparing Orange I (para) and Orange II (ortho).

Figure 3.3:- shows the results for sunset yellow with solution of Peracetic acid and hydrogen peroxide with without metals.

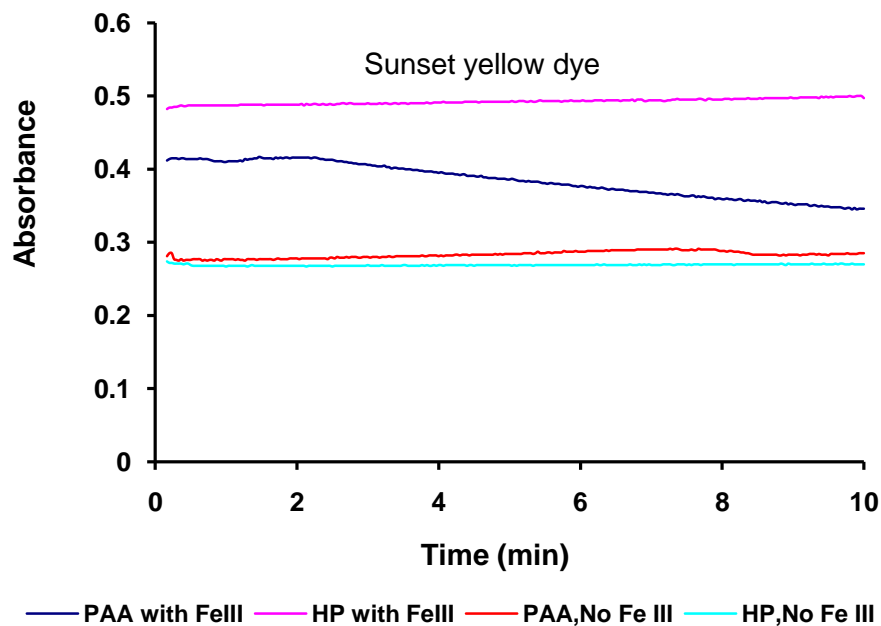


Figure 3.3A:- shows the change in dye Sunset yellow Absorption with, without the addition of FeIII

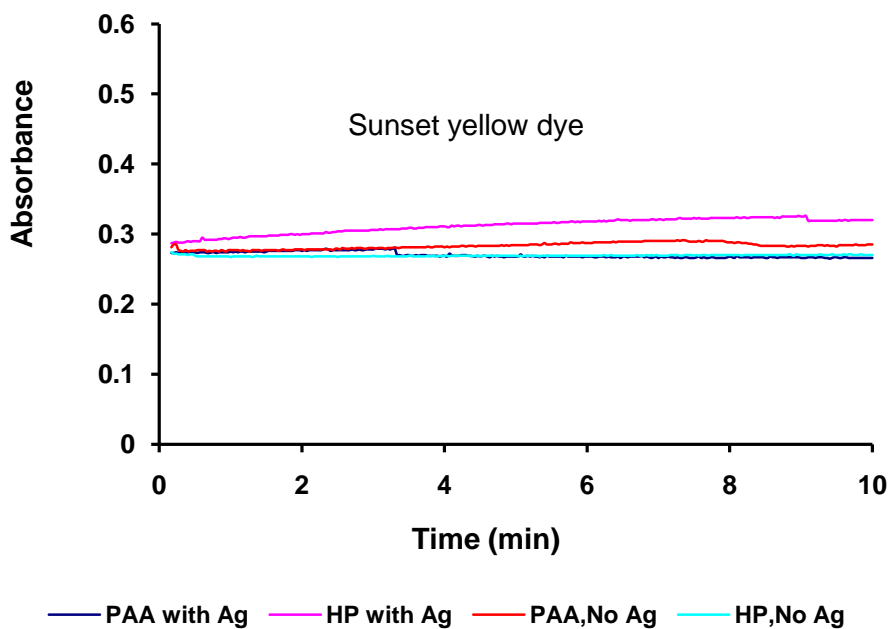


Figure 3.3B:- shows the change in dye Sunset yellow Absorption with, without the addition of Ag

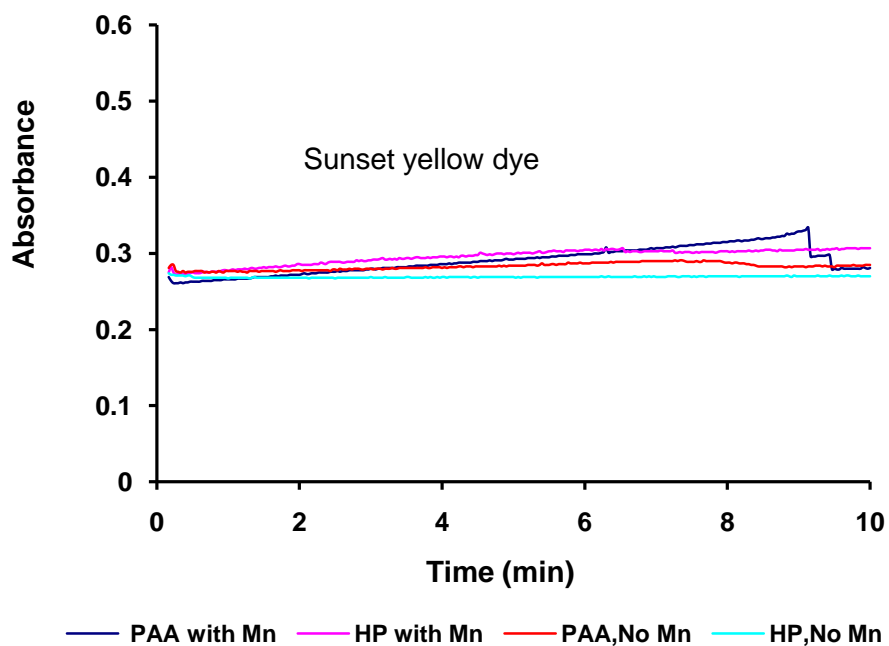


Figure 3.3C:- shows the change in dye Sunset yellow absorption with, without the addition of Mn

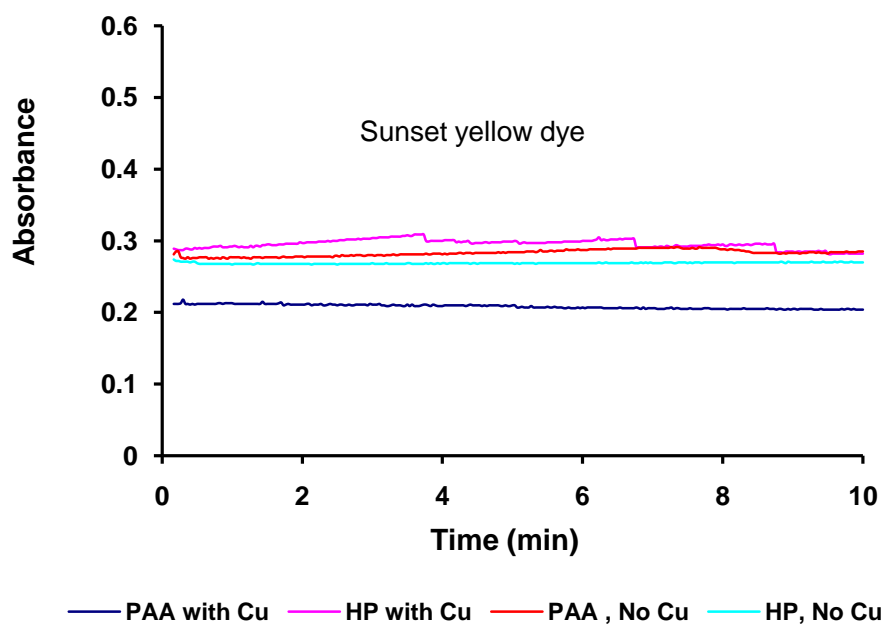


Figure 3.3D:- shows the change in dye Sunset yellow absorption with, without the addition of Cu

Figure 3.4:- shows the results for amaranth supra with solution of peracetic acid and hydrogen peroxide with without metals.

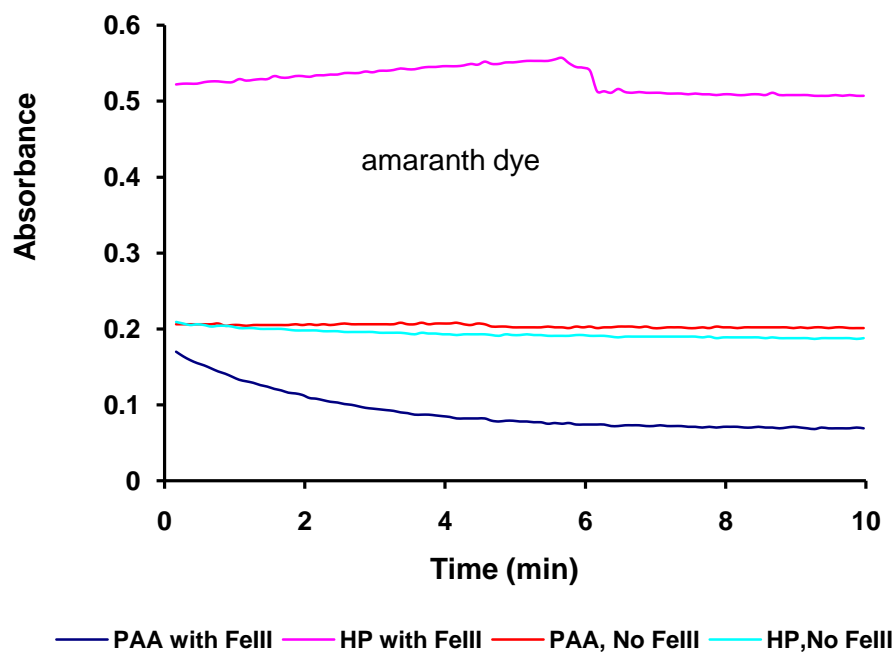


Figure 3.4A:- Shows the change in dye amaranth absorption with, without the addition of Fe III

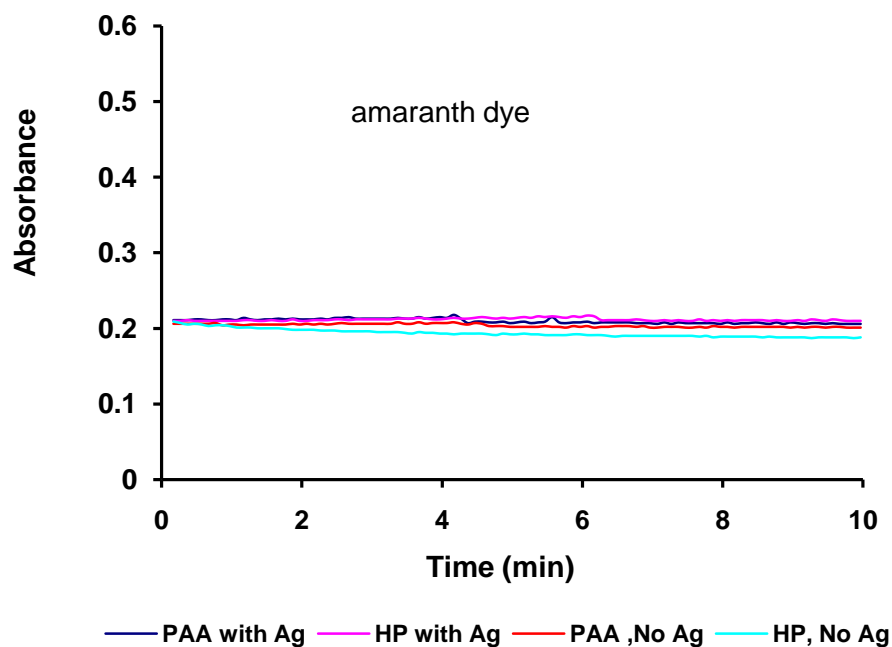


Figure 3.4B:- shows the change in dye amaranth absorption with, without the addition of Ag

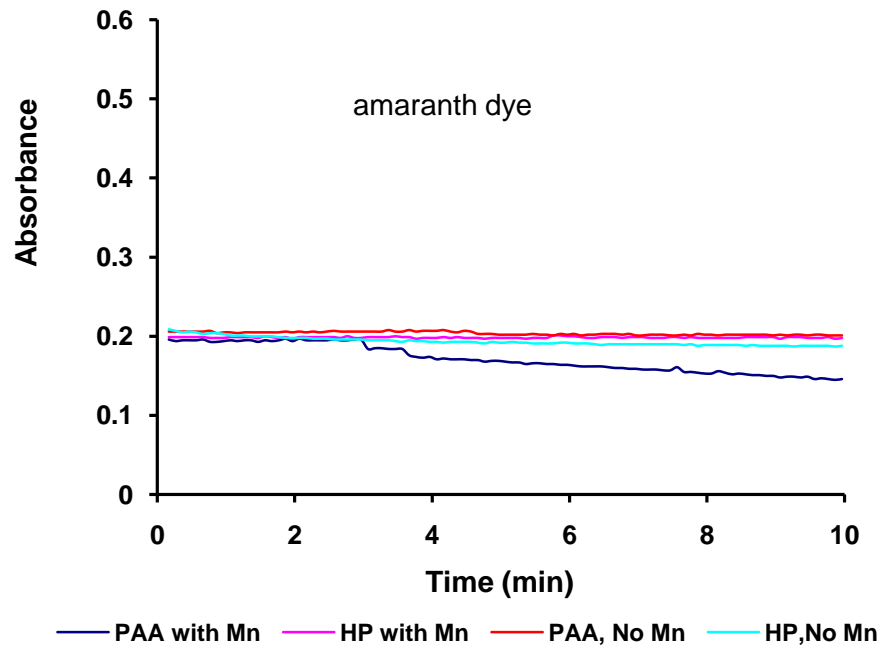


Figure 3.4C:- shows the change in dye amaranth absorption with, without the addition of Mn

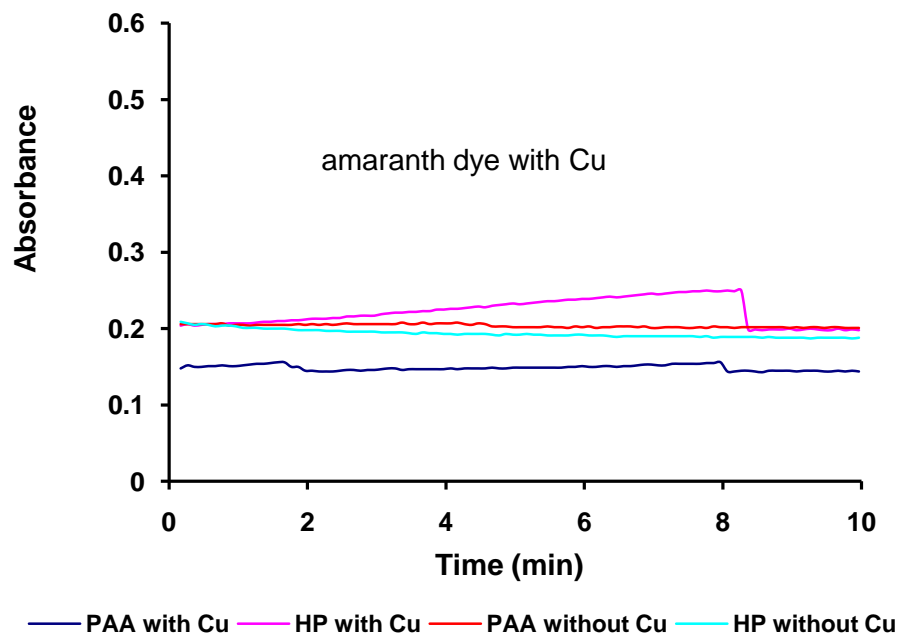


Figure 3.4D:- shows the change in dye amaranth absorption with, without the addition of Cu

Figure 3.5:- shows the results for carmosine supra with solution of peracetic acid and hydrogen peroxide with, without metals.

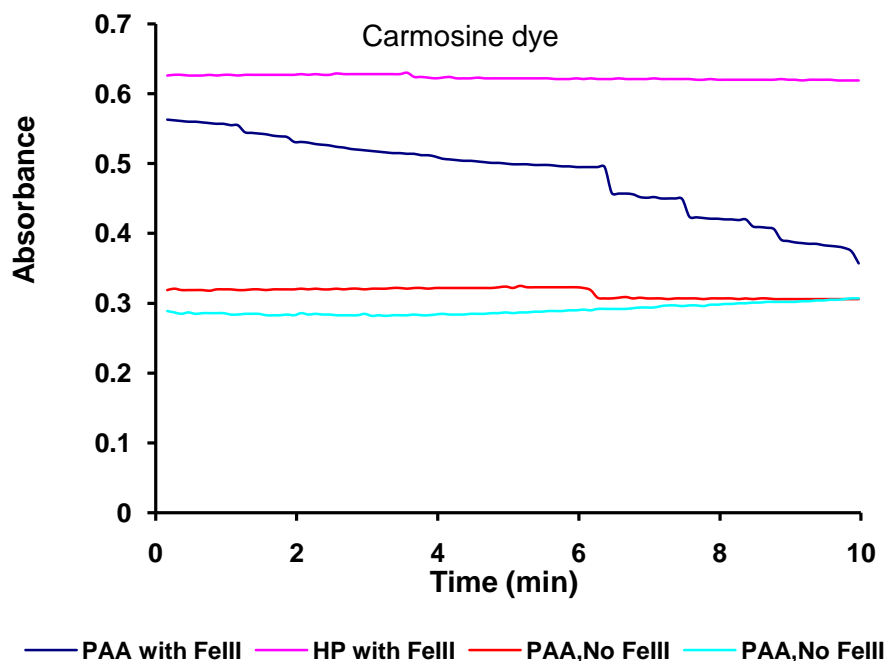


Figure 3.5A:- shows the change in dye Carmosine absorption with, without the addition of Fe (III)

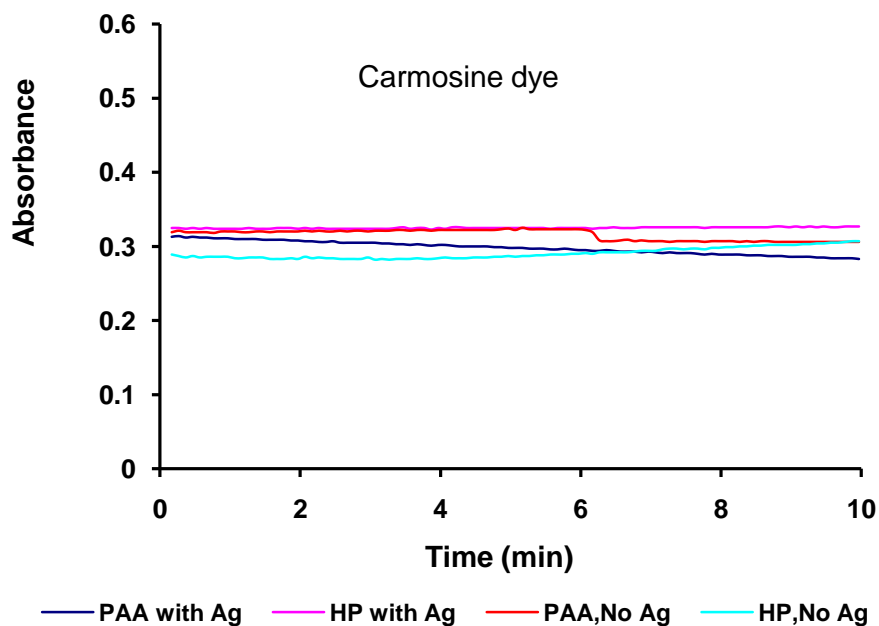


Figure 3.5B:- shows the change in dye Carmosine absorption with, without the addition of Ag

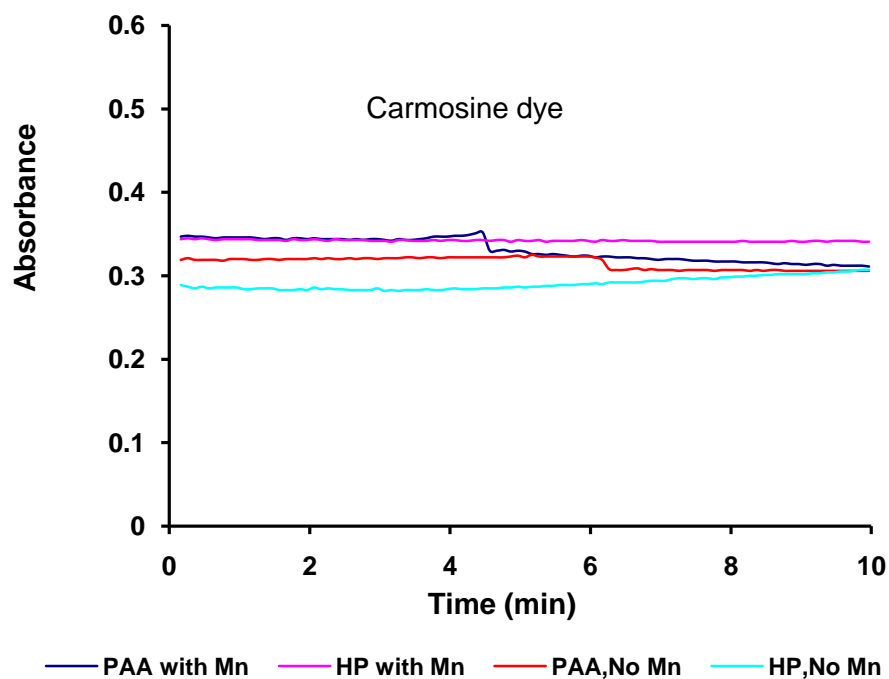


Figure 3.5C:- shows the change in dye Carmosine absorption with, without the addition of Mn

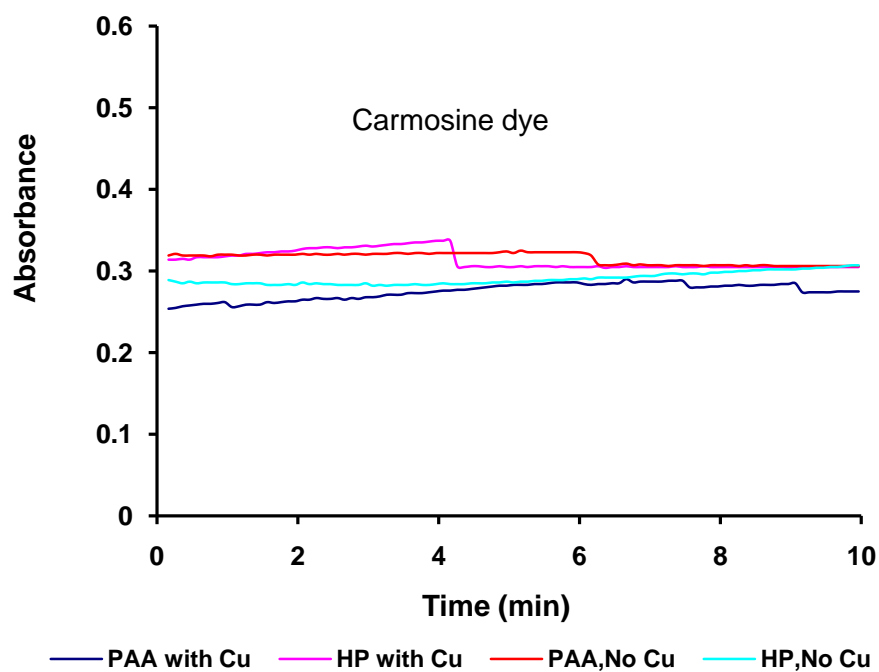


Figure 3.5D:- shows the change in dye Carmosine absorption with, without the addition of Cu

Figure 3.6:- shows the results for Red 2G with solution of peracetic acid and hydrogen peroxide with without metals.

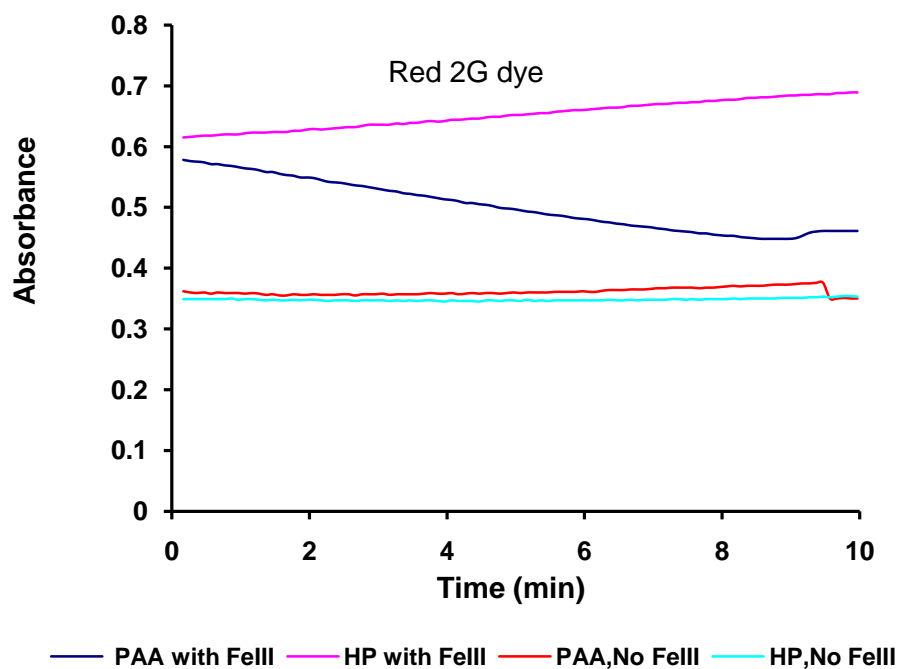


Figure 3.6A:- shows the change in dye Red 2G absorption with, without the addition of FeIII

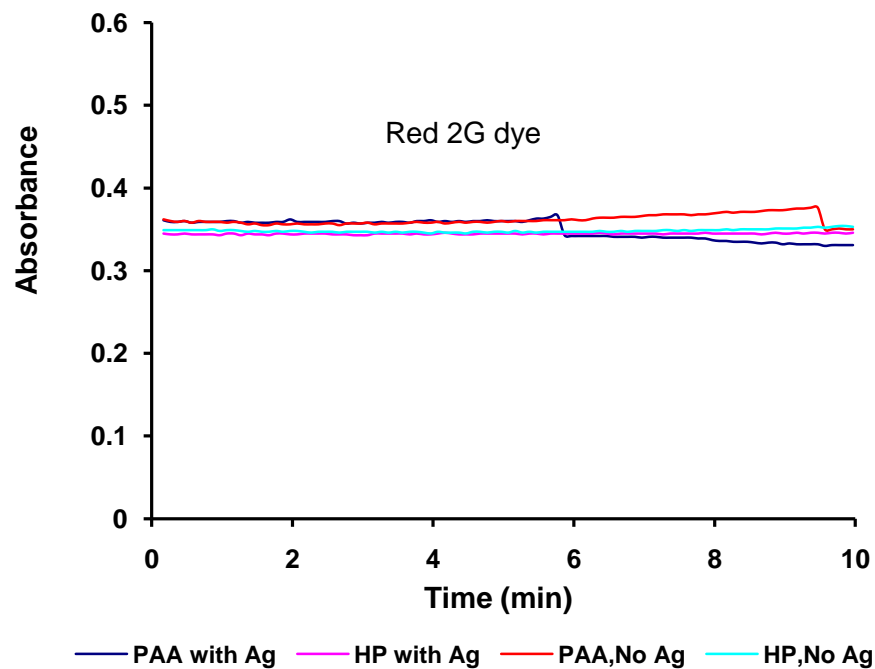
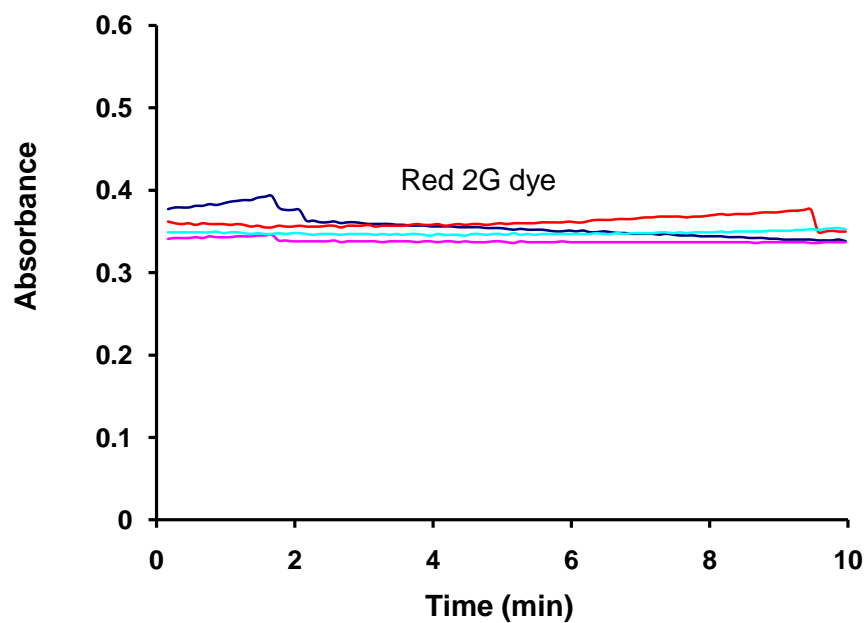
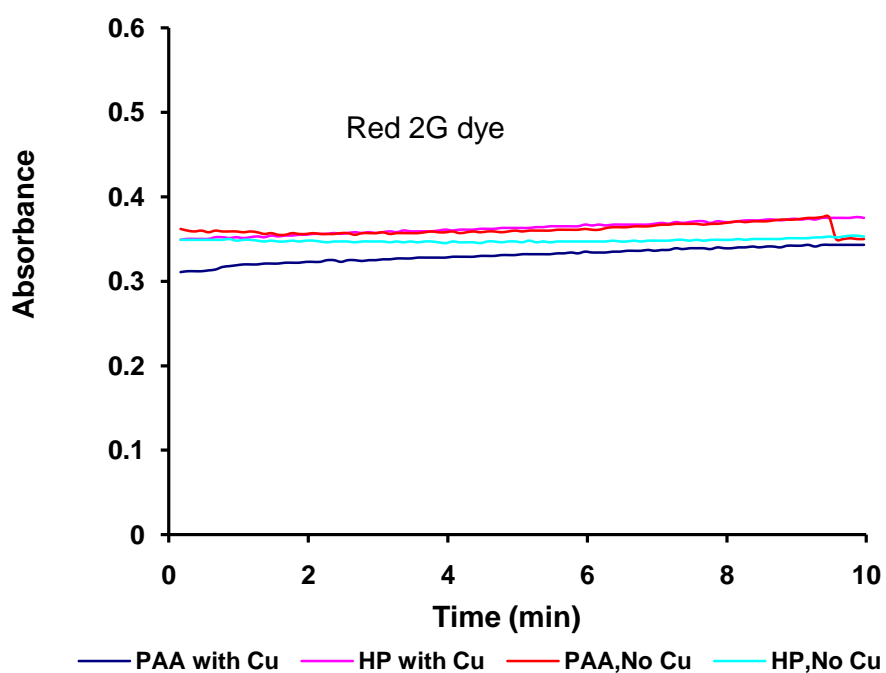


Figure 3.6B:- shows the change in dye Red 2G absorption with, without the addition of Ag



— PAA with Mn — HP with Mn — PAA, No Mn — HP, No Mn
 Figure 3.6C:- shows the change in dye Red 2G absorption with, without the addition of Mn



— PAA with Cu — HP with Cu — PAA, No Cu — HP, No Cu
 Figure 3.6D: - shows the change in dye Red 2G absorption with, without the addition of Cu

Figure 3.7:- shows the results for Tartrazine with solution of Peracetic acid and hydrogen peroxide with without metals.

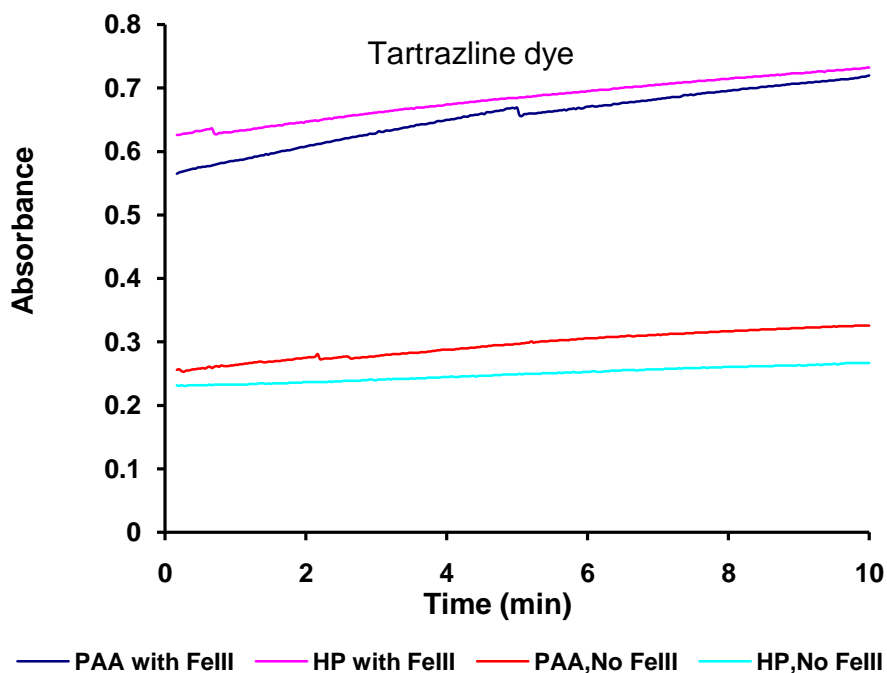


Figure 3.7A:- shows the change in dye Tartrazine absorption with, without the addition of Fe (III)

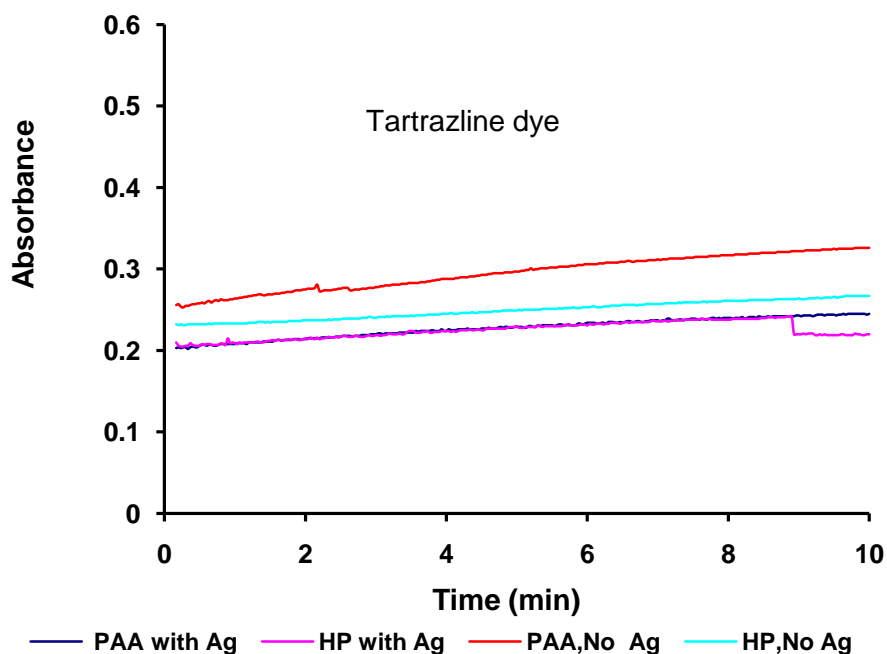


Figure 3.7B:- shows the change in dye Tartrazine absorption with, without the addition of Ag

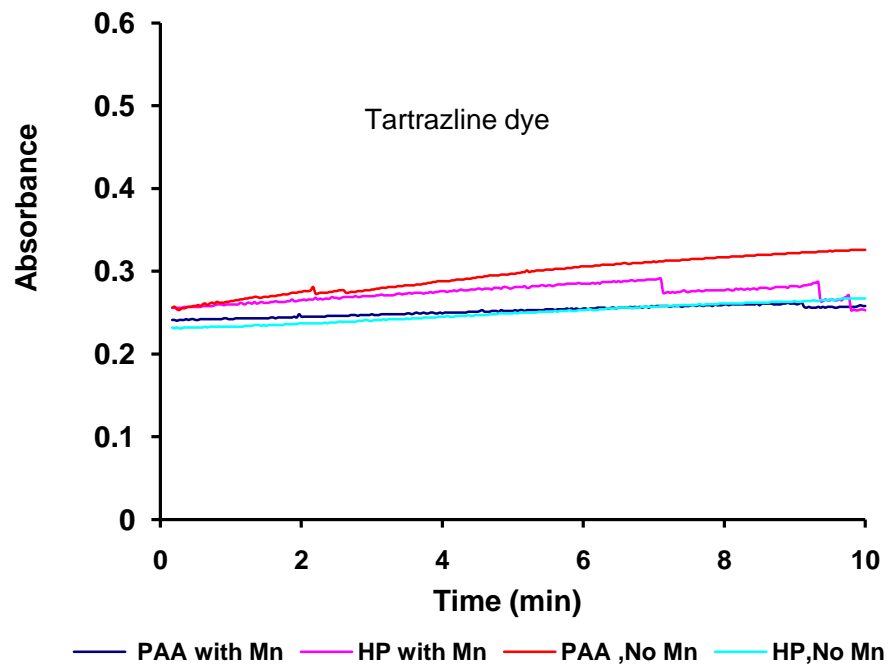


Figure 3.7C:- shows the change in dye Tartrazine absorption with, without the addition of Mn

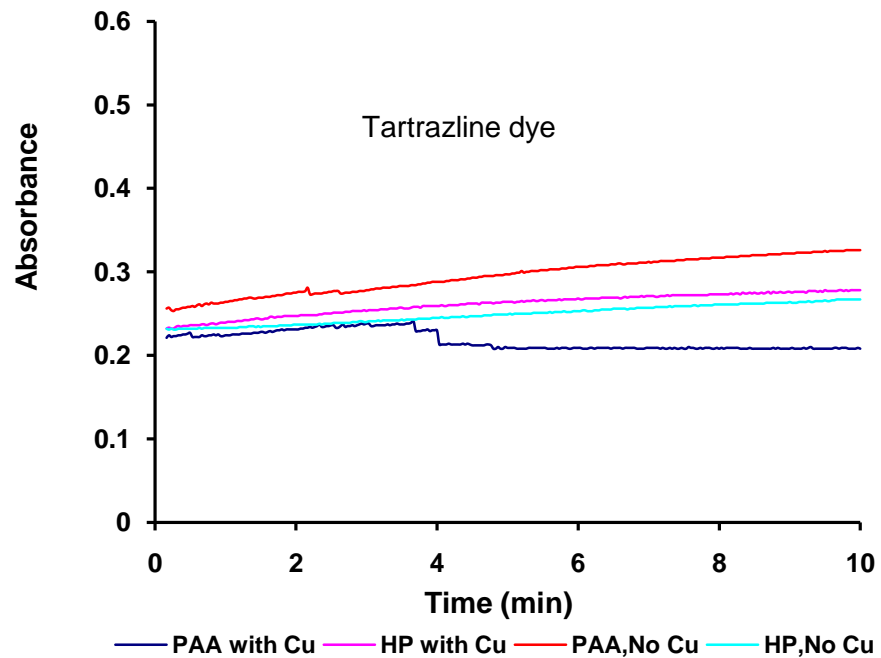


Figure 3.7D: - shows the change in dye Tartrazine absorption with, without the addition of Cu

Figure 3.8:- shows the results for Ponceau 4R with solution of Peracetic acid and hydrogen peroxide with without metals.

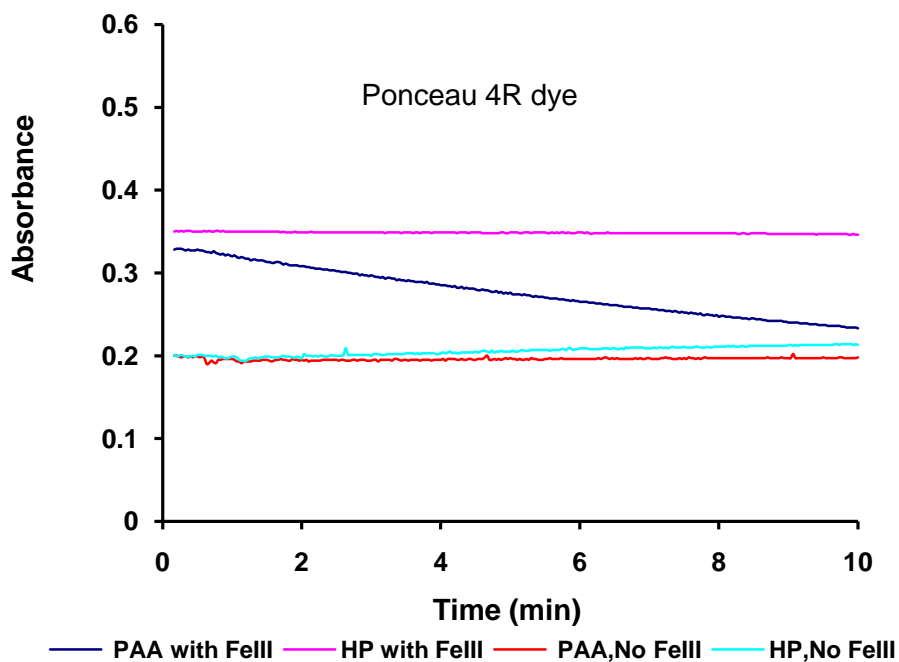


Figure 3.8A:- shows the change in dye Ponceau 4r absorption with, without the addition of Fe (III).

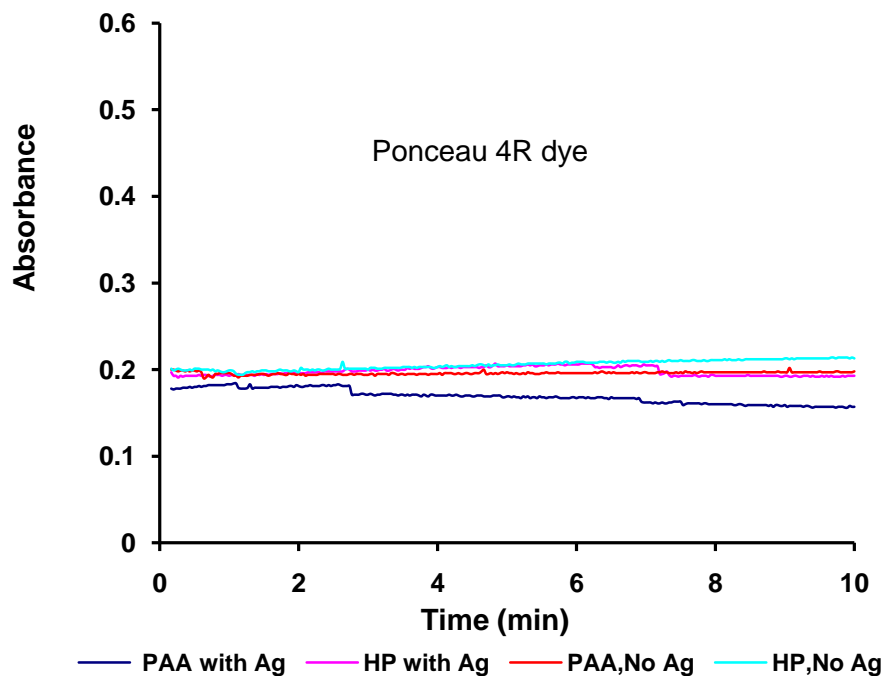


Figure 3.8B:- shows the change in dye Ponceau 4r absorption with, without the addition of Ag

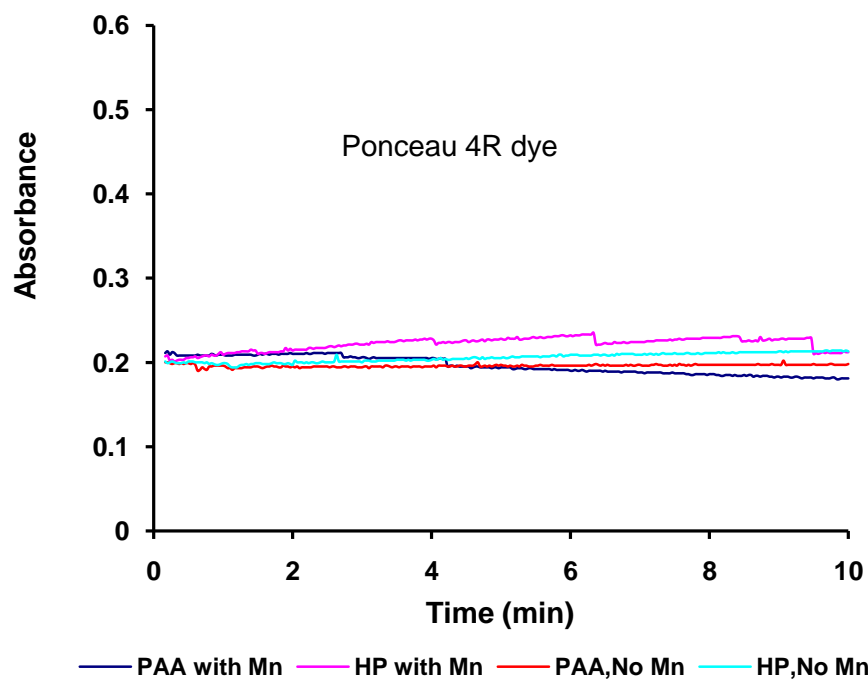


Figure 3.8C:- shows the change in dye Ponceau 4r absorption with, without the addition of Mn

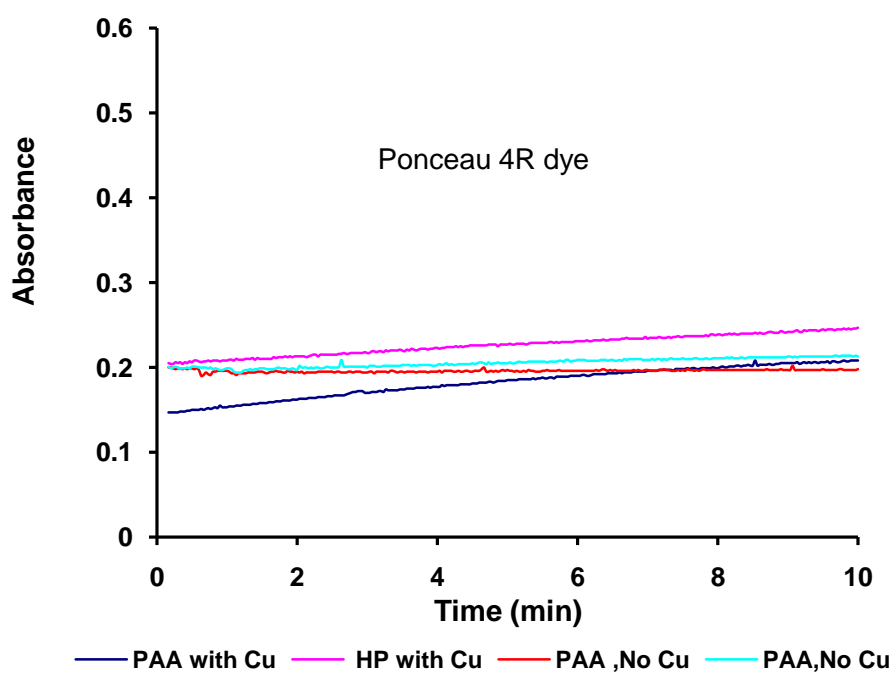


Figure 3.8D:- shows the change in dye Ponceau 4r absorption with, without the addition of Cu.

Figure 3.9:- shows the results for Orange I dye with solution of Peracetic acid and hydrogen peroxide with without metals.

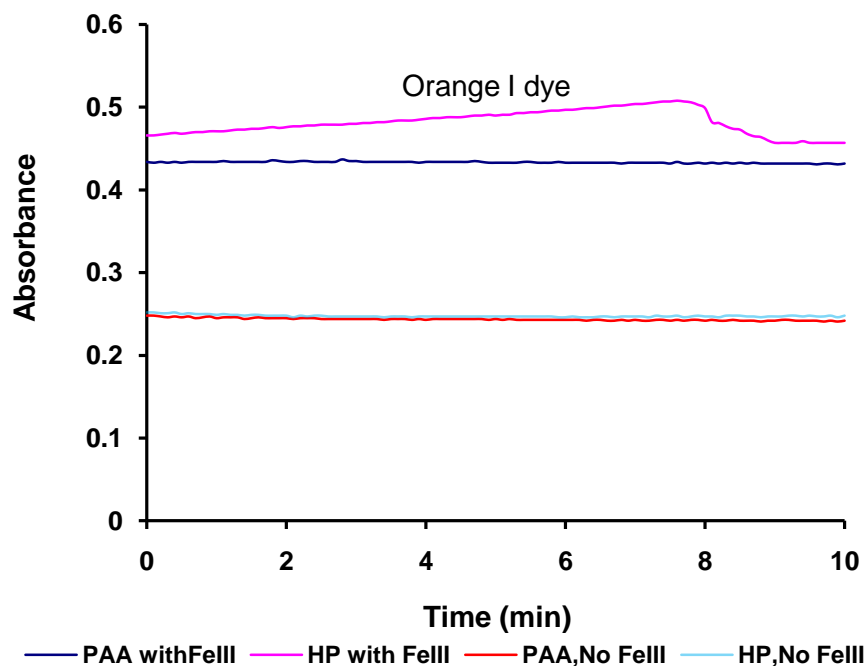


Figure 3.9A:- shows the change in Orange I dye absorption with, without the addition of Fe (III).

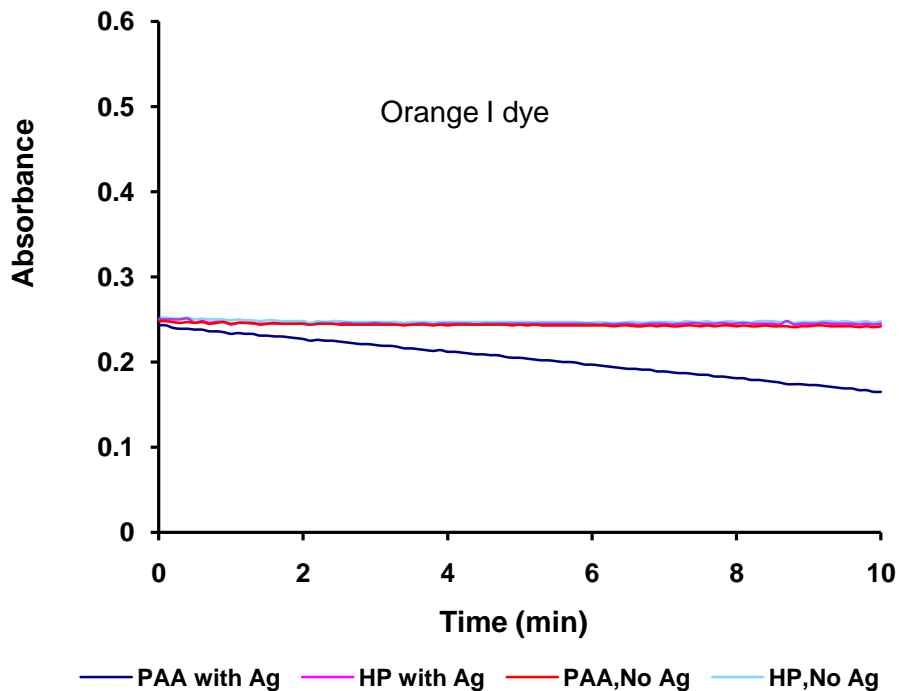


Figure 3.9B:- shows the change in Orange I dye absorption with, without the addition of Ag.

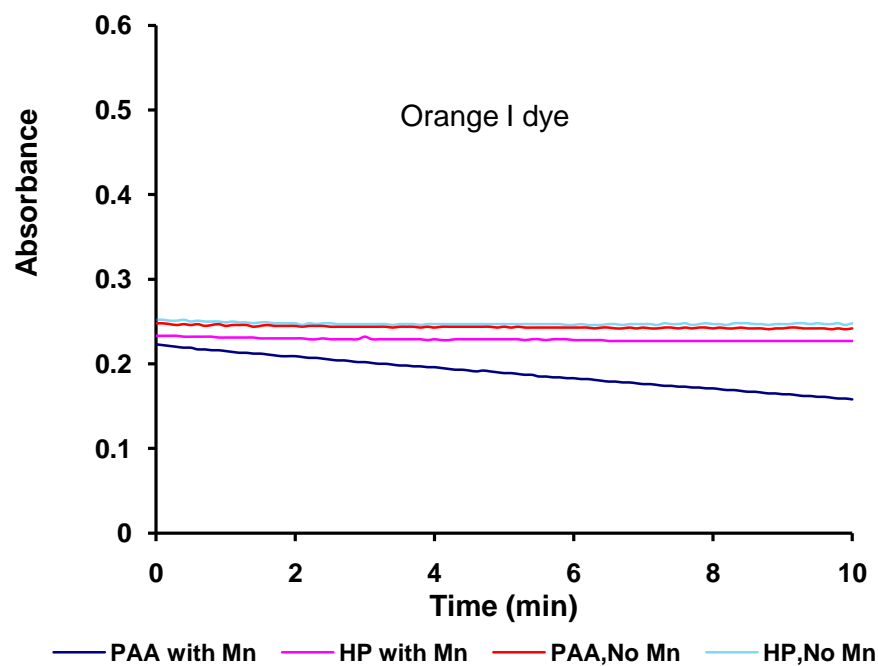


Figure 3.9C:- shows the change in Orange I dye absorption with, without the addition of Mn.

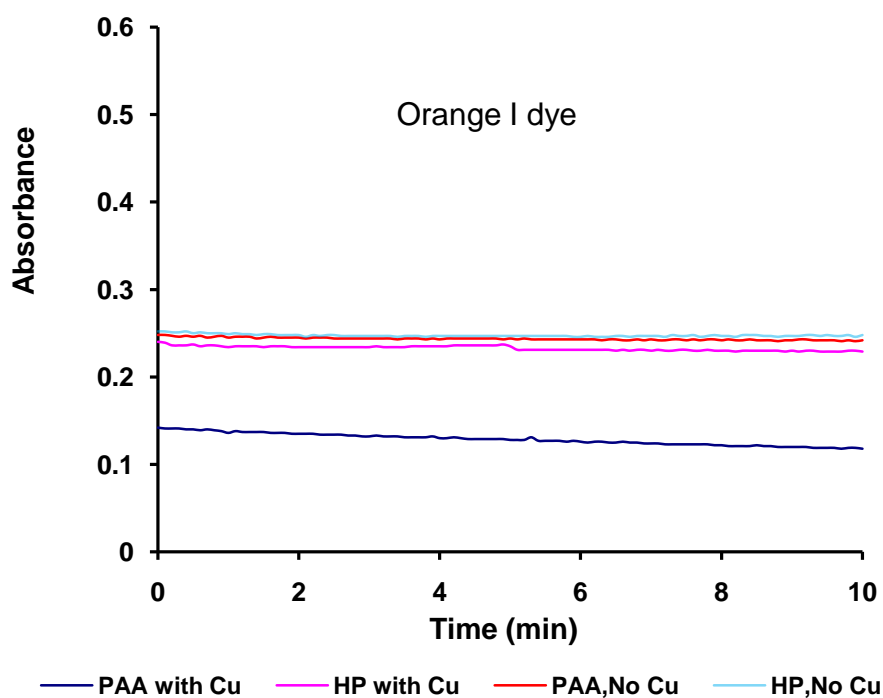


Figure 3.9D:- shows the change in Orange I dye absorption with, without the addition of Cu.

Figure 3.10:- shows the results for Orange II dye with solution of Peracetic acid and hydrogen peroxide with without metals

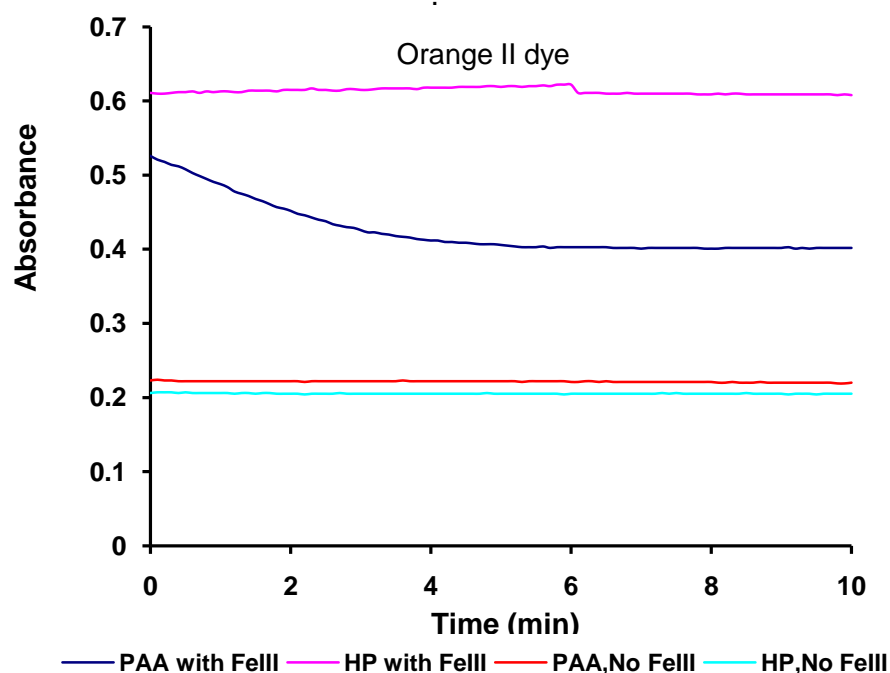


Figure 3.10A:- shows the change in Orange II dye absorption with, without the addition of Fe (III).

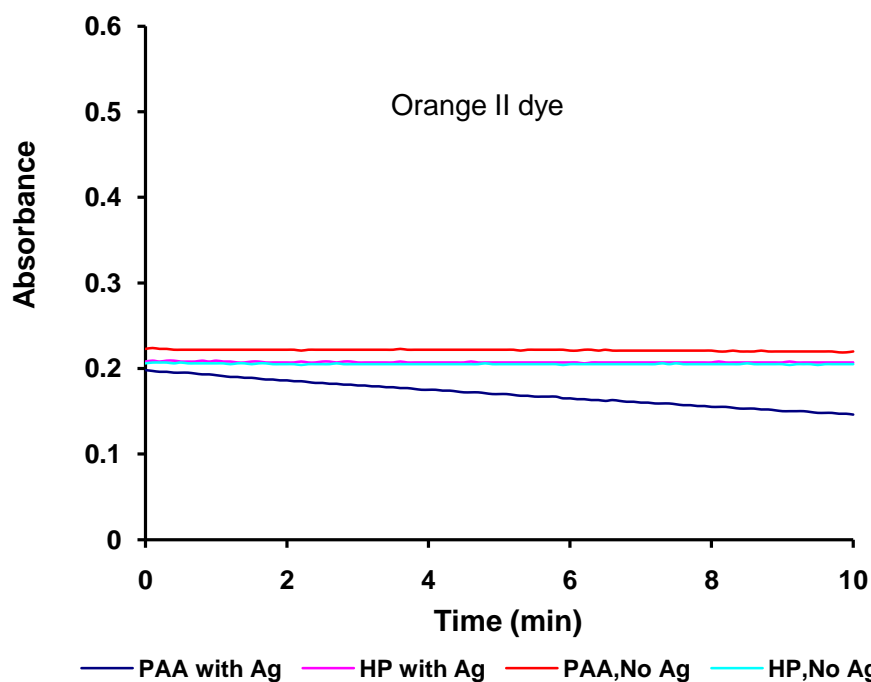


Figure 3.10B:- shows the change in Orange II dye absorption with, without the addition of Ag.

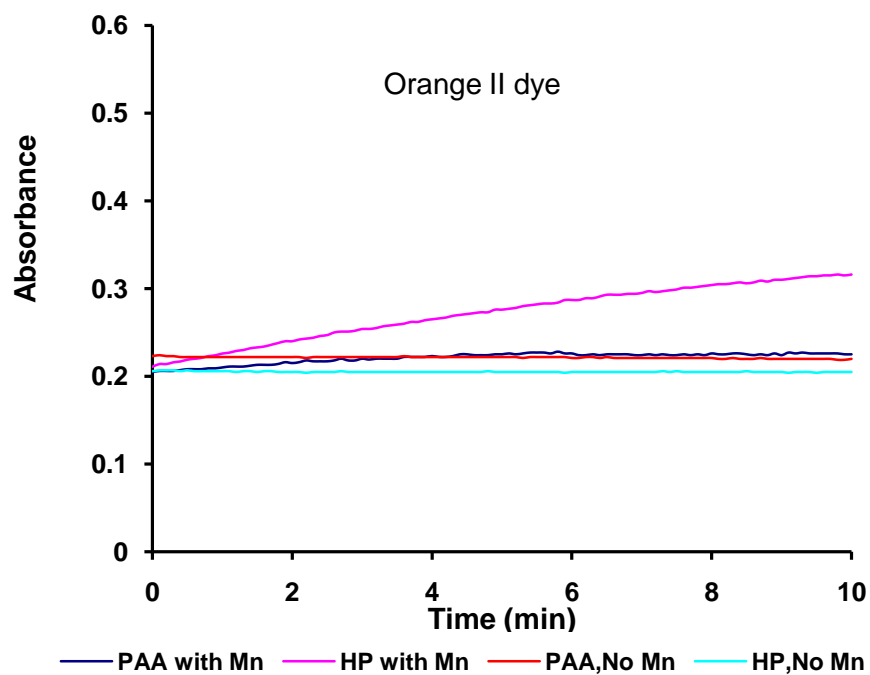


Figure 3.10C:- shows the change in Orange II dye absorption with, without the addition of Mn.

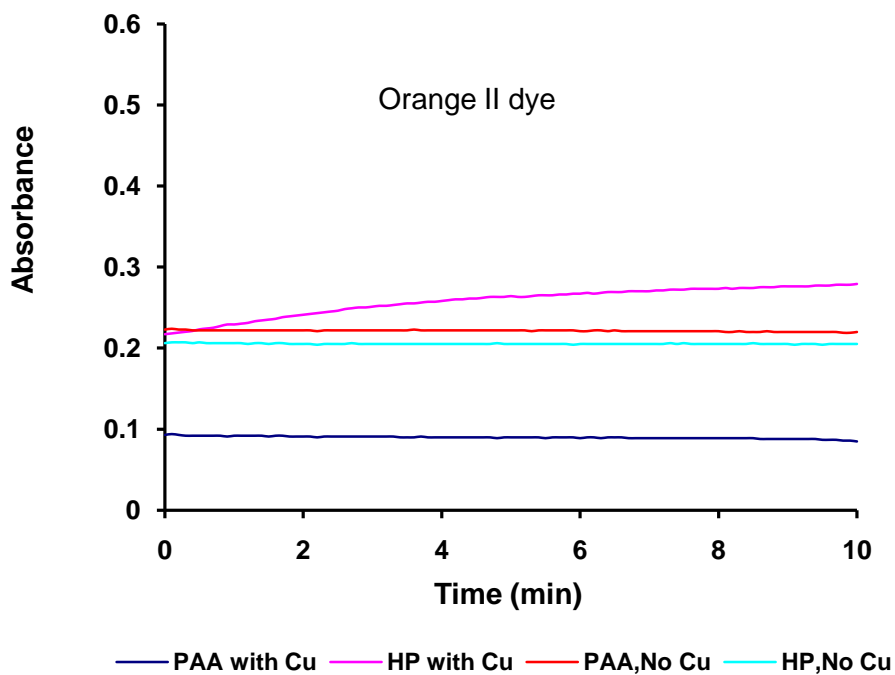


Figure 3.10D: - shows the change in Orange II dye absorption with, without the addition of Cu.

Figure 3.11:- shows the results for Black PN dye with solution of Peracetic acid and hydrogen peroxide with without metals.

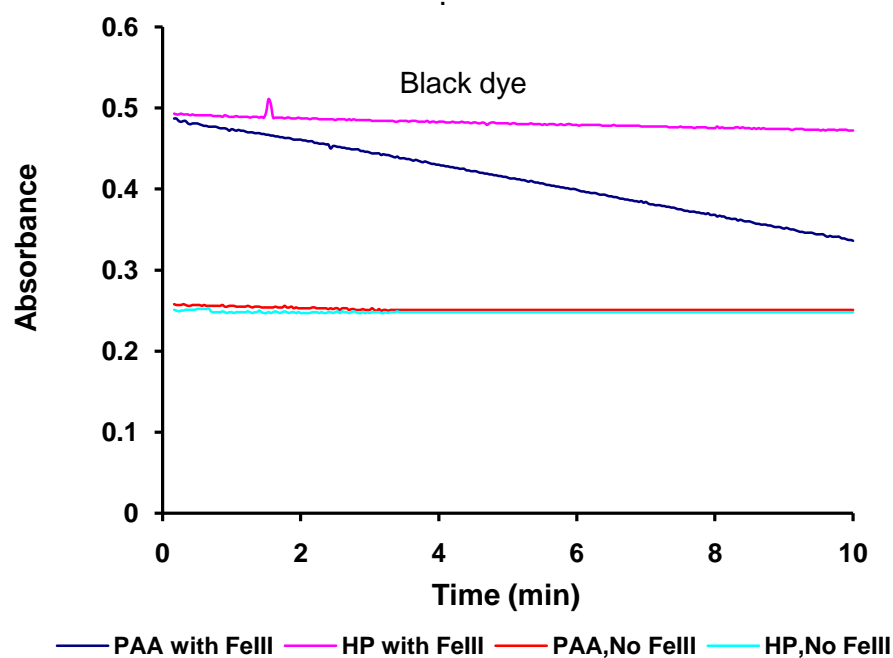


Figure 3.11A:- shows the change in dye Black PN absorption with, without the addition of Fe (III).

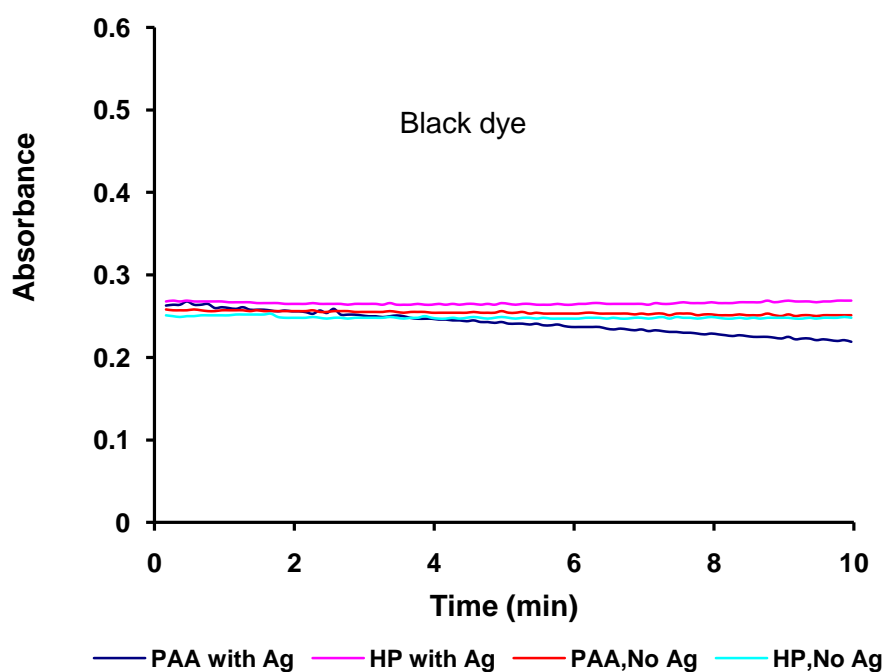


Figure 3.11B:- shows the change in dye Black PN absorption with, without the addition of Ag.

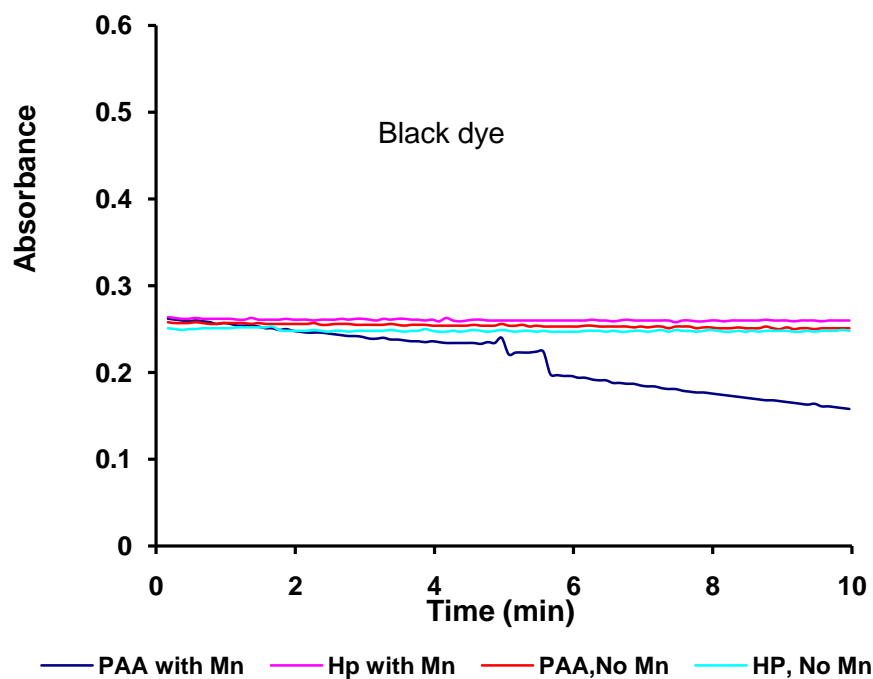


Figure 3.11C:- shows the change in Black PN dye absorption with, without the addition of Mn.

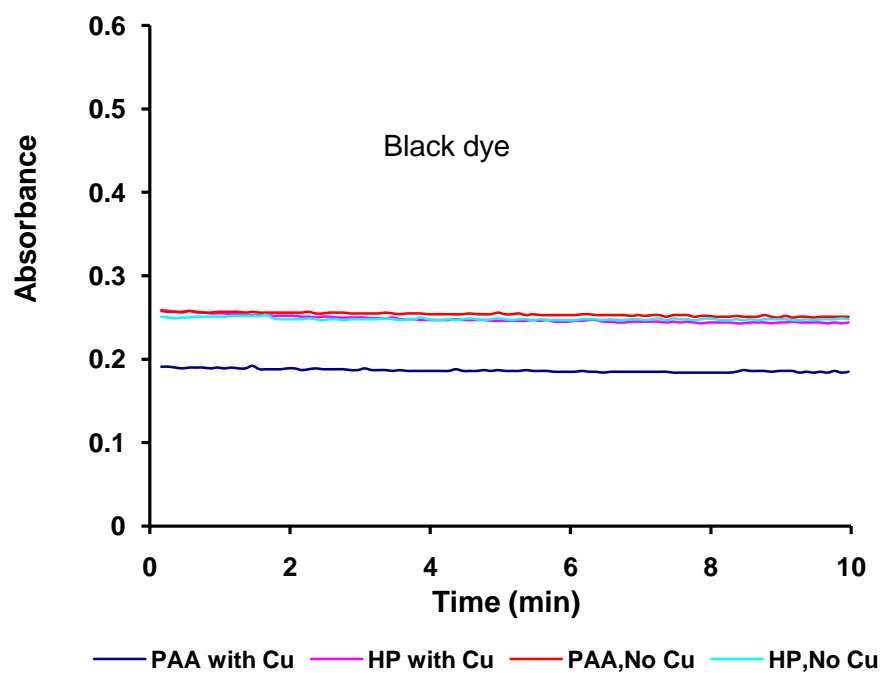


Figure 3.11D: - shows the change in Black PN dye absorption with, without the addition of Cu.

Figure 3.12:- shows the results for chocolate dye with solution of Peracetic acid and hydrogen peroxide with without metals

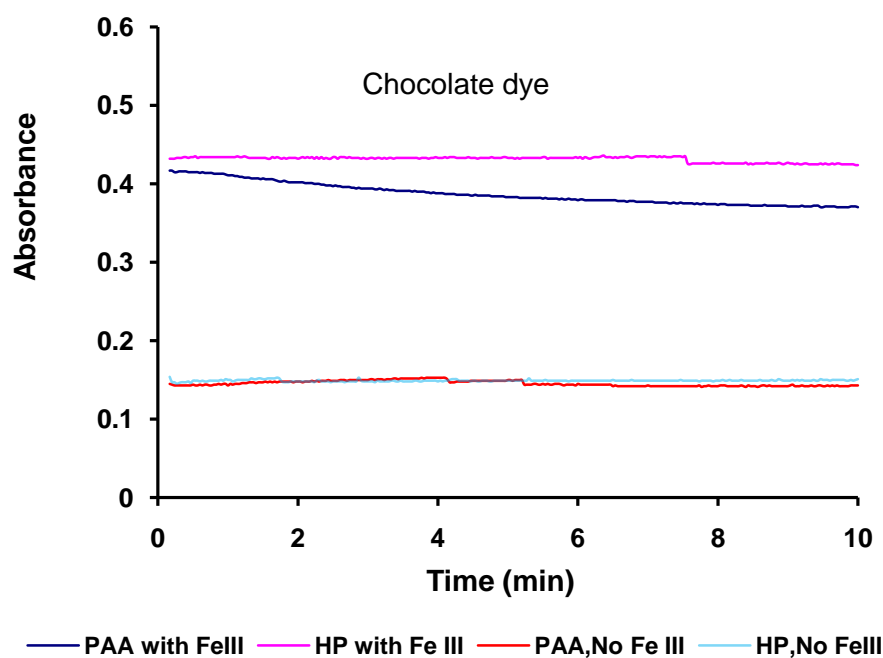


Figure 3.12A:- shows the change in dye chocolate absorption with, without the addition of Fe (III).

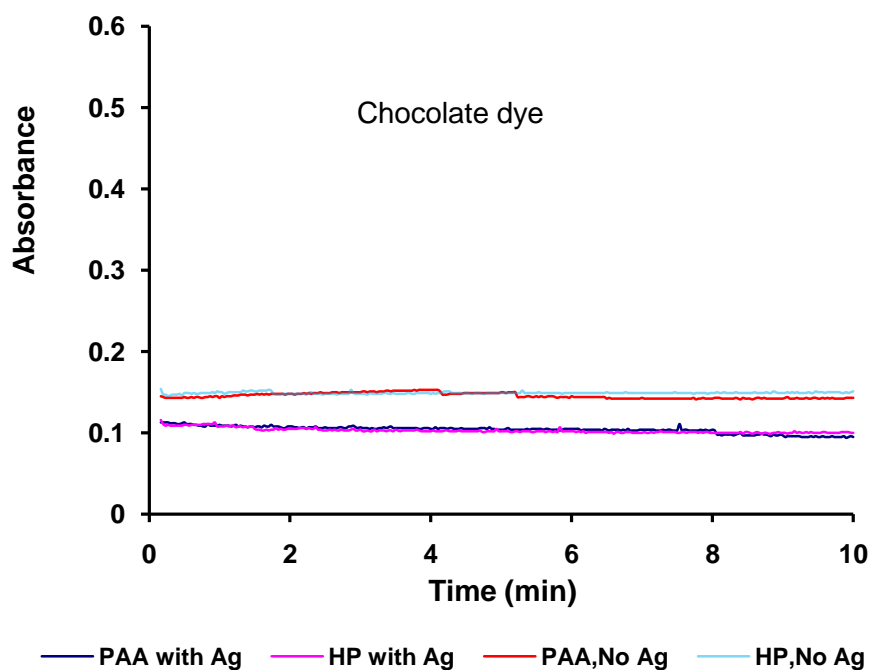


Figure 3.12B:- shows the change in dye chocolate absorption with, without the addition of Ag.

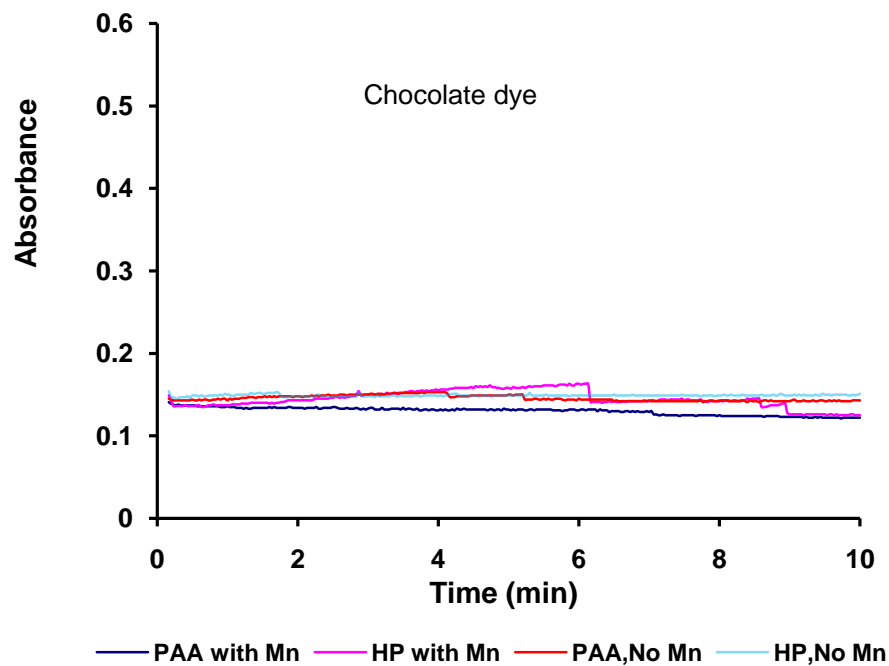


Figure 3.12C:- shows the change in dye chocolate absorption with, without the addition of Mn.

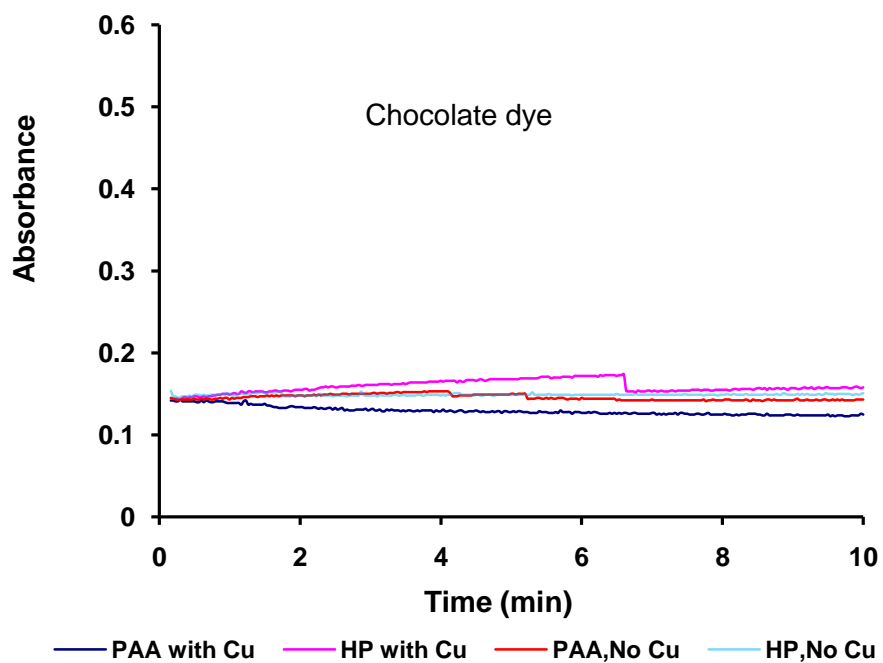


Figure 3.12D:- shows the change in dye chocolate absorption with, without the addition of Cu.

Figure 3.13:- shows the results for Green S with solution of Peracetic acid and hydrogen peroxide with without metals.

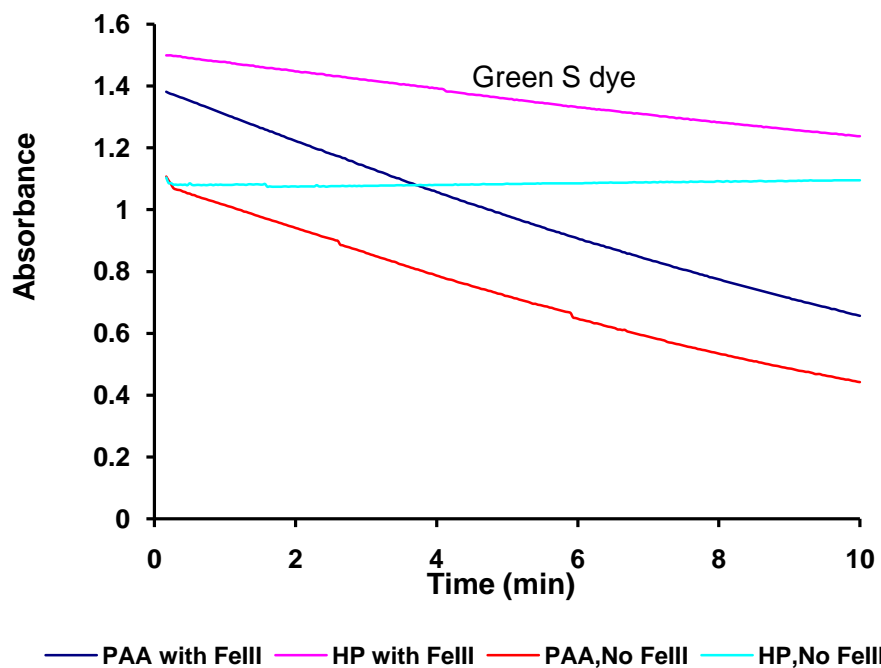


Figure 3.13A:- shows the change in dye Green S absorption with, without the addition of Fe (III).

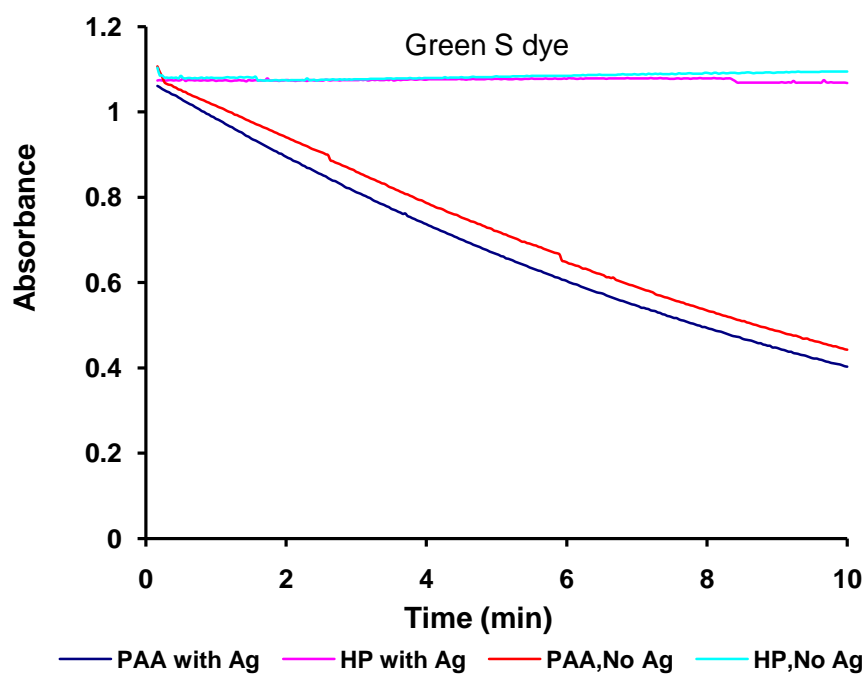


Figure 3.13B:- shows the change in dye Green S absorption with, without the addition of Ag.

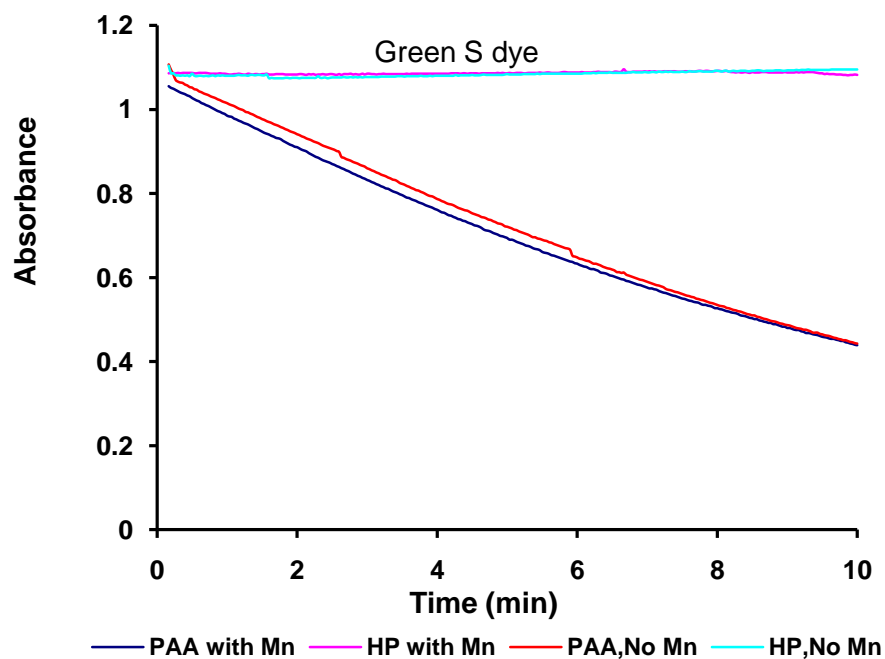


Figure 3.13C:- shows the change in dye Green S absorption with, without the addition of Mn.

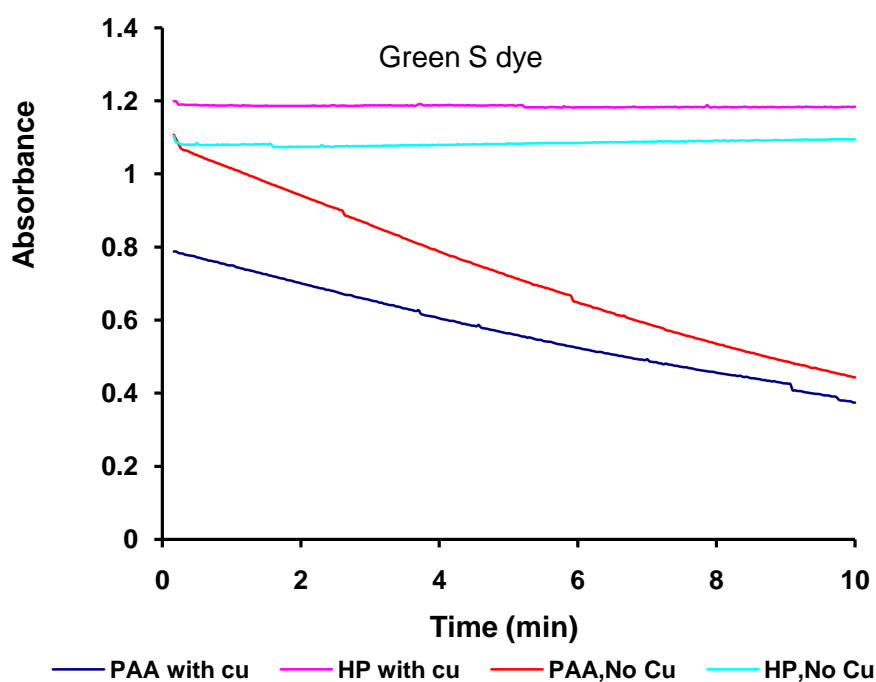


Figure 3.13D: - shows the change in dye Green S absorption with, without the addition of Cu.

Figure 3.14:- shows the results for Patent Blue dye with solution of Peracetic acid and hydrogen peroxide with without metals.

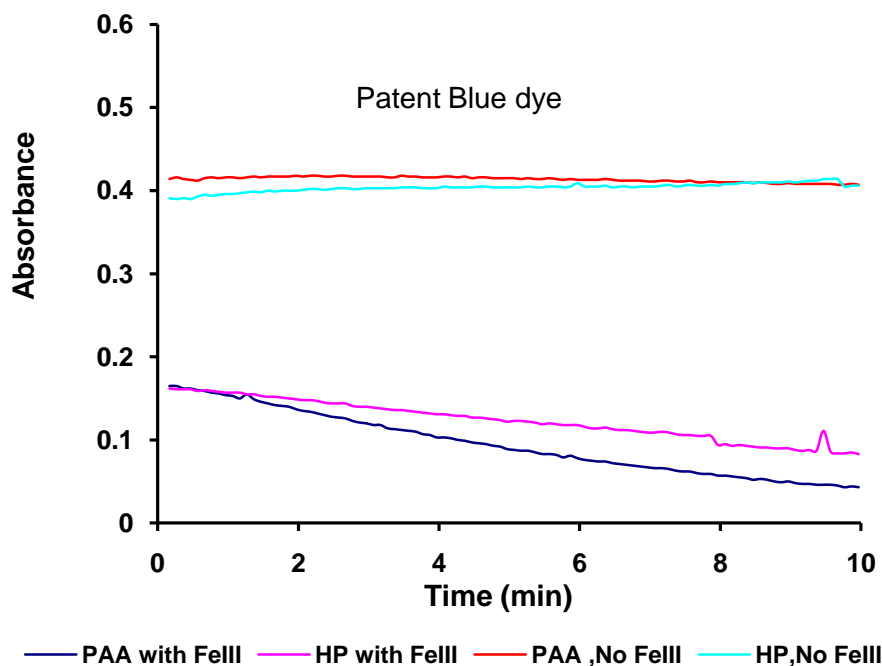


Figure 3.14A:- shows the change in dye Patent Blue absorption with, without the addition of Fe (III).

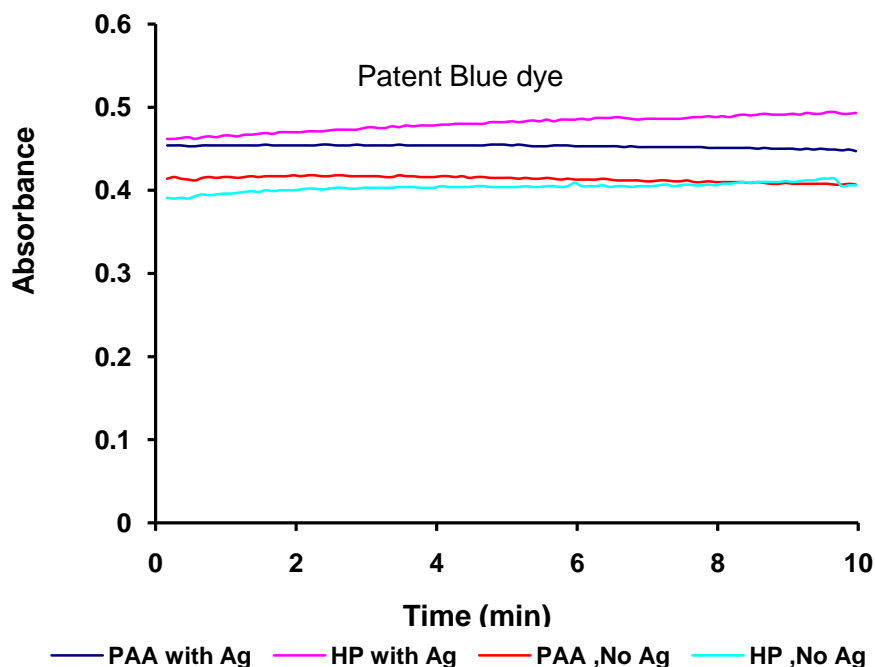


Figure 3.14B:- shows the change in dye Patent Blue absorption with, without the addition of Ag.

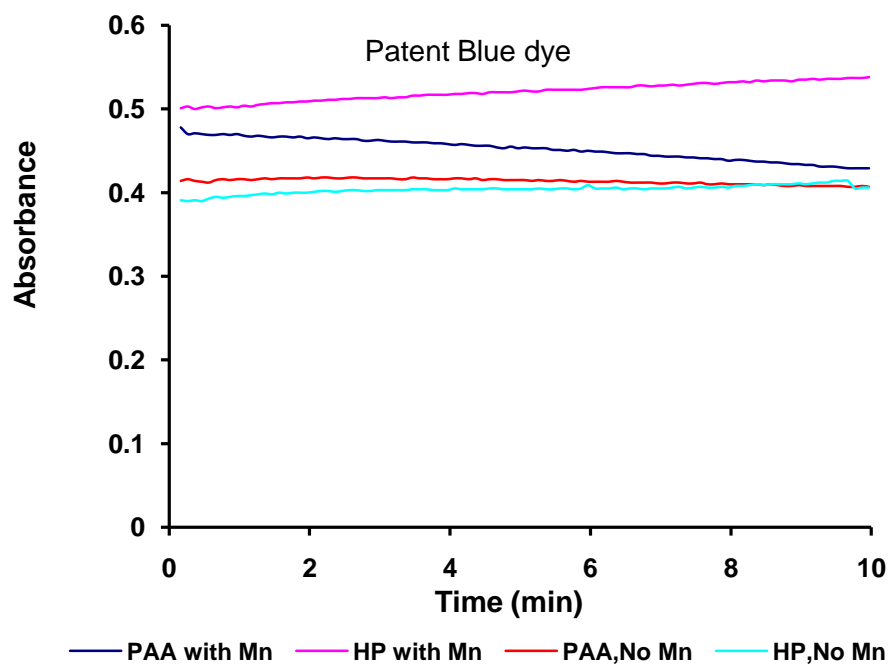


Figure 3.14C:- shows the change in dye Patent Blue absorption with, without the addition of Mn.

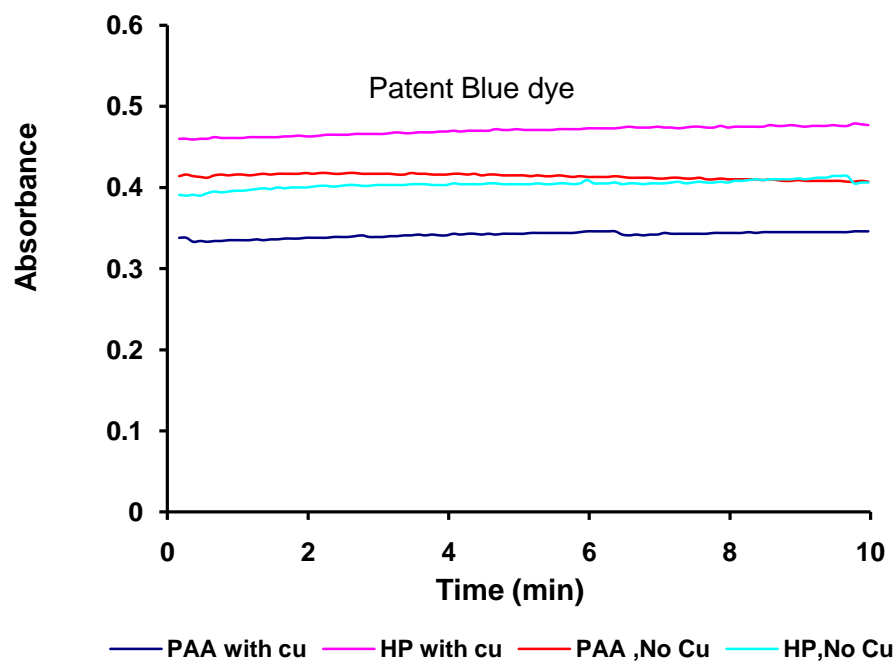


Figure 3.14D: - shows the change in dye Patent Blue absorption with, without the addition of Cu.

Figure 3.15: - shows the results for Brilliant Blue dye with solution of Peracetic acid and hydrogen peroxide with without metals.

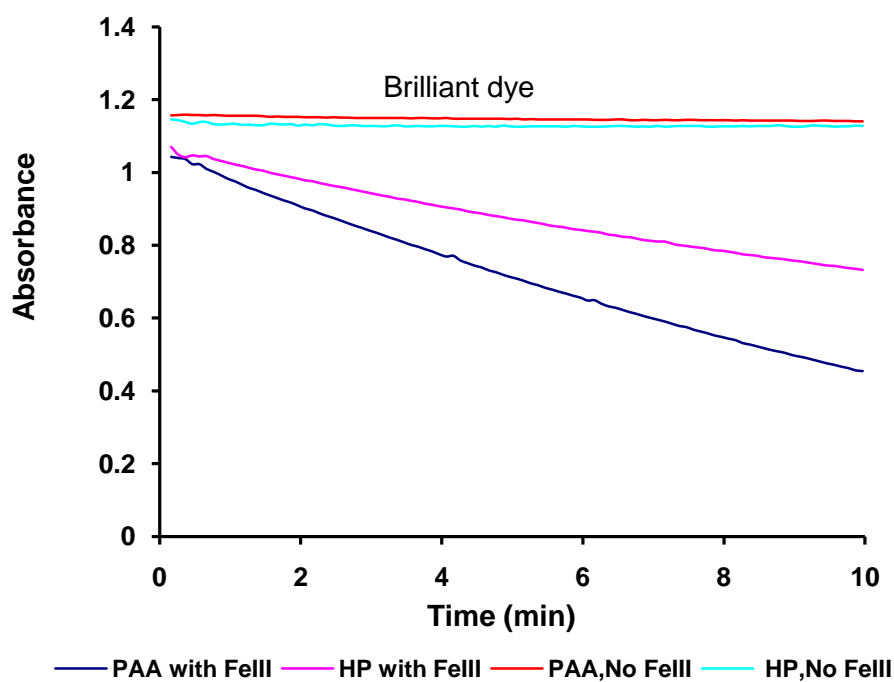


Figure 3.15A:- shows the change in dye Brilliant Blue absorption with, without the addition of Fe (III).

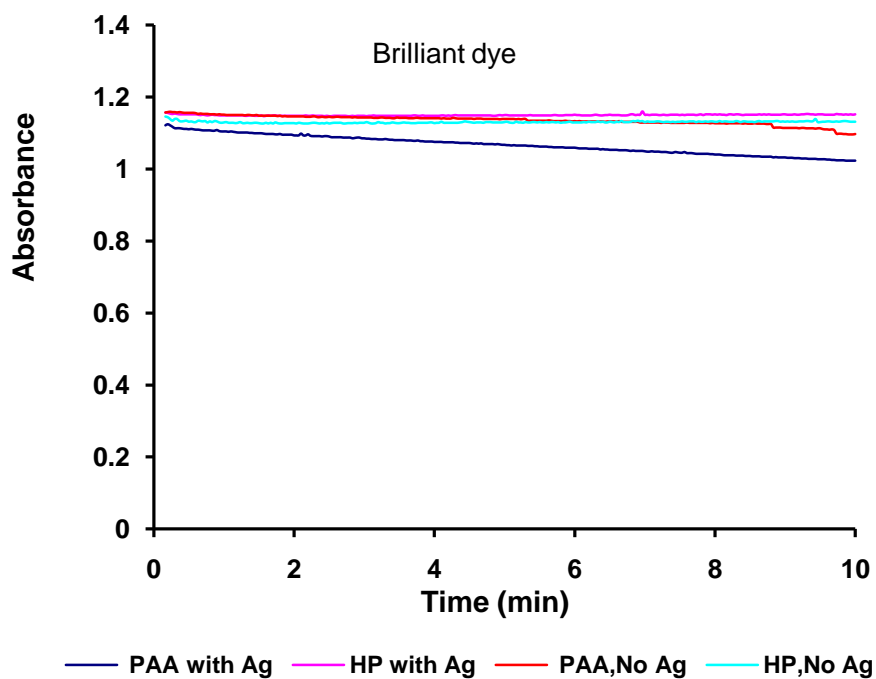


Figure 3.15B:- shows the change in dye Brilliant Blue absorption with, without the addition of Ag.

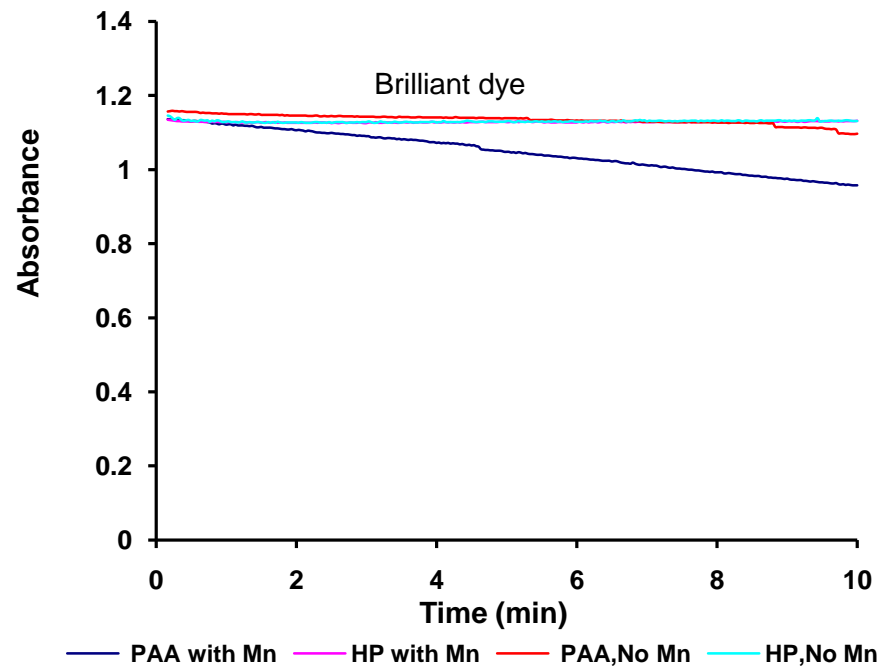


Figure 3.15C:- shows the change in dye Brilliant Blue absorption with, without the addition of Mn.

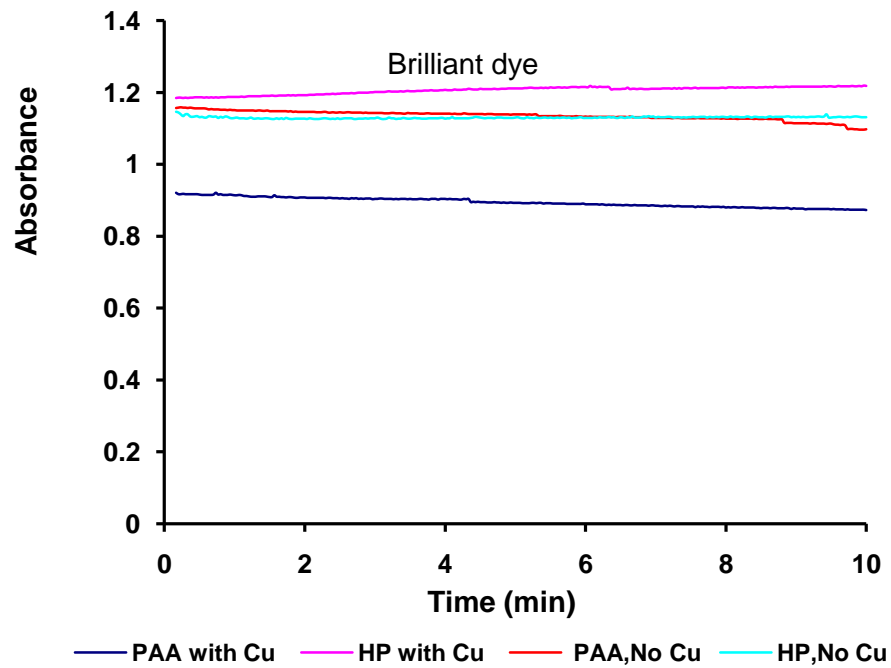
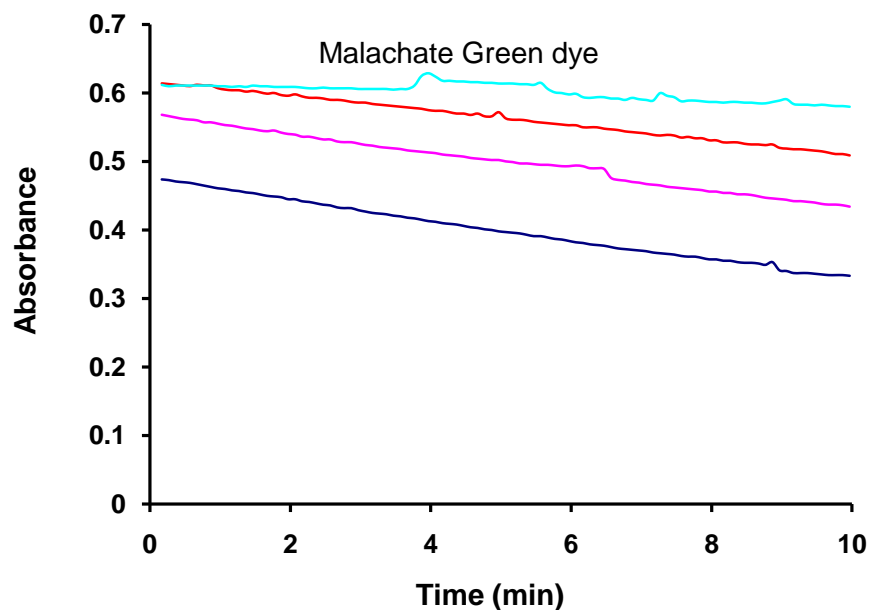


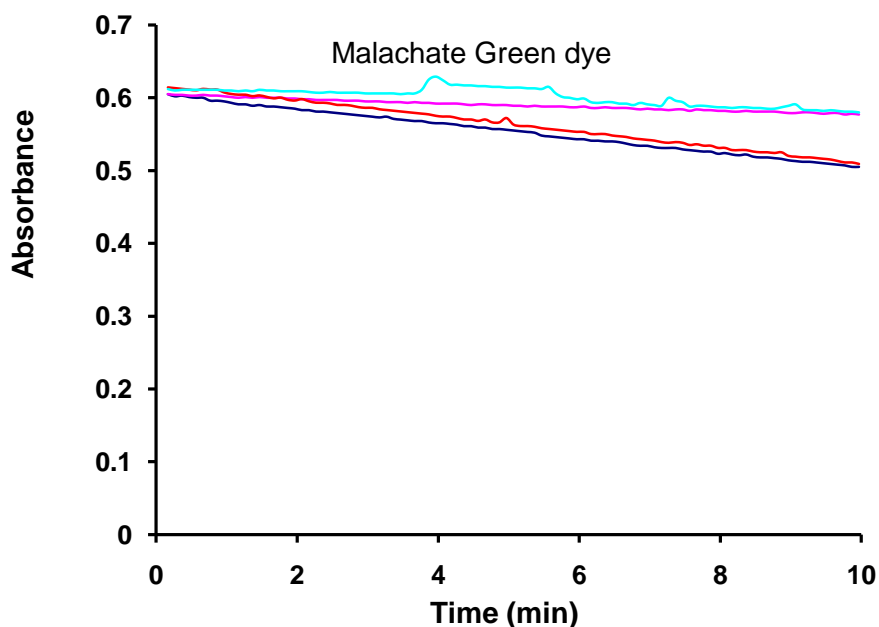
Figure 3.15D: - shows the change in dye Brilliant Blue absorption with, without the addition of Cu.

Figure 3.16:- shows the results for Malachite green dye with solution of Peracetic acid and hydrogen peroxide with without metals.



— PAA with FeIII — HP with FeIII — PAA No FeIII — HP No FeIII

Figure 3.16A:- shows the change in dye Malachite green absorption with, without the addition of Fe (III).



— PAA with Ag — HP with Ag — PAA, No Ag — HP, No Ag

Figure 3.16B:- shows the change in dye Malachite green absorption with, without the addition of Ag.

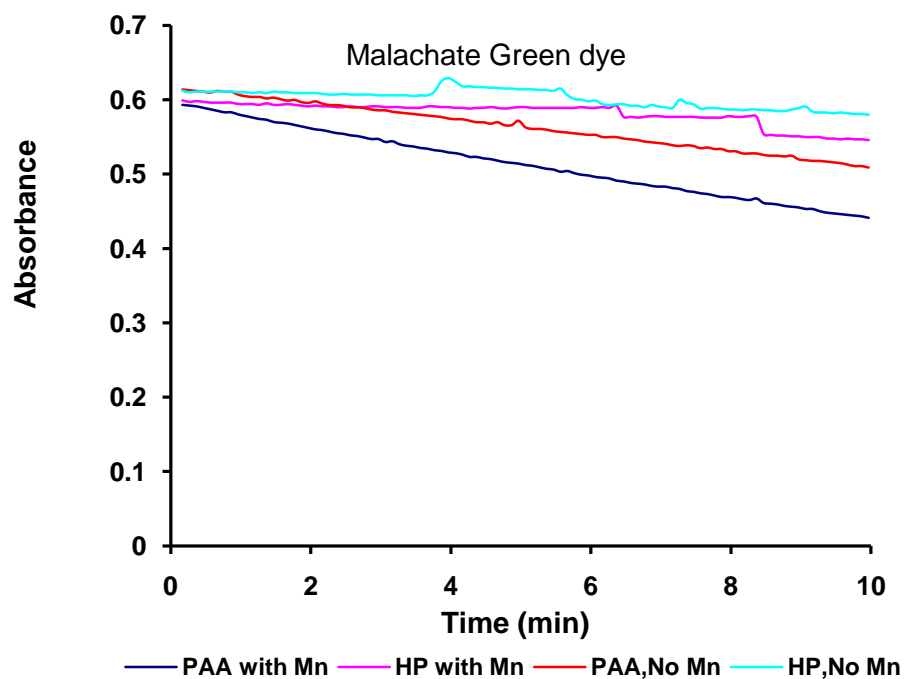


Figure 3.16C:- shows the change in dye Malachite green absorption with, without the addition of Mn.

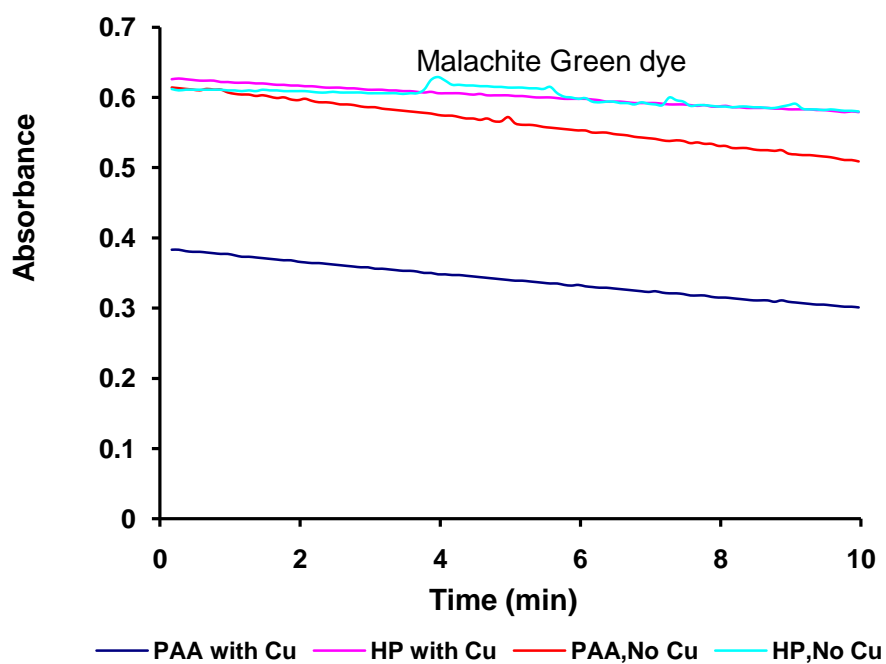
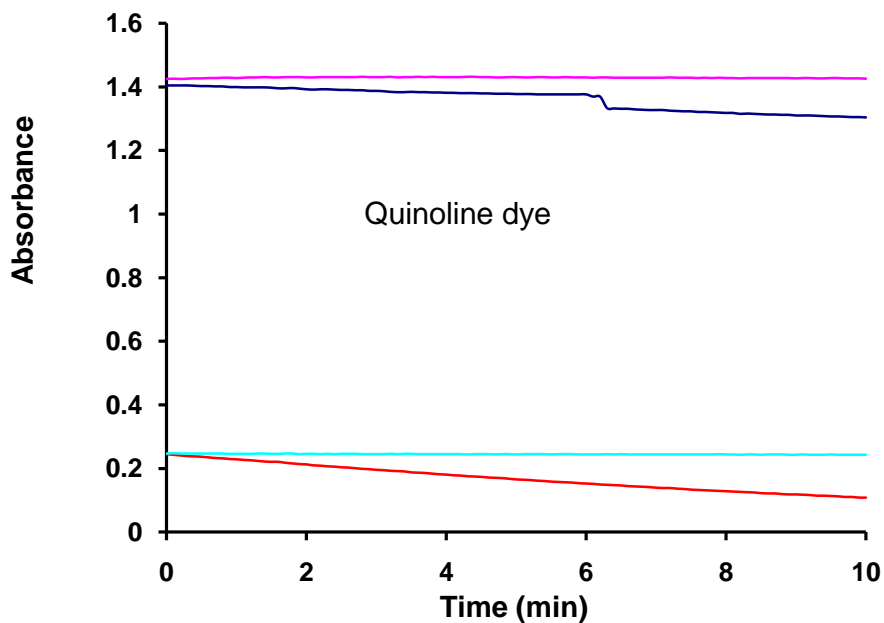


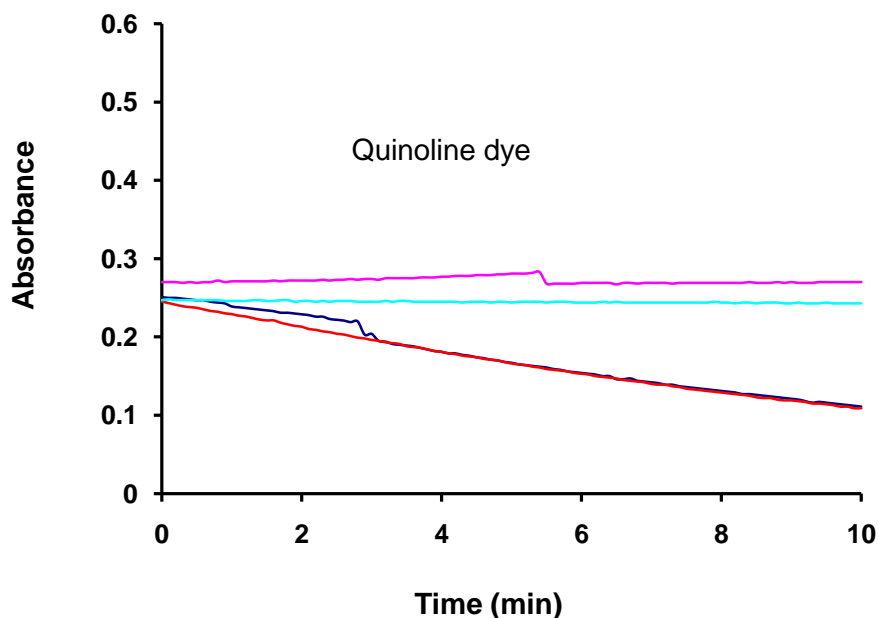
Figure 3.16D: - shows the change in dye Malachite green absorption with, without the addition of Cu.

Figure 3.17:- shows the results for Quinoline yellow dye with solution of Peracetic acid and hydrogen peroxide with without metals.



— PAA with FeIII — HP with FeIII — PAA, No FeIII — HP, No FeIII

Figure 3.17A:- shows the change in dye Quinoline yellow absorption with, without the addition of Fe (III).



— PAA with Ag — HP with Ag — PAA, No Ag — HP, No Ag

Figure 3.17B:- shows the change in dye Quinoline yellow absorption with, without the addition of Ag.

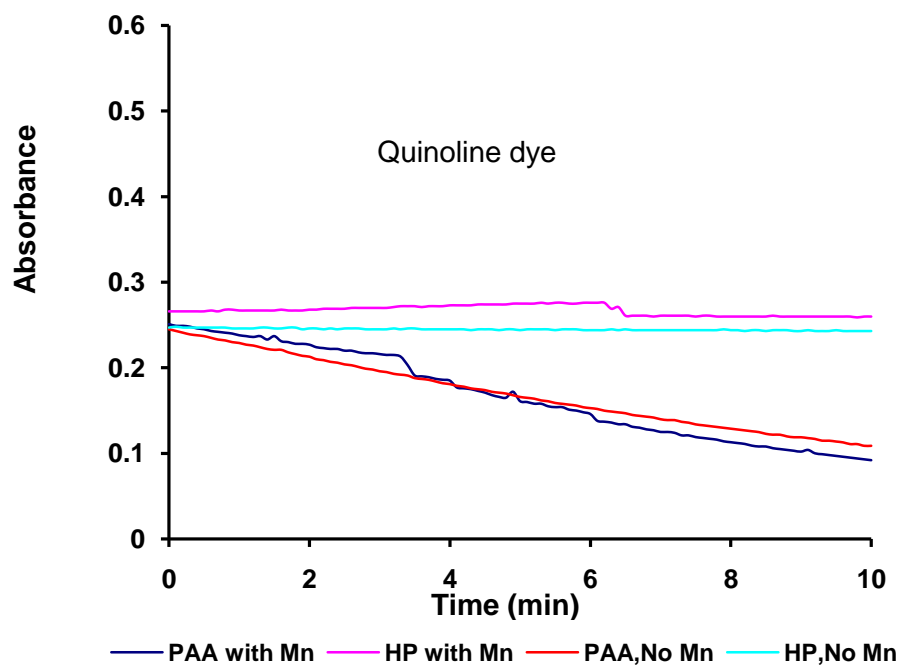


Figure 3.17C:- shows the change in dye Quinoline yellow absorption with, without the addition of Mn.

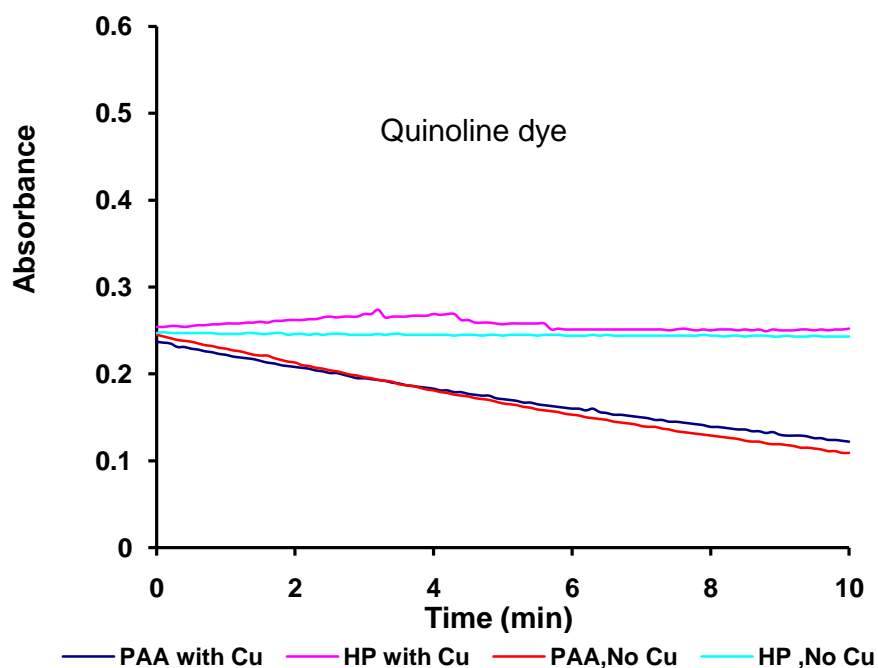


Figure 3.17D: - shows the change in dye Quinoline yellow absorption with, without the addition of Cu.

Figure 3.18:- shows the results for Erythrosine dye with solution of Peracetic acid and hydrogen peroxide with without metals.

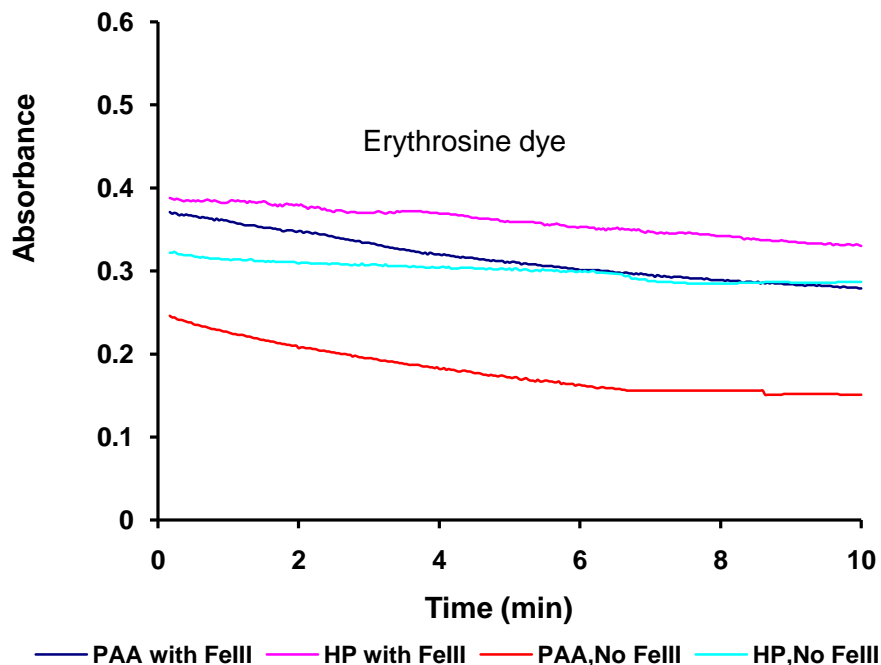


Figure 3.18A:- shows the change in dye erythrosine absorption with, without the addition of Fe (III).

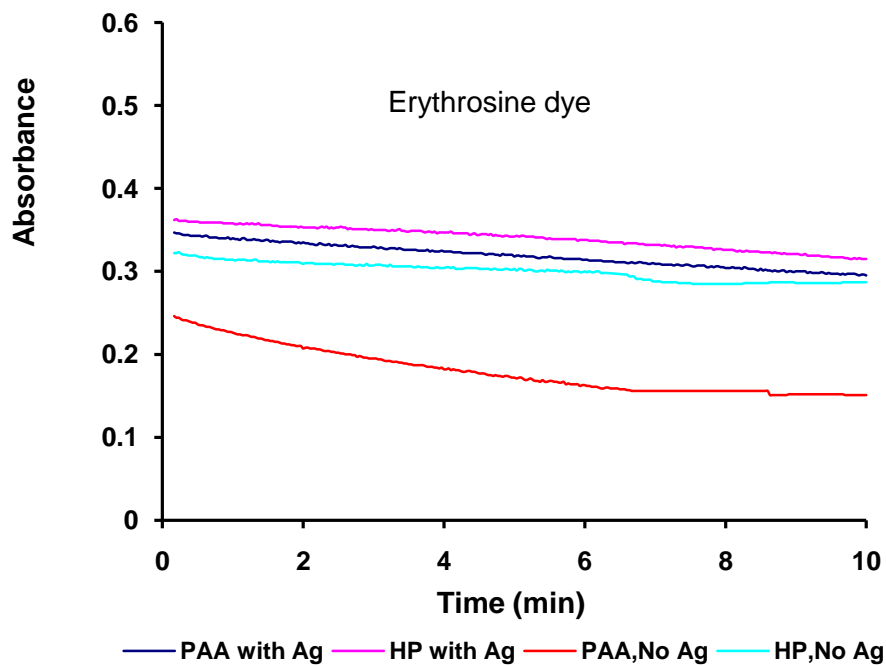


Figure 3.18B:- shows the change in dye erythrosine absorption with, without the addition of Ag.

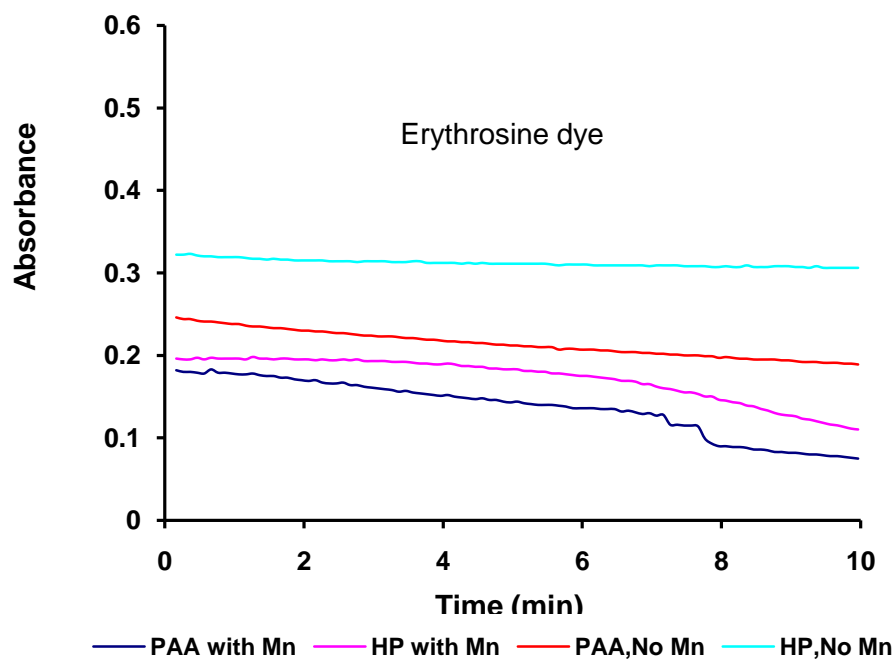


Figure 3.18C:- shows the change in dye erythrosine absorption with, without the addition of Mn.

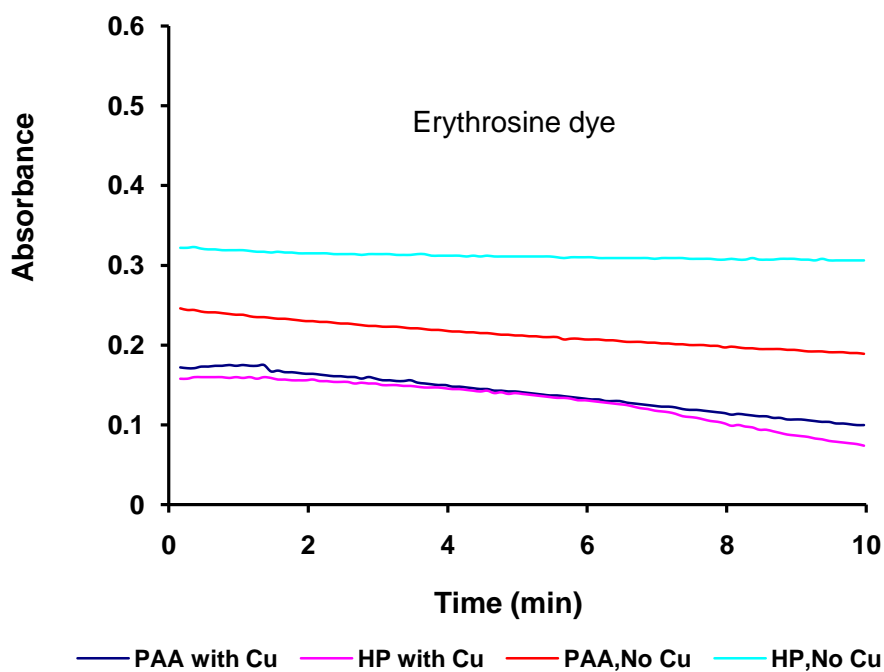


Figure 3.18D: - shows the change in dye erythrosine absorption with, without the addition of Cu.

Figure 3.19:- shows the results for indigo carmine dye with solution of Peracetic acid and hydrogen peroxide with without metals.

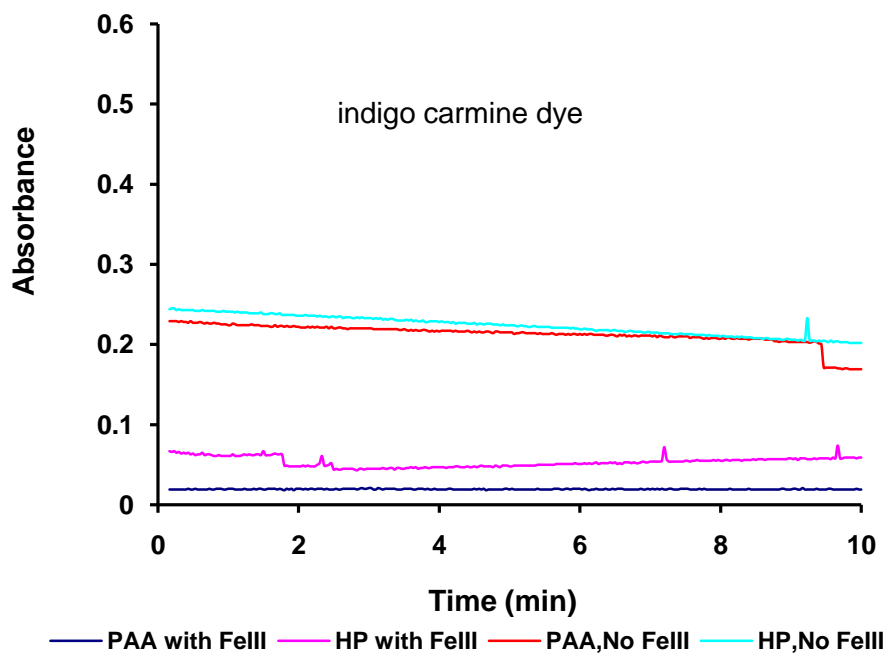


Figure 3.19A:- shows the change in indigo carmine dye absorption with, without the addition of Fe (III).

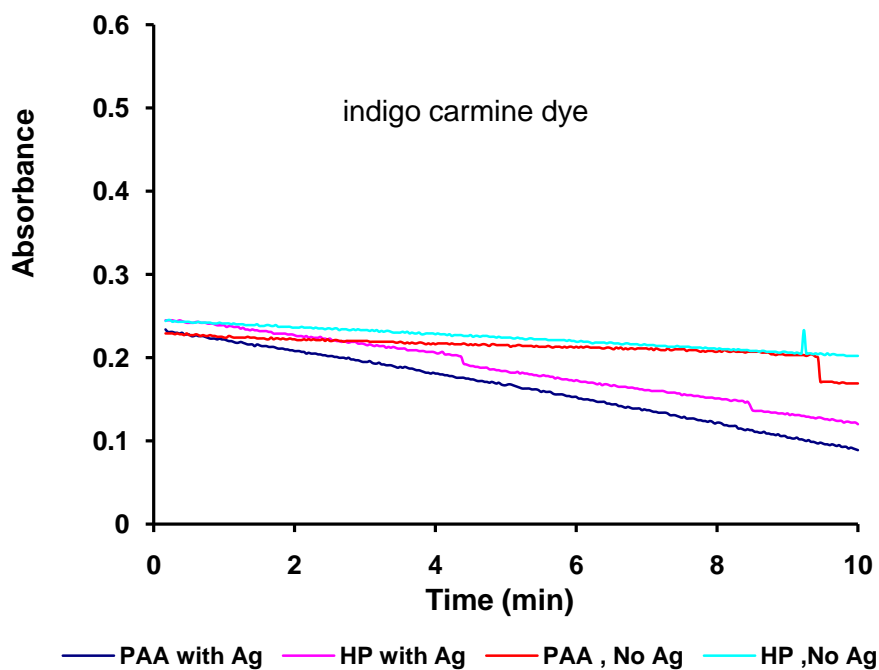


Figure 3.19B:- shows the change in indigo carmine dye absorption with, without the addition of Ag.

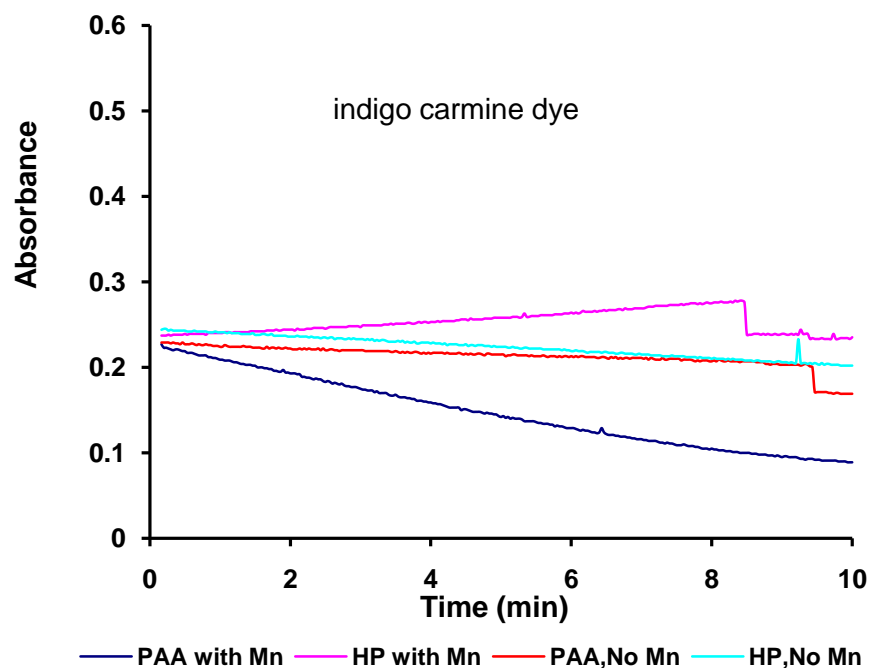


Figure 3.19C:- shows the change in indigo carmine dye absorption with, without the addition of Mn.

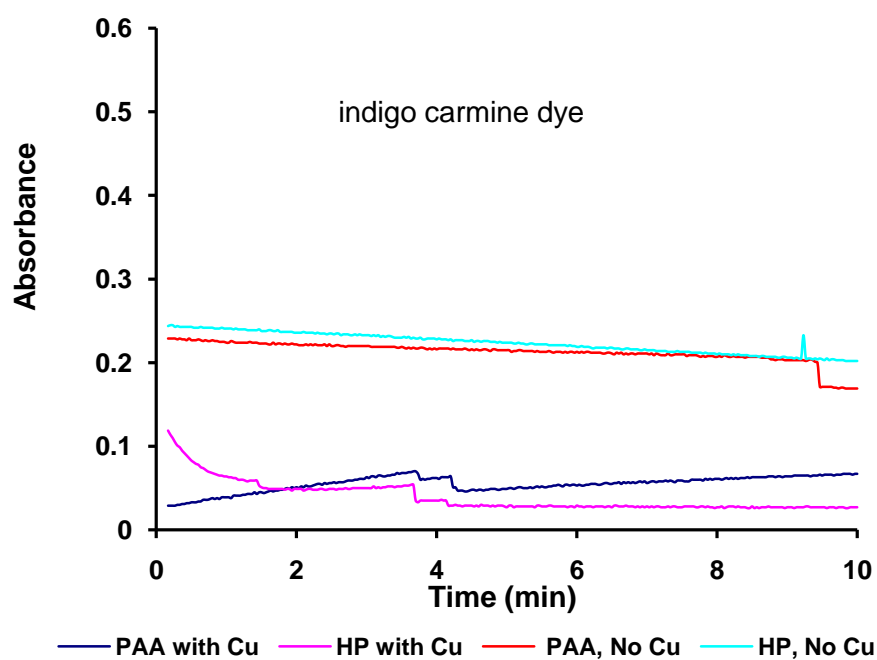


Figure 3.19D: - shows the change in indigo carmine dye absorption with, without the addition of Cu.

Figure 3.20:- shows the results for Acid Green 25 dye with solution of Peracetic acid and hydrogen peroxide with without metals.

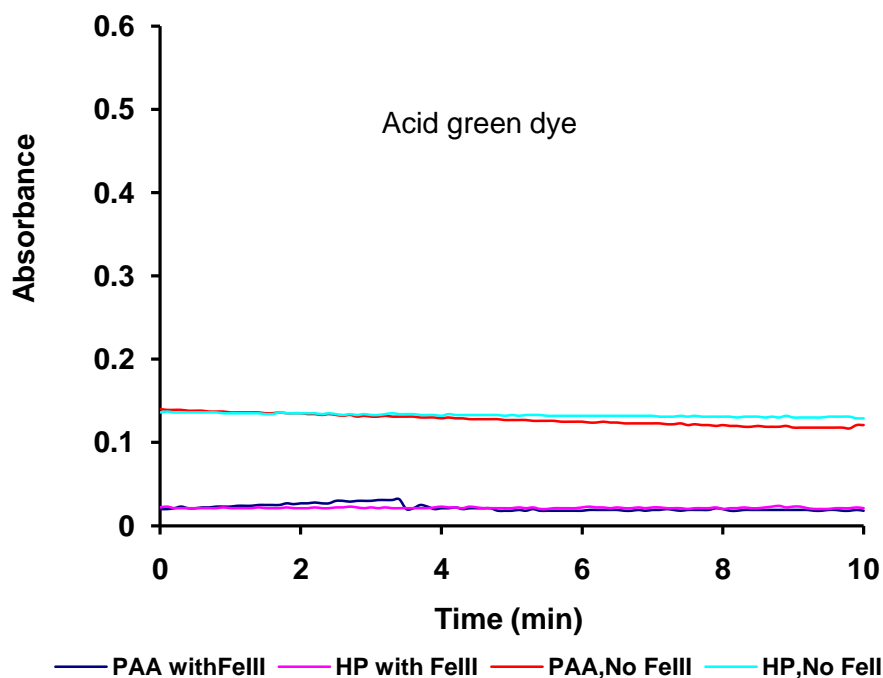


Figure 3.20A:- shows the change in Acid Green 25 dye absorption with, without the addition of Fe (III)

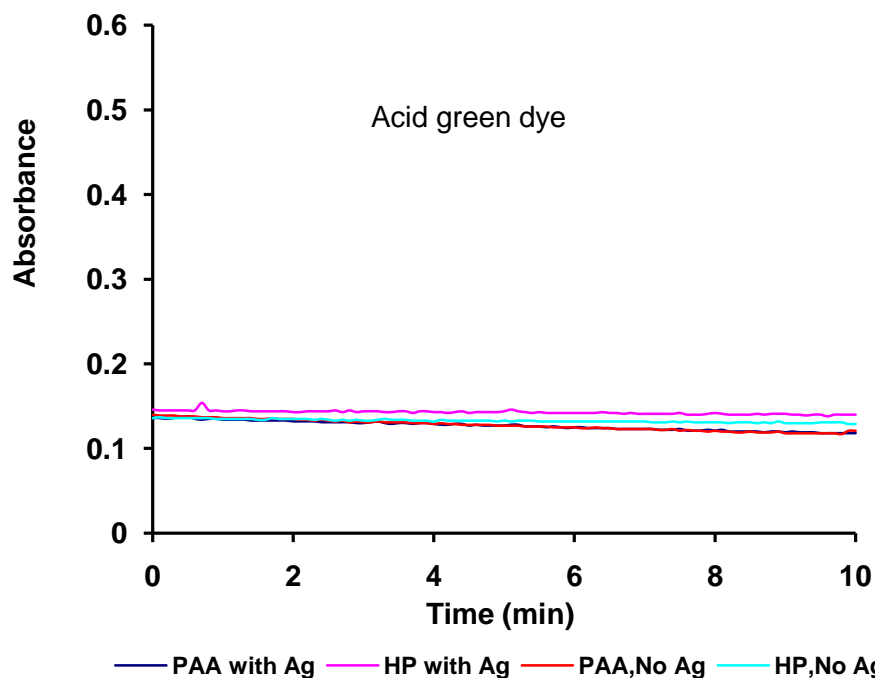


Figure 3.20B:- shows the change in Acid Green 25 dye absorption with, without the addition of Ag.

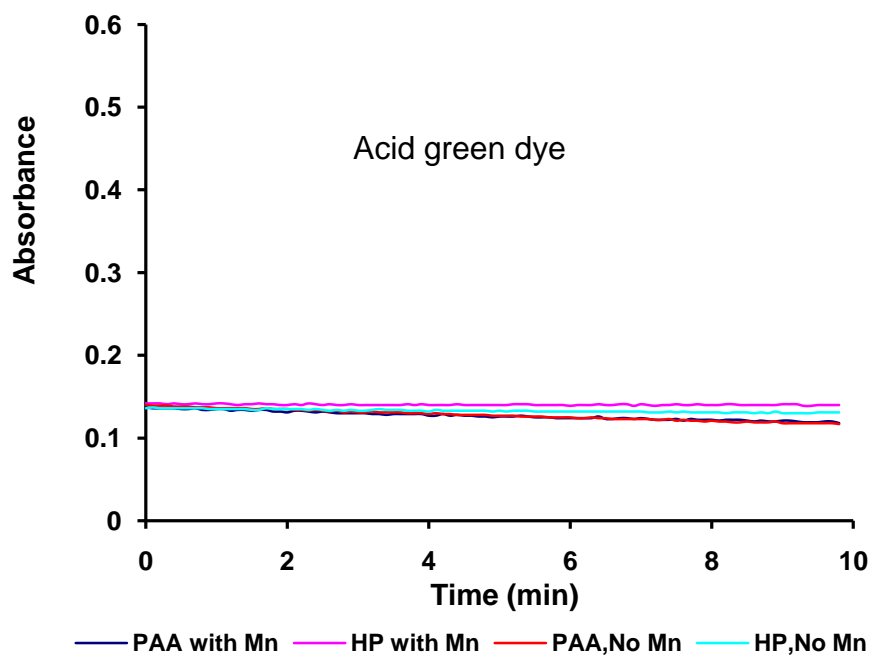


Figure 3.20C:- shows the change in Acid Green 25 dye absorption with, without the addition of Mn.

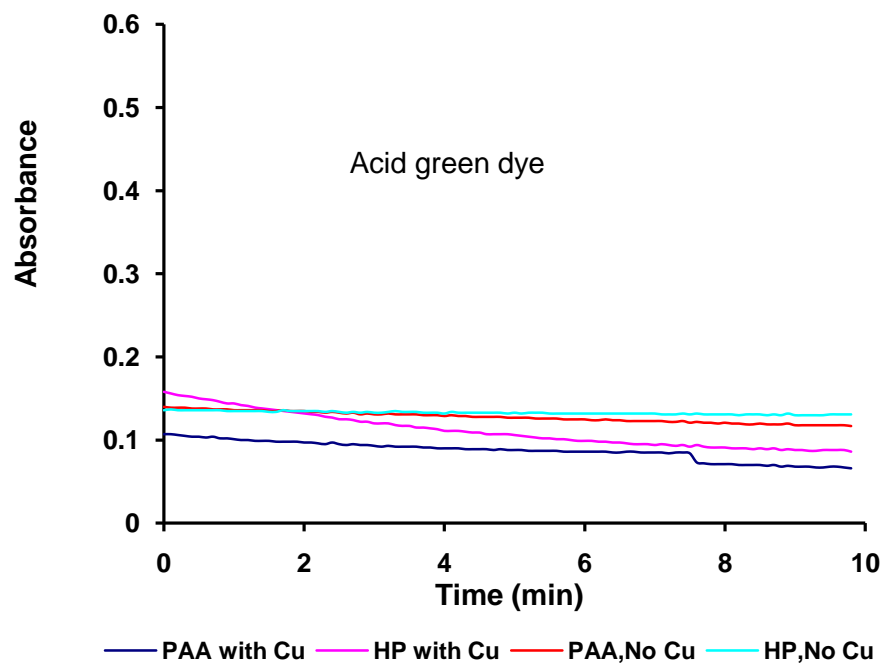


Figure 3.20D: - shows the change in Acid Green 25 dye absorption with, without the addition of Cu.

Chapter 4. Iron catalysed oxidation of azo dyes by peracetic acid.

4.1. Introduction

Many processes have been used and/or researched for dye decolourization. A brief description of each dye decolourization process compiled from the literature is given in Chapter 1. However, not all processes work for all coloured wastewaters and this has driven research in this area. Some studies have reported successful decolourization using different treatment schemes, despite the fact that the treated wastewater still has low colour intensity. Only a few cases have been reported with complete decolourization and dye mineralization.

Therefore, the aim of this chapter is to evaluate the decolourization of azo dyes under conditions of bleaching by peracetic acid in the presence of iron (III) as a catalyst. These conditions were applied to five azo dyes: Amaranth, Ponceau 4r, Orange II, Carmosine and Black PN dyes. From the bleaching studies carried out in Chapter 3 it is clear that all of these dyes react appreciably with peracetic acid in the presence of iron, yet only to a small extent with hydrogen peroxide in the presence of iron; other metal ions had variable effects. The lack of appreciable reaction of these dyes with hydrogen peroxide in the presence of iron may indicate that reactions involving the hydroxyl free radical, as discussed in Chapter 3, are not the main route in the degradation of these dyes. Moreover, the observation in Chapter 3 of significant absorbance changes (increases) upon mixing the dyes and iron ions indicates the formation of an iron-dye complex, as suggested in Scheme 3.3, in which the iron bridges an azo nitrogen and the oxygen of the hydroxyl group that is ortho to the azo group; this complex may activate the dye to attack by peracetic acid. It is also noteworthy that Orange I, in which the hydroxyl group is para to the azo group, also shows an absorbance increase in the presence of iron (Figure 3.7a) indicating that bridging between an azo nitrogen and the oxygen of an ortho-substituted hydroxyl group is not necessary for azo dye – iron complexes to form; in this case, however, neither the dye nor the dye-iron complex are reactive towards peracetic acid or hydrogen peroxide.

This chapter reports on the decolourization rates and extents of five azo dyes when reacted with peracetic acid in the presence of iron (III) as a catalyst. A range of experiments were carried out in which pH and the concentrations of the dye, peracetic acid and iron (III) were varied; this should give information on the optimal conditions for achieving maximum decolourisation..

4.2 . Experimental

4.2.1. Materials

4.2.1.1.Peracetic acid and other materials

Peracetic acid was prepared from acetic acid and hydrogen peroxide in sulphuric acid, as described in Chapter 2. Hydrogen peroxide, H₂O₂ (Fisher, 30% aqueous solution), and acetic acid (Fisher, Anal. Reagent Grade) were used without further purification. Potassium hydrogen phthalate COOHC₆H₄COOK, potassium iodide KI, sodium thiosulphate Na₂S₂O₃.5H₂O and ammonium heptamolybdate (AHM),(NH₄)₆Mo₇O₂₄.4H₂O, used in the determination of peroxide concentrations were obtained from BDH Chemicals Ltd, England. Ferric nitrate nono hydrate, Fe (NO₃)₃.9H₂O, used as a catalyst in the degradation experiments was also obtained from BDH Ltd.

4.2.1.2.Dye stuffs solution

Five dyes were used: Amaranth, Black PN, Carmosine, Orange II, which is also called Acid Orange 7; and Ponceau 4R. These dyes were in the purest form and therefore no further purification was needed. Dyes were obtained from L.G. Pointing and Sons Ltd, except for the Amaranth dye from which was obtained from BDH chemicals Ltd. A list of the dyes common and structural names is shown in Chapter 3, Table 3.3. Each dye was dissolved in distilled water. Initial absorbance was measured at the λ_{\max} values of each dye: Ponceau 4r ($\lambda_{\max} = 510\text{nm}$), Orange II ($\lambda_{\max} = 485\text{nm}$), Carmosine ($\lambda_{\max} = 514\text{nm}$), Black PN ($\lambda_{\max} = 571\text{nm}$), Amaranth ($\lambda_{\max} = 521\text{nm}$).For kinetic measurements The aqueous solution was prepared to provide an initial concentration of dye of $1.4 \times 10^{-5} \text{ mol dm}^{-3}$.

4.2.2. Reaction stoichiometry

The stoichiometry for the reaction between peracetic acid and each of the dyes used was determined by titrating the peracetic acid with dye until the point was reached where no further dye bleaching was observed, i.e. that all of the peracetic acid had reacted. The oxidations, using Fe (III) as a catalyst, were carried out on a Pharmacia Biotech Ultraspec 2000 spectrophotometer equipped with a thermostatic cell holder at 25°C. The procedure involved carrying out an initial run whereby dye, peracetic acid and iron (variable concentrations) were mixed in a cuvette and the absorbance change followed over a period of 60 seconds until most of the colour change had occurred.

Typically the concentrations in the cuvette would be $1.9 \times 10^{-2} \text{ mol dm}^{-3}$ peracetic acid, $1.1 \times 10^{-2} \text{ mol dm}^{-3}$ Fe (III) and $1.62 \times 10^{-2} \text{ mol dm}^{-3}$ dye. After the initial loss of colour, a 0.02ml aliquot of $5 \times 10^{-2} \text{ mol dm}^{-3}$ dye was pipetted into the cuvette and the absorbance change again followed over 60 seconds. This procedure was repeated until the point where no further bleaching of the dye occurred; the stoichiometry of the reaction could then be determined from the respective amounts of dye and peracetic acid added during the experiment. Absorbance changes were followed at the λ_{max} values of the dyes.

4.2.3. Kinetic measurements and percentage dye degradation

A series of kinetic runs were carried out in order to determine the effect of various experimental conditions on both the rate of reaction and the extent of bleaching; the experimental parameters that were varied were: pH, iron (III) catalyst concentration, dye concentration and peracetic acid concentration.

Kinetic runs were carried out at the λ_{max} of the dye. Measurements of the decolourisation of dye were conducted under pseudo first-order conditions, i.e. $[\text{Peracetic acid}]_{\text{T}} \gg [\text{Dye}]_{\text{T}}$.

The following experimental procedure was adopted. A suitable volume of solution (3.5ml) was transferred by pipette to a cuvette. The kinetic runs were carried out in 1cm path length cuvettes. The dye concentration ranged from 1×10^{-5} to $4 \times 10^{-5} \text{ mol dm}^{-3}$ and the iron (III) concentration varied from 0 to $1.2 \times 10^{-3} \text{ mol dm}^{-3}$. The reaction was started by pipetting a peracetic acid stock solution into the cuvette containing the dye and iron; the final concentration of peracetic acid ranged between 2.05×10^{-2} and $4.11 \times 10^{-2} \text{ mol dm}^{-3}$. Absorbance changes were monitored on a Pharmacia Biotech Ultraspec 2000 spectrophotometer which was maintained at $25^{\circ}\text{C} \pm 0.1^{\circ}\text{C}$ by a circulation of water from a thermostatically controlled bath; the reaction was followed for 3 minutes.

The kinetics of the oxidative degradation of the five azo dyes with Fe (III) and peracetic acid were studied in detail. The effects of the initial concentrations of dye, Fe (III), PAA and pH were investigated. The solutions of dyes were in the concentration range of $1 \times 10^{-5} - 4 \times 10^{-5} \text{ mol dm}^{-3}$. The dye was adjusted to pH 1.48, 1.88, 2.09, 2.29, 2.81 and 3.10 using sodium acetate; pH measurements were made on a Jenway 3010 pH meter. In all cases, kinetic rates were expressed as initial rates of absorbance decrease (dA/dt) in units of Absorbance units min^{-1} . This expression of rate was considered adequate for the purpose of comparing the relative effects of different

experimental conditions. In some cases, for the purpose of comparing rates between different dyes, these rates are further converted to observed second order rate constants by dividing the initial rate of absorbance decrease by molar absorptivity, dye concentration and peracetic acid concentration. Literature practice of expressing rates of dye bleaching include the approach we have adopted^{150, 193-197}, conversion to true initial rates^{190, 198, 199}, expression as observed second order rate constants^{187, 200} and, where the true reaction mechanism is known, for example electrophilic attack of the peracid on the dye, the expression of the rates as pH independent second order rate constants¹⁸⁷. For a second order reaction carried out under pseudo first order conditions (peroxide concentration in at least 10-fold excess over the dye concentration) then a plot of $\ln(A-A_\infty)$ against time could have been used to obtain pseudo first order rate constants; however the rates in the absence, or at low concentrations of iron(III), were too slow to allow an infinity reading to be obtained, hence the use of initial rates (of absorbance change). For each of the dyes, preliminary studies on dye bleaching were carried out whereby changes in the absorbance spectrum of the dye were followed upon reaction with peracetic acid.

The percentage of dye degradation was calculated from the same kinetic runs using Equation 4.1

$$\% \text{ Degradation} = \left(1 - \frac{A_t}{A_0}\right) \times 100 \quad \text{Equation 4.1}$$

Where A_0 is the initial absorbance and A_t is the absorbance after 3 minutes. Here the assumption is made that $A_\infty = 0$

4.3.Results

4.3.1. Ponceau 4r dye

4.3.1.1. Reaction stoichiometry

Figure 4.1 shows the results of one of the stoichiometry experiments conducted for the reaction of Ponceau 4r with peracetic acid in the presence of iron catalyst. The repeated cycles of absorbance decrease and increase correspond to the sequential additions of dye and subsequent reaction with peracetic acid. In this example, after about 800 seconds all of the peracetic acid has reacted and no further absorbance decreases are observed.

For all dyes, both in the absence and presence of iron nitrate as a catalyst, the reaction stoichiometry was determined as 1:1, in agreement with literature studies for azo dyes²⁰⁰.

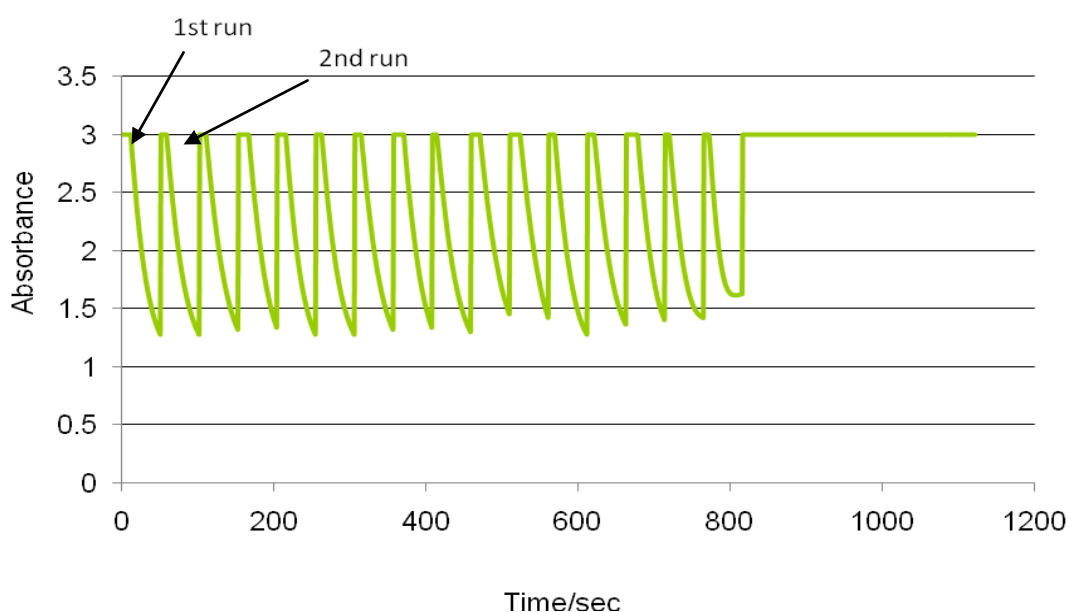


Figure 4.1:- Cyclic peracetic acid degradation of Ponceau 4r dye in the presence of Fe (III), initial concentrations of $[PAA] = 0.0187 \text{ mol dm}^{-3}$, $[Fe (III)] = 0.0109 \text{ mol dm}^{-3}$, total $[dye] = 0.0187$.

4.3.1.2. Preliminary study

For all dyes, preliminary studies were carried out in which changes in the absorbance spectrum during the reaction with peracetic acid were monitored over a period of time. Figure 4.2 shows a typical spectrum for Ponceau 4r dye.

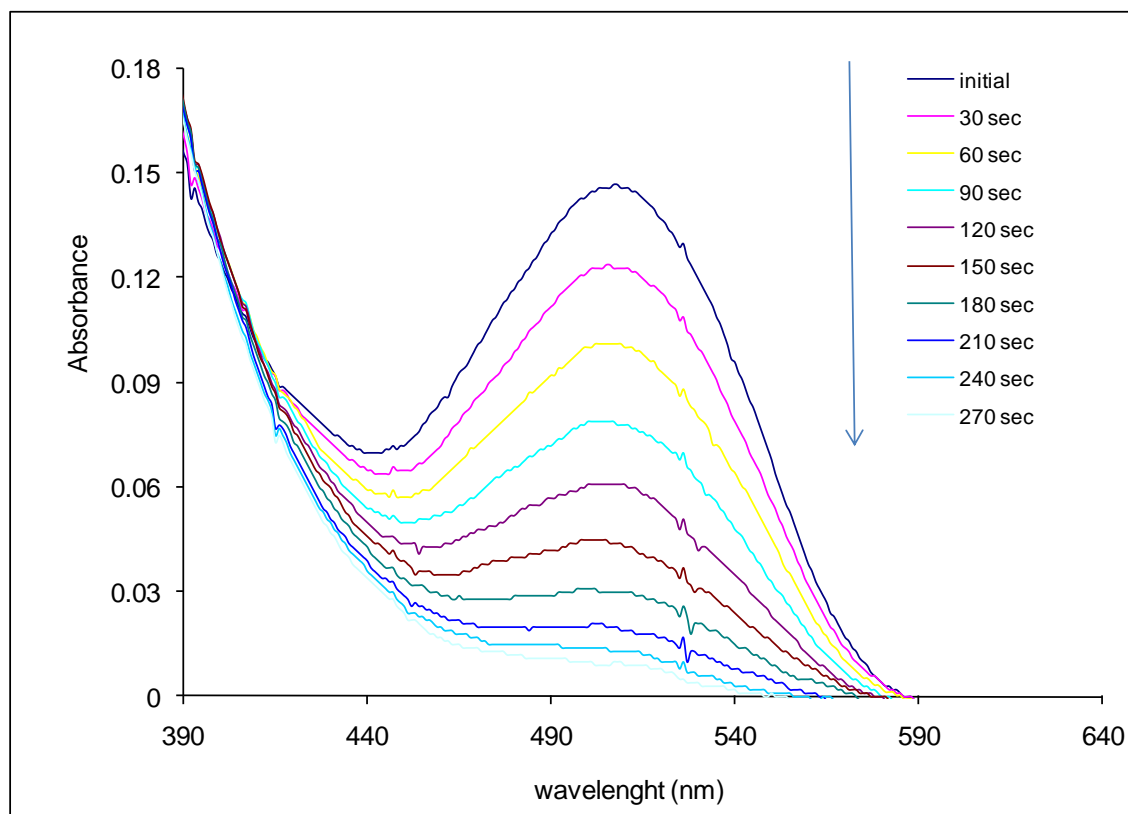


Figure 4.2:- Absorbance spectrum of Ponceau 4r dye on addition of peracetic acid. [PAA] = $2.05 \times 10^{-2} \text{ mol dm}^{-3}$, [Ponceau 4r] = $1 \times 10^{-5} \text{ mol dm}^{-3}$ at 25°C .

4.3.1.3 .Effect of peracetic acid concentration on the oxidation of Ponceau 4r.

Figure 4.3 shows a plot of dA/dt against peracetic acid concentration for the reaction of Ponceau 4r dye in the presence of iron catalyst at 510nm. Oakes and Gratton have shown the uncatalysed reaction between various substituted mono-azo dyes and the peracids *m*-chloroperbenzoic acid and monoperoxosulphate (Caro's acid) to be first order in each of the reactants, certainly over the pH range 5 to 10. Similar plots were obtained for the other dyes.

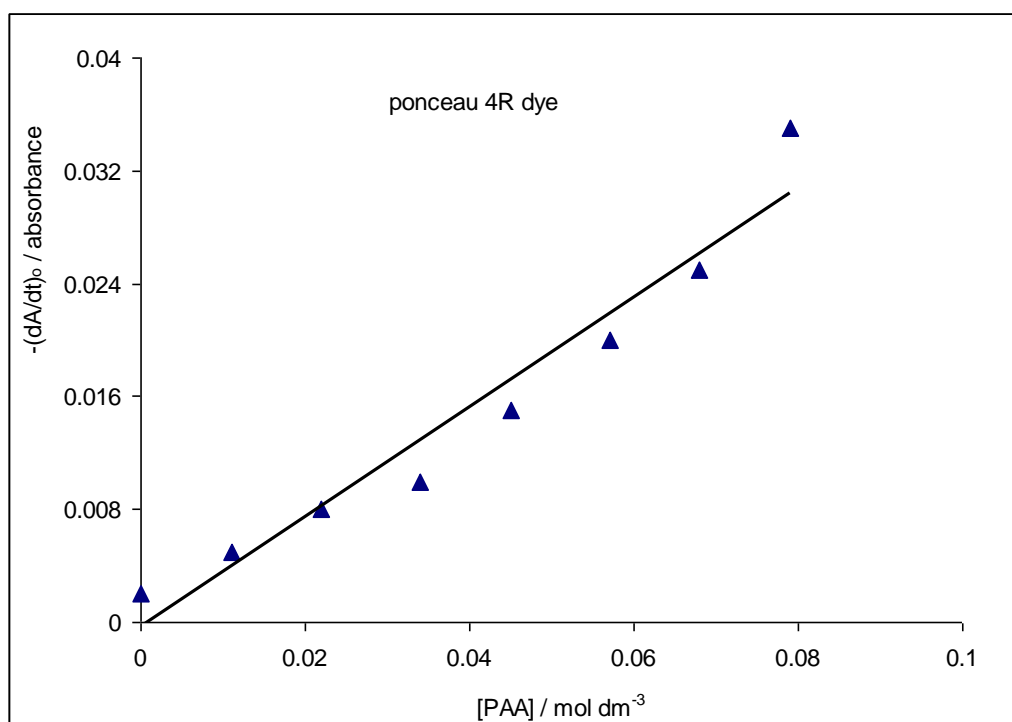


Figure 4.3 :- The reaction of Ponceau 4r dye and PAA, 25°C, $\lambda = 510\text{nm}$, $[\text{dye}] = 1 \times 10^{-5} \text{ mol dm}^{-3}$, $[\text{Fe (III)}] = 1.2 \times 10^{-2} \text{ mol dm}^{-3}$

4.3.1.4. Effect of pH, peracetic acid concentration and dye concentration on the on the oxidation of Ponceau 4r.

In order to investigate the effect of initial dye concentration on the rate of dye degradation, the following experiments were carried out using low dye concentrations to avoid the possibility of dye aggregation. The concentration of PAA was fixed at $2.05 \times 10^{-2} \text{ mol dm}^{-3}$ throughout this experiment. Dye solutions were prepared in a range of concentrations: $1 \times 10^{-5} \text{ mol dm}^{-3}$, $2 \times 10^{-5} \text{ mol dm}^{-3}$ and $4 \times 10^{-5} \text{ mol dm}^{-3}$.

These different concentrations were separately catalysed with iron (III). The amount of ferric ions is one of the main parameters tested in this study; various concentrations of Fe^{3+} were applied to obtain its optimal concentration. Therefore ferric nitrate was used to produce Fe^{3+} and the different Fe (III) concentrations used were: 0, $1.71 \times 10^{-4} \text{ mol dm}^{-3}$, $3.42 \times 10^{-4} \text{ mol dm}^{-3}$, $5.14 \times 10^{-4} \text{ mol dm}^{-3}$, $6.85 \times 10^{-4} \text{ mol dm}^{-3}$, $8.57 \times 10^{-4} \text{ mol dm}^{-3}$, $1.02 \times 10^{-3} \text{ mol dm}^{-3}$, $1.2 \times 10^{-3} \text{ mol dm}^{-3}$, $1.71 \times 10^{-3} \text{ mol dm}^{-3}$, $3.42 \times 10^{-3} \text{ mol dm}^{-3}$, $5.14 \times 10^{-3} \text{ mol dm}^{-3}$, $6.85 \times 10^{-3} \text{ mol dm}^{-3}$, $8.57 \times 10^{-3} \text{ mol dm}^{-3}$, $1.02 \times 10^{-3} \text{ mol dm}^{-3}$ and $1.2 \times 10^{-3} \text{ mol dm}^{-3}$.

Further experiments were carried out by increasing the peracetic acid concentration to $0.0411 \text{ mol dm}^{-3}$ at pHs of 1.48 and pH 1.88 under the same conditions.

An example of the effect of Fe (III) concentration on the oxidation of Ponceau 4r dye on the absorbance of $1 \times 10^{-5} \text{ mol dm}^{-3}$ dye and $2.05 \times 10^{-2} \text{ mol dm}^{-3}$ PAA is shown in Figure 4.4. Only a very small absorbance decrease was observed when the solution was prepared without the addition of Fe (III) however when the concentration of Fe (III) was gradually increased the rate of absorbance decrease significantly increased.

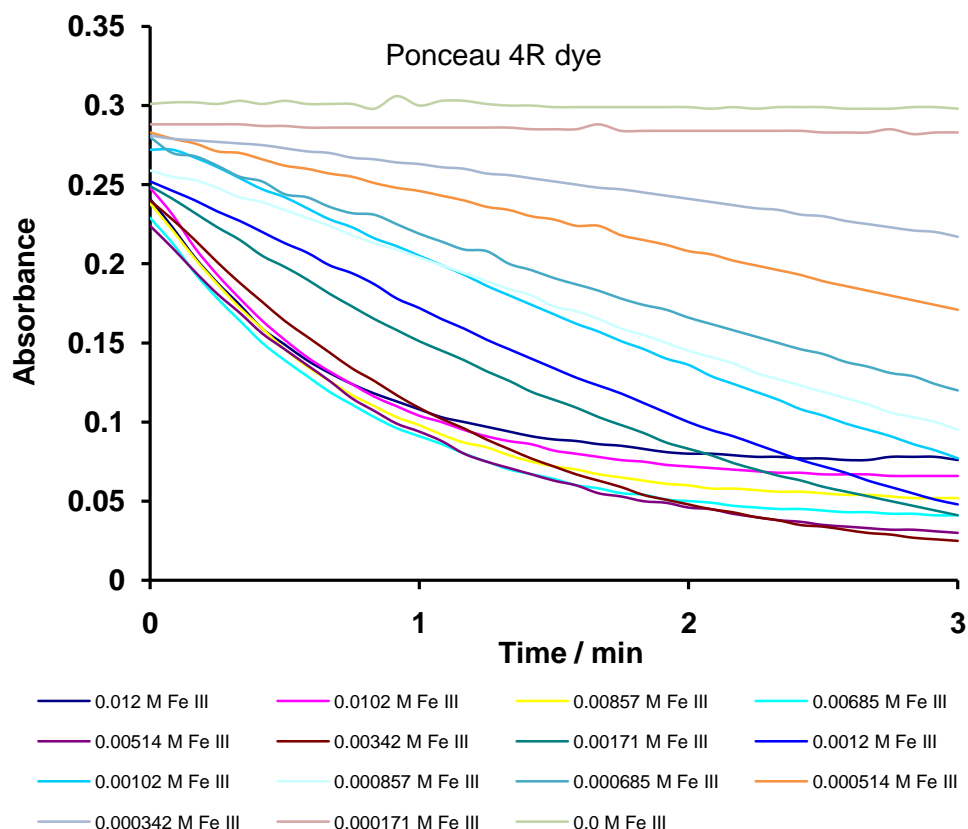


Figure 4.4 :- Effect of Fe (III) concentrations on the oxidation of Ponceau 4R dye absorbance change with time, $2.05 \times 10^{-2} \text{ mol dm}^{-3}$ PAA, on absorbance of $1 \times 10^{-5} \text{ mol dm}^{-3}$ dye with different concentrations of Fe (III), pH 2.09. Temp 25°C . $\lambda_{\text{max}} = 510\text{nm}$.

Table 4.1 shows the initial rates of the reaction of Ponceau 4r dye with peracetic acid; all of these results were calculated from a plot of change in absorbance against time.

The first four columns of Table 4.1 show the effect of changing the pH on the rate of the reaction. The experiment was carried out using different values of pH: 2.09, 2.29, 2.81 and 3.10. All the other factors, such as dye concentration, PAA concentration and temperature were kept constant during the study.

As a trend it was observed that as the pH of the solution increases, the rate of the reaction also increases, going across the table at pH 2.09 and without the addition of Fe (III) the rate of the reaction was 0.1 min^{-1} whereas at pH 3.10 the rate increases to

1.1. However the result at pH 2.81 did not follow this trend, which may be due to other factors affecting the rate of reaction. The overall results suggest that the reaction occurs faster at higher pH.

When the concentration of Fe (III) increased at pH 2.09 the rate of the reaction started to increase. The increase in the reaction rate was rapid at small concentrations of Fe (III), however when the Fe (III) concentration increased further to $6.857 \times 10^{-3} \text{ mol dm}^{-3}$ the reaction rate started to level off and then no major further difference in reaction rate was observed.

Table 4.1 shows a similar trend for the other pH values of 2.29, 2.82 and 3.10, when the rate of reaction starts to increase rapidly as the Fe (III) concentration increased, and after a certain concentration the rate of the reactions started to level and no more change can be observed.

Table 4.1 shows not only the influence of change in Fe (III) on the pH effect; it also shows the results obtained for the rate of reaction at different concentrations of PAA and dye. The result obtained for the increase in the concentration of PAA from 0.0205 to $0.041 \text{ mol dm}^{-3}$ shows a small increase in the rate of the reaction. Similar trends are shown for the other mono-azo dyes studied:

The increase in dye concentration from 1×10^{-5} to 2×10^{-5} then $4 \times 10^{-5} \text{ mol dm}^{-3}$ showed a proportionate effect on the rate of absorbance decrease; this was reassuring as it indicated that dye aggregation was not a particular issue for this dye at these low concentrations (Oakes and Gratton have pointed out that some azo dyes, e.g. Acid Red readily aggregate at low concentrations and high ionic strength¹⁸⁷).

It should be noted that for some runs there appeared to be a lag phase followed by a more rapid oxidation phase; typically this would occur for runs where the iron was at the lowest concentrations. Examples of this are shown in Figure A1.2 in the Appendix.

4.3.1.5. Effect of iron concentration on the rate of reaction for Ponceau 4r.

Table 4.1 shows that increasing the concentration of Fe (III) results in a large increase in the rate of the reaction, though the fact that the catalytic effect of the iron levels off at the higher iron concentrations has implications for the mechanism of catalysis.

There are two main potential pathways for the catalysis that is observed in the reaction of azo dyes with peracetic acid in the presence of iron: (a) rapid pre-equilibrium

between dye and iron(III) ion followed by reaction with peracid and (b) rapid pre-equilibrium between peracid and iron(III) ion followed by reaction with dye.

The evidence favours pathway (a), i.e. rapid pre-equilibrium between dye and iron(III) followed by reaction with the peracid, principally because in Chapter 3 we saw that adding iron to some azo dyes (all of those used in this chapter) results in an immediate absorbance increase that is indicative of complex formation.

Assuming that it is the iron(III)-Dye complex that reacts with the peracetic acid, and that $[Fe(III)] > [Dye]$ then from the rate, equilibria and mass balance relationships for this system we can define the initial rate of absorbance decrease by Equation 4.2.

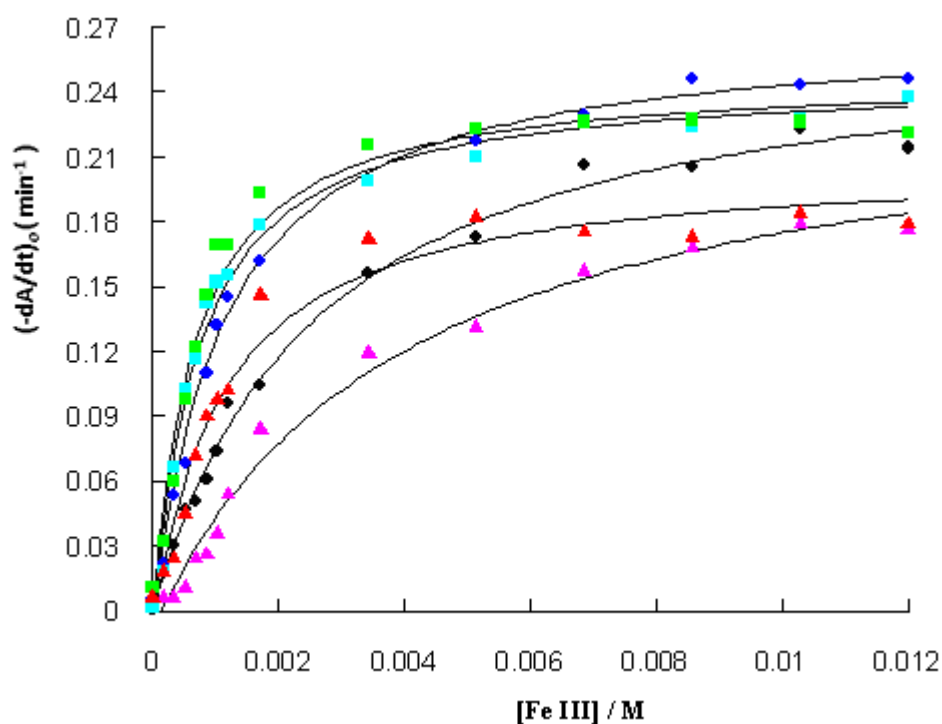
$$\left(\frac{dA}{dt}\right) = \frac{R_0 + R_{max} [FeIII]}{1 + K [Fe III]} \quad \text{Equation 4.2}$$

In Equation 4.2. R_0 and R_{max} are the uncatalysed and maximum rates of absorbance change (in absorbance units per minute) and K is the equilibrium constant for the 1:1 complex formed between iron and the dye. This equation predicts saturation in iron concentration, which is the relationship observed in the kinetic runs.

Figures 4.5 and 4.6 show the rate dependence on iron(III) concentration under various experimental conditions; the curves are the best fit to Equation 4.2 using the parameters listed in Table 4.1. These results were calculated using Grafit program version 3.01. Figure 4.6 shows that the pH has a significant effect on the rate of the reaction, with higher rates obtained as the pH is increased.

Table 4.1 :- The reaction of peracetic acid with Ponceau 4r dye at different concentrations of Fe (III): 25°C, [Dye]₀ = 1x10⁻⁵ M , [Dye]₀=2x10⁻⁵ mol dm⁻³,and [Dye]₀= 4x10⁻⁵ mol dm⁻³

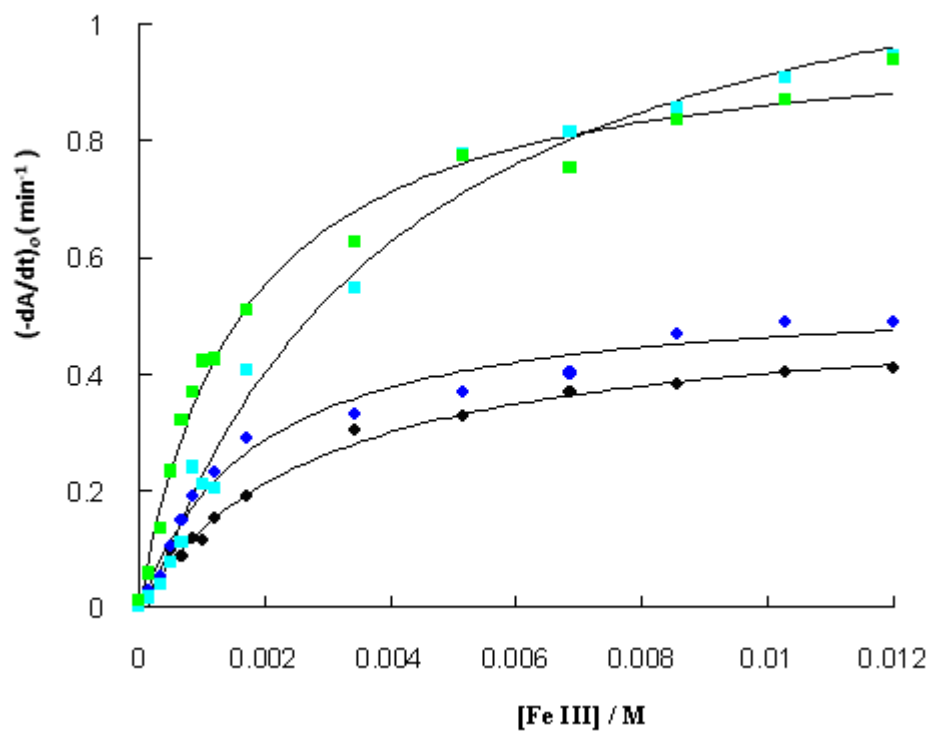
[Fe (III)] (M / 10 ³)	-(dA/dt) ₀ (min ⁻¹ x10 ⁻²) [dye]=1x10 ⁻⁵ M pH = 2.09 [PAA] = 0.0205M	-(dA/dt) ₀ (min ⁻¹ x10 ⁻²) [dye]=1x10 ⁻⁵ M pH = 2.29 [PAA] = 0.0205M	-(dA/dt) ₀ (min ⁻¹ x10 ⁻²) [dye]=1x10 ⁻⁵ M pH = 2.81 [PAA] = 0.0205M	-(dA/dt) ₀ (min ⁻¹ x10 ⁻²) [dye]=1x10 ⁻⁵ M pH = 3.10 [PAA]= 0.0205M	-(dA/dt) ₀ (min ⁻¹ x10 ⁻²) [dye]=1x10 ⁻⁵ M pH = 1.48 [PAA]= 0.0411M	-(dA/dt) ₀ (min ⁻¹ x10 ⁻²) [dye]=1x10 ⁻⁵ M pH = 1.88 [PAA]= 0.0411M	-(dA/dt) ₀ (min ⁻¹ x10 ⁻²) [dye]=2x10 ⁻⁵ M pH = 2.09 [PAA]= 0.0205M	-(dA/dt) ₀ (min ⁻¹ x10 ⁻²) [dye]=2x10 ⁻⁵ M pH = 2.81 [PAA]=0.0205M	-(dA/dt) ₀ (min ⁻¹ x10 ⁻²) [dye]=4x10 ⁻⁵ M pH = 2.09 [PAA] = 0.0205M	-(dA/dt) ₀ (min ⁻¹ x10 ⁻²) [dye]=4x10 ⁻⁵ M pH = 2.81 [PAA] = 0.0205M
No Fe (III)	0.1	0.5	0.2	1.1	0.6	0.6	1	0.5	0.2	1.1
0.17	1.7	2.2	1.8	3.2	0.6	1.8	2.5	2.7	1.7	5.8
0.342	3	5.3	6.6	6	0.6	2.4	4.8	5.4	0.04	13.4
0.514	4.7	6.8	10.2	9.8	1.1	4.5	9.7	10.5	7.7	23.3
0.685	5.1	12	11.6	12.2	2.4	7.2	8.6	15	11.2	32.2
0.857	6.1	11	14.2	14.6	2.6	9	11.9	19	24	37
1.02	7.4	13.2	15.2	16.9	3.6	9.8	11.4	21.1	21.2	42.2
1.2	9.6	14.5	15.5	16.9	5.4	10.2	15.3	23	20.5	42.5
1.714	10.4	16.2	17.8	19.3	8.4	14.6	18.9	29	40.6	51
3.429	15.6	19.9	19.9	21.5	11.9	17.2	30.2	33.1	54.8	62.5
5.143	17.3	21.7	21	22.3	13.1	18.2	32.9	36.8	77.7	77.5
6.857	20.6	22.9	22.6	22.6	15.7	17.5	37	40.1	81.4	75.2
8.571	20.5	24.6	22.4	22.7	16.8	17.3	38.2	46.7	85.4	83.5
10.286	22.3	24.3	22.7	22.6	17.9	18.4	40.2	49	90.8	86.9
12	21.4	24.6	23.8	22.1	17.6	17.9	41	49	94.6	93.8



- ◆ [dye]=0.00001M,[PAA]=0.0205M,pH2.09
- [dye]=0.00001M,[PAA]=0.0205M,pH3.10
- ◆ [dye]=0.00001M,[PAA]=0.0205M,pH2.29
- ▲ [dye]=0.00001M,[PAA]=0.0411M,pH1.48
- [dye]=0.00001M,[PAA]=0.0205M,pH2.81
- ▲ [dye]=0.00001M,[PAA]=0.0411M,pH1.88

Figure 4.5 :- The reaction of peracetic acid with Ponceau 4r dye with different concentrations of Fe (III): Temp 25°C, $\lambda = 510\text{nm}$, sodium acetate = 0.022 mol dm^{-3} , $[\text{Dye}]_0 = 1 \times 10^{-5}\text{ mol dm}^{-3}$, $[\text{Dye}]_0 = 2 \times 10^{-5}\text{ mol dm}^{-3}$ and $[\text{Dye}]_0 = 4 \times 10^{-5}\text{ mol dm}^{-3}$, different pH as shown in the above. $[\text{PAA}] = 2.05 \times 10^{-2}\text{ mol dm}^{-3}$ and $4.11 \times 10^{-2}\text{ mol dm}^{-3}$.

Figure 4.6 shows the rate of reaction at higher concentrations of dye against the increase in Fe (III) concentration. The PAA concentration was kept constant in this reaction, which was carried out at different pH values. As expected, doubling the dye concentration doubles the rate of absorbance loss.



- ◆ [dye]=0.00002M,[PAA]=0.0205,pH 2.09 ■ [dye]=0.00004M,[PAA]=0.0205,pH 2.09
- ◆ [dye]=0.00002M,[PAA]=0.0205,pH 2.81 ■ [dye]=0.00004M,[PAA]=0.0205,pH 2.81

Figure 4.6:- The reaction of peracetic acid with Ponceau 4r dye at different concentrations of Fe (III): Temp 25°C, $\lambda = 510\text{nm}$, $[\text{Dye}]_0 = 2 \times 10^{-5} \text{ mol dm}^{-3}$ and $[\text{Dye}]_0 = 4 \times 10^{-5} \text{ mol dm}^{-3}$, different pH as shown in the above. $[\text{PAA}] = 2.05 \times 10^{-2} \text{ mol dm}^{-3}$, at 25°C

Table 4.2 :- Best fit parameters for equilibrium constant (K), and maximum rate, R_{max} , for Ponceau 4R dye obtained from Equation 4. 2 and at Temp 25°C.

pH	[PAA]/ 10 ⁻² M	[NaAc]	[dye]/ 10 ⁻⁵ M	R_{max} (min ⁻¹)	K (mol dm ⁻³)
2.09	2.05	-	1	0.27±0.008	384±41
2.29	2.05	0.011 mol dm ⁻³	1	0.27±0.0066	894±104
2.81	2.05	0.022 mol dm ⁻³	1	0.24±0.0055	1445±171
3.10	2.05	0.034 mol dm ⁻³	1	0.24±0.0075	1549±266
1.48	4.11	-	1	0.24±0.017	252±52
1.88	4.11	0.022 mol dm ⁻³	1	0.2±0.009	920±194
2.09	2.05	-	2	0.51±0.016	343±39
2.81	2.05	0.022 mol dm ⁻³	2	0.54±0.022	572±97
2.09	2.05	-	4	1.29±0.079	249±43
2.81	2.05	0.022 mol dm ⁻³	4	0.99±0.031	624±84

4.3.1.6. Estimation of percentage of Ponceau 4r dye degradation at different dye concentrations and pH levels.

The kinetic runs described in the previous sections were also used to establish the optimum conditions for maximum degradation of the dye solutions. Reactions were carried out at a range of different pHs below 4 with dye concentrations of 1×10^{-5} mol dm^{-3} , 2×10^{-5} mol dm^{-3} and 4×10^{-5} mol dm^{-3} . The pH range was restricted when using iron as a catalyst because it is likely to precipitate out above 4 (though, as Oakes and Gratton have observed, the *uncatalysed* reaction shows a strong dependence on pH, with a maximum rate obtained ca. pH 9.5). The percentage degradation was calculated using Equation 4.1 for a run time of three minutes.

Figures 4.7 and 4.8 show the absorbance changes for individual runs under various experimental conditions; the overall percentage degradations after a three minute run time are summarised in Table 4.3. Clearly pH and iron (III) concentration have a significant effect on the overall degradation of the dye.

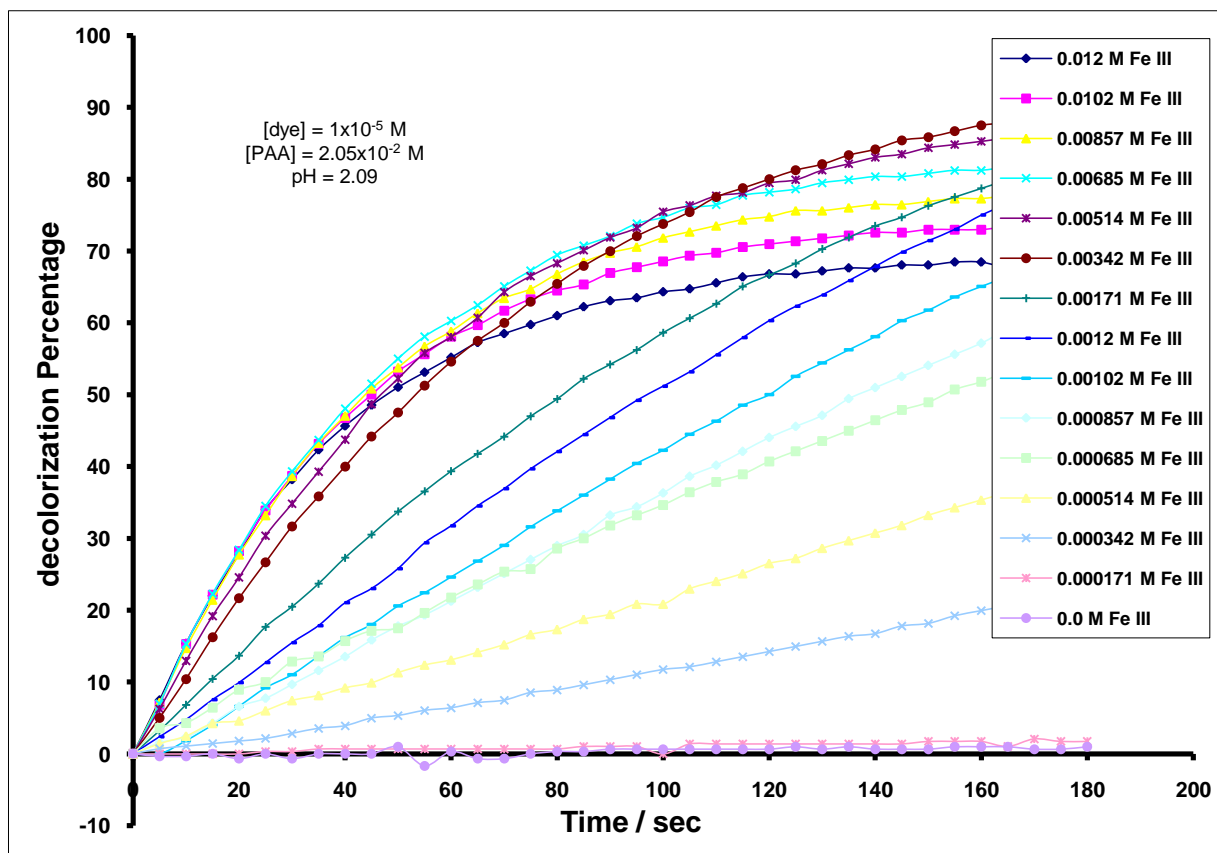


Figure 4.7 :- Effect of the initial concentration of Fe (III) on degradation of Ponceau 4r dye at pH = 2.09, [dye] = 1×10^{-5} mol dm^{-3} . [PAA] = 2.05×10^{-2} mol dm^{-3} , at 25°C .

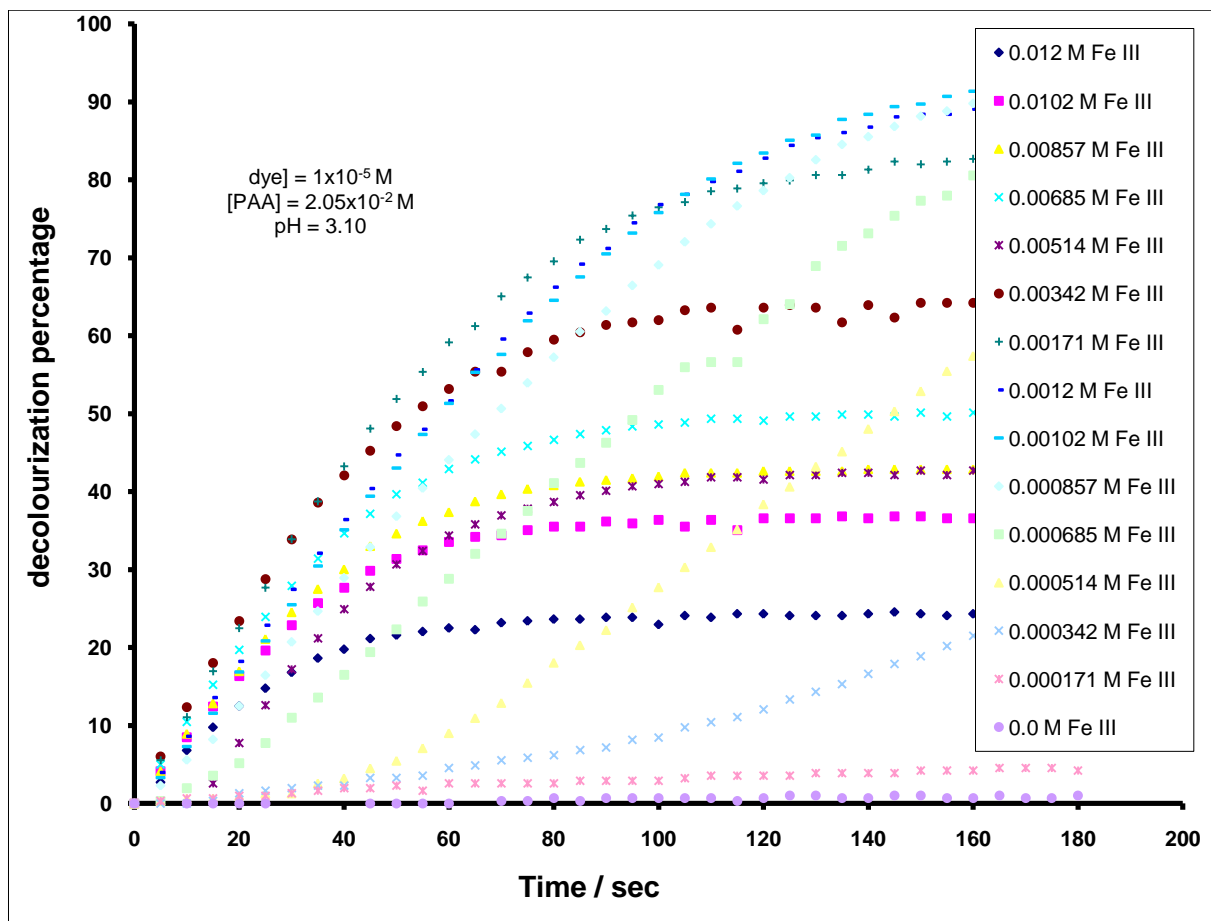


Figure 4. 8 :- Effect of the initial concentration of Fe (III) in degradation of Ponceau 4r dye at pH 3.10, [dye] = 1×10^{-5} mol dm⁻³. [PAA] = 2.05×10^{-2} mol dm⁻³, at 25^oC.

Table 4.3 :- Percentage decrease in Ponceau 4r dye absorbance over 180 seconds calculated from Equation 4.1 in the presence of $2.05 \times 10^{-2} \text{ mol dm}^{-3}$ and $4.11 \times 10^{-2} \text{ mol dm}^{-3}$ peracetic acid at different pH, and Dye concentrations with variations in Fe (III).

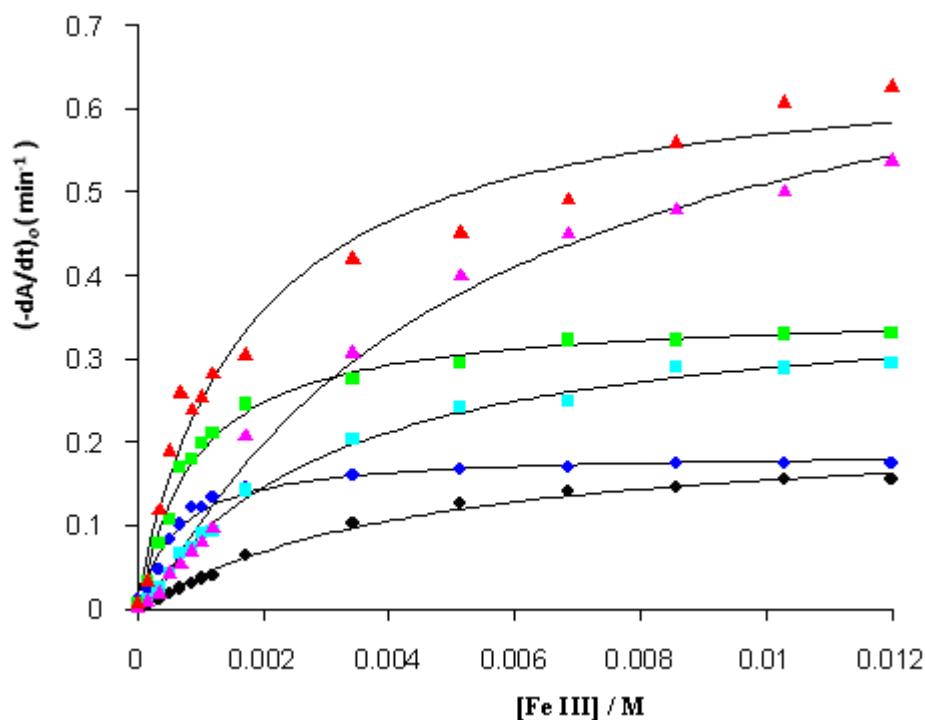
Reactant [Fe (III)] / 10^{-3} M	[dye] = $1 \times 10^{-5} \text{ M}$ [PAA] = $2.05 \times 10^{-2} \text{ M}$ % degradation				[dye] = $1 \times 10^{-5} \text{ M}$ [PAA] = $4.11 \times 10^{-2} \text{ M}$ % degradation		[dye] = $2 \times 10^{-5} \text{ M}$ [PAA] = $2.05 \times 10^{-2} \text{ M}$ % degradation		[dye] = $4 \times 10^{-5} \text{ M}$ [PAA] = $2.05 \times 10^{-2} \text{ M}$ % degradation	
	pH 2.09	pH 2.29	pH 2.81	pH 3.10	pH 1.48	pH 1.88	pH 2.09	pH 2.81	pH 2.09	pH 2.81
without Fe (III)	0.99	0.33	6.87	1.00	0.96	0.97	1.12	0.48	0.32	0.78
0.17	1.73	2.33	2.63	4.22	1.65	2.34	2.55	1.31	0.85	1.55
0.342	22.77	33.11	32.11	27.36	2.38	3.64	51.17	12.97	8.50	16.06
0.514	39.57	64.45	68.37	66.45	5.11	5.88	81.46	46.97	19.62	49.54
0.685	57.14	80.90	87.75	85.43	13.55	49.66	81.43	60.93	26.64	69.99
0.857	63.32	85.53	91	92.43	20.67	73.97	93.37	65.99	56.11	77.48
1.02	71.69	93.82	90.55	92.71	26.92	79.32	94.60	70.37	49.79	80.81
1.2	80.95	94.33	91.10	89.73	35.61	87.63	96.96	73.43	51.64	83.76
1.714	83.53	89.65	84.98	83.04	67.02	88.01	82.56	88.41	85.07	89.97
3.429	89.58	78.51	70.50	61.07	91.22	81.56	90.94	79.70	92.66	88.39
5.143	86.60	72.48	59.24	57.59	89.95	71.19	90.07	75	92.36	84.73
6.857	82.09	65.80	50.73	50.62	86.25	58.95	85.52	69.06	91.78	81.46
8.571	78.15	59.63	43.41	43.11	83.26	49.04	78.59	63.95	89.63	77.96
10.286	73.38	53.28	42.33	36.38	79.77	53.82	81.17	61.76	88.76	76.23
12	68.46	51.87	38.31	24.54	74.73	50.56	76.28	57.91	86.19	72.81

4.3.2. Other azo dyes

The stoichiometry, kinetics and percentage dye degradation experiments were repeated for the four other dyes being considered in this chapter, namely: Amaranth, Orange II, Carmosine and Diazo Black PN. These dyes were considered relevant to commercial bleaching problems since the composition and purity of commercial preparations of these compounds are well defined and quantified. They were chosen as a suitable class of model substrates for the study of bleaching reactions. Plots of absorbance decrease against time for the range of experimental parameters studied are shown in Appendix 1. It should be noted that as with Ponceau 4 dye, in several of the runs there appeared to be an induction period followed by a more rapid absorbance change, for example Figure A1.18 for Orange II, Figure A1.32 for Black PN, Figure A1.24 for Carmosine and Figure A1.34 for Amaranth. Runs that exhibited this behaviour general had a low iron concentration; i.e. it occurred at the lowest two iron concentrations used, though this wasn't a totally consistent observation.

Plots of initial rate of absorbance decrease against iron concentration are shown in Figures 4.9 to 4.13; the best fit curves for each set of data are obtained using Equation 4.2 and parameters from the appropriate table (Tables 4.4 to 4.7).

To estimate the percentage degradation of Amaranth, Carmosine, Black PN and Orange II dyes the same procedure as in section 4.3.1.6 was followed. The results were treated in a similar way to those for Ponceau 4r dye. Equation 4.1 was used to estimate the percentage of azo dye degradation; the data is summarised in Tables 4.8 to 4.11 for the five azo dyes.

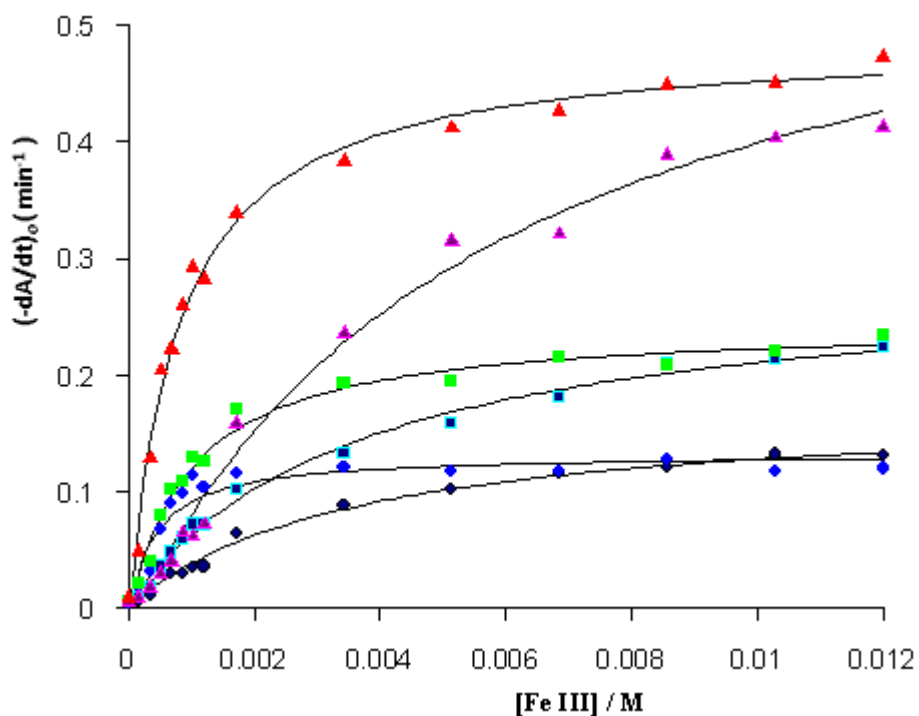


- ◆ [dye]=0.00001M, pH 2.09 ■ [dye]=0.00002M, pH 2.09 ▲ [dye]=0.00004M, pH 2.09
- ◆ [dye]=0.00001M, pH 2.81 ■ [dye]=0.00002M, pH 2.81 ▲ [dye]=0.00004M, pH 2.81

Figure 4.9 :- The reaction of peracetic acid concentrations $2.05 \times 10^{-2} \text{ mol dm}^{-3}$ with Amaranth dye at different concentrations of Fe (III): 25°C , pH 2.09 and 2.81, $\lambda = 521 \text{ nm}$. Curves are the best fits to Equation 4.2 using the parameters listed in Table 4.4.

Table 4.4 :- Best fit parameters for equilibrium constants (K), and maximum rates, R_{max} obtained from Equation 4. 2 and Temp 25°C for Amaranth dye

pH	[PAA]/ 10^{-2} M	[dye] / 10^{-5} M	$R_{\text{max}}(\text{Min}^{-1})$	K (mol dm^{-3})
2.09	2.05	1	0.22 ± 0.01	234 ± 33.5
2.81	2.05	1	0.18 ± 0.0056	1613 ± 259
2.09	2.05	2	0.37 ± 0.012	325 ± 37
2.81	2.05	2	0.35 ± 0.0083	1155 ± 134
2.09	2.05	4	0.79 ± 0.053	190 ± 33
2.81	2.05	4	0.66 ± 0.034	547 ± 120

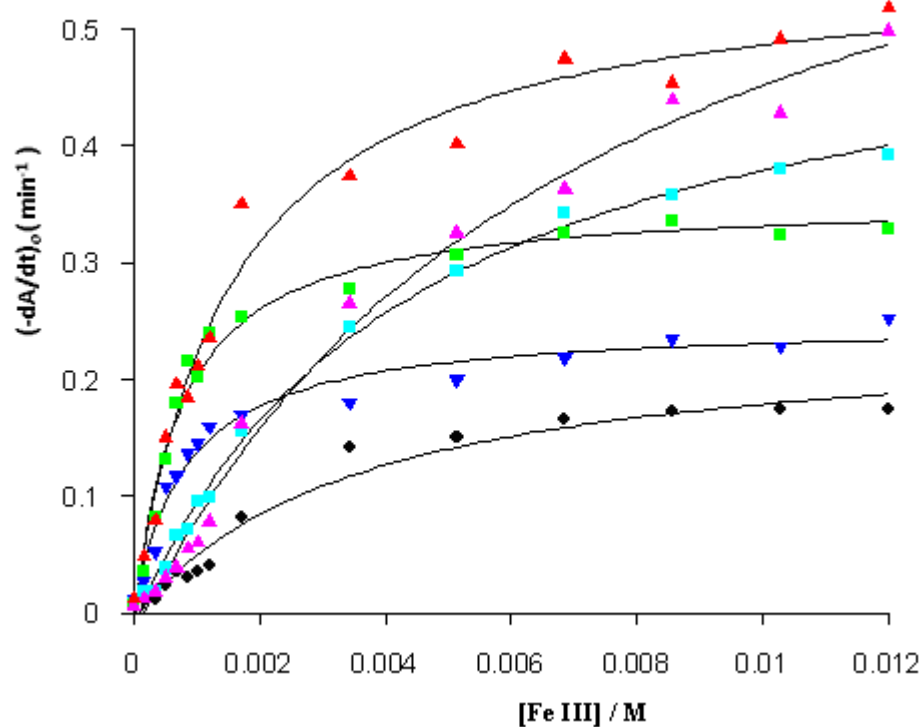


- ◆ [dye]=0.00001M, pH 2.09 ■ [dye]=0.00002M, pH 2.09 ▲ [dye]=0.00004M, pH 2.09
- ◆ [dye]=0.00001M, pH 2.81 ■ [dye]=0.00002M, pH 2.81 ▲ [dye]=0.00004M, pH 2.81

Figure 4.10:- The reaction of peracetic acid concentrations $2.05 \times 10^{-2} \text{ mol dm}^{-3}$ with Carmosine dye at different concentrations of Fe (III): 25°C , $\lambda = 514\text{nm}$. Curves are the best fits to Equation 4.2 using the parameters listed in Table 4.5.

Table 4.5:- Equilibrium constants (K), obtained from Equation 4. 2 and at Temp 25°C for Carmosine dye

pH	[PAA]/ 10^{-2} M	[dye]/ 10^{-5} M	$R_1(\text{Min}^{-1})$	(K)
2.09	2.05	1	0.17 ± 0.01	270 ± 52
2.81	2.05	1	0.13 ± 0.0068	2351 ± 798
2.09	2.05	2	0.28 ± 0.012	267 ± 35
2.81	2.05	2	0.24 ± 0.0071	1013 ± 143
2.09	2.05	4	0.63 ± 0.051	175 ± 34
2.81	2.05	4	0.48 ± 0.0096	1273 ± 130

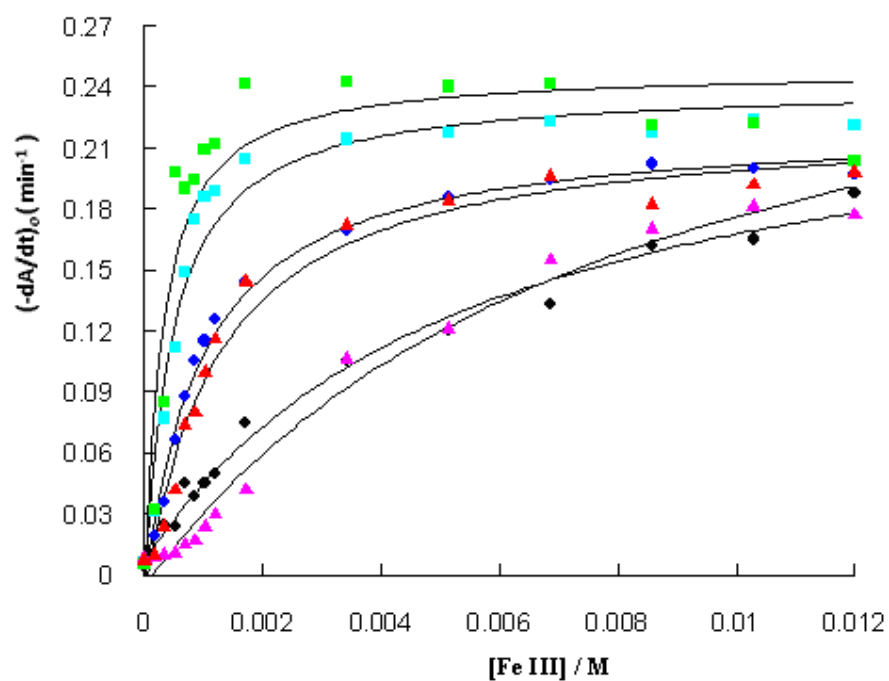


- ◆ [dye]=0.00001M, pH 2.09 ■ [dye]=0.00002M, pH 2.09 ▲ [dye]=0.00004M, pH 2.09
- ▼ [dye]=0.00001M, pH 2.81 ■ [dye]=0.00002M, pH 2.81 ▲ [dye]=0.00004M, pH 2.81

Figure 4.11 :- the reaction of peracetic acid concentrations $2.05 \times 10^{-2} \text{ mol dm}^{-3}$ with Black PN dye at different concentrations of Fe (III): 25°C , pH 2.09 and 2.81, $\lambda = 571\text{nm}$. Curves are the best fits to Equation 4.2 using the parameters listed in Table 4.6.

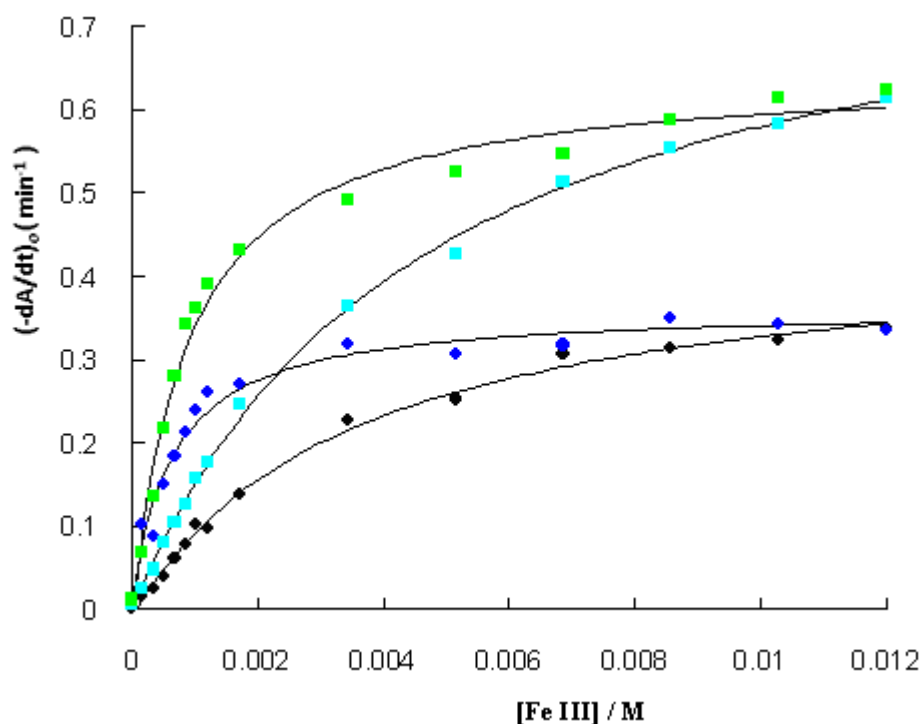
Table 4.6 :- Best fit parameters for equilibrium constants (K), and maximum rates, R_{max} obtained from Equation 4. 2 and at Temp 25°C for Black PN dye

pH	[PAA] / 10^{-2} M	[dye] / 10^{-5} M	$R_{\text{max}}(\text{Min}^{-1})$	K (mol dm^{-3})
2.09	2.05	1	0.24 ± 0.02	277 ± 79
2.81	2.05	1	0.24 ± 0.0089	1219 ± 219
2.09	2.05	2	0.55 ± 0.021	225 ± 25
2.81	2.05	2	0.35 ± 0.01	1418 ± 209
2.09	2.05	4	0.79 ± 0.075	137 ± 29
2.81	2.05	4	0.56 ± 0.02	650 ± 106



- ◆ [dye]=0.00001M,[PAA]=0.0205M,pH2.09
- [dye]=0.00001M,[PAA]=0.0205M,pH3.10
- ◆ [dye]=0.00001M,[PAA]=0.0205M,pH2.29
- ▲ [dye]=0.00001M,[PAA]=0.0411M,pH1.48
- [dye]=0.00001M,[PAA]=0.0205M,pH2.81
- ▲ [dye]=0.00001M,[PAA]=0.0411M,pH1.88

Figure 4.12 :- Reaction of peracetic acid concentrations $2.05 \times 10^{-2} \text{ mol dm}^{-3}$ with Orange II dye²⁰¹ at different concentrations of Fe (III): 25°C, pH 2.09 and 2.81, $\lambda = 571 \text{ nm}$. Curves are the best fits to Equation 4.2 using the parameters listed in Table 4.7.



- ◆ [dye]=0.00002M,[PAA]=0.0205M,pH2.09 ■ [dye]=0.00004M,[PAA]=0.0205,pH2.09
- ◆ [dye]=0.00002M,[PAA]=0.0205M, pH2.81 ■ [dye]=0.00004M,[PAA]=0.0205M,pH2.81

Figure 4.13 :- the reaction of peracetic acid concentrations $2.05 \times 10^{-2} \text{ mol dm}^{-3}$ with Orange II dye at different concentrations of Fe (III): 25°C , pH 2.09 and 2.81, $\lambda = 571\text{nm}$. Curves are the best fits to Equation 4.2 using the parameters listed in Table 4.7.

Table 4.7 :- Best fit parameters for equilibrium constant (K), and maximum rates, R_{max} obtained from Equation 4. 2 and at Temp 25°C for Orange II dye

pH	[PAA]/ 10^{-2} M	[dye] / 10^{-5} M	$R_{\text{max}}(\text{Min}^{-1})$	K (mol dm^{-3})
2.09	2.05	1	0.25 ± 0.019	178 ± 36
2.29	2.05	1	0.21 ± 0.0051	1018 ± 115
2.81	2.05	1	0.24 ± 0.0085	2262 ± 495
3.10	2.05	1	0.24 ± 0.014	3650 ± 1233
1.48	4.11	1	0.32 ± 0.044	122 ± 33
1.88	4.11	1	0.22 ± 0.009	826 ± 156
2.09	2.05	2	0.44 ± 0.015	278 ± 29
2.81	2.05	2	0.36 ± 0.01	1517 ± 251
2.09	2.05	4	0.84 ± 0.019	219 ± 14
2.81	2.05	4	0.64 ± 0.015	1139 ± 137

Table 4.8 :- Percentage decrease in Amaranth dye absorbance over 180 seconds. Calculated using Equation 4.1. Reactions were carried out in the presence of $2.05 \times 10^{-2} \text{ mol dm}^{-3}$ peracetic acid at pHs of 2.09 and 2.81. Dye and Fe concentrations as indicated in the table below.

Reactant [Fe (III)] / $10^{-3} \text{ mol dm}^{-3}$ [PAA] = $2.05 \times 10^{-2} \text{ mol dm}^{-3}$	[dye] = $1 \times 10^{-5} \text{ mol dm}^{-3}$ % degradation		[dye] = $2 \times 10^{-5} \text{ mol dm}^{-3}$ % degradation		[dye] = $4 \times 10^{-5} \text{ mol dm}^{-3}$ % degradation	
	pH 2.09	pH 2.81	pH 2.09	pH 2.81	pH 2.09	pH 2.81
without Fe (III)	1.8	0.4	1	1	0.3	1
0.17	1.9	4.2	2	2.2	0.5	1.1
0.342	6.7	33.7	10.5	23.9	5.7	23.3
0.514	20	84.5	28.8	57.8	12.7	54.9
0.685	28	96.6	39.4	88.6	17.4	66.3
0.857	45	95.9	48.4	94.9	24.7	71.5
1.02	60	94.4	59	96.4	30.9	82.9
1.2	51	91.8	71	95.3	34.9	84.7
1.714	94.7	83.4	93	89.8	75.1	91.9
3.429	91.2	64.7	95.5	76.9	91.5	89
5.143	88.9	56.2	91.6	72	92.8	82.7
6.857	77.6	42.9	86.8	62.7	91.7	80.5
8.571	75.7	42.1	84.6	60.4	90.3	70.6
10.286	69.7	33.8	79.7	55.9	87.2	74.9
12	64.7	33	76.9	50.9	87.3	73

Table 4.9 :- Percentage decrease in Carmosine dye absorbance over 180 seconds. Calculated using Equation 4.1. Reactions were carried out in the presence of 2.05×10^{-2} mol dm⁻³ peracetic acid at pHs of 2.09 and 2.81. Dye and Fe concentrations as indicated in the table below.

Reactant [Fe (III)] / 10^{-3} mol dm ⁻³ [PAA] = 2.05×10^{-2} mol dm ⁻³	[dye] = 1×10^{-5} mol dm ⁻³ % degradation		[dye]= 2×10^{-5} mol dm ⁻³ % degradation		[dye]= 4×10^{-5} mol dm ⁻³ % degradation	
	pH 2.09	pH 2.81	pH 2.09	pH 2.81	pH 2.09	pH 2.81
without Fe (III)	1	1.6	1.2	0.2	0.3	1.2
0.17	1.1	4.9	2.1	1.6	0.5	2.2
0.342	11.1	21.9	7.8	17.9	5.6	32.7
0.514	24.1	80.9	22.3	50.6	11.7	62.2
0.685	30.9	94.3	34	64	15.2	77.4
0.857	37.1	93.6	43.8	72	23.9	86.2
1.02	36.8	91.2	51	74.4	24.7	89.9
1.2	51.2	89.3	52	76.4	28.1	88.9
1.714	89.3	81.3	74.2	86.3	63.9	91.3
3.429	91.8	63.1	90.5	74.8	83.7	84.8
5.143	84.1	44.9	89.5	68.8	89.9	79.5
6.857	77.9	33.2	83.3	61.9	87.9	75.1
8.571	69.9	38.3	80.3	57.7	87.3	70
10.286	65.1	28.2	75.6	54.4	85.5	68.6
12	60.1	26.1	73.8	51.9	83.1	65.4

Table 4.10 :- Percentage decrease in Black PN dye absorbance over 180 seconds. Calculated using Equation 4.1. Reactions were carried out in the presence of 2.05×10^{-2} mol dm⁻³ peracetic acid at pHs of 2.09 and 2.81. Dye and Fe concentrations as indicated in the table below.

Reactant [Fe (III)] / 10^{-3} mol dm ⁻³ [PAA] = 2.05×10^{-2} mol dm ⁻³	[dye] = 1×10^{-5} mol dm ⁻³ % degradation		[dye]= 2×10^{-5} mol dm ⁻³ % degradation		[dye]= 4×10^{-5} mol dm ⁻³ % degradation	
	pH 2.09	pH 2.81	pH 2.09	pH 2.81	pH 2.09	pH 2.81
without Fe (III)	0.3	2	1.3	0.4	0.5	0.3
0.17	0.6	2.1	2.3	0.1	0.3	0.2
0.342	7.9	21.3	5.1	18.3	2.1	8
0.514	14.7	67.8	11.6	41.4	4.9	21.7
0.685	19.7	92.5	18	61.7	5.9	27.6
0.857	25.7	100	23.9	73.2	8.6	26.3
1.02	29	100	31.6	77.2	9.7	34.3
1.2	35	99.2	36.1	94.5	12	28.1
1.714	82	95.7	59.4	96.7	29.9	65.4
3.429	98.8	93.2	94.5	94.3	53.2	78
5.143	97.6	88.4	97.7	91.6	79.6	80.8
6.857	95	84.4	96.6	89.8	84	83.4
8.571	91.7	82.1	94	86.9	94.5	90
10.286	90.2	77	92.8	85.2	94.7	89.8
12	85.8	74.4	93.6	83.1	94.4	90.5

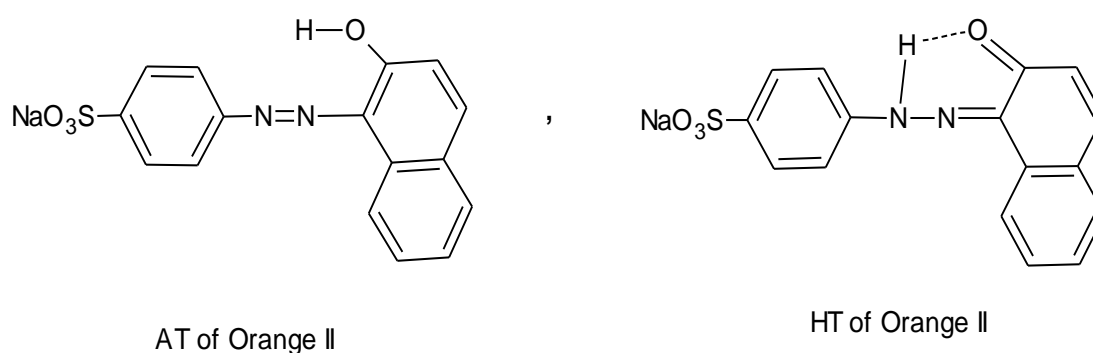
Table 4.11 :- Percentage decrease in Orange II dye absorbance over 180 seconds. Calculated using Equation 4.1. Reactions were carried out in the presence of $2.05 \times 10^{-2} \text{ mol dm}^{-3}$ peracetic acid at pHs of 2.09 and 2.81. Dye and Fe concentrations as indicated in the table below.

Reactant [Fe (III)] / $10^{-3} \text{ mol dm}^{-3}$	[dye] = $1 \times 10^{-5} \text{ M}$ [PAA] = $2.05 \times 10^{-2} \text{ mol dm}^{-3}$ % degradation				[dye] = $1 \times 10^{-5} \text{ mol dm}^{-3}$ [PAA] = $4.11 \times 10^{-2} \text{ mol dm}^{-3}$ % degradation		[dye]= $2 \times 10^{-5} \text{ mol dm}^{-3}$ [PAA] = $2.05 \times 10^{-2} \text{ mol dm}^{-3}$ % degradation		[dye]= $4 \times 10^{-5} \text{ mol dm}^{-3}$ [PAA] = $2.05 \times 10^{-2} \text{ mol dm}^{-3}$ % degradation	
	pH 2.09	pH 2.29	pH 2.81	pH 3.10	pH 1.48	pH 1.88	pH 2.09	pH 2.81	pH 2.09	pH 2.81
without Fe (III)	0.9	0.9	1.8	0.9	3.8	1.9	0.2	1.1	0.3	0.4
0.17	2.4	3.3	8.3	8.4	6.5	6.5	2.8	6.2	1.4	2.6
0.342	22.5	37.4	62.8	71.2	14.4	8.5	24.2	41.8	13.6	40.6
0.514	32.1	76.5	89.0	93.4	32.6	28.7	44.8	83.8	27.0	68.4
0.685	44.7	91.5	94.6	91.0	61.1	87.6	67.7	93.8	36.2	78.3
0.857	49.0	92.2	90.9	87.3	75.5	95.7	80.9	94.8	46.9	81.5
1.02	68.3	93	87.3	84.0	81.1	100	89.4	94.2	55.0	82.9
1.2	71.0	92.4	82.8	77.3	92.8	93.2	94.5	91.9	62.1	83.2
1.714	88.8	87.2	75	75.6	2.9	85.0	88.1	85.8	80.8	92.6
3.429	89.0	67.7	52.6	54.5	94.2	67.5	93.9	74.7	94.4	85.0
5.143	80.4	51.9	42.9	41.2	84.0	52.1	88.0	64.9	93.2	77.5
6.857	67.4	43.9	34.5	40.3	69.9	50.1	80.8	59.0	91.0	71.9
8.571	58.9	40.6	29.0	30	64.6	40.0	75.6	54.2	86.2	69.2
10.286	50.2	33.7	27.0	25.7	55.8	35.1	69.9	49.4	82.6	66.1
12	47.3	26.7	23.5	20.5	46.9	26.5	63.5	45.1	80.9	61.8

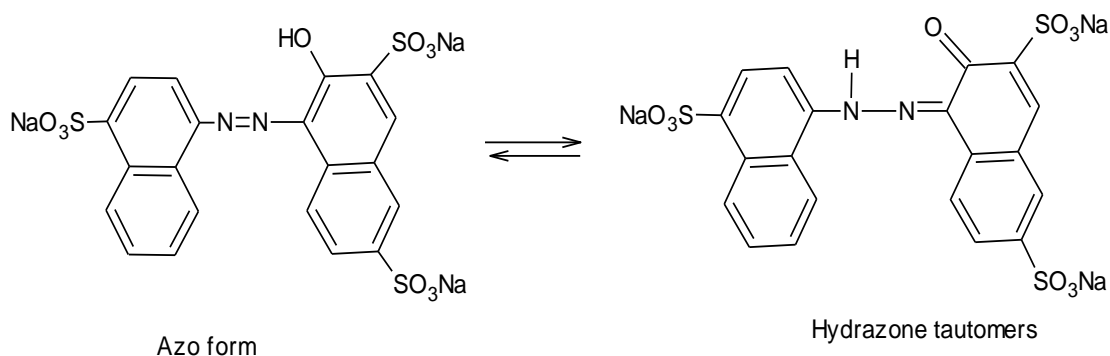
4.4. Discussion

As Oakes and Gratton have pointed out, whilst there have been a great many studies carried out to investigate the kinetics and mechanisms of reactions of azo dyes with various oxidants, many misconceptions about the reactive species involved have arisen from these. Dye oxidation systems are complex, involving several different dye and oxidant species, and are sensitive to the presence of trace metal ion contamination, which can catalyse the reactions (as we have seen in these experiments). In addition there is also the possibility of dye aggregation at low dye concentrations, which leads to complex kinetics¹⁸⁷.

Five of the azo dyes that have been studied in this chapter have a hydroxyl group on the naphthol ring that is ortho to the azo group. An example is Orange II, as shown in Scheme 4.1. Here there are two tautomers, an azo tautomer (AT) and hydrazone tautomer (HT). A naphthol hydroxyl that is ortho to the azo linkage tends to favour the hydrazone form, presumably through the formation of an intermolecular hydrogen bond stabilised structure as shown in Scheme 4.1. Orange II exists predominantly in this form in aqueous solution²⁰⁰. A further example of this azo-hydrazone tautomerism (AHT) is shown in Scheme 4.2 for Amaranth.

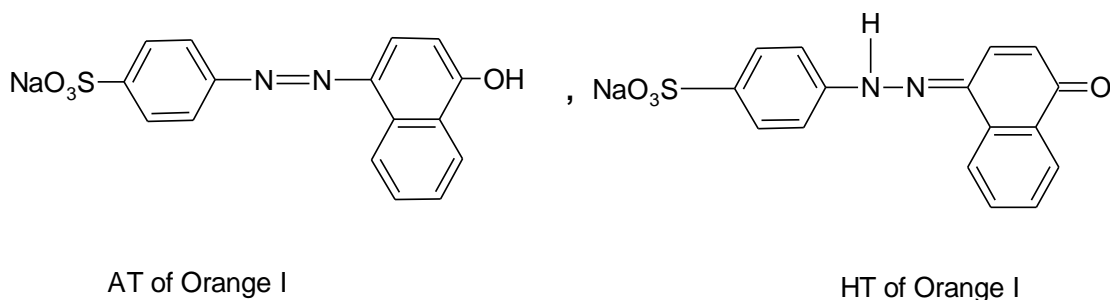


Scheme 4.1 Azo-hydrazone tautomerism (AHT) for Orange II²⁰²



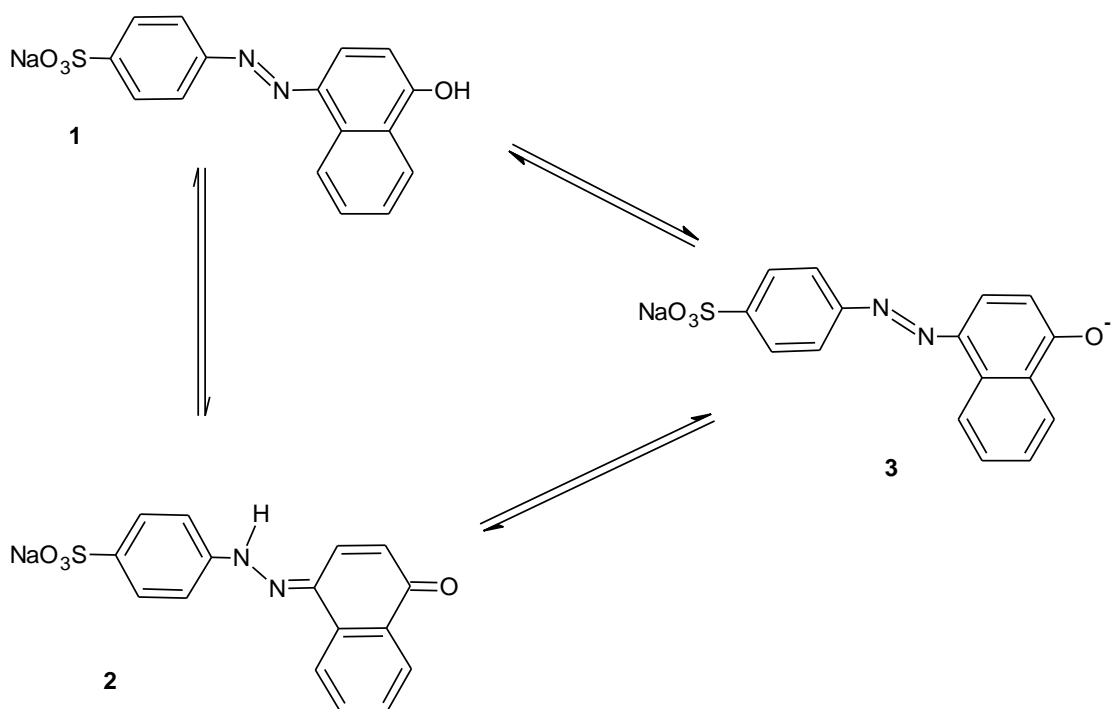
Scheme 4.2 Azo-hydrazone tautomerism (AHT) for Amaranth dye¹⁹⁵

In addition to the five ortho-hydroxyl substituted azo dyes used in this Chapter, a para-hydroxyl substituted azo dye, orange I was also used for comparison. The AHT tautomers for this dye are shown in Scheme 4.3, and whilst the hydrazone form is less favoured for p-substituted species, the hydrazone tautomer is still the most favoured form for this dye in aqueous solution²⁰⁰.



Scheme 4.3 Azo-hydrazone tautomerism (AHT) for Orange I²⁰⁰

In addition to the azo and hydrazone forms of these azo dyes, it is also important to consider that the conjugated hydroxyl group (ortho or para) will dissociate at high pH to form the 'common ion'. An example is shown in Scheme 4.4 for Orange II, which has a pKa of 11.4. pKa values for azo dyes can range from 8-12, with an ortho-hydroxyl group resulting in pKa values of approximately 2 units higher than p-substituted hydroxyl groups; ortho substituents on the aryl ring can further increase the pKa.



Scheme 4.4 Dissociation to form the common ion¹⁸⁷

The final consideration is the nature of the oxidant species involved in the oxidation reactions. In the case of peroxyacids and hydrogen peroxide there are two possibilities for the reactive species: (a) the undissociated peroxide acting as an electrophile and (b) the dissociated peroxide acting as a nucleophile. Oakes and Gratton (1998) through a series of detailed and eloquent studies have clarified which of the respective dye and peroxide species are involved in dye oxidation. In the case of peroxyacids, evidence gathered from (a) pH dependence studies (pH 6 to 12), (b) plots of dependence of rate on pKa of the peroxyacid (ranging from 7.15 to 8.2) and (c) the relationship between rate and dye substituent, shows conclusively that it is the undissociated peroxyacid that reacts with the common ion of the dye. This contradicts assertions in several studies that the hydrazone species of the dye is the most reactive. In the case of hydrogen peroxide, the authors showed that a different mechanism was involved whereby the highly nucleophilic hydroperoxide anion reacts with the hydrazone form of the dye.

This remainder of this section will discuss the results of uncatalysed and metal-ion catalysed dye oxidation reactions in the context of the mechanisms determined by Oakes and Gratton.

4.4.1. Uncatalysed reaction

Whilst values for the uncatalysed reaction, R_0 , were derived as parameters from non-linear regression to Equation 4.2 for the dependence on iron concentration, the very small intercept meant that there was considerable uncertainty associated with them, and in fact they often were output as small negative values.

Table 4.12 below shows the values for the uncatalysed reaction, converted to observed second order rate constants, $k_{2\text{obs}}$, that were obtained from initial rates of absorbance change for each of the dyes at several different pHs. $k_{2\text{obs}}$ values were obtained from the quotient of the initial rate of absorbance change and the product of the molar absorptivity and the concentrations of the dye and peracetic acid.

Table 4.12 Second order rate constants, $k_{2\text{obs}}$, for the reaction between $4 \times 10^{-5} \text{ mol dm}^{-3}$ azo dyes and $0.0205 \text{ mol dm}^{-3}$ peracetic acid at pH 2.81.

Dye	$k_{2\text{obs}} (\text{dm}^3 \text{ mol}^{-1} \text{ min}^{-1})$	$k_{2\text{obs}} (\text{dm}^3 \text{ mol}^{-1} \text{ s}^{-1})$
Amaranth	0.32	0.0053
Black PN	0.43	0.0072
Carmosine	0.58	0.0097
Orange II	0.70	0.0112
Ponceau R	0.44	0.0073

From a consideration of the reaction mechanism determined by Oakes and Gratton²⁰⁰, it is the undissociated peracetic acid that is reacting with the common ion in this reaction system. At the pH used in this study, 2.81, which is well below the lowest pH used by Oakes and Gratton¹⁸⁷, the peracetic acid is completely undissociated; however the dye is in the hydrazone form, with an extremely small amount of common ion available (for example: the pKa of Orange II is 11.4, so only $2.57 \times 10^{-7} \%$ is in the form of the common ion). Consequently it is expected that the reaction will be extremely slow at this pH, increasing to a maximum at a pH midway between the pHs of the peroxyacid and dye (expected to be at pH 9.9 for Orange II).

It is difficult to find comparison data for this reaction in the literature: Oakes and Gratton have looked at the reaction of peracetic acid with Orange II at 40°C , but at a much higher pH range; however they have published a value for the second order rate constant for the electrophilic reaction, termed k_2^E , which takes into account the respective concentrations of the specific reactant species, the undissociated peroxyacid and the common ion, rather than the total concentrations of peracid and

dye. k_2^E can be calculated from the observed second order rate constant, the pH and the pKa values of the reactants, as detailed in Equation 4.3, in which K_A and K_D are the dissociation constants of the peroxyacid and dye respectively.

$$k_2^E = k_{2\text{obs}} / (\{1/(1 + K_A/[H^+])\} \{1/(1 + [H^+] / K_D)\}) \quad \text{Equation 4.3}$$

Carrying out this calculation for the reaction of Orange II with peroxyacid gives a k_2^E value of $4.5 \times 10^6 \text{ dm}^3 \text{ mol}^{-1} \text{ s}^{-1}$, which is several orders of magnitude higher than the value of $112 \text{ dm}^3 \text{ mol}^{-1} \text{ s}^{-1}$ published by Oakes and Gratton (read off from a graph). There are problems with this comparison, namely the different experimental conditions employed, yet a difference of several orders of magnitude indicates a significant mechanistic difference. The most likely explanation is that in the present study, even though no metal ion catalyst was added for the uncatalysed studies, there were still trace metal ions present that catalysed the reaction, possibly as impurities in the dye itself. Figures 4.12 and 4.13, reporting on the results of the catalysed reaction, show that at low metal ion (Fe^{3+}) concentrations the rate is extremely sensitive to the concentration used. Oakes and Gratton used EDTA to alleviate the problem of metal ion catalysis, as well as avoiding commercially produced dyes which tend to have significant metal ion content. No metal ion chelators were used in the present study because the bulk of the study was designed to elucidate the effect of metal ion concentration on reaction rate.

4.4.2. Catalysed reaction

The azo dyes used in this study are listed in Table 3.2 with experimentally determined values of the wavelength of maximum absorbance in the visible spectrum. Table 3.3 in Chapter 3 shows their systematic names.

In order to make a relative comparison of the catalysed reaction of the five different dyes, the initial rates of absorbance changes were converted to initial rates of reaction by dividing by the *apparent* molar absorptivity of the dye in the presence of 0.012M iron ions (i.e. the iron-dye complex); molar absorptivities in the presence and absence iron are given in Table 4.13. In most cases $0.012 \text{ mol dm}^{-3}$ iron approximates to the maximum observed rate of reaction. The plots, shown in Figure 4.14, show a reactivity order of Ponceau 4R > Amaranth > (Orange II & Carmosine) > Black PN; Orange I is unreactive under these conditions. Ponceau is more reactive than the diazo dye, Black PN by a factor of 5.5 and is 2.8 fold more reactive than Carmosine and Orange II. The order of reactivity shown in is not the same as that observed for the uncatalysed

reaction where it was observed that Orange II was the most reactive dye, though, as discussed in Section 4.4.1, the role of trace metal contaminants is likely to have been significant.

Table 4.13: Molar absorptivities of dyes in the absence and presence of $0.012 \text{ mol dm}^{-3}$ iron (III) ions at pH 2.81

Dye	Molar absorptivity in water ($\text{dm}^3 \text{ mol}^{-1} \text{ cm}^{-1}$)	Apparent molar absorptivity in the presence of $0.012 \text{ mol dm}^{-3}$ iron (III). ($\text{dm}^3 \text{ mol}^{-1} \text{ cm}^{-1}$)
Ponceau 4r	30,550	34,500
Amaranth	22570	52,200
Carmosine	19,050	62,000
Orange I	Not determined	43,000
Orange II	21,000	61,000
Black PN	33,700	49,500

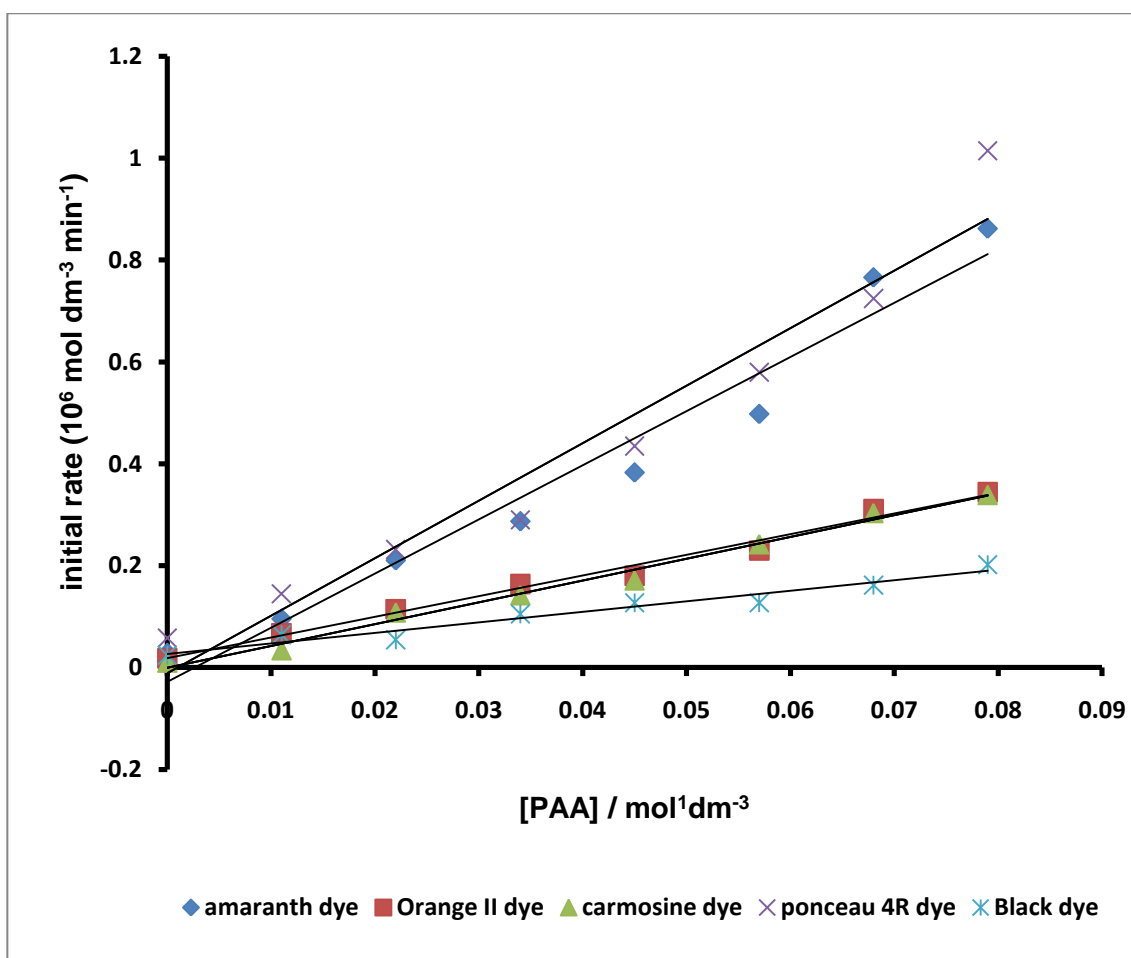


Figure 4.14 :- The reaction of azo dyes Amaranth ,Orange II Carmosine , Ponceau 4r and diazo Black PN dye at ($\lambda = 521\text{nm}, 485\text{nm}, 514\text{nm}, 510\text{nm}, \text{and } 571 \text{ nm}$) respectively with PAA, Temp = 25°C , $[\text{dye}] = 1 \times 10^{-5} \text{ mol dm}^{-3}$, $[\text{FeIII}] = 1.2 \times 10^{-2} \text{ mol dm}^{-3}$

Regarding the mechanism of catalysis the excellent fit of the data to curves described by Equation 4.2 indicate that rapid pre-equilibrium between the dye and iron is followed by attack of the peroxyacid. Moreover, the alternative mechanism of rapid pre-equilibrium between peracid and iron followed by reaction with the dye would not give saturation in iron, as is observed in this case. Additional evidence for an equilibrium complex between iron and dye is given by the significant increases in absorbance observed when mixing the dye with the iron. It is interesting to note, however, that Orange I also complexes with iron, yet is not reactive towards peracetic acid; this dye, of course, has the naphthol hydroxyl group in the para position, compared to the ortho position for the other azo dyes studied in this section.

Several studies have noted the formation of dye metal complexes^{198, 203, 204}, though the precise structure of these complexes is unclear. It is possible that in the case of ortho-hydroxyl azo-dyes that a five membered ring is formed whereby the iron ion bridges the hydroxyl group and the azo nitrogen adjacent to the naphthol ring, thus activating this

nitrogen to attack by the peracid anion (i.e. a switch from the peracid acting as an electrophile to a nucleophile), as shown in Scheme 3.2 in the preceding chapter. We should not of course discount the possibility of free radical mechanisms through a Fenton-like process, even though the corresponding reactions with hydrogen peroxide, reported in the previous chapter, were not significantly accelerated by the presence of iron. As reported in the results, some runs with peracetic acid and iron, particularly at the lowest iron concentrations, demonstrated behaviour whereby there was a lag phase in absorbance change followed by a more rapid bleaching phase. This behaviour could be explained by either: (a) that the complex between iron and dye at the lowest iron concentrations takes some time to form (this is supported to some extent by the initial absorbance values) or (b) a free radical mechanism whereby there is a lag in the formation of the free radicals. Nevertheless, by comparison to the higher concentration that show no lag phase, this process, whichever the mechanism, is slow.

4.4.3. Effect of pH on K

Values for K, the apparent association constant between dye and iron (III) ions, have been obtained from curve fitting to Equation 4.2 at several pHs for each of the dyes. The relationship between strength of association and pH is shown in Figures 4.15 to 4.19 for each of the five azo dyes studied in this section. Each plot has data obtained at different dye several dye concentrations.

The general trends of the data are as follows. Firstly, there is a consistent trend of increasing strength of association with increasing pH, at all dye concentrations used. Secondly, the strength of association seems to decline with increasing dye concentration, and the slope of K against pH is reduced. The increase in K with pH may be due to the ease of deprotonation of the hydroxyl group at higher pHs, facilitating complexation with iron, though this study was restricted to a narrow range of pHs. The decrease in K with higher dye concentrations may suggest dye aggregation, perhaps facilitated by the iron ions, though it is also possible that it is a systematic error arising from the curve fitting procedure.

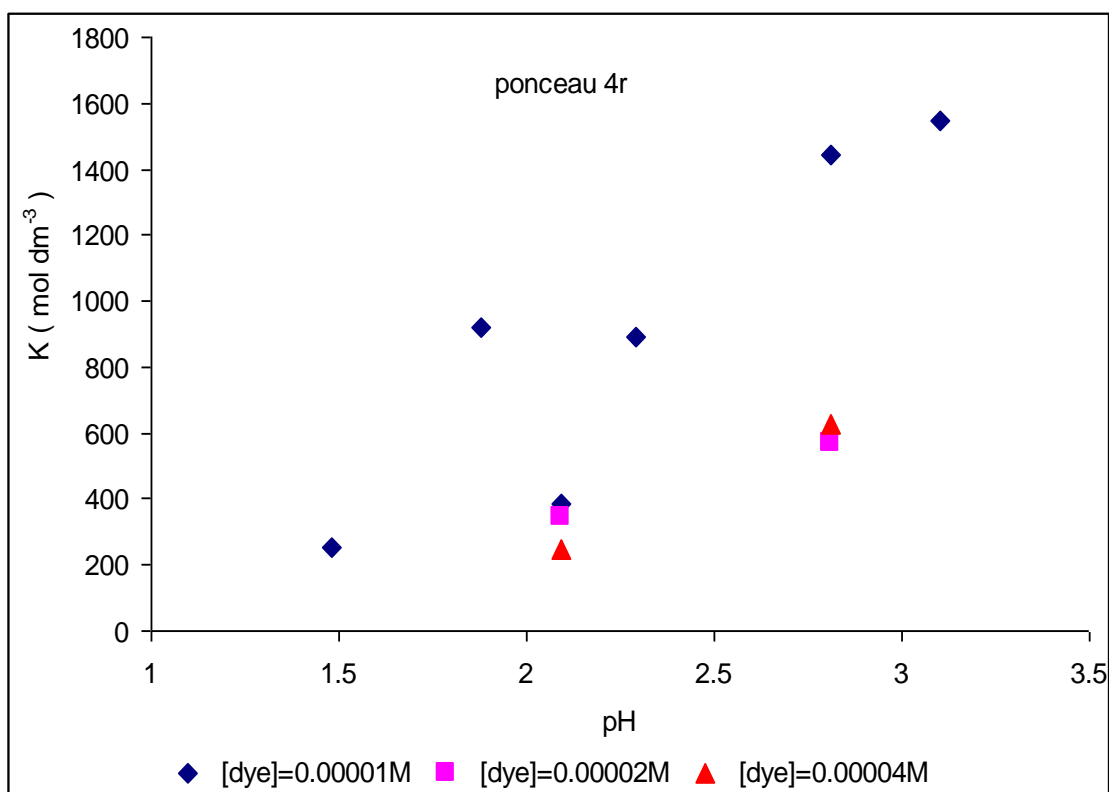


Figure 4.15:- A plot of the equilibrium rate constant K (mol dm^{-3}) vs. pH for the oxidation reactions of Ponceau 4r dye with peracetic acid, at 25°C

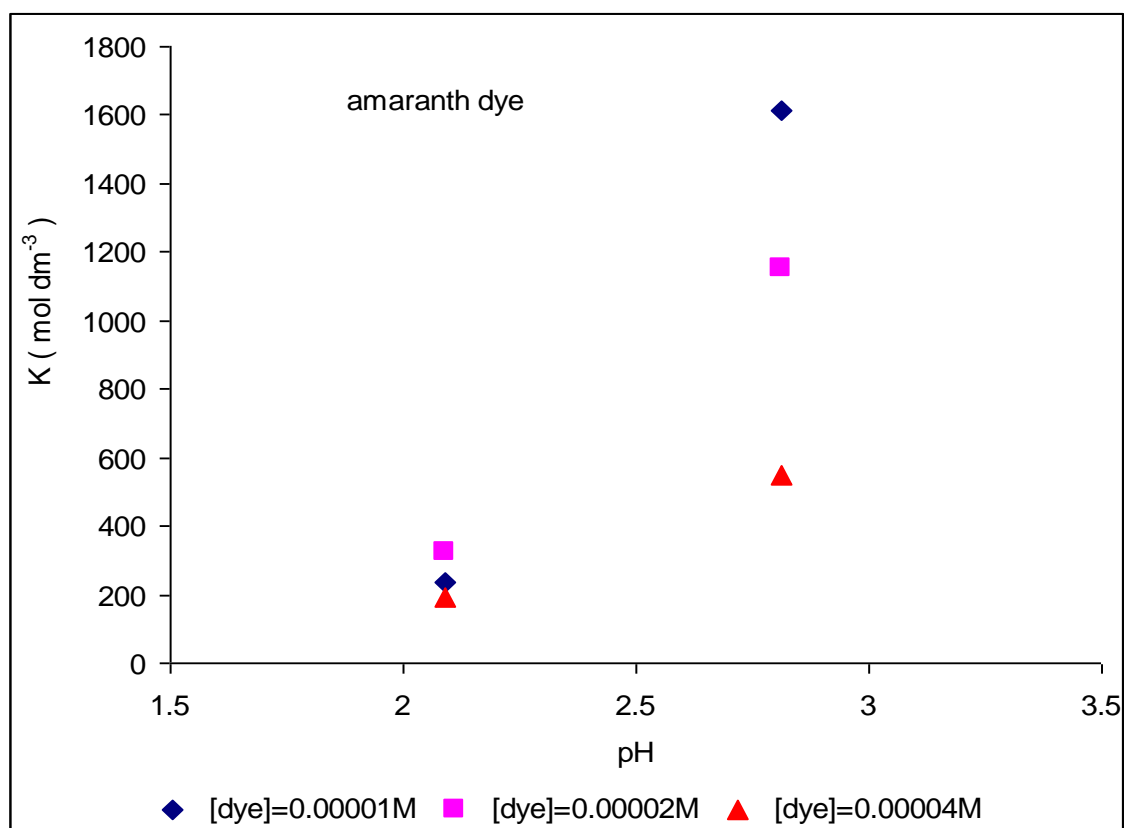


Figure 4.16 :- A plot of the equilibrium rate constant K (mol dm^{-3}) vs. pH for the oxidation reactions of Amaranth dye with peracetic acid, at 25°C

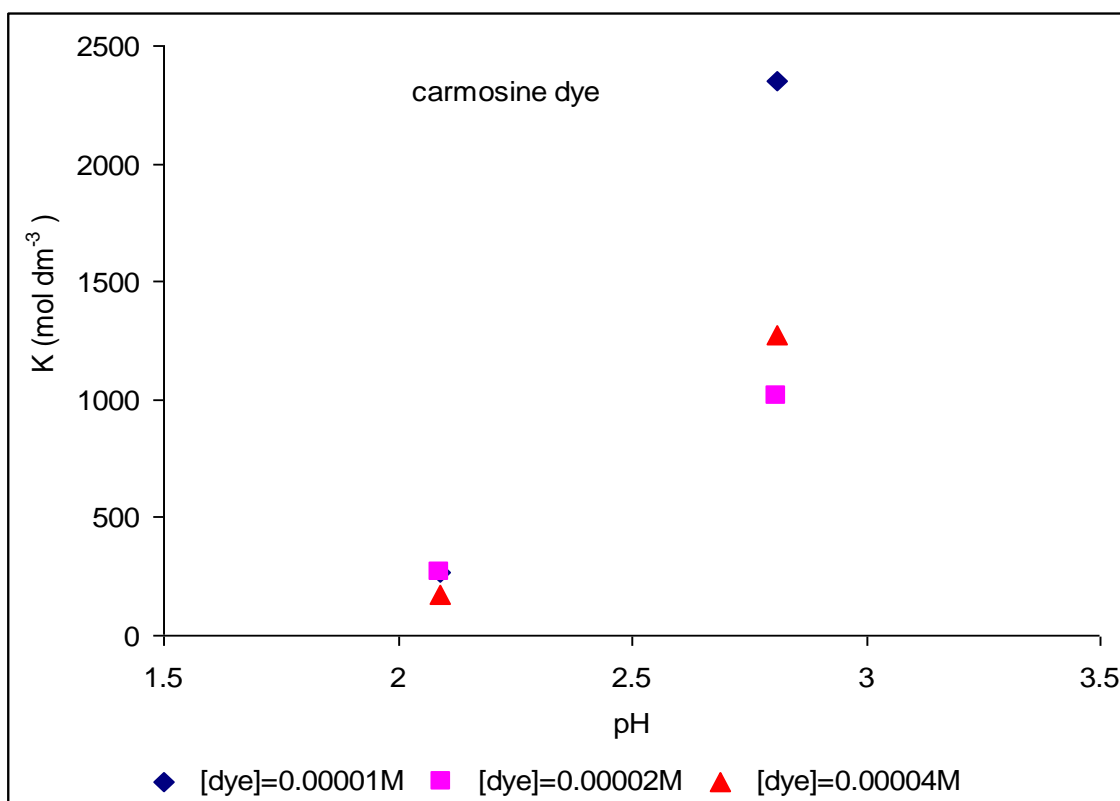


Figure 4.17 :- A plot of the equilibrium rate constant K (mol dm^{-3}) vs. pH for the oxidation reactions of Carmosine dye with peracetic acid, at 25°C

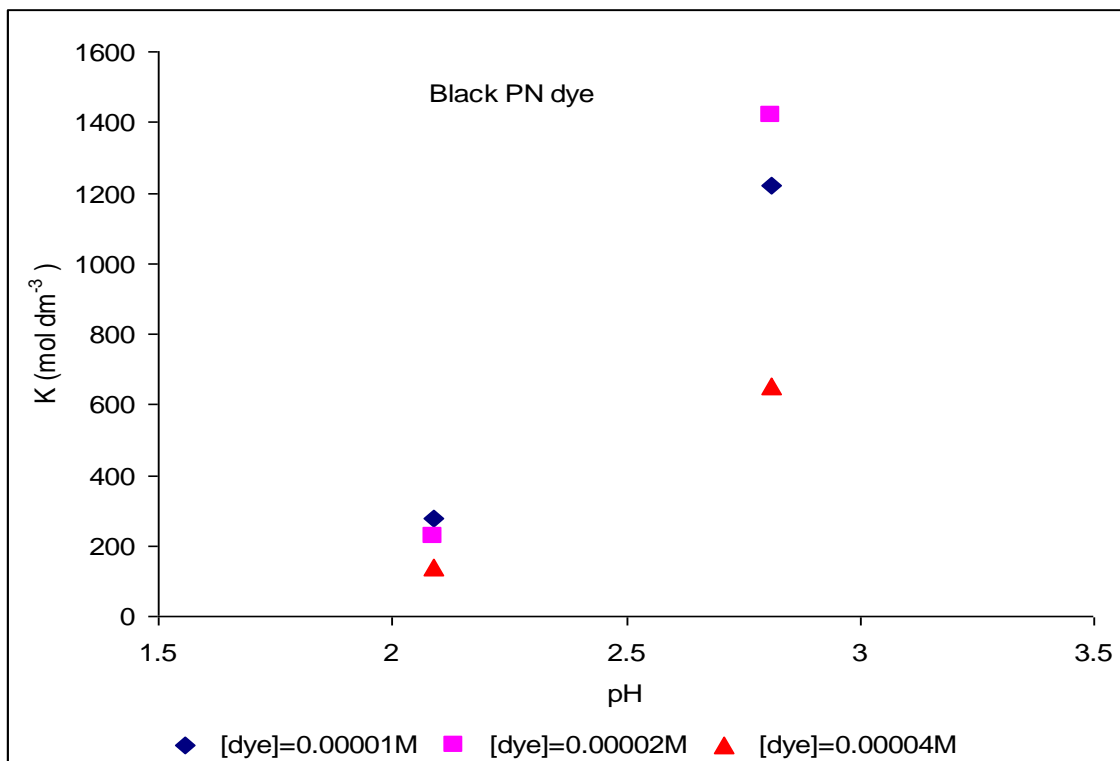


Figure 4.18 :- A plot of the equilibrium rate constant K (mol dm^{-3}) vs. pH for the oxidation reactions of Black PN dye with peracetic acid, at 25°C

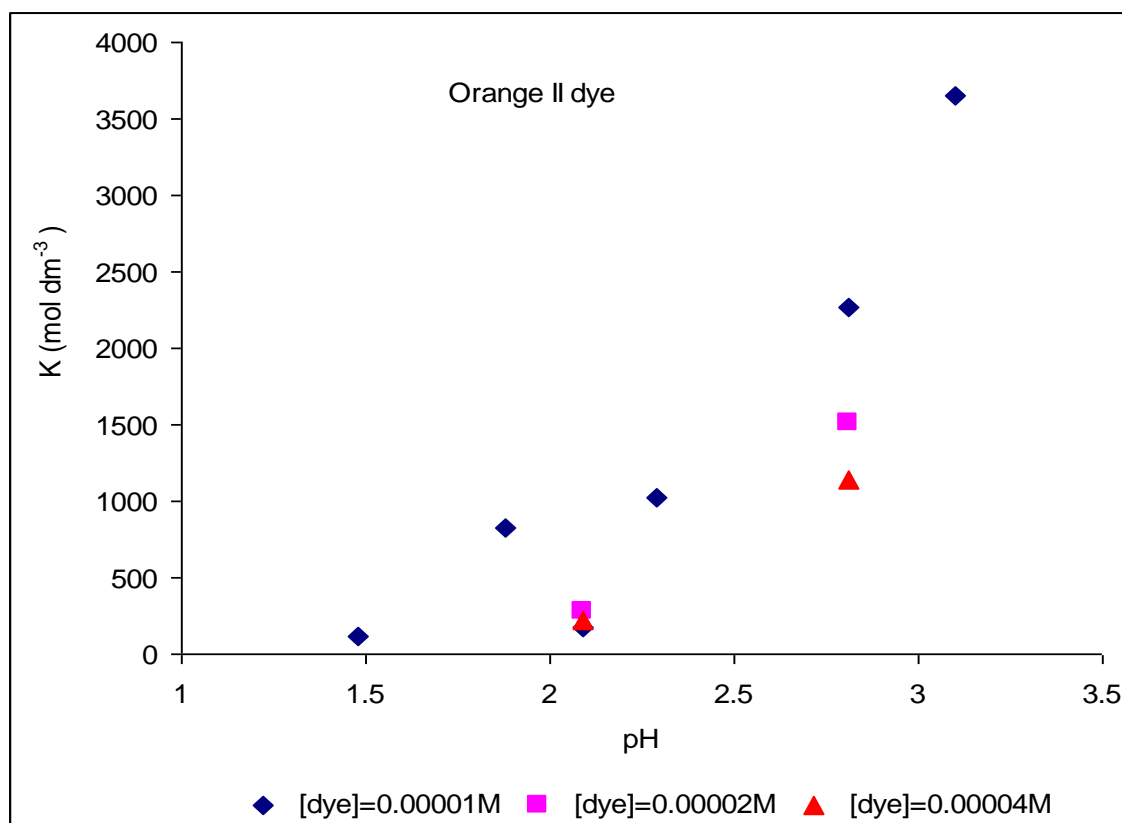


Figure 4.19 :- A plot of the equilibrium rate constant K (mol dm^{-3}) vs. pH for the oxidation reactions of Orange II dye with peracetic acid, at 25°C

4.4.4. Factors affecting dye degradation

One of the key objectives of this section was to determine the optimum conditions for dye degradation, i.e. oxidant concentration, catalyst concentration, and pH. Percent degradation is shown in Tables 4.8 to 4.11 in the results section; however a far more intuitive approach to elucidating the main factors affecting degradation is to plot clustered bar graphs of % degradation against iron concentration for each pH, as shown in Figures 4.20 to 4.24 for each of the dyes (note that this is the percent dye degradation after 180 seconds). What is quite evident from all of the plots is that maximum degradation occurs at the highest pH (generally pH 3.1) and at a fairly low iron concentration; the optimum % degradation appears to be about 1×10^{-3} M iron for each of the dyes. Lower pHs have a significant reduction in overall degradation, whereas higher iron concentrations result in a reduction in dye degradation. Dye degradation is highly sensitive to iron concentration at lower iron concentrations; this reflects the similar dependence observed for reaction rate. The decline in degradation at higher iron concentrations may be due to the formation of degradation products that are complexed with iron, increasing their molar absorptivity; there is evidence from the kinetic studies that this is the case. The dependence of % degradation on pH almost

certainly reflects the greater strength of association between iron and dye at higher pHs, as discussed in the previous section.

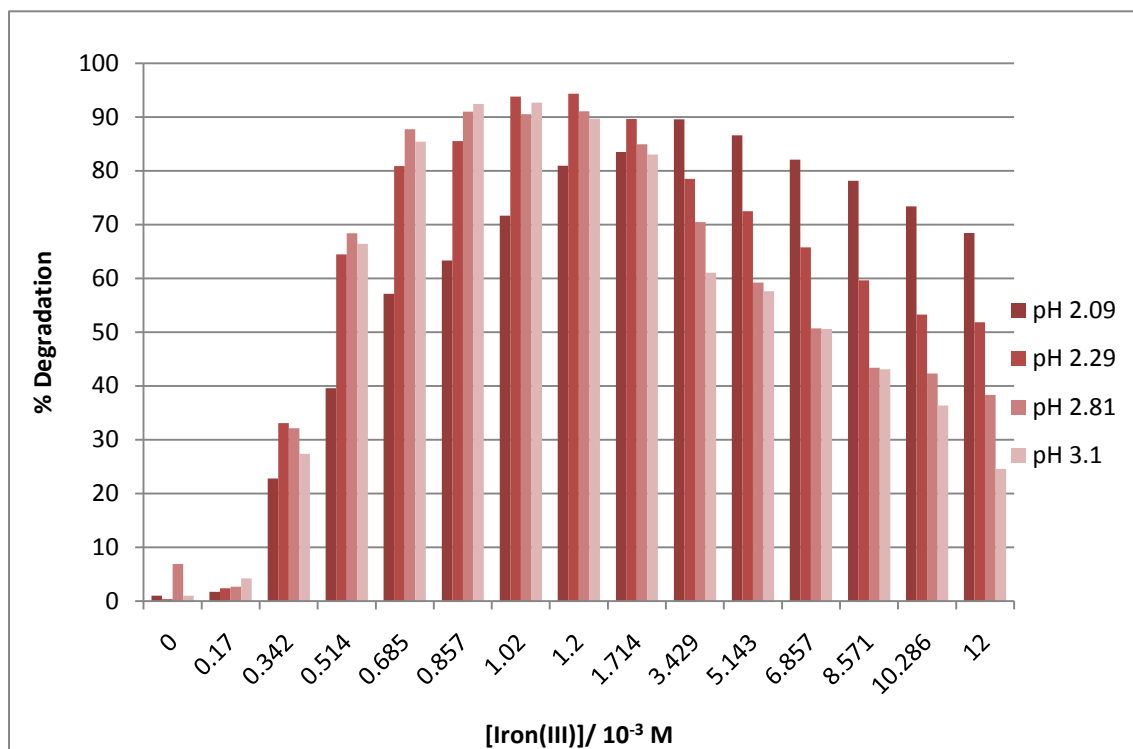


Figure 4.20 Effect of pH and iron concentration on the degradation of Ponceau 4r dye

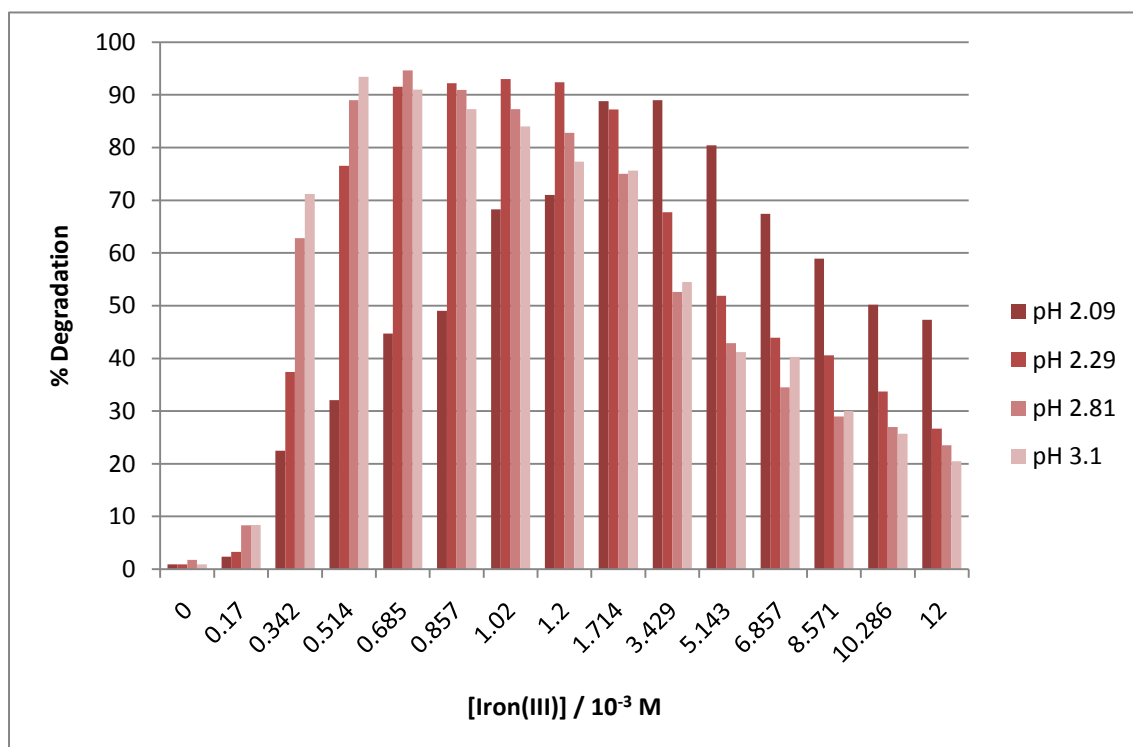


Figure 4.21 Effect of pH and iron concentration on the degradation of Orange II dye

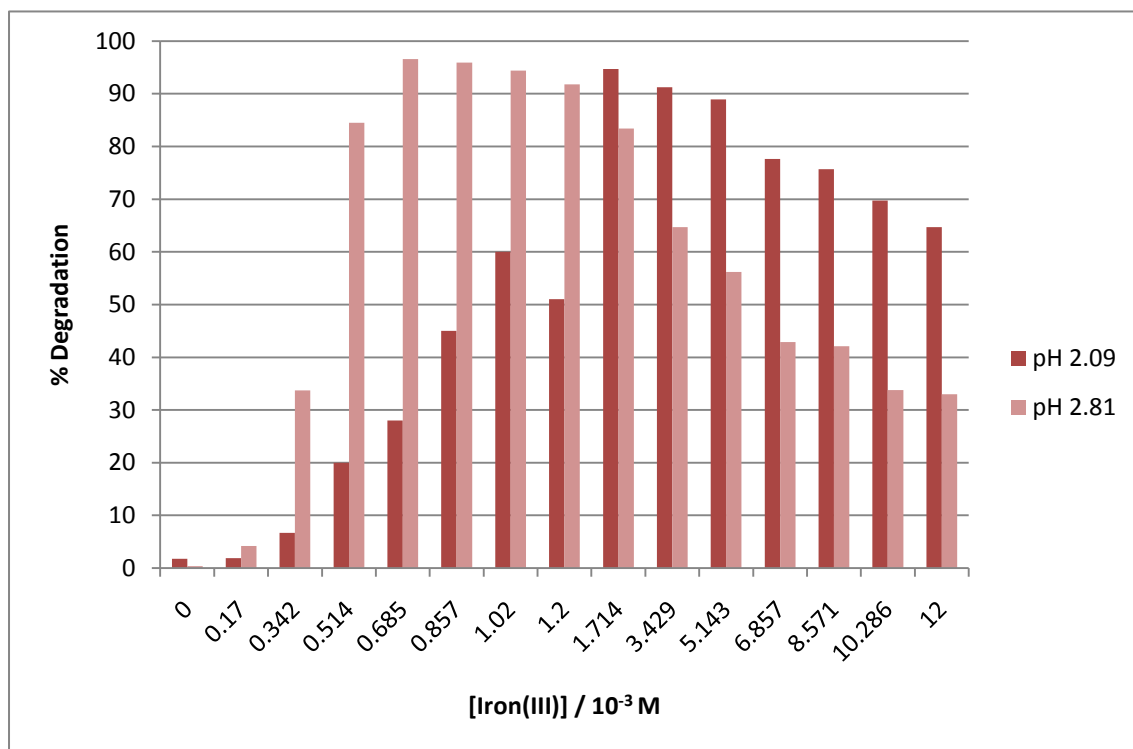


Figure 4.22 Effect of pH and iron concentration on the degradation of Amaranth dye

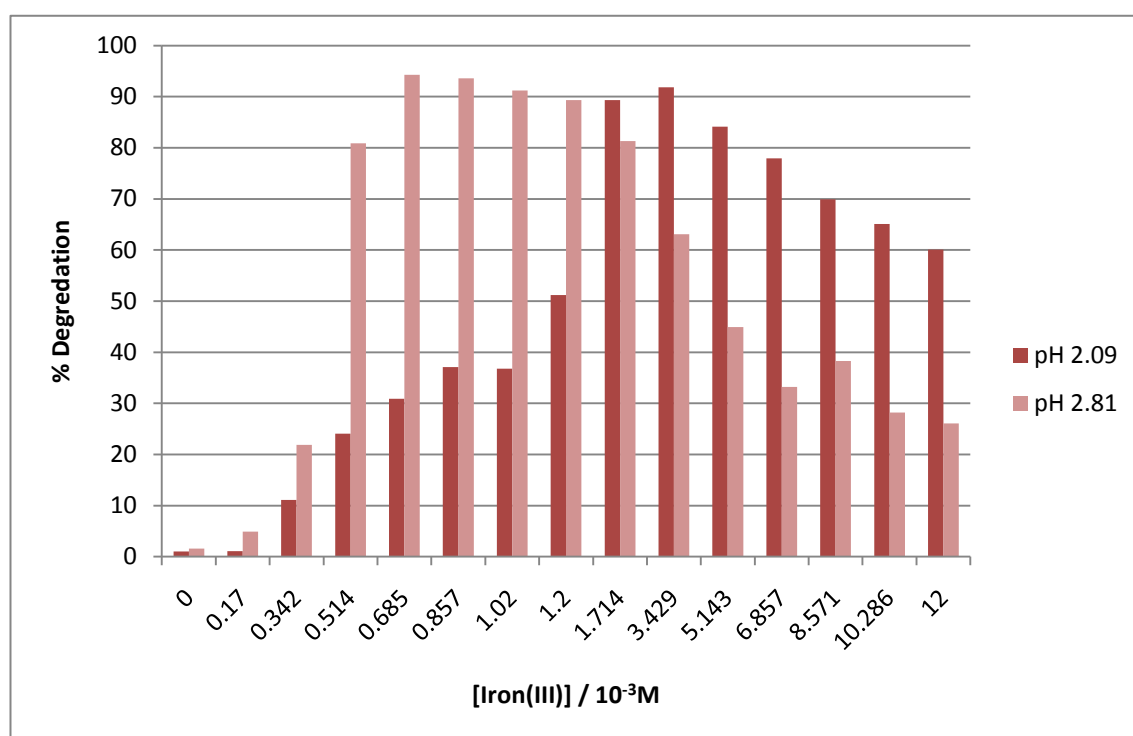


Figure 4.23 Effect of pH and iron concentration on the degradation of Carmosine dye

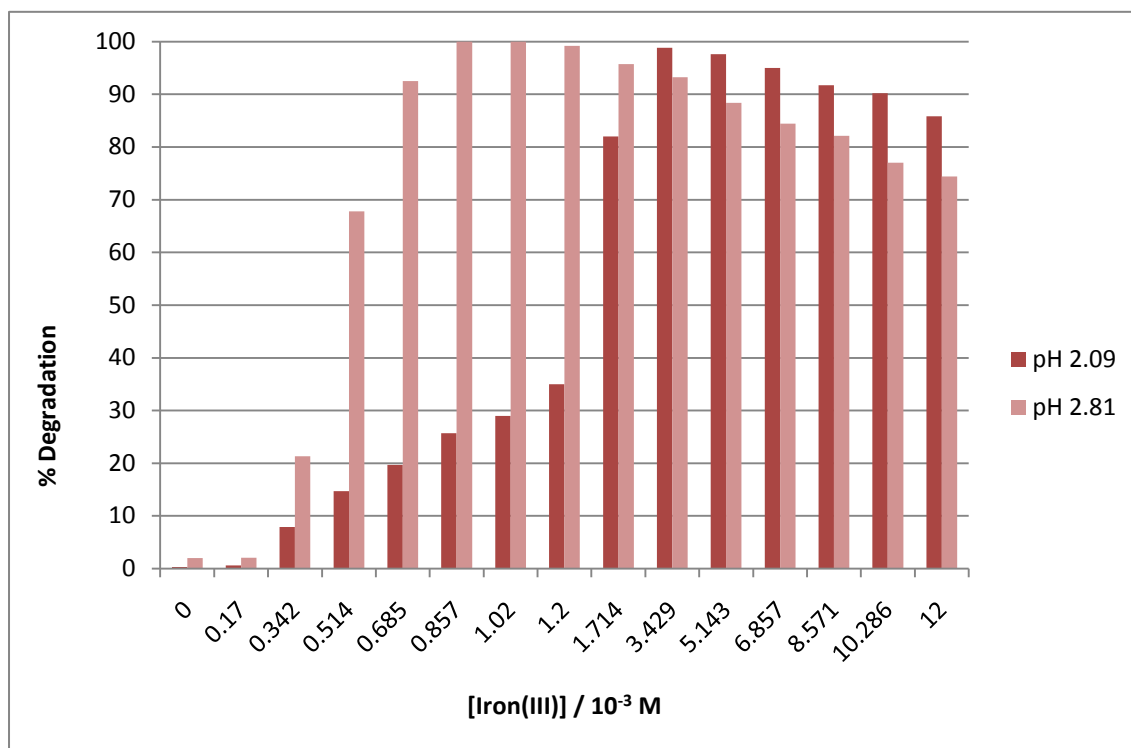


Figure 4.24 Effect of pH and iron concentration on the degradation of Black PN dye

The range of pHs that can be used in these studies is limited, because, as Modirshahla et al. have found²⁰⁵, at pH values above 4, the % degradation decreases because the iron starts to precipitate as hydroxide. Similar results have been reported by Pignatello (1992)²⁰⁶.

4.5. Conclusions

Oakes and Gratton¹⁸⁷ have conclusively shown that *in the absence of metal ion catalysts*, peroxyacids such as *m*-chloro and *p*-sulfo perbenzoic acid, the mechanism of azo dye oxidation involves the reaction of the azo dye common ion and the undissociated peroxyacid; i.e. that the peroxyacid is acting as an electrophile. Furthermore, a correlation between pKa of the peroxyacid and rate, which included peracetic acid, showed that all peroxyacids react in the same way. The most likely mechanism would be nucleophilic attack of an azo nitrogen on the outer peroxidic oxygen of the protonated peracid, though no specific mechanism has been proposed by Oakes and Gratton²⁰⁰. Hydrogen peroxide, a much more powerful nucleophile has been shown by the same authors to oxidise azo dyes by reaction of the perhydroxyl anion with the hydrazone tautomer of the azo dye.

The results obtained in this study for the reaction of azo dyes with peroxyacids without added iron, when converted to the second order rate constant for the electrophilic reaction, k_2^E , give values that are several orders of magnitude higher than those derived from literature studies²⁰⁰. It is likely, because no chelating agents were used in our study, for example EDTA as used by Oakes and Gratton¹⁸⁷, that trace metal impurities catalysed the reaction. We have seen that the reaction rate is extremely sensitive to iron concentration at low iron concentrations, so only a small amount of metal ions, present as either impurities in the dye, or on glassware, would be necessary to significantly enhance the rate. Further studies are needed to clarify this point; i.e. the addition of EDTA to the reaction solution to obtain comparison rate constants.

For the catalysed reaction we observed a significant dependence of observed rate of absorbance decrease on iron concentration that also demonstrated saturation in iron concentration at high iron concentrations. This, together with the observation of an increase in absorbance when adding iron to dye solutions, suggested the formation of an iron(III)-dye complex which then reacts with peracetic acid. An equation derived for this pathway (Equation 4.2) in which the dye-iron(III) association constant, the maximum rate, and the uncatalysed rate were parameters, showed an excellent fit to the data for all dyes and conditions. It is uncertain whether the reaction mechanism remains the same as for the catalysed reaction (as determined by Oakes and Gratton²⁰⁰). All of the dyes studied in this chapter had naphthol hydroxyl groups in an ortho position to the azo linkage. This facilitates an iron complex in which the iron bridges the hydroxyl oxygen and the azo nitrogen. The resulting complex, with electron deficient nitrogen would then be susceptible to nucleophilic attack by the perhydroxyl anion, thus changing the mechanism from that for the uncatalysed reaction. Orange I, which has the hydroxyl in the para position to the azo linkage does form a complex with iron, as evidenced by the absorbance enhancement upon adding iron(III) to a solution of the dye, however it cannot form the same bridged complex as the ortho-hydroxy azo dyes, which may explain the much lower reactivity for the catalysed reaction. The association constant for the complexes with the ortho-hydroxyl azo dyes, obtained from the fits to the kinetic data, is found to increase with pH. Further studies are required to investigate the nature of the complex formed between the dyes and iron (III).

In this discussion, the emphasis has been on reaction mechanisms that involve the peracetic acid reacting as either an electrophile (uncatalysed reaction), or, possibly, as a nucleophile (catalysed reaction). There is of course a large body of literature that has

looked at Fenton-like and photo Fenton reactions for systems involving peroxides and azo dyes^{126, 150, 193, 198, 203, 205, 207-215}. For these systems, the formation of hydroxyl and perhydroxyl radicals and their subsequent attack on the azo dye is seen as the main mechanism of reaction. Davies and Jones²¹⁶, have suggested that at pHs less than 9, the predominant reaction mechanism for the bleaching of the ortho-hydroxyl azo dye, Amaranth, by peroxyacids is the metal ion catalysed decomposition of the perbenzoic acid to form free radicals; the reaction is suppressed by the metal ion chelator, EDTA.

It is notable in this study, however, that the Fenton-like system of Iron(III) and hydrogen peroxide reacting with a range of azo dyes gave relatively low reaction rates compared to the corresponding reactions with peracetic acid (Chapter 3). Nevertheless, evidence of the possible involvement of radicals in our studies comes from the observation of a lag phase followed by a more rapid bleaching phase in the oxidation of azo dyes by peracetic acid at the lowest iron concentrations (another possibility is that at these iron concentrations the reactive iron complex forms at a much slower rate). However, this process is slow by comparison with the rate of oxidation at higher iron concentrations that do not exhibit this lag phase; consequently, if free radical mechanisms are suggested then they are not significant compared to the proposed formation of a reactive iron-dye complex.

Finally, from the point of view of practical application of this work, percent dye degradation under various experimental conditions has been studied for five azo dyes. The results were remarkably consistent, and showed that the optimum conditions are pH 3, with approximately 0.001M added iron; further addition of iron is wasteful since it results in a reduction of degradation, most probably through the formation of coloured complexes between degradation products and iron²⁰⁶.

Chapter 5. Reaction of hydrogen peroxide with p-nitrophenyl acetate (PNPA) in the presence of different buffers.

5.1. introduction

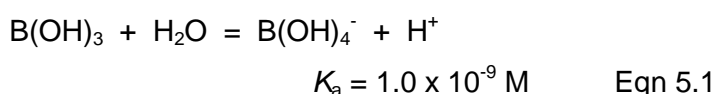
Depending on the type of reaction under study, peroxides, such as hydrogen peroxide and peracetic acid used in this work, can act as either nucleophiles or electrophiles. This was highlighted in the previous chapter for the oxidation of azo dyes by peracetic acid where potential reaction pathways included (a) the reaction of the undissociated peracetic acid with the common ion form of the azo dye, whereby a nitrogen on the azo dye acts as the nucleophile and (b) the reaction of the dissociated peracetate anion with the hydrazone tautomer of the azo dye in which the peracid acts as the nucleophile. Oakes and Gratton (1998) have shown that for peracids, it is the former pathway that is the significant one, contrary to other literature reports. The same authors also showed that for hydrogen peroxide, the predominant pathway is the nucleophilic attack of the dissociated perhydroxyl anion on the hydrazone form of the azo dye. The switch in mechanism is presumably because hydrogen peroxide is a much better nucleophile than peroxyacids.

In this chapter, similar issues are explored for the reactions of peroxyborates, which are a complex, pH dependent, system of species formed from the equilibrium between hydrogen peroxide and boric acid. As discussed in previous chapters, hydrogen peroxide, whilst a powerful oxidant, tends to react quite slowly, hence the extensive literature on systems that can speed up these reactions, including some of the advanced oxidation systems used in this work, for example the transformation into peracetic acid and the use of metal ion catalysts. Peroxoborates, particularly monoperoxoborate, $\text{HOOB}(\text{OH})_3^-$, which is formed in significant proportions at pHs above 7, have been shown to significantly accelerate the rate of oxidation of substituted phenyl methyl sulfides²¹⁷. It is almost certainly the case that monoperoxoborate is acting as an electrophile in these reactions, even though at first sight this seems strange, owing to the presence of a negative charge. Nevertheless, there is some uncertainty in the literature about the nature of peroxoborates, with several papers reporting that they are in fact nucleophiles: for example Thompson et al (1993)²¹⁸ observed a small (14%) increase in the rate of reaction between hydrogen peroxide and phenolphthalein, which is proposed to commence with the nucleophilic attack of the perhydroxyl anion on the

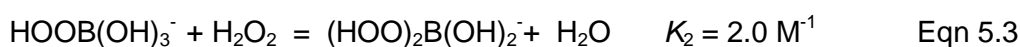
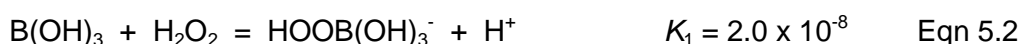
central carbon of the substrate. In addition, McKillop and Sanderson (1995) in their review of the use of sodium perborate and sodium percarbonate in synthetic organic chemistry²¹⁹, state that the BOOH group has nucleophilic activity. It is this ambiguity that the work in this chapter seeks to clarify: whilst the reaction between organic sulphides and peroxides is generally well understood, involving attack of the sulphur on the outer peroxidic oxygen of the peroxide, there is the possibility of some latent electrophilicity associated with the sulphur atom and that in the case of peroxoborate species, which are known to catalyse the reaction with hydrogen peroxide, they may be acting as nucleophiles.

The work in this chapter involves the reaction of hydrogen peroxide with p-nitrophenyl acetate (PNPA) in the presence of different buffer components and at different pHs. This reaction is well characterised and involves the nucleophilic attack of the perhydroxyl anion on the carbonyl carbon of the PNPA to form peracetic acid and p-nitrophenol, the anion of which is highly coloured and is used to follow the progress of the reaction. If peroxoborate species are indeed capable of acting as nucleophiles then some catalysis of the reaction will be observed, depending on the respective concentrations of hydrogen peroxide and borate, and the pH. If on the other hand, peroxoborates act as electrophiles then some inhibition of the reaction is likely to be observed.

It is perhaps pertinent at this point to review the complex system of peroxoborate species that exist in aqueous solution when hydrogen peroxide and boric acid are mixed together. In water, boric acid is in equilibrium with the borate anion, which predominates above pH 9, as detailed in Equation 5.1.

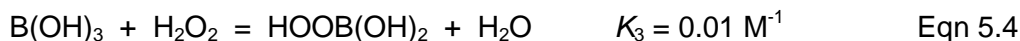


In aqueous hydrogen peroxide boric acid is in rapid equilibrium with mono- and diperoxoborates, as defined by Equations 5.2 and 5.3.

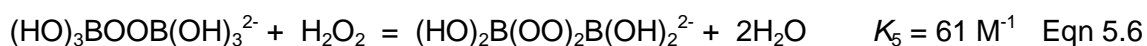


The peroxyborates are the predominant species between about pH 7 and 13, depending on the total concentrations of peroxide and boron species.

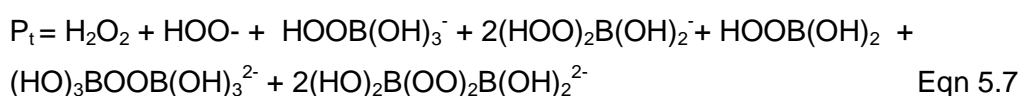
In addition, at lower pHs, the $\text{HOOB}(\text{OH})_2$ species is in equilibrium with hydrogen peroxide, according to Equation 5.4, though the low formation constant ensures that it is only present at about 1% of the total peroxide concentration.



In addition, recent studies by Rey and Davies²²⁰ and Deary and Davies²¹⁷ have shown conclusive evidence for the formation of two other significant peroxoborate species at higher pHs, namely peroxodiborate, BOOB , and diperoxodiborate, $\text{B}(\text{OO})_2\text{B}$, according to Equations 5.5 and 5.6 respectively. It is certainly possible that other peroxoborate species exist in addition to those listed above, though this system has been found to adequately describe the kinetic and absorption data associated with the above studies.



Using Equations 5.1 to 5.6, in addition to the mass balance equation for total peroxide, P_t , (5.7), it is possible to simulate the concentrations of each of these species in solution at different pHs and peroxide / borate concentrations. Figures 5.1 and 5.2 show the results of two simulations that were produced using Grafit, version 6.0.5, in which the peroxide concentrations were solved numerically, and the borate concentration solved using an analytical equation derived from Equations 5.1 to 5.6 (utilising a model previously constructed for work carried out in references²²⁰ and²¹⁷)



In the simulations shown in Figures 5.1 and 5.2, it is assumed that sodium borate is used as the source of peroxide, dissociating to yield equimolar concentrations of hydrogen peroxide and boric acid. In Figure 5.1, where the amount of peroxide is 0.2M, the plots clearly show that above pH 6 the concentrations of the various peroxyborates significantly increase, especially the monoperoxoborate and the diperoxodiborate. In Figure 5.2 where the simulated peroxide concentration is 0.05M, the monoperoxoborate starts to increase in concentration after pH 6.5, though it remains the only significant peroxoborate species until pH 8.

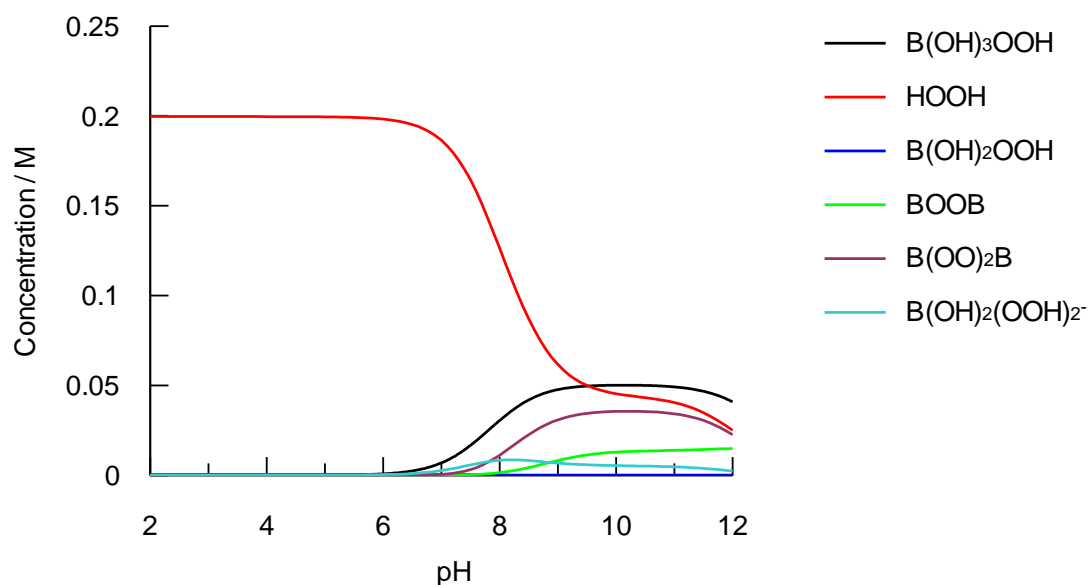


Figure 5.1: Simulated distribution of the peroxoborate species and hydrogen peroxide as a function of pH for a system containing 0.2M sodium borate and 0.2M total hydrogen peroxide.

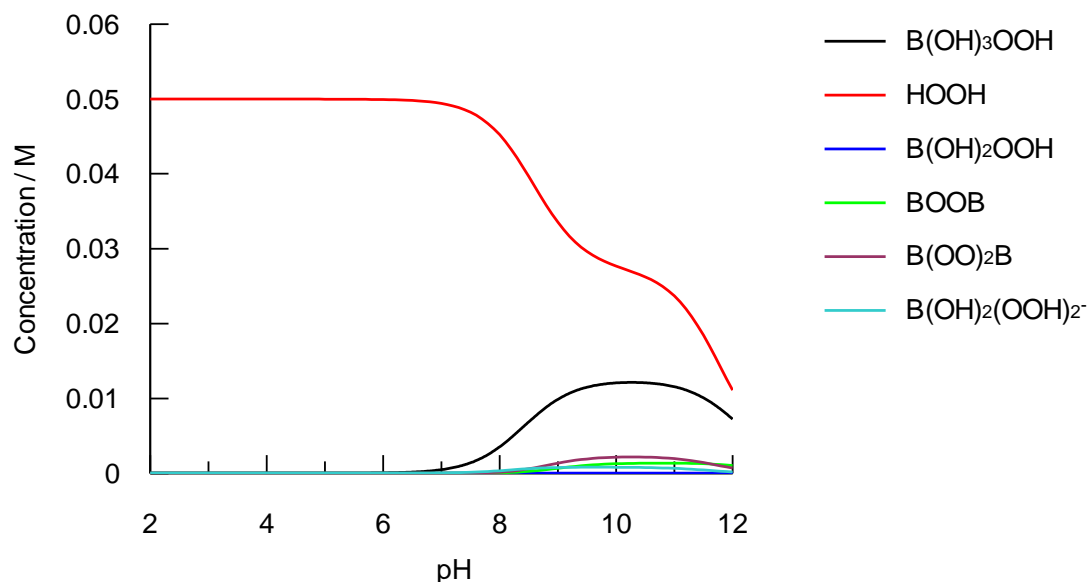


Figure 5.2: Simulated distribution of the peroxoborate species and hydrogen peroxide as a function of pH for a system containing 0.05M sodium borate and 0.05M total hydrogen peroxide.

From Figures 5.1 and 5.2 it can be seen that by observing the reaction of hydrogen peroxide with PNPA in the presence of borate buffer at a pH range between 6 and 8, any borate species present that are capable of acting as nucleophiles should cause an upward deflection in a plot of rate against sodium borate concentration at the higher pH values, and that the pH dependence should indicate if any catalysis is occurring. As a comparison, studies were also conducted in carbonate and phosphate buffers.

5.2. Experimental

As rationalised above, the experiments described in the following section had the aim of determining the rate of reaction between hydrogen peroxide and the ester, p-nitrophenyl acetate, in the presence of different buffer systems. The borate system is of particular interest and it is predicted that pH and concentration dependence studies should show up any nucleophilic character of borate species through the enhancement of rate compared to other buffer systems. Conversely, if borate is solely an electrophile then some depression in rate might be observed.

5.2.1. Materials

Analytical grade materials were used wherever possible. paranitrophenyl acetate ($C_8H_7NO_4$), sodium hydrogen carbonate ($NaHCO_3$). Sodium carbonate 10-hydrate ($Na_2CO_3 \cdot 10H_2O$). sodium perborate of the best available grade were obtained from BDH chemicals Ltd pool England ($NaBO_3 \cdot 4H_2O$). Sodium phosphate, mono basic 99%. (NaH_2PO_4).sodium phosphate, dibasic , 99% (Na_2HPO_4).Boric acid (H_3BO_3), sodium hydroxide ($NaOH$). Hydrogen peroxide, H_2O_2 (Fisher, 30% aqueous solution), Potassium hydrogen phthalate, $COOHC_6H_4COOK$. Potassium iodide KI. Sodium thiosulphate $Na_2S_2O_3 \cdot 5H_2O$. Ammonium heptamolybdate (AHM), $(NH_4)_6Mo_7O_{24} \cdot 4H_2O$, from BDH Chemicals Ltd, England. All solutions were prepared in distilled water.

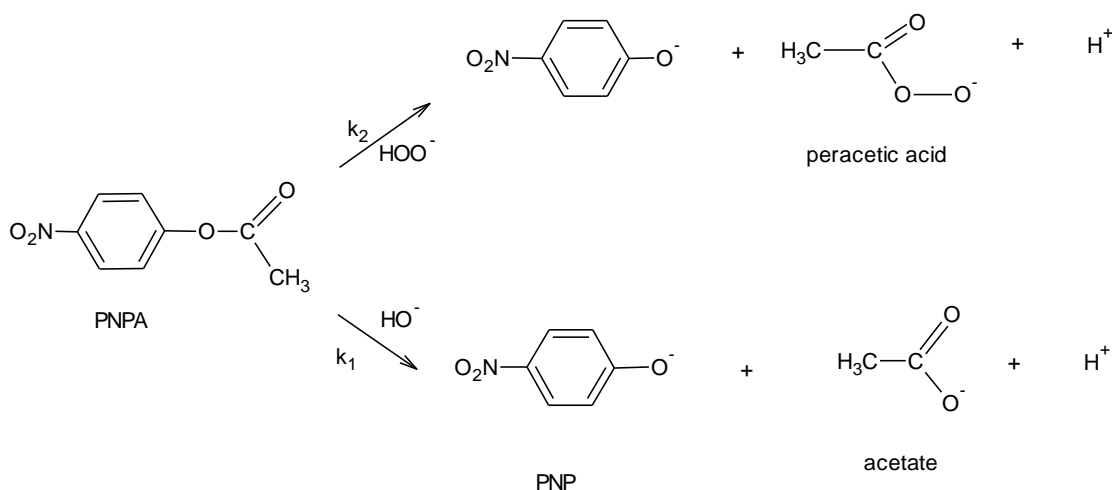
A stock solution of paranitrophenylacetate of approximately $0.001 \text{ mol dm}^{-3}$ concentration was prepared by adding an appropriate amount of the solid PNPA to 250 ml of distilled water and allowed to stir for one hour before filtering through a $10 \mu\text{m}$ sintered-glass funnel to remove any undissolved PNPA. The solution could be stored for up to a week without appreciable hydrolysis taking place.

Hydrogen peroxide, either added directly or as sodium perborate was determined iodometrically using the procedure that has been described previously in Chapter two.

5.2.3. Kinetic measurements

Under pseudo first order conditions, the rate of release of PNP at 400nm was followed for solutions of PNPA (approximately $3 \times 10^{-5} \text{ mol dm}^{-3}$) in the presence of excess hydrogen peroxide (see Figures for details) using a Pharmacia Biotech Ultraspec 2000 spectrophotometer.

Colourless p-nitrophenyl acetate (PNPA) reacts with the perhydroxyl anion to form p-nitrophenol (PNP) which has a λ_{\max} at 400 nm. In addition, PNPA hydrolyses by reaction with the hydroxide ion. These reactions are shown in Scheme 5.1 below, where the rate constants for hydrolysis and perhydrolysis are denoted as k_1 and k_2 respectively.



Scheme 5.1

For convenience, total hydrogen peroxide concentration $[\text{H}_2\text{O}_2]_T$ is used rather than the concentration of the reactive species, $[\text{HOO}^-]$, which is dependent on pH. We can, therefore, define an observed second order rate constant, $k_{2\text{obs}}$, which has the relationship to k_2 shown in Equation 5.8:

$$k_{2\text{obs}} = k_2 \frac{K_a}{(K_a + [\text{H}^+])} \quad \text{Eqn 5.8}$$

where K_a is the acid dissociation constant for hydrogen peroxide.

The rate law for the reaction can now be defined, as shown in Equation 5.9

$$\frac{d[\text{PNPA}]}{dt} = k_{2\text{obs}} [\text{H}_2\text{O}_2]_T [\text{PNPA}] + k_1 [\text{PNPA}] \quad \text{Eqn 5.9}$$

The reaction was followed spectrophotometrically, for which the following relationships hold:

$$A = [\text{PNPA}] \varepsilon_{\text{PNPA}} + [\text{PNP}] \varepsilon_{\text{PNP}} \quad \text{Eqn 5.10}$$

$$A_0 = [PNPA]_0 \varepsilon_{PNPA} \quad \text{Eqn 5.11}$$

Now, $[PNPA]_0 = [PNP]_\infty$

Thus:

$$A_0 = [PNP]_\infty \varepsilon_{PNPA} \quad \text{Eqn 5.12}$$

Also,

$$A_\infty = [PNP]_\infty \varepsilon_{PNP} \quad \text{Eqn 5.13}$$

$$A_\infty = [PNPA]_0 \varepsilon_{PNP} \quad \text{Eqn 5.14}$$

Where A is the absorbance, with the subscripts indicating the initial and infinity values; and ε is the molar absorptivity of the species indicated by the subscript.

Now,

$$[PNPA]_0 = [PNP] + [PNPA] \quad \text{Eqn 5.13}$$

And

$$[PNPA]_0 = [PNP] + [PNPA] \quad \text{Eqn 5.14}$$

Substituting 5.13 into 5.10:

$$A = [PNPA] \varepsilon_{PNPA} + [PNPA]_0 \varepsilon_{PNP} - [PNPA] \varepsilon_{PNP} \quad \text{Eqn 5.15}$$

Collecting on [PNPA]:

$$A = [PNPA] \varepsilon_{PNPA} + [PNPA]_0 \varepsilon_{PNP} - [PNPA] \varepsilon_{PNP} \quad \text{Eqn 5.16}$$

$$A = [PNPA] (\varepsilon_{PNPA} - \varepsilon_{PNP}) + [PNPA]_0 \varepsilon_{PNP} \quad \text{Eqn 5.17}$$

Substituting 5.14 into 5.17:

$$A = [PNPA] (\varepsilon_{PNPA} - \varepsilon_{PNP}) + A_\infty \quad \text{Eqn 5.18}$$

Solving for [PNPA]:

$$[PNPA] = \frac{A - A_\infty}{(\varepsilon_{PNPA} - \varepsilon_{PNP})} \quad \text{Eqn 5.19}$$

Substituting 5.19 into 5.9

$$\frac{d(A - A_\infty)}{(\varepsilon_{PNPA} - \varepsilon_{PNP}) dt} = k_{2obs} [H_2O_2]_T \frac{A - A_\infty}{(\varepsilon_{PNPA} - \varepsilon_{PNP})} + k_1 \frac{A - A_\infty}{(\varepsilon_{PNPA} - \varepsilon_{PNP})} \quad \text{Eqn 5.20}$$

$\varepsilon_{PNPA} - \varepsilon_{PNP}$ cancels out, thus:

$$\frac{d(A - A_\infty)}{dt} = k_{2obs} [H_2O_2]_T (A - A_\infty) + k_1 (A - A_\infty) \quad \text{Eqn 5.21}$$

Multiplying both sides by -1 (because the absorbance increases during the reaction)

$$\frac{d(A_{\infty} - A)}{-dt} = -k_{2obs}[H_2O_2]_T(A_{\infty} - A) - k_1(A_{\infty} - A) \quad \text{Eqn 5.22}$$

Rearranging:

$$\frac{d(A_{\infty} - A)}{(A_{\infty} - A)} = (-k_{2obs}[H_2O_2]_T - k_1)(-dt) \quad \text{Eqn 5.23}$$

Integrating

$$\ln(A_{\infty} - A) = (-k_{2obs}[H_2O_2]_T - k_1)t + C \quad \text{Eqn 5.24}$$

Where C is the constant of integration

When t=0, C = ln(A_∞ - A₀)

Substituting into 5.24:

$$\ln(A_{\infty} - A) = (-k_{2obs}[H_2O_2]_T - k_1)t + \ln(A_{\infty} - A_0) \quad \text{Eqn 5.25}$$

These reactions were carried out under pseudo first order conditions, i.e. at least a 10-fold excess of hydrogen peroxide, for which the following holds:

$$k_{obs} = k_{2obs}[H_2O_2]_T + k_1 \quad \text{Eqn 5.26}$$

Where k_{obs} is the pseudo first order rate constant.

Substituting into 5.25:

$$\ln(A_{\infty} - A) = -k_{obs}t + \ln(A_{\infty} - A_0) \quad \text{Eqn 5.27}$$

Raising both sides to the power of e and rearranging:

$$A = A_{\infty} + (A_0 - A_{\infty})e^{-k_{obs}t} \quad \text{Eqn 5.28}$$

Pseudo first order rate constants, k_{obs}, for each run were obtained from non-linear least squares using Equation 5.28. Plots of k_{obs} against [H₂O₂]_T will yield a slope of k_{2obs} and an intercept of k₁ (as defined by Equation 5.26).

5.3. Results

A typical series of sequential spectra over 180 seconds for the reaction of PNPA with hydrogen peroxide in the presence of carbonate buffer at pH 9.14 is shown in Figure 5.3. The main peaks represent PNPA (275 nm), and the anionic form of PNP (400 nm). There are isobestic points at 245 nm and at 318 nm. Typical absorbance traces for the reaction over a range of hydrogen peroxide concentrations are shown in Figure 5.4. For the reaction in the absence of hydrogen peroxide (hydrolysis of the PNPA), the cell was left overnight in order to obtain an infinity absorbance reading. At the highest

hydrogen peroxide concentration the reaction was almost complete by the time the first absorbance reading was made.

Figures 5.5 and 5.6 show plots of the pseudo first order rate constant, obtained from Equation 5.8, against hydrogen peroxide concentration at two different pHs (8.00 and 9.14) in carbonate buffer. The rate of hydrolysis, i.e. in the absence of hydrogen peroxide, was determined directly in some cases, as shown in Figures 5.5 and 5.6 (and the corresponding Table 5.1). However, this reaction is slow compared to the rate in the presence of hydrogen peroxide and so throughout this chapter the plots of k_{obs} against $[\text{H}_2\text{O}_2]_{\text{T}}$ have been fitted to Equation 5.26 in which k_1 (i.e. the intercept) is set to zero; the slope yields $k_{2\text{obs}}$ the observed second order rate constant for the reaction with hydrogen peroxide. Table 5.1 summarises the k_{obs} values at each hydrogen peroxide concentration and derived $k_{2\text{obs}}$ values (± 1 standard deviation).

Figures 5.7 to 5.14 show similar plots of the pseudo first order rate constant against hydrogen peroxide concentration for the reaction in the presence of phosphate buffer (pH range: 5.28 to 7.42). Again the plots are linear: the kinetic data, including derived observed second order rate constants, $k_{2\text{obs}}$, values are summarised in Table 5.2.

Figures 5.15 to 5.19 show plots of pseudo first order rate constant against hydrogen peroxide concentration added as sodium borate (pH range: 5.50 to 8.00). Here the hydrogen peroxide concentration and borate concentration are equivalent to the sodium borate concentration, and it is in these runs, particularly at the higher pHs, that some deviation from linearity, either upward or downward curvature, would be expected if the peroxoborate species were having a significant effect on the reaction, as discussed in the introduction. In fact there is no obvious curvature for these reactions. The kinetic data, including derived observed second order rate constants are summarised in Table 5.3.

Finally, Figures 5.20 to 5.24 show kinetic data for the reaction of PNPA with hydrogen peroxide in the presence of a boric acid buffer (pH 6.25 to 10.5). As with the case where sodium perborate was used to add both the hydrogen peroxide and borate, the plots are all linear, suggesting that there is no significant effect of peroxoborates on the reaction. The kinetic data for this set of data, including derived observed second order rate constants are summarised in Table 5.4.

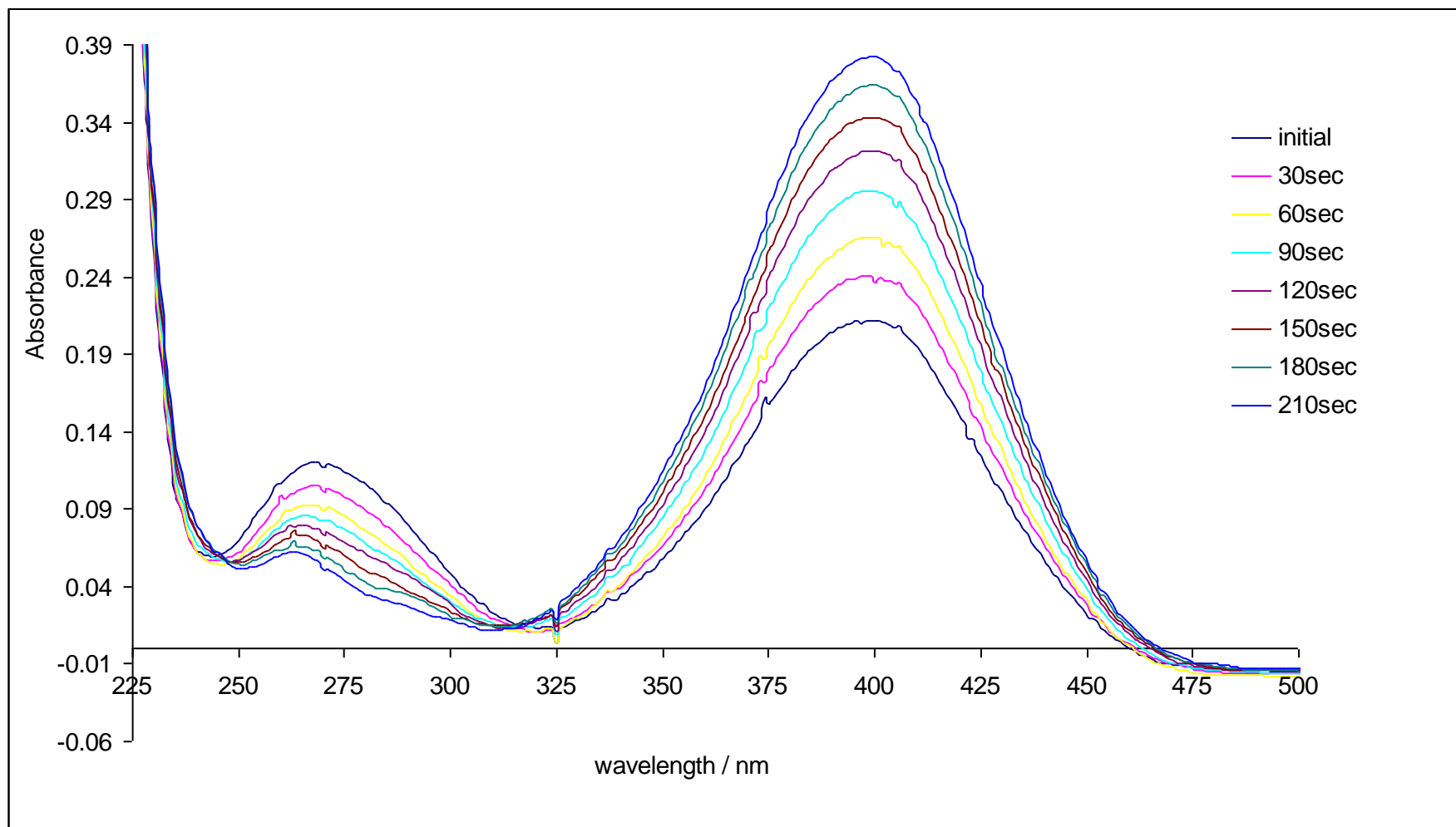


Figure 5.3:- sequential spectra taken subsequent to mixing solutions of p-nitrophenylacetate(PNPA) and hydrogen peroxide; pH 9.14 carbonate buffer solution 0.1M NaHCO₃ and 0.01M Na₂CO₃; [PNPA]_o = 3.03x10⁻⁵ mol dm⁻³ ; [H₂O₂] = 5.0x10⁻⁴ mol dm⁻³ ; 25°C.

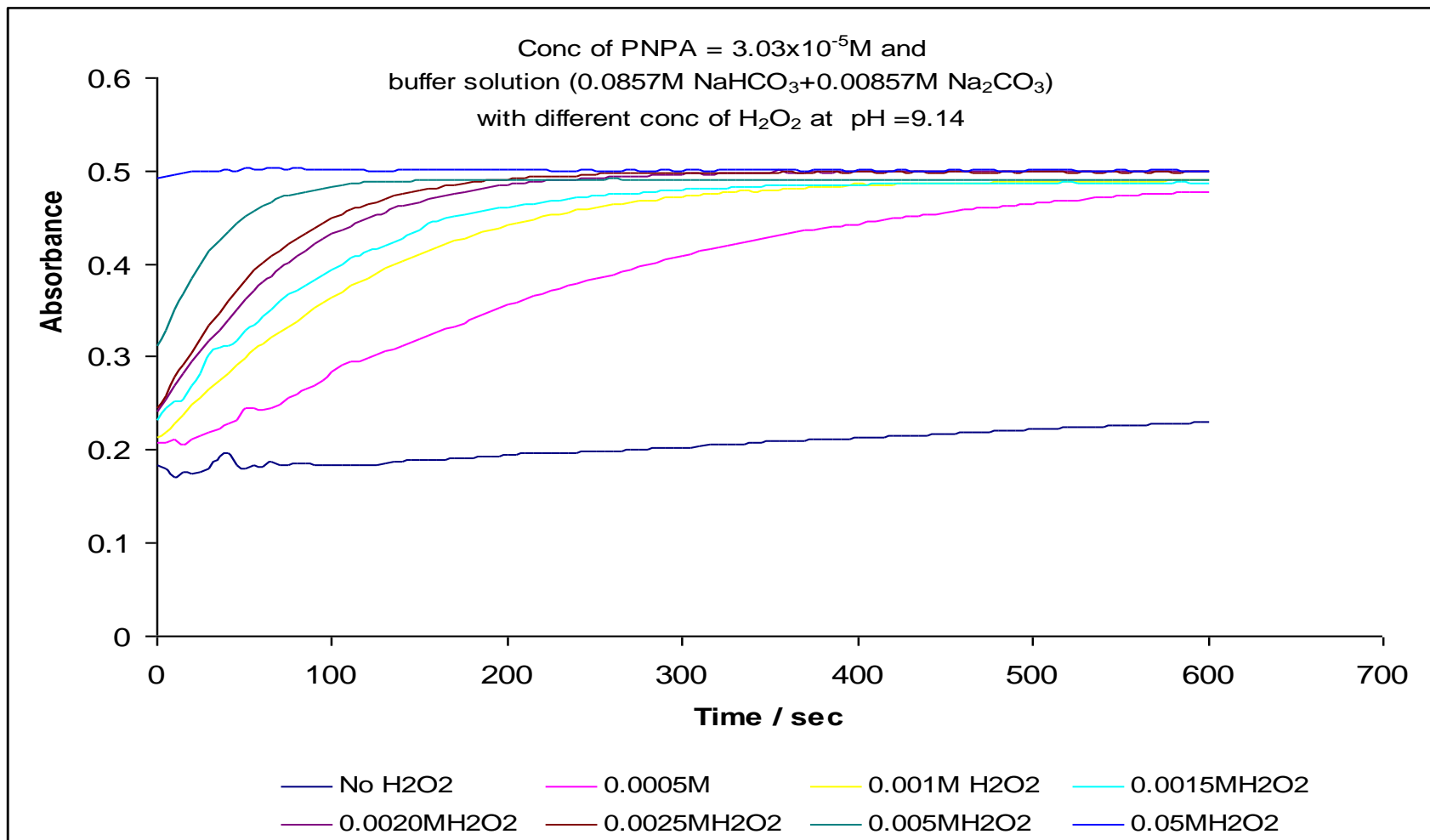


Figure 5.4:- plot showing the increase in absorbance at 400nm due to p-nitrophenol formation during the reaction between p-nitrophenylacetate and hydrogen peroxide : pH 9.14 , buffer solution 0.0857M NaHCO_3 and $0.00857 \text{M Na}_2\text{CO}_3$. $[\text{PNPA}]_0 = 3.03 \times 10^{-5} \text{ mol dm}^{-3}$ $[\text{H}_2\text{O}_2]$ as indicated on graph; 25°C .

Table 5.1: Observed first order rate constants (k_{obs}) for the reaction between p-nitrophenylacetate and hydrogen peroxide. Conditions were: pH 8.0 and pH 9.14 carbonate buffers, $[\text{PNPA}]_0 = 3.03 \times 10^{-5} \text{ mol dm}^{-3}$, 25°C .

Buffer (0.0857M $\text{NaHCO}_3 + 0.00857\text{M Na}_2\text{CO}_3$), $[\text{PNPA}]_0 = 3.03 \times 10^{-5} \text{ mol dm}^{-3}$		
	pH = 8.0	pH = 9.14
$[\text{H}_2\text{O}_2]/10^{-3} \text{ M}$	$k_{\text{obs}} / 10^{-4} \text{ s}^{-1}$	$k_{\text{obs}} / 10^{-4} \text{ s}^{-1}$
0	0.33	8.7
0.5	2.5	34.4
1	8.5	83.9
1.5	16.9	106.4
2	26.2	136
2.5	37.2	164.6
5	69.3	302
Observed second order rate constants, $k_{2\text{obs}} / \text{dm}^3 \text{ mol}^{-1} \text{ s}^{-1} (\pm \alpha)$	1.36 ± 0.05	6.33 ± 0.21

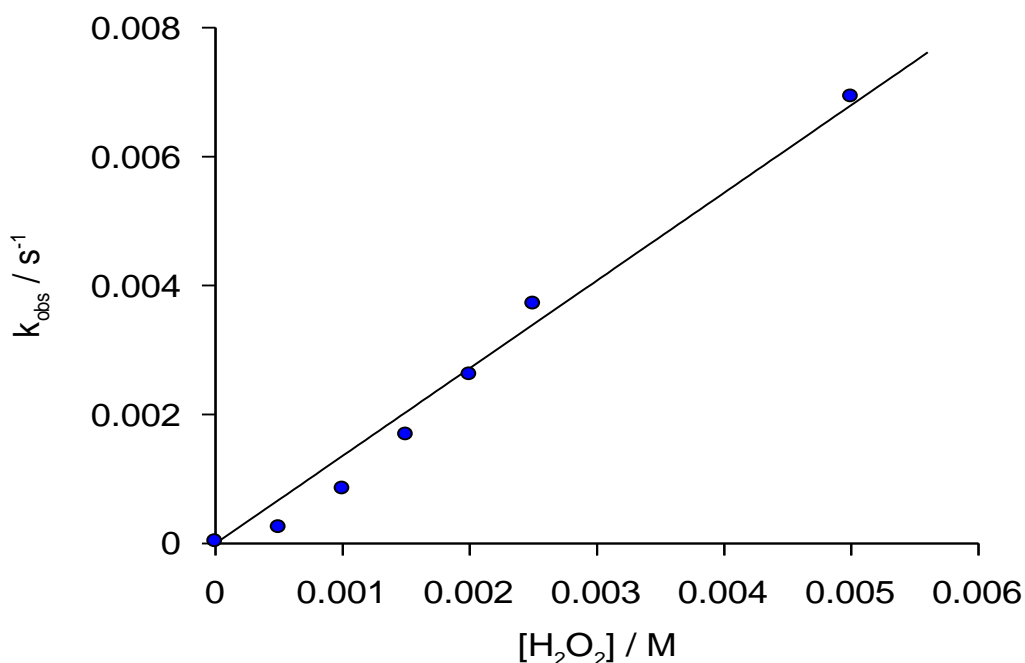


Figure 5.5:- Observed pseudo first order rate constants (k_{obs}) for the reaction between the p-nitrophenylacetate and hydrogen peroxide. Conditions were: pH 8.0 sodium hydrogen carbonate (NaHCO_3) and sodium carbonate (Na_2CO_3) buffers, $[\text{PNPA}]_0 = 3.03 \times 10^{-5} \text{ mol dm}^{-3}$, 25°C .

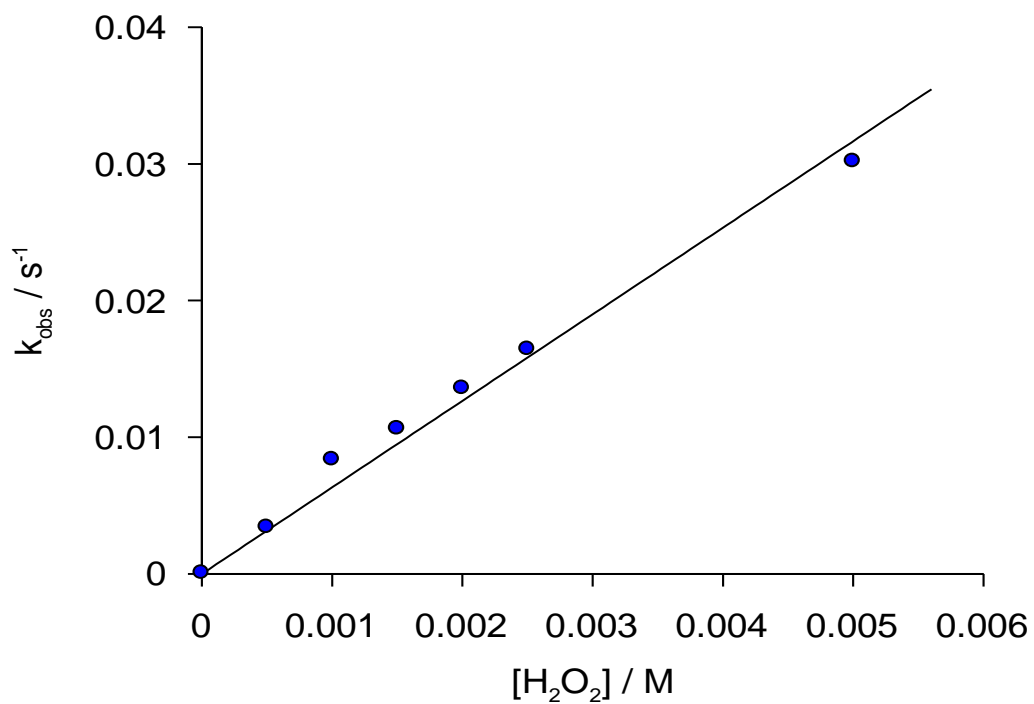


Figure 5.6:- Observed first order rate constants (k_{obs}) for the reaction between the p-nitrophenylacetate and hydrogen peroxide. Conditions were: pH 9.14 sodium hydrogen carbonate ($NaHCO_3$) and sodium carbonate (Na_2CO_3) buffers, $[PNPA]_0 = 3.03 \times 10^{-5} M$, $25^\circ C$.

Table 5.2 : Observed first order rate constants (k_{obs}) for the reaction between p-nitrophenylacetate and hydrogen peroxide. Conditions were: pH and concentration of hydrogen peroxide as indicated on Table, phosphate buffer buffers, $[\text{PNPA}]_0 = 2.85 \times 10^{-5} \text{ mol dm}^{-3}$, 25°C .

Buffer($\text{Na}_2\text{HPO}_4 + \text{NaH}_2\text{PO}_4$)								
	pH =5.28	pH = 5.56	pH = 5.93	pH = 6.29	pH =6. 34	pH = 6.92	pH = 7.16	pH = 7.42
$[\text{H}_2\text{O}_2] / 10^{-1} \text{ M}$	$k_{\text{obs}} / 10^{-4} \text{ s}^{-1}$	$k_{\text{obs}} / 10^{-4} \text{ s}^{-1}$	$k_{\text{obs}} / 10^{-4} \text{ s}^{-1}$	$k_{\text{obs}} / 10^{-4} \text{ s}^{-1}$	$k_{\text{obs}} / 10^{-4} \text{ s}^{-1}$	$k_{\text{obs}} / 10^{-4} \text{ s}^{-1}$	$k_{\text{obs}} / 10^{-4} \text{ s}^{-1}$	$k_{\text{obs}} / 10^{-4} \text{ s}^{-1}$
1.8	3.6	7	14.9	31.5	29.6	129	159	383
3.6	7.4	13.3	26.4	61.1	65.5	241	329	649
5.4	11.4	18.7	39.2	79.4	92.2	312	510	928
7.2	18.5	22.3	46	92.2	138	373	724	1158.6
9	21.4	26.6	55.5	116.3	156	414	947	1280
Observed second order rate constants, $k_{2\text{obs}} / 10^{-3} \text{ dm}^3 \text{ mol}^{-1} \text{ s}^{-1}$ ($\pm \alpha$)	2.36±0.090	3.15±0.12	6.53±0.25	13.6±0.7	17.9±0.4	51.6±3.3	101±2	156±7

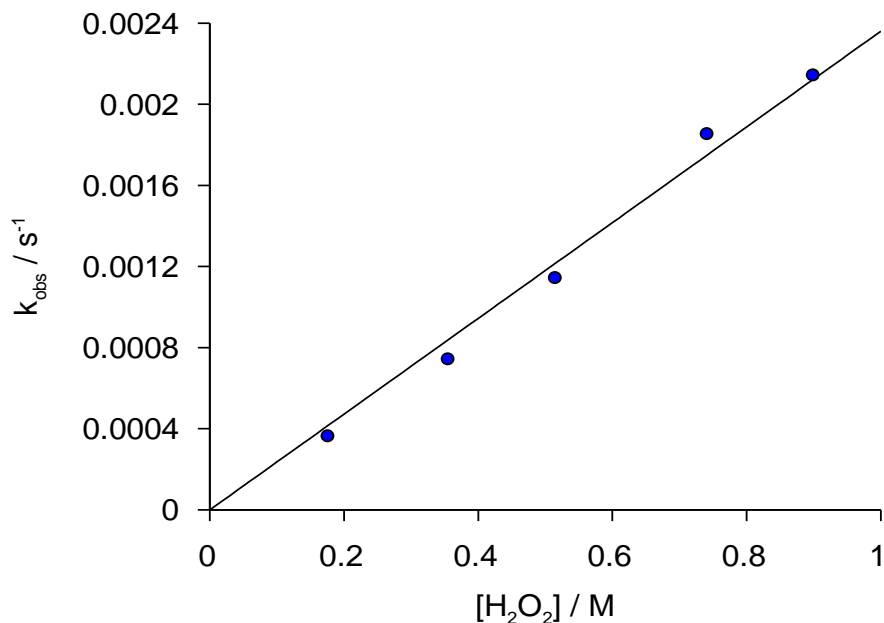


Figure 5.7: Observed first order rate constants (k_{obs}) for the reaction between the p-nitrophenylacetate and hydrogen peroxide. Conditions were: pH 5.28 sodium hydrogen phosphate – disodium hydrogen phosphate buffers, [PNPA] = 2.85×10^{-5} M, 25°C.

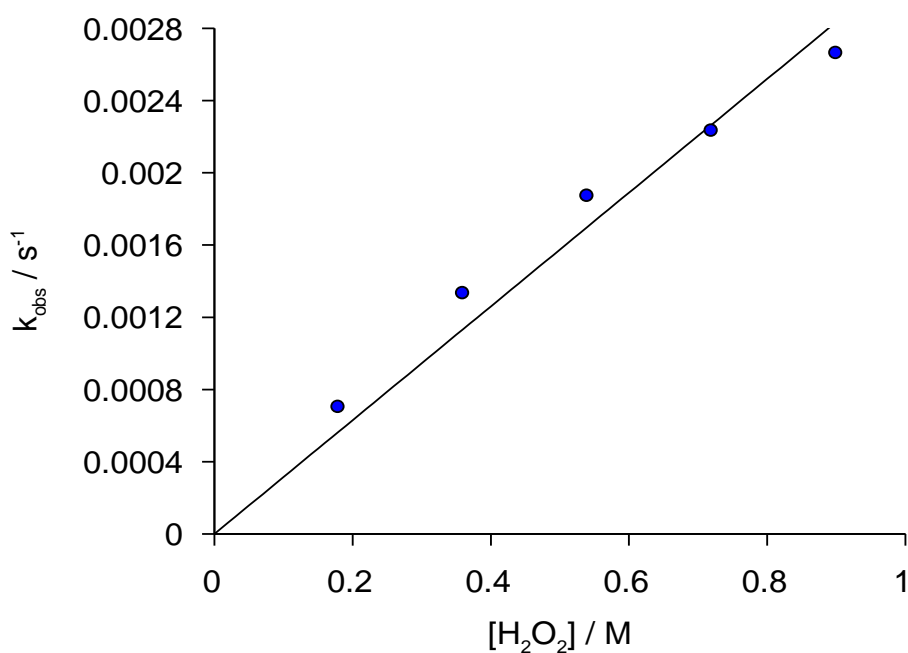


Figure 5.8: Observed first order rate constants (k_{obs}) for the reaction between the p- nitrophenylacetate and hydrogen peroxide. Conditions were: pH 5.56 sodium hydrogen phosphate – disodium hydrogen phosphate buffers, [PNPA] = 2.85×10^{-5} M, 25°C.

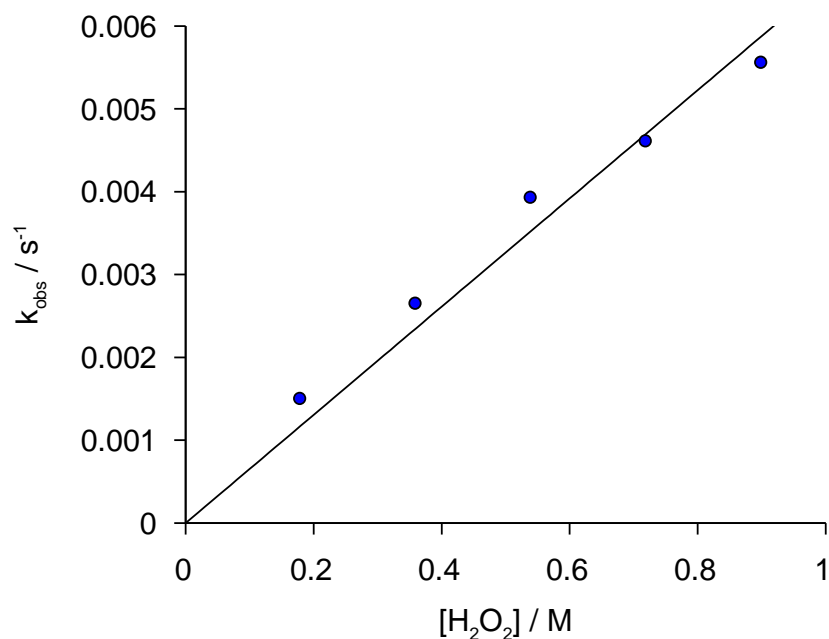


Figure 5.9: Observed first order rate constants (k_{obs}) for the reaction between the p-nitrophenylacetate and hydrogen peroxide. Conditions were: pH 5.93 sodium hydrogen phosphate – disodium hydrogen phosphate buffers, $[\text{PNPA}] = 2.85 \times 10^{-5} \text{ M}$, 25°C .

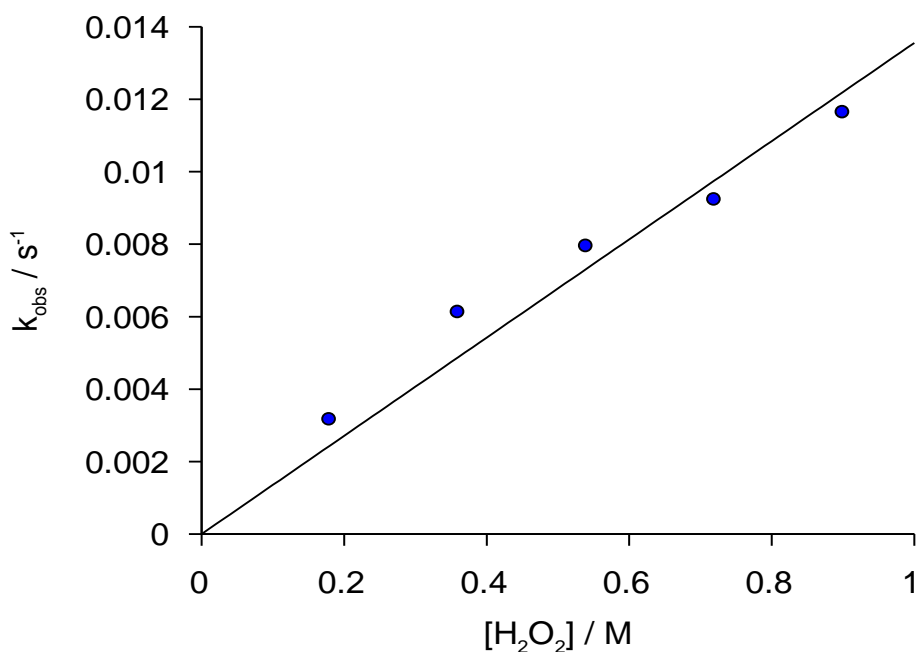


Figure 5.10: Observed first order rate constants (k_{obs}) for the reaction between the p-nitrophenylacetate and hydrogen peroxide. Conditions were: pH 6.29 sodium hydrogen phosphate – disodium hydrogen phosphate buffers, $[\text{PNPA}] = 2.85 \times 10^{-5} \text{ M}$, 25°C .

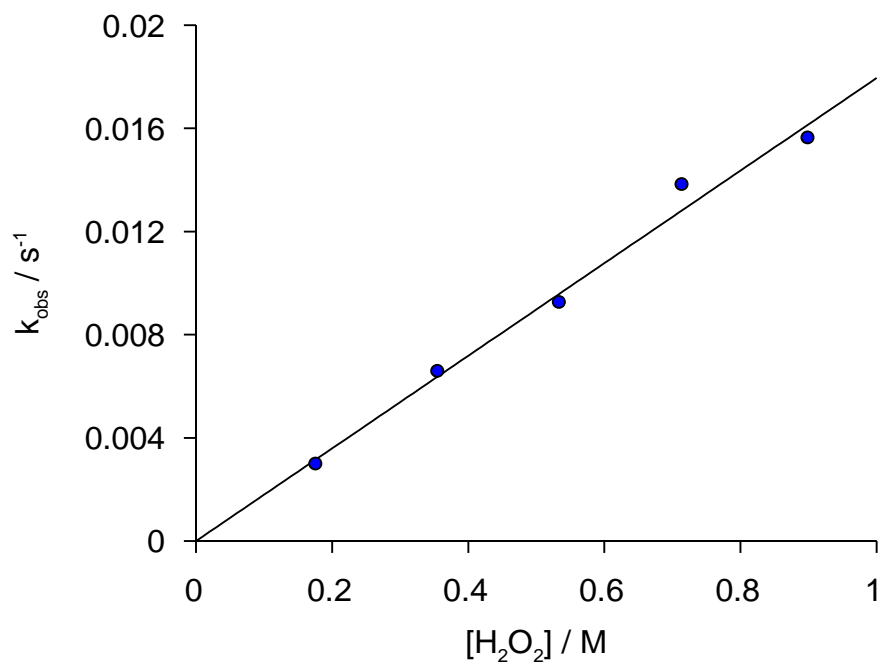


Figure 5.11: Observed first order rate constants (k_{obs}) for the reaction between the p-nitrophenylacetate and hydrogen peroxide. Conditions were: pH 6.34 sodium hydrogen phosphate – disodium hydrogen phosphate buffers, $[\text{PNPA}] = 2.85 \times 10^{-5} \text{ M}$, 25°C .

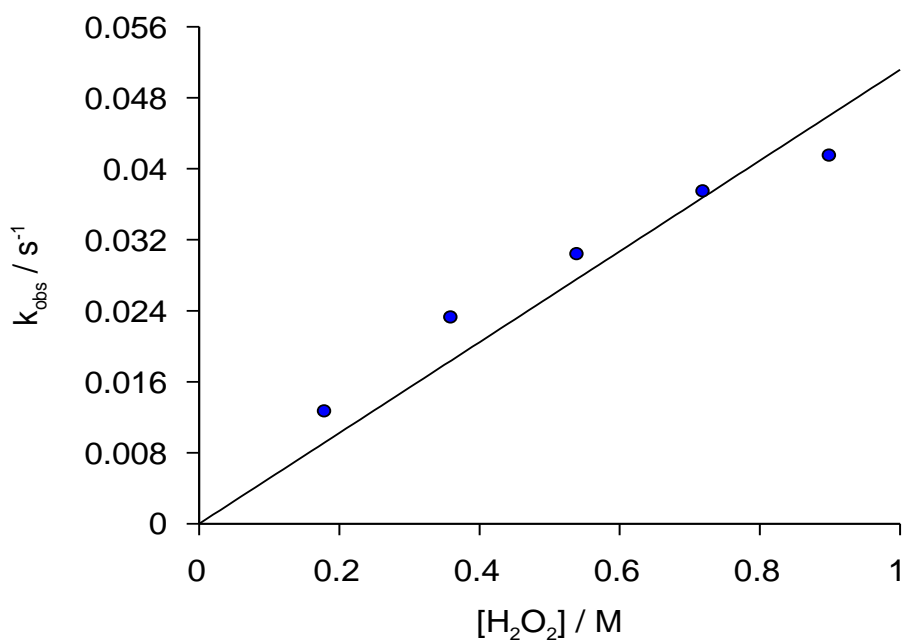


Figure 5.12: Observed first order rate constants (k_{obs}) for the reaction between the p-nitrophenylacetate and hydrogen peroxide. Conditions were: pH 6.92 sodium hydrogen phosphate – disodium hydrogen phosphate buffers, $[\text{PNPA}] = 2.85 \times 10^{-5} \text{ M}$, 25°C .

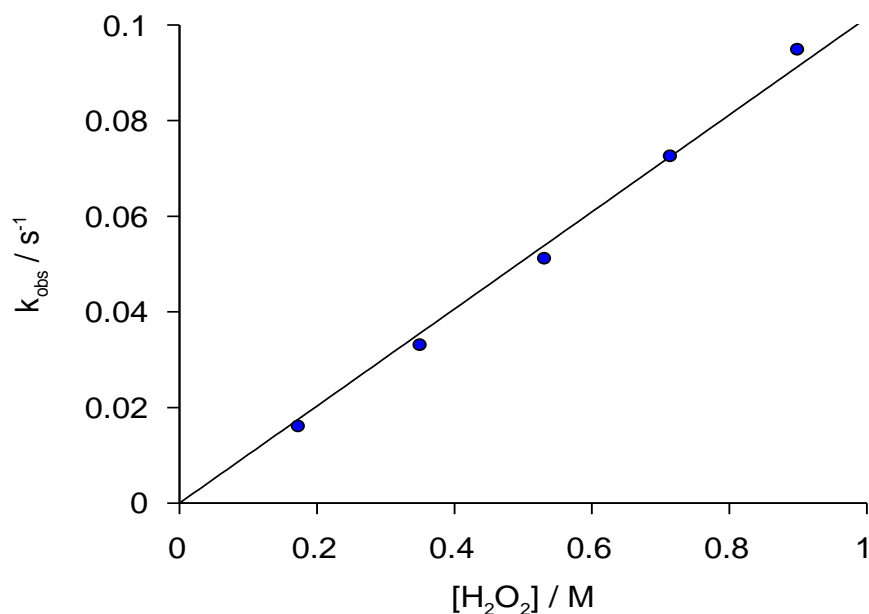


Figure 5.13: Observed first order rate constants (k_{obs}) for the reaction between the p-nitrophenylacetate and hydrogen peroxide. Conditions were: pH 7.16 sodium hydrogen phosphate – disodium hydrogen phosphate buffers, $[\text{PNPA}] = 2.85 \times 10^{-5} \text{ M}$, 25°C .

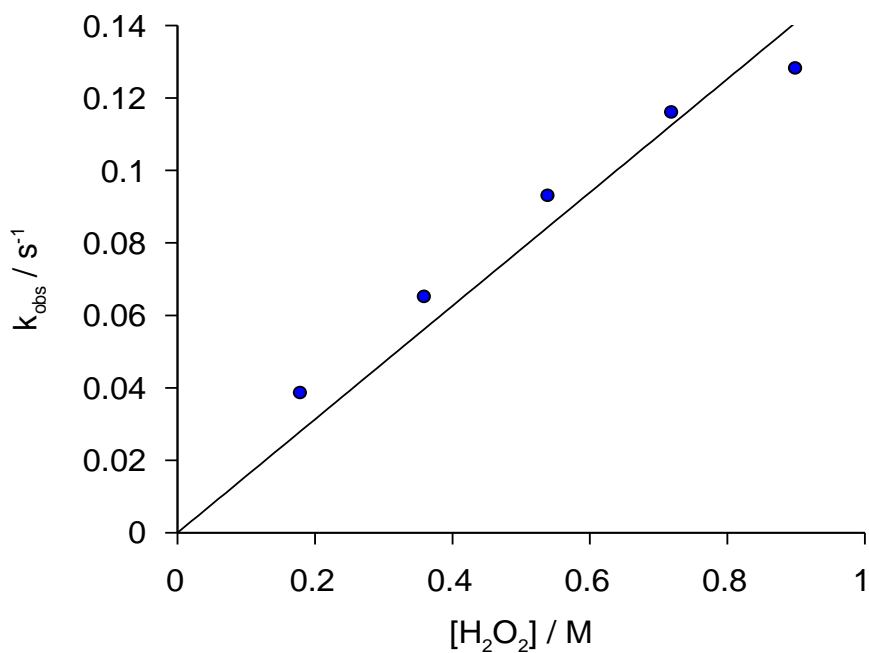


Figure 5.14: Observed first order rate constants (k_{obs}) for the reaction between the p-nitrophenylacetate and hydrogen peroxide. Conditions were: pH 7.42 sodium hydrogen phosphate – disodium hydrogen phosphate buffers, $[\text{PNPA}] = 2.85 \times 10^{-5} \text{ M}$, 25°C .

Table 5.3 : Observed first order rate constants (k_{obs}) for the reaction between p-nitrophenylacetate and sodium perborate. Conditions were: pH and concentration of sodium perborate as indicated on Table, $[\text{PNPA}]_0 = 2.85 \times 10^{-5} \text{ mol dm}^{-3}$, 25°C .

Sodium perborate (NaBO_3)					
	pH = 5.50	pH = 6.0	pH = 6.5	pH = 7.0	pH = 8.0
$[\text{NaBO}_3] / \text{M}$	$k_{\text{obs}} / 10^{-4} \text{ s}^{-1}$	$k_{\text{obs}} / 10^{-4} \text{ s}^{-1}$	$k_{\text{obs}} / 10^{-4} \text{ s}^{-1}$	$k_{\text{obs}} / 10^{-4} \text{ s}^{-1}$	$k_{\text{obs}} / 10^{-4} \text{ s}^{-1}$
0.0508	2.1	5.2	17.1	38.6	238
0.0959	3.8	9.3	29.5	68.7	462
0.135	5.6	16.8	46.4	94	636
0.1724	7.5	20.2	54.3	134	929
0.2063	8.9	27.6	75.7	154	
Observed second order rate constants, $k_{2\text{obs}} / 10^{-3} \text{ dm}^3 \text{ mol}^{-1} \text{ s}^{-1} (\pm \alpha)$	4.26 ± 0.05	12.3 ± 0.6	34.1 ± 1.2	74.4 ± 1.4	506 ± 19

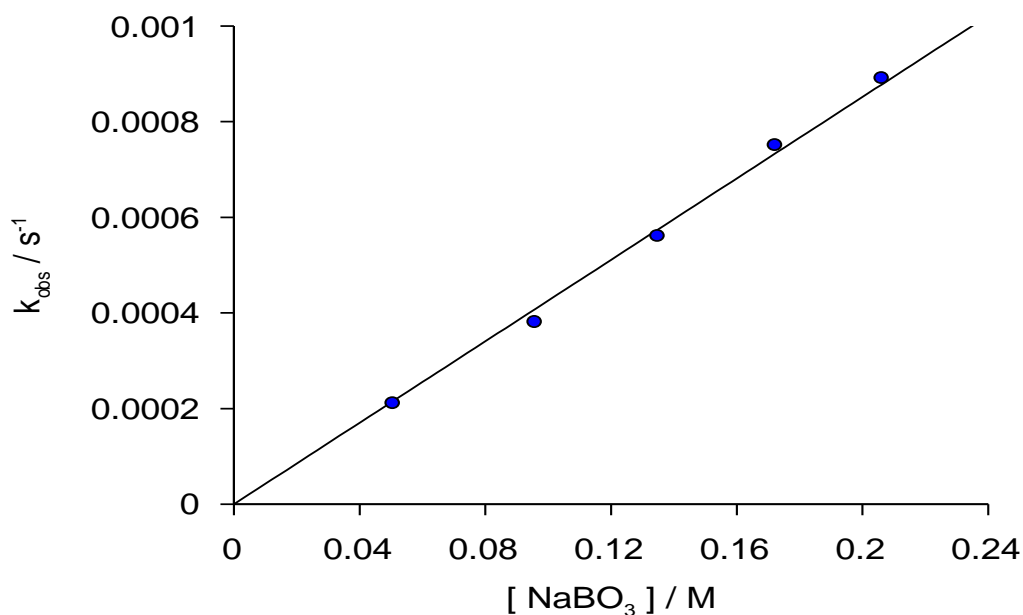


Figure 5.15: Observed first order rate constants (k_{obs}) for the reaction between the p-nitrophenylacetate and hydrogen peroxide (from NaBO_3). Conditions were: pH 5.50, $[\text{PNPA}] = 2.85 \times 10^{-5} \text{ M}$, 25°C .

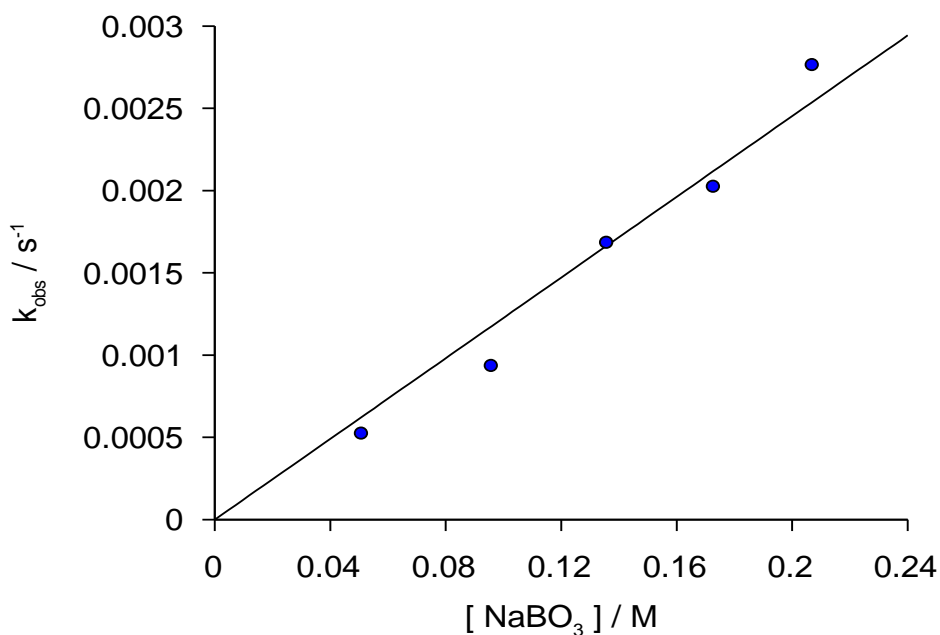


Figure 5.16: Observed first order rate constants (k_{obs}) for the reaction between the p-nitrophenylacetate and hydrogen peroxide (from NaBO_3). Conditions were: pH 6.0, $[\text{PNPA}] = 2.85 \times 10^{-5} \text{ M}$, 25°C

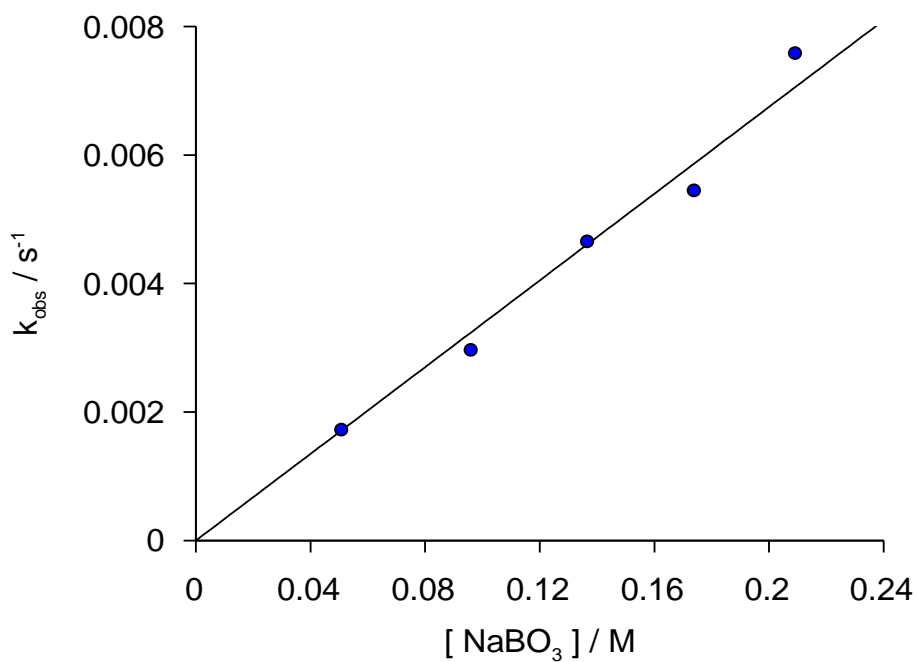


Figure 5.17: Observed first order rate constants (k_{obs}) for the reaction between the p-nitrophenylacetate and hydrogen peroxide (from NaBO_3). Conditions were: pH 6.5, $[\text{PNPA}] = 2.85 \times 10^{-5} \text{ M}$, 25°C .

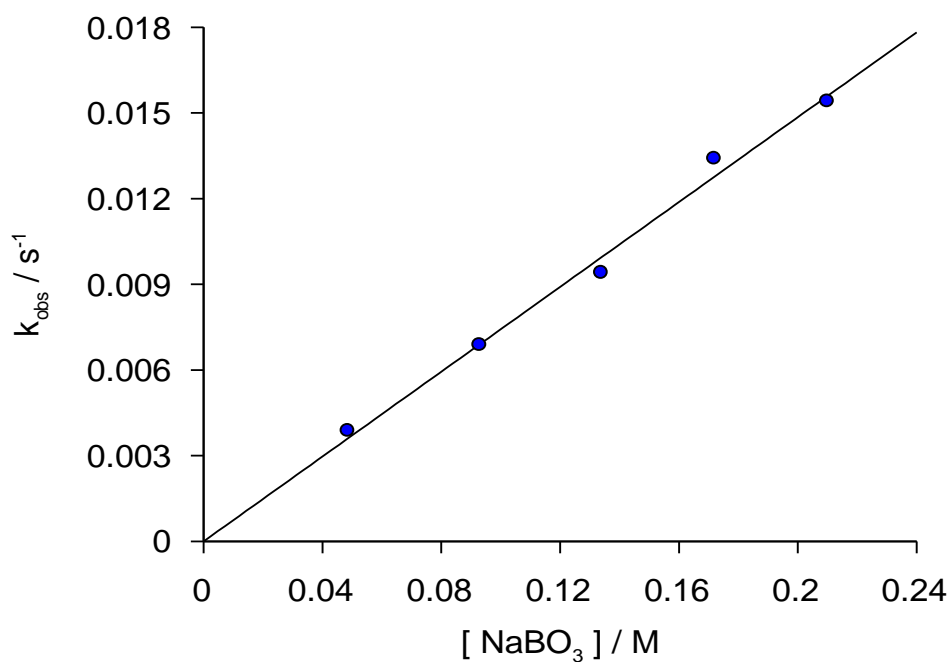


Figure 5.18: Observed first order rate constants (k_{obs}) for the reaction between the p-nitrophenylacetate and hydrogen peroxide (from NaBO_3). Conditions were: pH 7.0, $[\text{PNPA}] = 2.85 \times 10^{-5} \text{ mol dm}^{-3}$

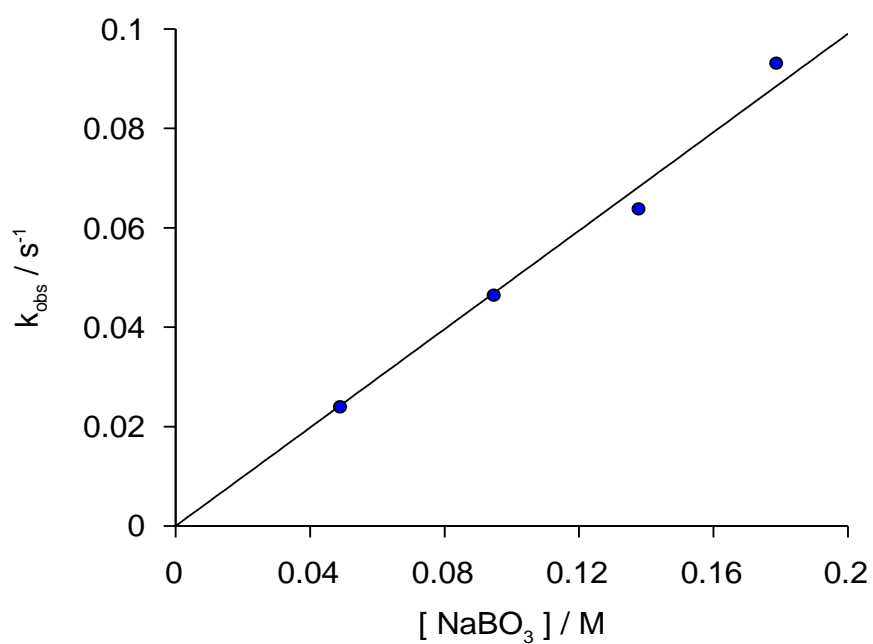


Figure 5.19: Observed first order rate constants (k_{obs}) for the reaction between the p-nitrophenylacetate and H_2O_2 at 25°C. Conditions were: pH 8.0, $[\text{PNPA}] = 2.85 \times 10^{-5} \text{ mol dm}^{-3}$, 25°C.

Table 5.4: Observed first order rate constants (k_{obs}) for the reaction between p-nitrophenylacetate and hydrogen peroxide. Conditions were: pH and concentration of hydrogen peroxide as indicated on Table, buffers(boric acid – sodium hydroxide), $[\text{PNPA}]_0 = 2.85 \times 10^{-5} \text{ mol d m}^{-3}$, 25°C .

Buffer boric acid and sodium hydroxide (H_3BO_4 and NaOH)						
	pH = 6.25		pH=9.0	pH=9.4	pH=9.8	pH=10.5
$[\text{H}_2\text{O}_2] / 10^{-1} \text{ M}$	$k_{\text{obs}} / 10^{-4} \text{ s}^{-1}$	$[\text{H}_2\text{O}_2] / 10^{-3} \text{ M}$	$k_{\text{obs}} / 10^{-4} \text{ s}^{-1}$	$k_{\text{obs}} / 10^{-4} \text{ s}^{-1}$	$k_{\text{obs}} / 10^{-4} \text{ s}^{-1}$	$k_{\text{obs}} / 10^{-4} \text{ s}^{-1}$
0	0.4	0	3.1	8.1	6.5	39.5
0.9	6.5	0.0588	11	18	29.3	77.4
1.8	14.5	0.147	35.7	36.5	42	126.2
3.6	57.7	0.368	20.1	37.5	81.5	311.4
5.4	111.2	0.92	44.1	103.5	188.1	870.2
9	188.6	2.3	92.8	175.1	473.5	1467.8
		5.7	207.6	428.9	858	
		14	367.2			
Observed second order rate constants, $k_{2\text{obs}} / \text{dm}^3 \text{ mol}^{-1} \text{ s}^{-1} (\pm \alpha)$	0.020 ± 0.001		2.81 ± 0.18	7.64 ± 0.30	15.9 ± 0.85	68.6 ± 4.9

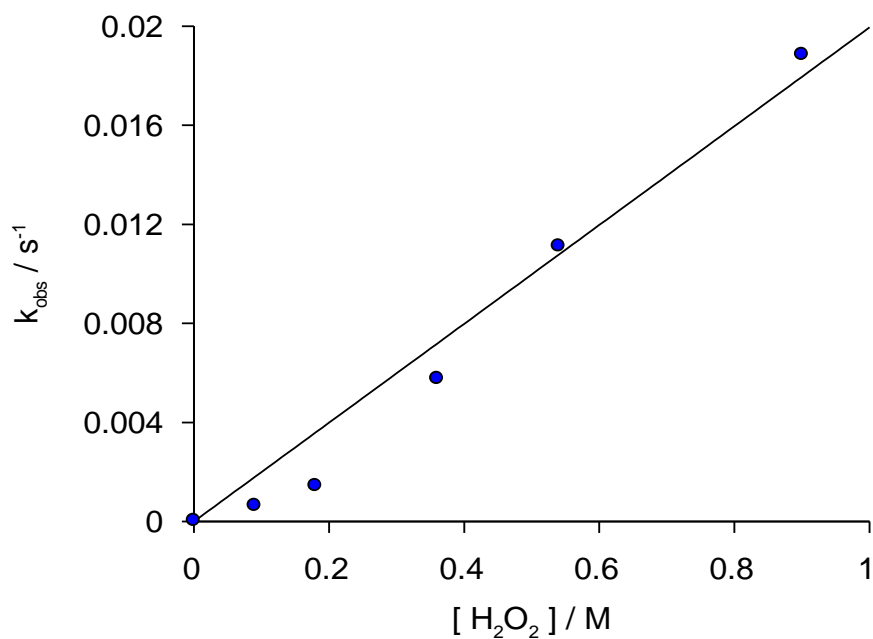


Figure 5.20: rate constants (k_{obs}) for the reaction between the p-nitrophenylacetate and hydrogen peroxide. Conditions were: pH 6.25, buffers ($0.0428 \text{ mol dm}^{-3}$ boric acid – sodium hydroxide $0.00428 \text{ mol dm}^{-3}$), [PNPA] $\approx 2.85 \times 10^{-5} \text{ mol dm}^{-3}$, 25°C .

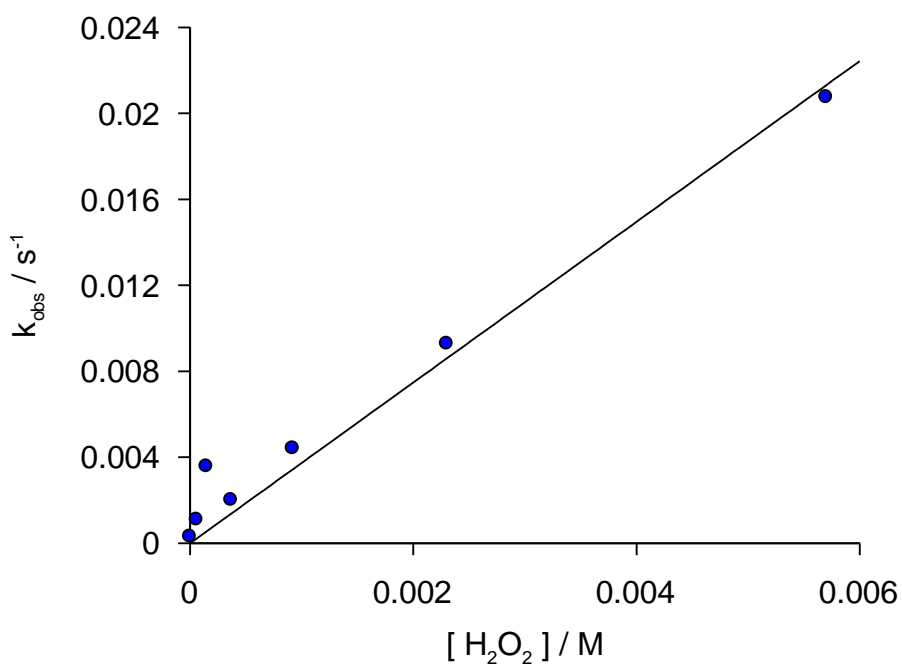


Figure 5.21: rate constants (k_{obs}) for the reaction between the p-nitrophenylacetate and hydrogen peroxide. Conditions were: pH 9.0, buffers ($0.0428 \text{ mol dm}^{-3}$ boric acid – sodium hydroxide $0.01714 \text{ mol dm}^{-3}$), [PNPA] $\approx 2.85 \times 10^{-5} \text{ mol dm}^{-3}$, 25°C .

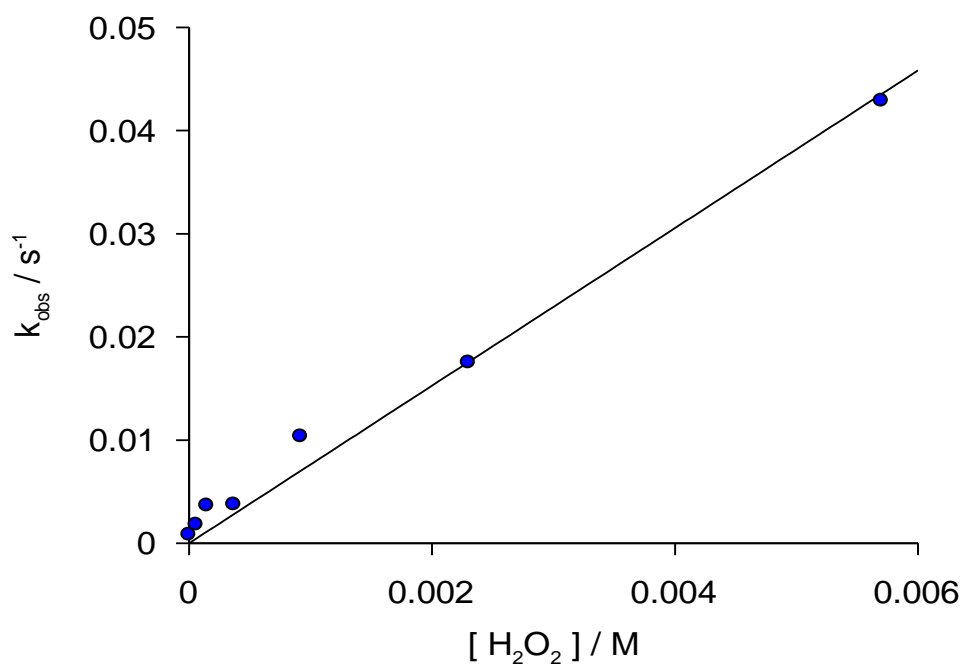


Figure 5.22: rate constants (k_{obs}) for the reaction between the p-nitrophenylacetate and hydrogen peroxide. Conditions were: pH 9.45, buffers ($0.0428 \text{ mol dm}^{-3}$ boric acid – sodium hydroxide $0.0257 \text{ mol dm}^{-3}$), [PNPA] $=2.85 \times 10^{-5} \text{ mol dm}^{-3}$, 25°C

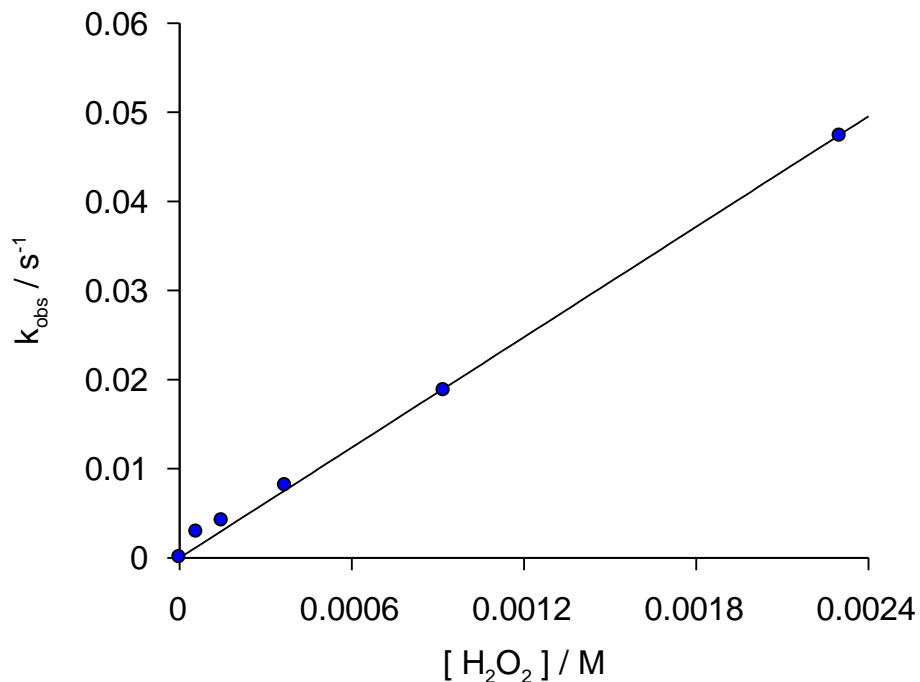


Figure 5.23: rate constants (k_{obs}) for the reaction between the p-nitrophenylacetate and hydrogen peroxide. Conditions were: pH 9.8, buffers ($0.0428 \text{ mol dm}^{-3}$ boric acid – sodium hydroxide $0.0342 \text{ mol dm}^{-3}$), [PNPA] $=2.85 \times 10^{-5} \text{ mol dm}^{-3}$, 25°C .

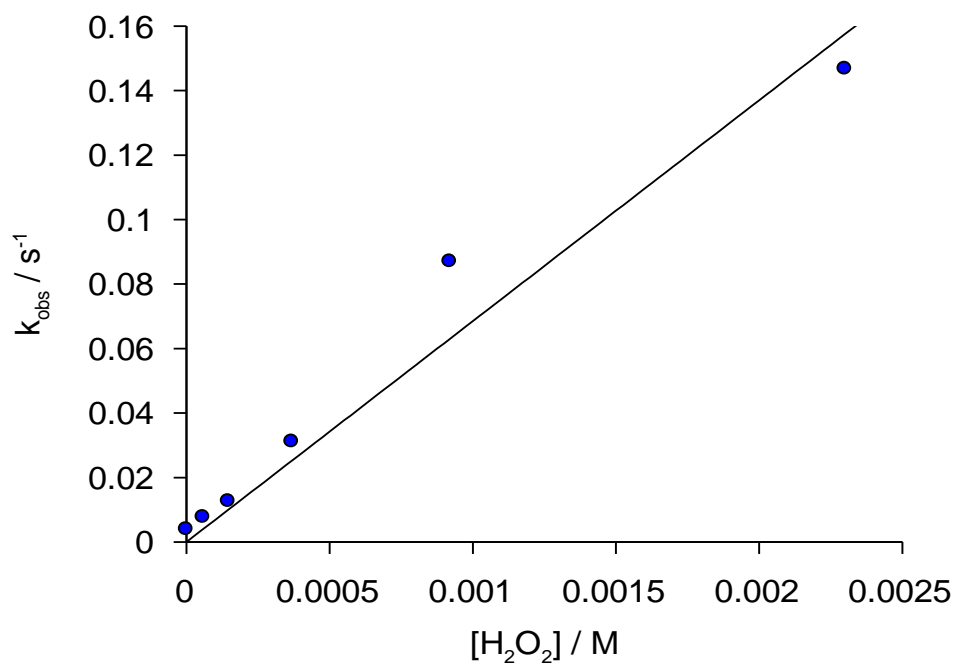


Figure 5.24: rate constants (k_{obs}) for the reaction between the p-nitrophenylacetate and hydrogen peroxide. Conditions were: pH 10.53, buffers ($0.0428 \text{ mol dm}^{-3}$ boric acid – sodium hydroxide $0.04285 \text{ mol dm}^{-3}$), $[\text{PNPA}] = 2.85 \times 10^{-5} \text{ mol dm}^{-3}$, 25°C .

5.4. Discussion

5.4.1. General

The literature contains several warnings about the careful selection of buffer systems for studies that use hydrogen peroxide. Wilson, for example, states that “use of borate buffers in reactions which involve hydrogen peroxide should only be made with care”²²¹. In another paper, Jones *et al* warn on the “notorious behaviour of borate buffers in complicating the kinetics of peroxide reactions”²²². It is certainly true that borate-hydrogen peroxide systems are complex because of the significant number of species that are formed over the pH range, yet these systems are now reasonably well understood^{217, 220, 223} and, moreover, rather than proving potentially troublesome in terms of complicating chemical kinetics, they actually present opportunities for catalysis²¹⁷ and synthetic organic chemistry²¹⁹.

The aim of this chapter was to clarify whether any of the peroxyborate species display nucleophilic character and thus accelerate the rate of reaction of hydrogen peroxide with p-nitrophenyl acetate (PNPA). There is some ambiguity in the literature as to whether peroxoborates can act as nucleophiles, though recent studies strongly suggest they behave as electrophiles²¹⁷.

As outlined in the introduction the pH range 6.0 to 8.0 is critical in terms of the distribution of peroxoborate species. Depending on the borate and hydrogen peroxide concentrations, below about pH 6.5, the only significant peroxoborate species is the trianol peroxoboric acid, $\text{B(OH)}_2\text{OOH}$, which has a low formation constant and represents only about 1% of the total peroxide at these pHs. However, above pH 6.5, increasing concentrations of the monoperoxoborate anion, $\text{B(OH)}_3\text{OOH}^-$, the peroxodiborate anion $(\text{HO})_3\text{BOOB(OH)}_3^{2-}$, and the diperoxodiborate anion $(\text{HO})_2\text{B(OO)}_2\text{B(OH)}_2^{2-}$, are formed, with diperoxoborate, $\text{B(OH)}_2(\text{OOH})_2^-$ forming at higher hydrogen peroxide concentrations. Consequently this is the ideal pH range in which to elucidate any effects of borate on the reaction of hydrogen peroxide and PNPA. Comparisons are made with the reaction in the presence of phosphate buffer, which does not form complexes with hydrogen peroxide, and carbonate, which does²²⁴

5.4.2. Second order rate constants

The reaction of PNPA with hydrogen peroxide proceeds according to Scheme 5.1, where k_1 is the first order rate constant for PNPA hydrolysis and k_2 is the second order rate constant for the reaction of the PNPA with the perhydroxyl anion, HOO^- .

The expectation is that with increasing concentrations of different peroxoborate species, any rate accelerations would manifest as upward curvature in plots of observed pseudo-first order rate constants against peroxide concentration. With one notable exception (Figure 5.20), the plots are generally linear, although there is perhaps a hint of some slight downward curvature in some of the plots.

As explained in Section 5.2.3, for convenience the total hydrogen peroxide was used in the tables and plots. It has been well established that it is the perhydroxyl anion that is the reactive species, as indicated in Scheme 5.1. The second order rate constant (k_2) for the reaction between PNPA and the perhydroxyl anion can be calculated from Equation 5.29, where K_a is the acid dissociation constant for hydrogen peroxide ($\text{p}K_a = 11.6$).

$$k_2 = k_{2obs} \times \frac{(K_a + [H^+])}{K_a} \quad \text{Equation 5.29}$$

In the absence of buffer or ionic strength effects, the second order rate constants should be pH independent, whereas any equilibrium processes that result in the formation of less, or more, reactive peroxide species will decrease or increase the rate.

Figure 5.25 shows a similar distribution diagram to those presented in the introduction to this chapter, but with the addition of curves for the perhydroxyl anion in the presence and absence of borate. This demonstrates the reduction in the concentration of the perhydroxyl anion through the formation of peroxoborate complexes. Moreover, the reduction in the perhydroxyl anion concentration is very pH dependent, as can be ascertained from Figure 5.25, though this is much more clearly seen in Figure 5.26, which shows the percentage reduction in perhydroxyl anion concentration as a function of pH for the same conditions as in Figure 5.25.

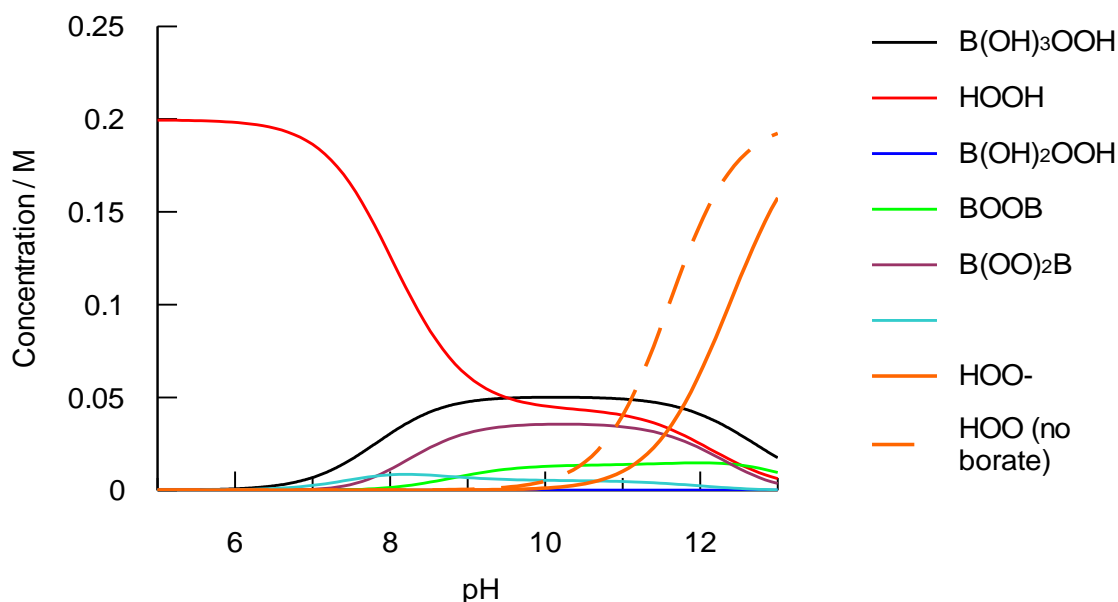


Figure 5.25: Simulated distribution of the peroxoborate species, hydrogen peroxide and the perhydroxyl anion as a function of pH for a system containing 0.20 mol dm^{-3} sodium borate and 0.20 mol dm^{-3} total hydrogen peroxide. The expected concentration of the perhydroxyl anion in the absence of borate is shown as a broken line.

As can be seen from Figure 5.26, at pHs up to about 6.5 the perhydroxyl anion is almost 100% of that expected in the absence of borate (though present at very low concentrations since it is some 5 pH units below the pK_a). The formation of peroxyborate species above this pH then results in the reduction of the perhydroxyl anion to approximately 30% of that expected in the absence of borate. If the formed peroxoborate species are largely unreactive towards PNPA then the second order rate constant at this pH should be only 30% of that expected in the absence of borate.

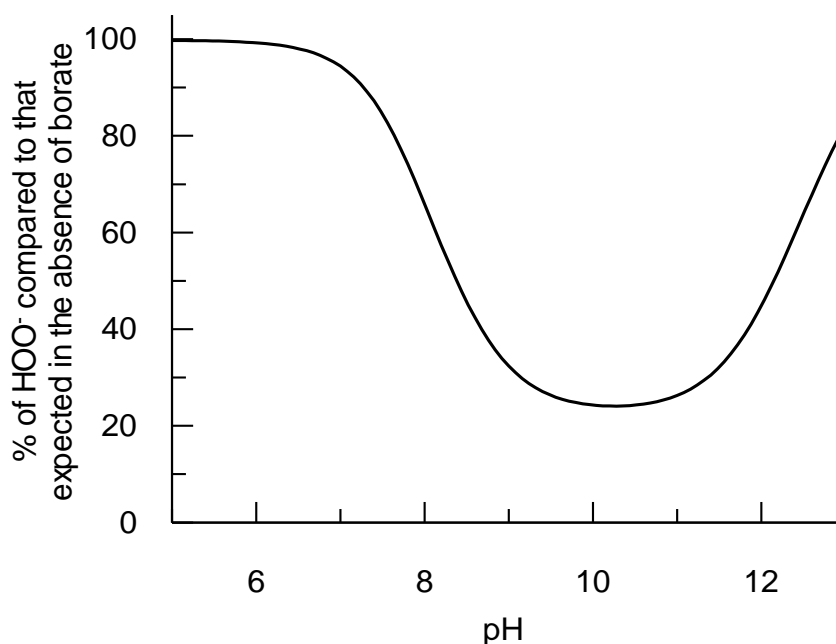


Figure 5.26: Simulated pH dependence of HOO^- concentration in the presence of 0.20 mol dm^{-3} borate and 0.20 mol dm^{-3} total hydrogen peroxide, as a percentage of that expected when no borate is present.

Table 5.5 shows a summary of the observed second order rate constants at a particular pH, $k_{2\text{obs}}$, and the calculated second order rate constants for the reaction of PNPA with the perhydroxyl anion, k_2 . Considering, firstly, the k_2 values for runs conducted in a phosphate buffer, clearly from Table 5.5 there is some variability, but no obvious trend; the rate at pH5.28 is significantly higher than the others. Phosphate is not known to form complexes with hydrogen peroxide, and so the k_2 values should be pH independent. The rates in phosphate compare reasonably well with literature values of 3140 and 3520 $\text{dm}^3 \text{mol}^{-1} \text{s}^{-1}$ obtained at pH 6.8 in ionic strengths of 0.02 and 0.10M respectively²²⁵. In carbonate buffer (pH10, I=0.1M) the literature k_2 value is 3785 $\text{dm}^3 \text{mol}^{-1} \text{s}^{-1}$.

Looking now at the results in the presence of borate buffer, there are conflicting results: on one hand the k_2 values at lower pH are considerably higher than the published values; however as the pH increases beyond 6.5, the rate significantly decreases. This is particularly notable for the $\text{H}_3\text{BO}_3/\text{NaOH}$ buffer system, where a reduction to almost one fifth of the rate at low pH occurs. For the system where sodium borate is added as the source of both peroxide and borate, thus ensuring equimolar concentrations of both, a similar effect is seen, though the pH range in this system is more restricted than for the $\text{H}_3\text{BO}_3/\text{NaOH}$ system.

It is clear from these results that the pattern followed mirrors the reduction in the concentration of the perhydroxyl anion as a result of the formation of non-reactive (towards PNPA) peroxoborate complexes as discussed earlier. It is known that this happens at higher pHs, for example Davies and Deary report a 75% reduction in k_2 in the presence of 0.1M borate at pH 9.25²²⁵, but there was the possibility that perborate species formed between pH6 and pH8 may have exhibited some nucleophilicity; clearly this is not the case. For the $\text{H}_3\text{BO}_3/\text{NaOH}$ system, the decrease in rate is greater than might be expected from the predicted reduction in HOO^- , as can be seen from Figures 5.27, where the reduction, compared to lower pH should be to about 60%: in fact the reduction is to about 20% of the low pH rate, so there may be other unreactive borate species that have not been accounted for.

In Figure 5.28, all of second order rate constants have been plotted as a pH dependence and this reveals some interesting extra detail that was not obvious from the Table alone. The first point is that all of the rates derived for borate buffer, either from the sodium perborate runs or the boric acid / NaOH runs, actually fall on the same curve (not drawn), even though the reduction in the perhydroxyl anion concentration

should have differed between the two modes of adding borate and hydrogen peroxide. It is also clear from Figure 5.28 that the curve resembles that predicted for the reductions in perhydroxyl anion concentration as a result of hydrogen peroxide forming perborate species, e.g. as in Figures 5.26 and 5.27. The rates in phosphate buffer appear to join the curve at higher pHs, but at lower pHs they form a separate series. For the two points in carbonate buffer, the higher pH one falls on the curve formed by the borate runs, but at the lower pH there is a significant deviation. Richardson has shown that peroxy carbonate species are formed from the equilibrium between carbonate buffer and hydrogen peroxide and that these species act as electrophiles, for example in sulphide oxidation and epoxidation reactions^{224, 226, 227}. The peroxy carbonate system, which is only reported to have one species (HCO_4^-) is also likely to result in the reduction of the concentration of the perhydroxyl anion, which is consistent for the results observed.

The second point to discuss from Figure 5.28 is the consistently high values obtained for k_2 in the borate buffers and carbonate buffers at pHs of 6 or lower. This contrasts with the lower values obtained in phosphate buffer with the exception of the value at pH 5.28. There is the suggestion here of some form of catalysis, which because it seems common across all buffer types (though the result for phosphate is debatable), may be a form of general acid base catalysis. This might take the form of deprotonation of the nucleophile in the transition state^{228, 229} or protonation of the leaving group²³⁰. There is also the possibility that reactive species are formed in the equilibrium between the buffer and hydrogen peroxide. In the case of borate, this would be the $\text{HOOB}(\text{OH})_2$ species, though the low formation constant means that it would have to be very reactive indeed to demonstrate the rate enhancements that are being observed; it would also have to be nucleophilic and there is little evidence of this; in fact a recent study by Deary and Davies have suggested that it is a very effective electrophile²¹⁷.

Table 5.5: A summary of the observed second order rate constants ($k_{2\text{obs}}$) for the reaction between p-nitrophenylacetate and hydrogen peroxide, and the corresponding second order rate constants, k_2 for the reaction of the perhydroxyl anion with PNPA. Conditions as stated in the relevant plots.

Buffer	pH	Ionic strength / mol dm ⁻³	$k_{2\text{obs}} / \text{dm}^3 \text{mol}^{-1} \text{s}^{-1}$	$k_2 / \text{dm}^3 \text{mol}^{-1} \text{s}^{-1}$
Carbonate	8.0	0.09	1.36	5415
Carbonate	9.14	0.12	6.33	1823
Phosphate	5.28	0.11	0.0023	4805
Phosphate	5.56	0.13	0.0031	3399
Phosphate	5.93	0.09	0.0065	3040
Phosphate	6.29	0.07	0.0136	2654
Phosphate	6.34	0.07	0.0179	3093
Phosphate	6.92	0.06	0.0516	2441
Phosphate	7.16	0.11	0.101	2754
Phosphate	7.42	0.21	0.156	2270
NaBO ₃	5.50	Variable	0.0043	5287
NaBO ₃	6.00	Variable	0.012	4777
NaBO ₃	6.50	Variable	0.034	4154
NaBO ₃	7.00	Variable	0.074	2946
NaBO ₃	8.00	Variable	0.51	1951
H ₃ BO ₃ /NaOH	6.25	0.00	0.019	4253
H ₃ BO ₃ /NaOH	9.00	0.01	2.81	1121
H ₃ BO ₃ /NaOH	9.40	0.01	7.64	1216
H ₃ BO ₃ /NaOH	9.80	0.02	15.9	1018
H ₃ BO ₃ /NaOH	10.50	0.02	68.6	931

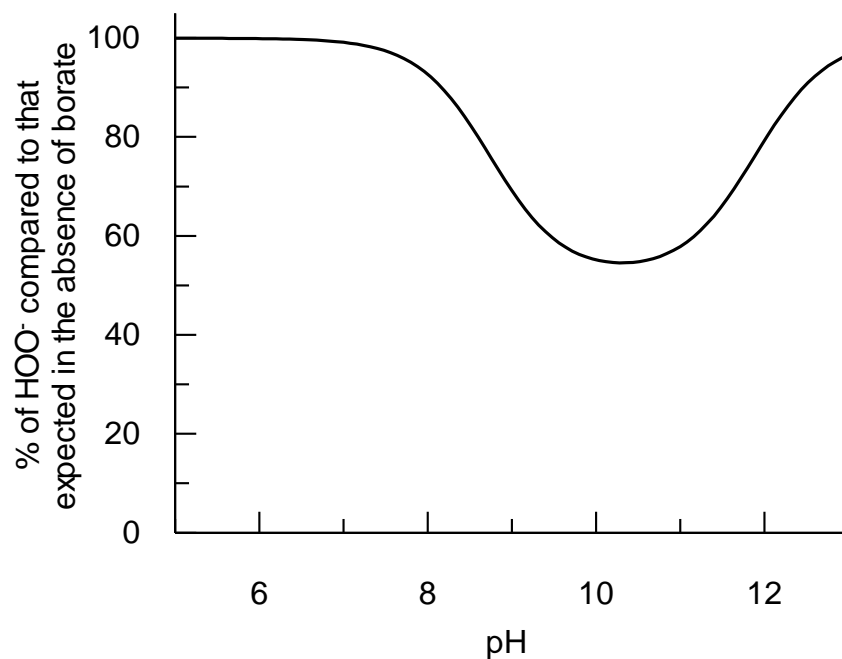


Figure 5.27: Simulated pH dependence of HOO^- concentration in the presence of $0.0428 \text{ mol dm}^{-3}$ borate and 0.001M total hydrogen peroxide, as a percentage of that expected when no borate is present.

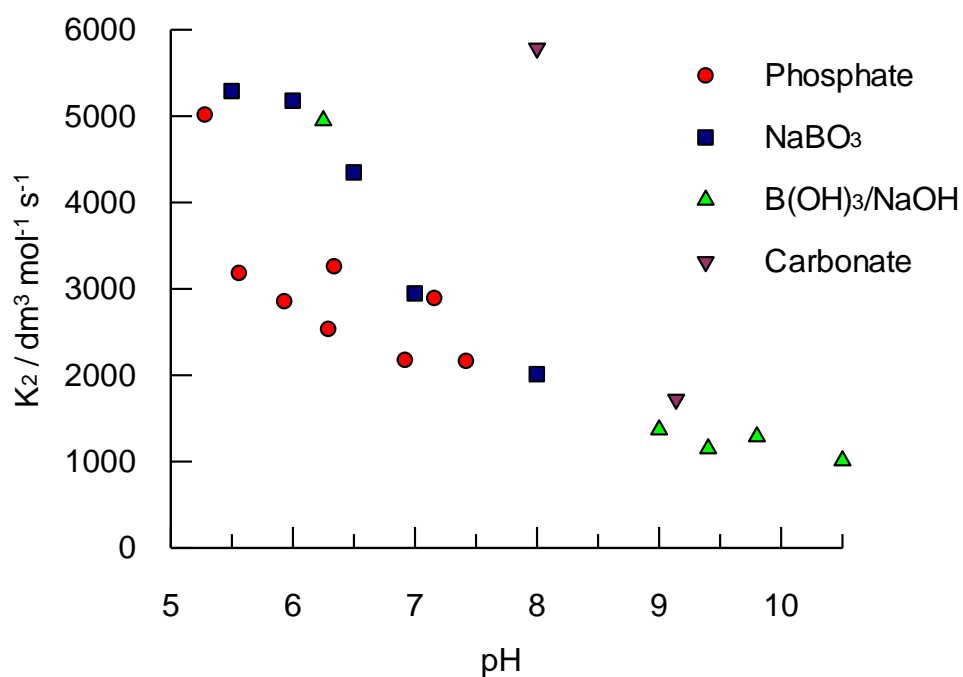


Figure 5.28: pH dependence for the second order rate constant, k_2 , obtained for the reaction of PNPA with hydrogen peroxide in various buffers.

5.4.2. Limitations of the work

The main limitations of this work centre around the wide range of pH's used for a given buffer system and the lack of control of ionic strength.

Looking first at buffering capacity, for sodium carbonate – sodium bicarbonate buffer solutions the recommended working range of pHs is 9.2 to 10.8 (Sigma Aldrich), whereas one run in this work was conducted at pH 8. For phosphate buffers the recommended range is pH 5.8 to 8.0, whereas one run was carried out at pH 5.28. For borate buffers the recommended range is 8.2 to 10.2, however runs were conducted at pH 6.25 and 10.5. Scheme 5.1 indicates that protons are generated during the hydrolysis and perhydrolysis reactions, and so when the buffering capacity is weak, as in the case of the runs specified above, the pH may decrease during the reaction, leading to a reduction in rate; experimentally this would manifest as a deviation from the expected curve described by Equation 5.28. In fact, no significant deviations were observed for these plots, and taken together with the fact that only four of the runs fell into this category the overall implications for the main discussion points are minimal.

Regarding ionic strength, It has been shown^{231, 232} that for alkaline hydrolysis of esters the kinetic salt effects are negative and usually small. For example, for the alkaline hydrolysis of ethyl malonate, increasing the ionic strength from 0 to 0.1 mol dm⁻³ results in less than 5% reduction in rate²³². Similar negative salt effects should be expected for other nucleophilic substitution reactions with esters. Table 5.5 shows the calculated ionic strengths for each of the buffer/pH systems used. For carbonate and phosphate buffers the ionic strength is approximately 0.1 mol dm⁻³, except in one case and so the effects across this pH range should not be significant. For borate buffers the ionic strength is 0.01 to 0.02 mol dm⁻³ when using boric acid and variable (0.01 to 0.20 mol dm⁻³) when using sodium borate (which is also the source of the hydrogen peroxide). Based on literature studies reported above, is unlikely that this range of ionic strengths will significantly affect the rate of either the hydrolysis or perhydrolysis reactions.

5.5. Conclusions and Further work

The studies carried out in this chapter have shown, fairly conclusively, that borate buffers inhibit the rate of reaction of hydrogen peroxide with PNPA and that this rate reduction is consistent with the formation of unreactive (to PNPA) peroxyborate species that reduce the equilibrium concentration of the perhydroxyl anion.

There was the possibility that some of the peroxyborate species may have demonstrated nucleophilic tendencies, as reported in the literature, and that this nucleophilicity might have manifest as rate accelerations at pHs between 6 and 8. This was not the case, and this can be taken as evidence that peroxyborate species act only as electrophiles.

There is evidence of buffer effects producing rate accelerations at lower pHs (6 or less), which may be due to either general acid base catalysis by the buffers, or, possibly through the formation of the $\text{HOOB}(\text{OH})_2$ species in the case of borate.

Further work should be carried out to determine the nature of this catalysis at lower pHs; this would take the form of a buffer dependence at constant ionic strength.

Chapter 6. Conclusions and recommendations for further research

6.1. Novel aspects arising from the study

The main objective of this research programme was to determine the factors influencing the decolourisation of dyes at low pH by different peroxide species, both in the presence and absence of metal ion catalysts and, therefore, to find a set of optimal conditions for application to wastewater treatment processes. An additional study looked at whether peroxoborates were capable of acting as nucleophiles.

The novel aspects arising from this study were as follows:

(a) The development of a new method for the *in-situ* generation of peracetic acid that gives the same equilibrium yield as established methods yet does not require the addition of an acid catalyst. The reaction was slow, but there was minimal decomposition and so it is ideal for circumstances that allow the preparation of peracetic acid well in advance of use.

(b) The first comprehensive study of the bleaching potential of peracetic acid and hydrogen peroxide towards a wide structural range of dyes both in the presence and absence of metal ions (iron, manganese, silver and copper).

(c) The inference that for iron-catalysed bleaching of azo dyes by peracetic acid the catalytic mechanism involves pre-complexation of iron and dye, followed by reaction of the 'activated' complex with peracetic acid rather than a free radical mechanism that might have been expected for such systems.

(d) The evidence that, in contradiction of literature studies, peroxoborate species do not act as nucleophiles.

6.2. Main conclusions

The work carried out in Chapter 2 described the study of the formation of peracetic acid from the equilibrium between hydrogen peroxide and a large excess of glacial acetic acid, both in the presence and absence of an acid catalyst (sulphuric acid). The reaction is slow in the absence of sulphuric acid, taking about 12 days to achieve equilibrium, compared to only 7 hours for the sulphuric acid catalysed reaction.

Notwithstanding the slow time to reach equilibrium, our study has shown that if time is not a factor in producing the peracetic acid, then there are many advantages of not using a catalyst. The yield itself is not affected by employing a much longer equilibrium time (we have shown almost identical equilibrium constants of 2.04 and 2.1 for catalysed and uncatalysed respectively), and there is no overall loss of peroxide over the 12 days. The main advantage of not using sulphuric acid is that there is a reduced requirement for neutralisation once the peracetic acid is formed (which also reverses the reaction) and that the requirement to use an environmentally hazardous material has been eliminated, in line with current industry efforts.

In Chapter 3 the relative reactivities of hydrogen peroxide and peracetic acid (generated using the methods developed in Chapter 2) towards a range of dyes were studied; these included monoazo, diazo, triarylmethane, quinoline, xanthene, indigoid and anthraquinone dyes. The catalytic effect of iron, silver, manganese and copper ions on the bleaching reactions were compared. The study showed that there were a variety of different behaviours observed for the different dye/peroxide/metal combinations. In some cases, such as for Green S, Malachite Green (both triarylmethane dyes), and Erythrosine Supra, with peracetic acid as the oxidant, the rates in the presence and absence of metal ions are similar, suggesting that radical mechanisms are not so significant compared to reaction with the peracetic acid directly. For Quinoline Yellow, which complexes with iron, the rate is actually lower in the presence of iron (and silver), and it is possible that the complex is less reactive to peracetic acid. There were also several examples of dye bleaching by peracetic acid being significantly accelerated by the presence of metal ions: Patent Blue and Brilliant Blue, and most of the azo dyes. Here, radical mechanisms might be suggested, but as shown in Chapter 4, it is more likely that the catalytic effect arises because the complex formed between iron and azo dyes activates the dye to attack by peracetic acid.

When hydrogen peroxide is used as the oxidant, all of the azo dyes are virtually unreactive in either the presence or absence of metal ions, though significant catalysis is observed for the triarylmethane dyes, probably through the formation of radicals. Radical mechanisms are also suggested for Indigo Carmine, Acid Green and Erythrosine Supra; copper and iron are particularly effective in this respect.

Chapter 4 extended the broad study carried out in Chapter 3 to look in detail at the oxidation of a range of azo dyes by peracetic acid in the presence of iron (III) as a

catalyst. The focus on peracetic acid and iron was because this was found to be the most effective oxidation system for across the range of dyes. The focus on azo dyes allowed the importance of structural features, such as having a hydroxyl group ortho or para to the azo linkage, to be investigated. The influence of catalyst concentration, pH, peracetic acid concentration and dye concentration on the reaction rate and overall percentage decolourisation were investigated.

It is known that for peroxyacids such as *m*-chloro and *p*-sulfo perbenzoic acid *in the absence of metal ion catalysts*, the mechanism of azo dye oxidation involves the reaction of the azo dye common ion and the protonated peroxyacid; i.e. that the peroxyacid is acting as an electrophile. Hydrogen peroxide, a much more powerful nucleophile has been shown oxidise azo dyes by reaction of the perhydroxyl anion with the hydrazone tautomer of the azo dye.

The results obtained in this study for the reaction of azo dyes with peroxyacids without added iron, when converted to the second order rate constant for the electrophilic reaction, k_2^E , give values that are several orders of magnitude higher than those derived from literature studies. It is possible that trace metal impurities catalysed the reaction. We have shown that the reaction rate is extremely sensitive to iron concentration at low iron concentrations, so only a small amount of metal ions, present as either impurities in the dye, or on glassware, would be necessary to significantly enhance the rate.

For the catalysed reaction, it was observed that there was a significant dependence of observed rate of absorbance decrease on iron concentration; moreover, saturation in iron concentration was observed at high iron concentrations. This, together with the observation of an increase in absorbance when adding iron to dye solutions, suggested the formation of an iron(III)-dye complex which then reacts with peracetic acid. An equation derived for this pathway showed an excellent fit to the data for all dyes and conditions. All of the dyes studied in Chapter 4 had naphthol hydroxyl groups in an ortho position to the azo linkage. This facilitates an iron complex in which the iron bridges the hydroxyl oxygen and the azo nitrogen. The resulting complex, with electron deficient nitrogen would then be susceptible to nucleophilic attack by the perhydroxyl anion. Orange I, which has the hydroxyl in the para position to the azo linkage also forms a complex with iron, as evidenced by the absorbance enhancement upon adding iron(III) to a solution of the dye, however it cannot form the same bridged complex as the ortho-hydroxy azo dyes, which may explain the much lower reactivity for the catalysed reaction.

Evidence of the possible involvement of radicals in our studies comes from the observation of a lag phase followed by a more rapid bleaching phase in the oxidation of azo dyes by peracetic acid at the lowest iron concentrations (another possibility is that at these iron concentrations the reactive iron complex forms at a much slower rate). However, this process is slow by comparison with the rate of oxidation at higher iron concentrations that do not exhibit this lag phase; consequently, if free radical mechanisms are suggested then they are not significant compared to the proposed formation of a reactive iron-dye complex.

The other main finding from Chapter 4 concerned the potential practical application of this work to wastewater treatment processes. In this regard percent dye degradation under various experimental conditions has been studied for five azo dyes. The results were remarkably consistent, and showed that the optimum conditions are pH 3, with approximately 0.001M added iron; further addition of iron is wasteful since it results in a reduction of degradation, most probably through the formation of coloured complexes between degradation products and iron.

The concept of nucleophilic / electrophilic reactions of peroxide species, which was raised in Chapter 4 was further explored in the final experimental chapter (Chapter 5) where the reactivity of peroxoborate species towards an ester, *p*-nitrophenyl acetate, was investigated. Above pH 6 hydrogen peroxide in equilibrium with boric acid forms a complex system of peracid-like peroxoborate species. Several of these species, for example monoperoxoborate have been found to be better electrophiles than hydrogen peroxide (for example in the reaction with organic sulphides), the suspicion remains that there may be some peroxide species that may also be good nucleophiles.

However, the studies carried out in Chapter 5 showed, that borate buffers inhibit the rate of reaction of hydrogen peroxide with PNPA and that this rate reduction is consistent with the formation of unreactive (to PNPA) peroxyborate species that reduce the equilibrium concentration of the perhydroxyl anion.

There was evidence of buffer effects producing rate accelerations at lower pHs (6 or less), which may be due to either general acid base catalysis by the buffers, or, possibly through the formation of the $\text{HOOB}(\text{OH})_2$ species in the case of borate.

6.3. Recommendations for further research

This work has produced some useful information on the bleaching of a wide range of dyes by hydrogen peroxide and hydrogen peroxide in the presence of metal catalysts; however a number of questions have been raised that should be addressed by further studies as detailed below.

1. Extend the range of dye substrates on which bleaching studies are carried out, including dyes that have structural features that assist in dye degradation, for example hydroxy groups in ortho positions to the reaction centre, as in some azo dyes, and in Green S.
2. Extend the study of factors affecting dye degradation, looking at temperature, concentrations of dyes, an extended PH range for the uncatalysed reaction (pHs 2 – 11) or dye related parameters such as class and type of dye.
3. Explore other catalysts and systems such as UV-visible light irradiation with or without metals ion catalysts. Many active homogeneous catalysts and their complexes are toxic and thus potentially environmentally problematic, under these circumstances development of heterogeneous catalytic processes is the most suitable solution so a further potential avenue for study might be to characterise the catalytic effect of heterogeneous magnetically separable iron mixed oxides Cu(II), Mn(II) ferrite and magnetite on decolourisation by peroxides.
4. Carry out pilot scale studies in either batch or continuous mode.
5. The precise nature of the iron catalysed azo dye oxidation by peracetic acid needs to be elucidated, i.e. the role of the iron complex, the extent of any radical mechanisms and the nature of the peroxide species involved in the reaction. The unexpectedly large rate constant for the uncatalysed reaction also needs to be clarified: there was the suggestion that trace metal ions were catalysing the reaction, and so metal ion chelators such as EDTA and radical scavengers could be added to the solution to see if the reaction rate is decreased.
6. Bleaching of dye colour in the visible region of the spectrum is required aesthetically; however the dye fragments that are produced may themselves be toxic and persistent in the environment. Ideally an oxidation process should

achieve complete mineralisation. We have not analysed the reaction products or the overall mineralisation rates, and this is an aspect of the study that should be addressed in further studies. Mineralisation could be measured by chemical oxygen demand (COD): this method is used as a measure of oxygen requirement of a sample that is susceptible to oxidation by strong chemical oxidant. The potassium dichromate reflux method is preferred over procedures or using other oxidants e.g. potassium permanganate because of its superior oxidizing ability; COD is expressed in milligrams per litre (mg/l) which indicates the mass of oxygen consumed per litre of solution.

7. Understanding the dye structures and how they are degraded is crucial to understanding how toxic by-products are created, it is very important to analyse products of dyes after degradation so it is recommended that a time series of product analyses be carried out for different dye/peroxide systems. Suitable methods for this include: UV/visible spectrophotometry, high performance liquid chromatography (HPLC), liquid chromatography and electrospray ionization mass spectrometry (LC/ESI-MS).
8. Finally, regarding the peroxoborate work, further work should be carried out to determine the nature of general acid base catalysis by the buffers at lower pHs; this would take the form of buffer dependence at constant ionic strength.

References

1. J. R. Rittenhouse, W. Lobunez, D. Swern and J. G. Miller, *Journal of the American Chemical Society*, 1958, **80**, 4850-4852.
2. G. J. Minkoff, *Proceedings of the Royal Society of London. Series A. Mathematical and Physical Sciences*, 1954, **224**, 176-191.
3. M. C. R. Symons, in 'Peroxide Reaction Mechanisms', Ed. JO Edwards, Wiley-Interscience, New York 1962, , 1962, p137.
4. D. Littlejohn and S. G. Chang, *Industrial & Engineering Chemistry Research*, 1990, **29**, 1420-1424.
5. D. Swern and L. S. Silbert, *Analytical chemistry*, 1963, **35**, 880-885.
6. D. Swern, *Organic peroxides. Wiley Interscience, New York*,, 1970, **1**, 207.
7. A. J. Everett and G. J. Minkoff, *Transaction of the Faraday Society*,, 1953, **49**, 410.
8. J. P. Goodman and P. Robson, *J. Chem. Soc*, 1963, 2871.
9. C. J. Battaglia and J. O. Edwards, *Inorganic Chemistry*, 1965, **4**, 552-558.
10. R. Curci and Edwards. J.O., *Organic Peroxides* , ed.Swern, D., Wiley-Interscience, New york,ch.4, 1970.
11. C. Schmidt and A. H. Schon., *Canadian Journal of Chemistry*, 1963, **41**, 1819-1825.
12. F. W. Evans and A. H. Schon, *canadian Journal of chemistry*,, 1963, **41**, 1826.
13. D. Lefort, J. Fossey, M. Gruselle, J.-Y. Nedelec and J. Sorba, *Tetrahedron*, 1985, **41**, 4237-4252.
14. Y. Sawaki and W. Ando, *Organic peroxides, Ed.;*John Wiley & sons:New York, 1992, 425-477.
15. D. L. Ball and J. O. Edwards, *The Journal of Physical Chemistry*, 1958, **62**, 343-345.
16. E. Koubek, M. L. Haggett, C. J. Battaglia, K. M. Ibne-Rasa, H. Y. Pyun and J. O. Edwards, *Journal of the American Chemical Society*, 1963, **85**, 2263-2268.
17. B. J.D'Ans and W. Frey, 45 , 1845(1912);Z. Anorg.Chem.,84, 145 ,1914.J . D'Ans , German Patent 251,802,1911.
18. B. Phillips, P. S. Starcher and B. D. Ash, *The Journal of Organic Chemistry*, 1958, **23**, 1823-1826.
19. F. P. Greenspan, *Journal of the American Chemical Society*, 1946, **68**, 907-907.
20. B. Phillips, F. C. Frostick and P. S. Starcher, *Journal of the American Chemical Society*, 1957, **79**, 5982-5986.
21. D. Swern, T. W. Findley and J. T. Scanlan, *Journal of the American Chemical Society*, 1944, **66**, 1925-1927.
22. C. R. Dick and R. F. Hanna, *The Journal of Organic Chemistry*, 1964, **29**, 1218-1220.
23. I. M. Kolthoff, T. S. Lee and M. A. Mairs, *Journal of Polymer Science*, 1947, **2**, 199-205.
24. A. D. Baeyer and V. Villiger, *Berichte der deutschen chemischen Gesellschaft*, 1900, **33**, 1569-1585.
25. A. Baeyer and V. Villiger, *Berichte der deutschen chemischen Gesellschaft*, 1901, **34**, 762-767.
26. G. B. Bachman and D. E. Cooper, *The Journal of Organic Chemistry*, 1944, **09**, 302-309.
27. A. Kergomard and J. Bigou, *Bull. Soc. Chem. France* 1956, 486.
28. M. Vilkas, *Bull. Soc. France*,, 1959, 1401.
29. J. D'Ans and J. Mattner, *Journal. Chem.Ztg*, 1950, **74**, 435.
30. R. Adams, et al., *Chem.Rev.*, 1, *Organic Reactions*, Wiley,New York, , 1949, **VII Chapter 7**.
31. B. C. Brodie, *Ann.(Suppl.)*,, 1864, **3**, 200.

32. P. C. Freer and F. G. Novy, *Journal of the American Chemical Society*,, 1902, **27**, 161.
33. A. M. Clover and A. C. Houghton, *Journal of the American Chemical Society*,, 1904, **32**, 43.
34. J. S. Reichert, S. A. McNeight and A. A. Elston, *United States Patent*,, 1945, **2**, 377.
35. C. A. Bunton, T. A. Lewis and D. L. Llewellyn, *Journal of Chemical Society*,, 1956, **78**, 1226.
36. K. Murai, F. Akazame and Y. Murakami, *J.Chem. Soc.Japan, Ind. Chem.Sect.*, 1960, **63**, 803.
37. E. Pungor, J. Trompler, Z. Rempert and E. Schulek, *Acta Chimica Academiae Scientiarum Hungaricae*,, 1956, **8**, 321.
38. H. Krimm, *United States Patent 2*, 1957, **813**, 896.
39. H. Krimm, *German Patent*, 1, 1959, **048**, 569.
40. J. D'Ans, and Gold, H., Ber, 92, 2559(1959). German patent 1,099,528 (1961).
41. W. H. Hatcher and G. W. Holden, *Transactions of Royal Society of Canada*,, 1927, **21**, 237.
42. S. Havel and J. A. Weigner, *Chem.Prumysl.*, 1960, **10**, 293.
43. B. Phillips and D. L. MacPeck, *Encyclopedia of Chemical Technology*,, 1957., **622**, edited by R.E.Kirk and D.F. Othmer, First Supplement
44. Y. Sawaki and Y. Ogata, *Bulletin of the Chemical Society of Japan*,, 1965, **38**, 2103-2106.
45. D. H. Fortnum, C. J. Battaglia, S. R. Cohen and J. O. Edwards, *Journal of the American Chemical Society*, 1960, **82**, 778-782.
46. G. M. Badger, R. G. Buttery and G. E. Lewis, *Journal of Chemical Society*,, 1953, 214.
47. J. O. Edwards and R. G. Pearson, *Journal of the American Chemical Society*, 1962, **84**, 16-24.
48. F. Secco and M. Venturini, *J. Chem. Soc. Perkin Transaction II*,, 1972, 2305.
49. J. O. Edwards and R. Curci, *Wiley Interscience, New York.Vol I "ed. Swern,D.*, , 1970.
50. A. Battaglia, A. Dondoni, G. Maccagnani and G. Mazzanti, *J. Chem. Soc. Perkin Transaction II*,, 1974, 609.
51. Y. Ogata, Y. Sawaki and H. Inoue, *The Journal of Organic Chemistry*, 1973, **38**, 1044-1045.
52. J. d'Ans and W. Frey, *Berichte der deutschen chemischen Gesellschaft*, 1912, **45**, 1845-1853.
53. F. P. Greenspan and D. G. MacKellar, *Analytical chemistry*, 1948, **20**, 1061-1063.
54. B. D. Sully and P. L. Williams, *Analyst*,, 1962, **87**, 653.
55. H. Krüssmann and J. Bohnen, *Tenside Surfactants Detergents*,, 1994, **31**, 229.
56. Petra Forte Tavčer., *Tekstilc.*, 2003, **46**, 19.
57. J. E. Frew, P. Jones and Scholes., *Analytica Chimica Acta*,, 1983, **155**, 139.
58. U. L. k. Pinkernell, H.-J.; Karst, U. , *Analyst*, 1997, **122**, 567-571.
59. D. M. Davies and M. E. Deary, *Analyst*,, 1988, **113**, 1477.
60. E. Saltzman and N. Gilbert, *Analytical Chemistry*,, 1959, **31**, 1914.
61. T. C. Parcell and I. R. Coben, *Environ. Sci. Technol.*, 1967, **1**, 431.
62. F. P. Di Furia, U. M.; Quintly, S. Salvagno and G. Scorrano, *Analyst* 1984, **109**, 985-987.
63. F. Di Furia, M. Prato, G. Scorrano and M. Stivanello, *Analyst*, 1988, **113**, 793.
64. U. Pinkernell, S. Effkemann and U. Karst, *Analytical chemistry*, 1997, **69**, 3623-3627.
65. S. Effkemann, U. Pinkernell, R. Neumuller, F. Schwan, H. Engelhardt and U. Karst, *Analytical chemistry*, 1998, **70**, 3857-3862.
66. T. T. Boon, P. A. Kok and G. Haritharan, *Analyst*,, 1988, **113**, 617-620.
67. P. Westbroek, B. Haute and E. Temmerman, *Fresenius' Journal of Analytical Chemistry*, 1996, **354**, 405-409.

68. D. C. Gottschalk, D. J. A. Libra and D.-I. A. Saupe, *Ozonation of Water and Waste Water*, 2000, i-xiii.
69. J. Staehelin and J. Hoigne, *Environmental Science & Technology*, 1982, **16**, 676-681.
70. G. Eisenberg, *Industrial & Engineering Chemistry Analytical Edition*, 1943, **15**, 327-328.
71. M. S. Robin, *Analyst*, 1980, **105**, 950-954.
72. J. W. Ogleby and J. Williams, *Analytical proceedings*, 1985, **22**, 181.
73. I. R. Cohen, T. C. Purcell and A. P. Altshuler, *Environmental Science and Technology*, 1967, **1**, 247.
74. T. C. Purcell and I. R. Cohen, *Environmental Science and Technology*, 1967, **1**, 431.
75. D. Harms and U. Karst, *Anal Chim. Acta*, 1999, **389**, 233.
76. G. Boullion, C. Lick and K. Schank, *John Wiley&Sons, London*, , 1983, 287.
77. S. Effkemann, U. Pinkernell and U. Karst, *Analytica Chimica Acta*, 1998, **363**, 97.
78. N. Higashi, H. Yokota, S. Hiraki and Y. Ozaki, *Analytical chemistry*, 2005, **77(7)**, 2272-2277.
79. M. I. Karayannis, A. C. Pappas and C. D. Stalikas, *J. Ins. Sci. Techn.* , 2000, **2 (2)**, **2nd AACD**.
80. P. F. Tavčer, *Tekstilec* 2003, **46(1-2)**, 19-24.
81. J. Clayden, N. Greeves, S. Warren and P. Wothers, *Oxford:Oxford University Press*,, 2001, 506.
82. P. A. CARNEIRO, E. OSUGI Marly, J. J. SENE, M. A. ANDERSON and Z. M. V. BOLDRIN, *Electrochim. Acta* 2004, **49 (22-23)** 3807-3820.
83. P. Rys and H. Zollinger, in *Wiley-Interscience, Division of John Wiley & Sons Ltd*, , Belfast, Editon edn., 1972, vol. SA 23 (3) pp. 193-199
84. <http://stainsfile.info/StainsFile/dyes/dyecolor.htm>.
85. G. J. Rocha, *Estrutura e propriedades dos corantes*, 2002, 12-16.
86. T. M. Cooper and M. O. Stone, *Langmuir*, 1998, **14**, 6662-6668.
87. M. Kasha, H. R. Rawls and M. Ashraf El-bayoumi, *Pure and Applied Chemistry*,, 1965, **11**, 371-392.
88. E. G. McRae and M. Kasha, *physical Processes in Radiation Biolog eds. Augenstein, L., Rosenberg, B. and Mason, R., Academic Pres New York*, p23., 1964.
89. E. R. Trotman, *Dyeing and Chemical Technology of Textile Fibers*, Sixth Edition. edn., Edward Arnold, A Division of Hodder & Stoughton, , London, 1990.
90. J. Shore, *Society of Dyers and Colourists*, 1990. BTTG. volume 1. Manchester, England.
91. J. Bell, J. J. Plumb, C. A. Buckley and D. C. Stuckey, *J. Environ. Eng*, 2000, **126(11)**, 1026.
92. X.-Y. Yang and B. Al-Duri, *Chemical Engineering Journal*, 2001, **83**, 15-23.
93. T. O'Mahony, E. Guibal and J. M. Tobin, *Enzyme and Microbial Technology*, 2002, **31**, 456-463.
94. J. E. M. Sarina, M. T. Brian and A. R. M. Reckhow, *Journal of Environmental Engineering*,, 2006, **3**, 315-322.
95. E. K. Raymond and F. Dunald, *John Wiley, New York, USA.*, 1984.
96. S. Papic, N. Koprivanac, A. Loncaric Bozic and A. Metes, *Dyes and Pigments*, 2004, **62**, 291-298.
97. J. F. Jeremy, A. T. Coen, L. P. Smith and J. Oakes, *Journal of Chemical Society, Perkin Transaction 2*,, 2001, 2125-2129.
98. L. Rehn, *Blasengeschwulste bei Fuchsin Arbeitern. Arch. Klin. Chir.*,, 1895, **50**, 588-600.
99. K. T. Chung and C. E. Cerniglia, *Mutation research. Reviews in genetic toxicology*,, 1992, **277**, 201-220.

100. H. M. Pinheiro, E. Touraud and O. Thomas, *Dyes and Pigments*, 2004. , **61**, 121-139.
101. O. Legrini, E. Oliveros and A. M. Braun, *Chemical Reviews*, 1993, **93**, 671-698.
102. A. Mittal, L. Kurup and V. K. Gupta, *Journal of Hazardous Materials*, 2005, **117**, 171-178.
103. T.-H. Kim, C. Park, J. Lee, E.-B. Shin and S. Kim, *Water Research*, 2002, **36**, 3979-3988.
104. R. Liu, H. Chiu and R. Yeh., *International Journal of Environmental Studies*, , 2003, **59**, 143-158.
105. R. Sanghi and B. Bhattacharya, *Canadian Journal of Forest Research*, 2002, **38**, 553.
106. A. Alinsafi, M. Khemis, M. N. Pons, J. P. Leclerc, A. Yaacoubi, A. Benhammou and A. Nejmeddine, *Chemical Engineering and Processing*, 2004, **44**, 461-470.
107. G. Jiantuan and J. Qu, *Journal of Hazardous Materials*, 2003, **100**, 197-207.
108. I. Arslan, Balcioglu, I. A. and Tuhkanen, T. , *Environ. Technol.*, 1999, **20**, 921-931.
109. S. Parra, V. Sarria, S. Malato, P. Perring and C. Pulgarin, *Applied Catalysis B: Environmental*, 2000, **27**, 153-168.
110. E. H. Snider and J.J. Porter, *J. Water Poll. Cont. Fed*, 1994, **46**, 886.
111. S. Beszedits, *American Dyestuffs Report*, 1980, **69**, 38-40.
112. J. M. Green and C. Sokol, *American Dyestuff Rept*, , 1985, **74**, 67-72.
113. J. P. Gould and K. A. Groff, *Ozone Science & Engineering*, 1987, **9**, 153.
114. I. Arslan, I. A. Balcioglu and T. Tuhkanen, *Journal of Environmental Science and Health, Part A*, 2000, **35**, 775-793.
115. V. López-Grimau and M. C. Gutiérrez, *Chemosphere*, 2006, **62**, 106-112.
116. P. A. Carneiro, M. E. Osugi, C. S. Fugivara, N. Boralle, M. Furlan and M. V. B. Zanoni, *Chemosphere*, 2005, **59**, 431-439.
117. J. H. Ramirez, C. A. Costa and L. M. Madeira, *Catalysis Today*, 2005, **107-108**, 68-76.
118. M. M. Hassan and C. J. Hawkyard, *Journal of Chemical Technology & Biotechnology*, 2002, **77**, 834-841.
119. G. Muthuraman and K. Palanivelu, *Dyes and Pigments*, 2006, **70**, 99-104.
120. P. Venkateswaran and K. Palanivelu, *Journal of Hazardous Materials*, 2006, **131**, 146-152.
121. J. Naumczyk, L. Szpyrkowicz and F. Zilio-Grandi, *Water Science and Technology*, 1996, **34**, 17-24.
122. A. T. King, *Journal of the Society of Dyers and Colourists*, 1930, **46**, 225-227.
123. H. Phillips, *Journal of the Society of Dyers and Colourists*, 1938, **54**, 503-512.
124. U. Rott and R. Minke, *Water Science and Technology*, 1999, **40**, 137-144.
125. M. Neamtu, A. Yediler, I. Siminiceanu and A. Kettrup, *J. Photochem. Photobiol A: Chem.*, , 2001, **141**, 247-254.
126. M. S. Lucas and J. A. Peres, *Dyes and Pigments*, 2006, **71**, 236-244.
127. P. Forte-Tavcer, *Dyes and Pigments*, 2004, **63**, 181-189.
128. K. Pavla, K. Franci and F. Petra, *Coloration technology*, 2005, **121** 304-309.
129. W. H. Glaze, J. W. Kang and D. H. Chapin, *Ozone: Science & Engineering*, , 1987, **9**, 335-352.
130. N. Azbar, T. Yonar and K. Kestioglu, *Chemosphere*, 2004, **55**, 35-43.
131. U. Pagga and D. Brown, *Chemosphere*, 1986, **15**, 479-491.
132. T. Reemtsma and M. Jekel, *Water Research*, 1997, **31**, 1035.
133. R. Andrezzi, V. Caprio, A. Insola and R. Marotta, *Catalysis Today*, 1999, **53**, 51-59.
134. M. Pera-Titus, V. García-Molina, M. A. Baños, J. Giménez and S. Esplugas, *Applied Catalysis B: Environmental*, 2004, **47**, 219-256.
135. M. Rein, *Proceedings of the Estonian Academy of Sciences Chemistry*, 2001, **50**, 59-80.
136. A. F. Martins, *Pure and Applied Chemistry*, 1998, **70**, 2271-2279.

137. O. J. Hao, H. Kim and P.-C. Chiang, *Critical Reviews in Environmental Science and Technology*, 1999, **30**, 449 - 505.
138. O. Tünay, I. Kabdasli, G. Eremektar and D. Orhon, *Water Science and Technology*, 1996, **34**, 9-16.
139. C. Gottschalk, J. A. Libra and A. Saupe, *Wiley-VCH*, 2000.
140. Y. S. Shen and D. K. Wang, *Journal of Hazardous Materials*, 2002, **89**, 267-277.
141. H. Y. Shu and C. R. Huang, *American Dyestuff Reporter*, , 1995, 30-34.
142. M. Pittroff and K. H. Gregor, *Melliand English 6, translation of Melliand Textilberichte*, 1992, **73**, 526.
143. J. M. Hoigne, rates and selectivities of oxidations of organic compounds initiated by ozonation of water. In *Handbook of Ozone Technology and Applications*. Ann Arbor and A. A. Science Publ., MI, 1982.
144. TECHCOMMENTARY: Advanced Oxidation Processes for Treatment of Industrial Wastewater. An EPRI Community Environmental Center Publ. No. 1.
145. H. J. Fenton, *Journal of Chemical Society*,, 1884, **65**, 889-899.
146. S.-F. Kang, C.-H. Liao and M.-C. Chen, *Chemosphere*, 2002, **46**, 923-928.
147. Y. Zuo and J. Hoigne, *Environmental Science and Technology*, , 1992, **26**, 1014-1022.
148. W. Feng and D. Nansheng, *Chemosphere*, 2000, **41**, 1137-1147.
149. W. Feng, D. Nansheng and Z. Yuegang, *Chemosphere*, 1999, **39**, 2079-2085.
150. S. Nam, V. Renganathan and P. G. Tratnyek, *Chemosphere*, 2001, **45**, 59-65.
151. C. Bauer, P. Jacques and A. Kalt, *Journal of Photochemistry and Photobiology A: Chemistry*, 2001, **140**, 87-92.
152. E. S. Huyser and G. W. Hawkins, *The Journal of Organic Chemistry*, 1983, **48**, 1705-1708.
153. G. McMullan, C. Meehan, A. Conneely, N. Kirby, T. Robinson, P. Nigam, I. M. Banat, R. Marchant and W. F. Smyth, *Applied Microbiology and Biotechnology*, 2001, **56**, 81-87.
154. M. Bhaskar, A. Gnanamani, R. J. Ganeshjeevan, R. Chandrasekar, S. Sadulla and G. Radhakrishnan, *Journal of Chromatography A*, 2003, **1018**, 117-123.
155. A. Stolz, *Applied Microbiology and Biotechnology*, 2001, **56**, 69-80.
156. D. Sponza. and M. Isik, *Process Biochemistry*,, 2005, **40**, 35-44.
157. W. Azmi, R. K. Sani and U. C. Banerjee, *Enzyme and Microbial Technology*, , **1998**, **22**, , 185-191.
158. G. M. Walker and L. R. Weatherley, *Environmental Pollution*, 2000, **108**, 219-223.
159. M. I. Beydili, R. D. Matthews and S. G. Pavlostathis, *Water science and technology*,, 2001, **43(2)**, 333-340.
160. A. S. Mahmoud, A. E. Ghaly and M. S. Brooks, *American Journal of Environmental Sciences*,, 2007, **3 (4)**, 205-218.
161. J. J. Rook, *Water Treatment Exam*,, 1974, **23**, 234- 243.
162. S. Monarca, D. Feretti, I. Zerbini, C. Zani, A. Alberti, S. D. Richardson, A. D. Thruston Jr., P. Ragazzo and L. Guzzella, *Water Science and Technology: Water Supply* 2002, **2**, 199-204.
163. Kri, P. man, Kova, Franci, Tav and P. F. er, *Coloration Technology*, 2005, **121**, 304-309.
164. Y. Cai and S. K. David, *Clothing and Textiles Research Journal*,, 1997, **67**, 459-464.
165. Z. Yuan, Y. Ni and Van Heiningen., *Appita J*,, 1998, **51(5)** 377-380.
166. Q. Yang, F. Tang and Y. Zhang, *China's pulp and paper sector*,, 2003, **22**, 5-8.
167. D. H. Stormont., *Oil Gas Journal*,, 1960, **58**, 78-79.
168. R. L. Musante, R. J. Grau and M. A. Baltanas, *Applied Catalysis A: General*,, 2000, **197(1)**, 165-173.
169. R. Gehr, M. Wagner, P. Veerasubramanian and P. Payment, *Water Research*, 2003, **37**, 4573-4586.
170. M. Kitis, *Environment International*, 2004, **30**, 47-55.

171. Swern, D. *Organic Peroxides*; Wiley-Interscience: New York, 1970; p 360.
172. <http://www.epa.gov/oppbppd1/biopesticides/ingredients/factsheets/factshe>.
173. J. A. John and F. J. Weymouth, *Society of Chemical Industry*, , 1962, **2**, 62–69.
174. C. H. Wang and R. S. Fang, *Chin. J. Disinfection*, 2006, **23**, 100–102(in Chinese).
175. L. Dul'neva and A. Moskvin, *Russian Journal of General Chemistry*, 2005, **75**, 1125-1130.
176. X. B. Zhao, T. Zhang and Y. J. Zhou, *Journal of Molecular Catalysis A: Chemical*, , 2007, **271**, 246-252.
177. Z. Yuan, Y. Ni and A. Van Heiningen, *The Canadian Journal of Chemical Engineering*,, 1997, **75**, 37-41.
178. E. Koubek and J. O. Edwards, *The Journal of Organic Chemistry*, 1963, **28**, 2157-2160.
179. M. Rubio, G. Ramírez-Galicia and L. J. López-Nava, *Journal of Molecular Structure: THEOCHEM*, 2005, **726**, 261-269.
180. R. Stewart and K. Yates, *Journal of the American Chemical Society*, 1960, **82**, 4059-4061.
181. L. Kunigk, D. R. Gomes, F. Forte, K. P. Vidal, L. F. Gomes and P. F. Sousa, *Brazilian Journal of Chemical Engineering*, 2001, **18**, 217-220.
182. V. G. Kharchuk, I. P. Kolenko and L. A. Petrov, *Journal Name: J. Appl. Chem. USSR (Engl. Transl.); (United States); Journal Volume: 58:6, PT.2*, 1985, Medium: X; Size: Pages: 1228-1232.
183. C. W. Jones, *Royal Society of Chemistry*, , **1999**, , Chapter 6.
184. C. W. Jones, *Royal Society of Chemistry*,, 1999, chapter 2.
185. A. Samuni, D. Meisel and G. Czapski, *Journal of Chemical Society, Dalton Transaction I*,, 1972, 1273-1277.
186. I. A. Salem, M. El-Maazawi and A. B. Zaki, *International Journal of Chemical Kinetics*, 2000, **32**, 643-666.
187. J. Oakes and P. Grantton, *Journal .Chem. Soc, Perkin Transaction 2*,, 1998, 1857-1864.
188. K. Rajeshwar, M. E. Osugi, W. Chanmanee, C. R. Chenthamarakshan, M. V. B. Zaroni, P. Kajitvichyanukul and R. Krishnan-Ayer, *Journal of Photochemistry and Photobiology C: Photochemistry Reviews*, 2008, **9**, 171-192.
189. A. U. Moozyckine and D. M. Davies, *Green Chem*, 2002, **4**, 452 - 458.
190. D. M. Davies and A. U. Moozyckine, *J. Chem. Soc., Perkin Trans. 2* 2000, 1495 - 1503.
191. B. H. Hameed and T. W. Lee, *Journal of Hazardous Materials*, 2009, **164**, 468-472.
192. C. Galindo, P. Jacques and A. Kalt, *Journal of Photochemistry and Photobiology A: Chemistry*, 2001, **141**, 47-56.
193. M. Morita, R. Ito, T. Kamidate and H. Watanabe, *Textile Research Journal*, 1996, **66**, 470-473.
194. T. Bigg and S. J. Judd, *Process Safety and Environmental Protection*, 2001, **79**, 297-303.
195. M. P. Paul, *Journal of Chem. Research (S)*,, 1999, 340-341.
196. J. P. Lorimer, T. J. Mason, M. Plattes, S. S. Phull and D. J. Walton, *Pure and Applied Chemistry*, , 2001, **73(12)**, 1957–1968
197. H. Ouml, zsoy, Ali, Uuml, nyayar and M. Mazmanc, *Biodegradation*, 2005, **16**, 195-204.
198. N. Chahbane, D. L. Popescu, D. A. Mitchell, A. Chanda, D. Lenoir, A. D. Ryabov, ., K. W. Schramm and T. J. Collins, *Green Chem.*, , 2007, **9**, 49-57.
199. C. Bruce, L. John R, S. N. Marurice, O. John and P. P. Roger, *Organic and Biomolecular Chemistry*,, 2003, **1**, 1568-1577.
200. J. Oakes and P. Grantton, *Journal. Chem. Soc., Perkin Transaction 2*,, 1998, 2563-2568.

201. Y. Mu, H. Q. Yu and S. J. Zhang, *J. Photochem. Photobiol.*, 2004, **A163**, 311-316.
202. T. Hihara, Y. Okada and Z. Morita, *Dyes and Pigments*, 2003, **59**, 25-41.
203. G. R. Hodges, J. R. L. Smith and J. Oakes, *Journal. Chem. Soc., Perkin Trans. 2*, 1999, 1943-1952.
204. A. H. Gemeay, I. A. Mansour, R. G. El-Sharkawy and A. B. Zaki, *Journal of Chemical Technology & Biotechnology*, 2004, **79**, 85-96.
205. N. Modirshahla, M. A. Behnajady and F. Ghanbary, *Dyes and Pigments*, 2007, **73**, 305-310.
206. J. J. Pignatello, *Environmental Science & Technology*, 1992, **26**, 944-951.
207. X.-R. Xu, H.-B. Li, W.-H. Wang and J.-D. Gu, *Chemosphere*, 2004, **57**, 595-600.
208. P. K. Malik and S. K. Saha, *Separation and Purification Technology*, 2003, **31**, 241-250.
209. M. Neamtu, C. Catrinescu and A. Kettrup, *Applied Catalysis B: Environmental*, 2004, **51**, 149-157.
210. C. L. Hsueh, Y. H. Huang, C. C. Wang and C. Y. Chen, *Chemosphere*, 2005, **58**, 1409-1414.
211. D. Kabita, B. Sekhar, C. Basab and M. Subrata, *Journal of Environmental Monitoring*, 2002, **4**, 754-760.
212. S. H. Lin and C. C. Lo, *Water Research*, 1997, **31**, 2050-2056.
213. L. Szpyrkowicz, C. Juzzolino and S. N. Kaul, *Water Research*, 2001, **35**, 2129-2136.
214. K. Swaminathan, S. Sandhya, A. Carmalin Sophia, K. Pachhade and Y. V. Subrahmanyam, *Chemosphere*, 2003, **50**, 619-625.
215. J. Chen and L. Zhu, *Chemosphere*, 2006, **65**, 1249-1255.
216. D. M. Davies and P. Jones, *Journal. Soc. Dyers Colour*, 1983, **98**, 17-21.
217. D. M. Davies, M. E. Deary, K. Quill and R. A. Smith, *Chemistry - A European Journal*, 2005, **11**, 3552-3558.
218. K. M. Thompson, W. P. Griffith and M. Spiro, *Journal of the Chemical Society, Faraday Transactions*, 1993, **89(8)**, 1203-1209
219. A. McKillop and W. R. Sanderson, *Tetrahedron*, 1995, **51**, 6145-6166.
220. S. Rey and D. M. Davies, *Chemistry - A European Journal*, 2006, **12**, 9284-9288.
221. I. R. Wilson, *Short Communications*, 1960, 582-584.
222. S. B. Brown, P. Jones and A. Sugget, *Progress in Inorganic Chemistry*, 1970, **13**, 159 - 204.
223. R. Pizer and C. Tihal, *Inorganic Chemistry*, 1987, **26**, 3639-3642.
224. D. E. Richardson, H. Yao, K. M. Frank and D. A. Bennett, *Journal of the American Chemical Society*, 2000, **122**, 1729-1739.
225. D. M. Davies. and M. E. Deary., *journal of chemical research synopses*, 1988, 354 - 355.
226. C. A. S. Regino and D. E. Richardson, *Inorganica Chimica Acta*, 2007, **360**, 3971-3977.
227. H. Yao and D. E. Richardson, *Journal of the American Chemical Society*, 2000, **122**, 3220-3221.
228. M. N. Khan, *Journal .Chem. Soc, Perkin Transaction 2*, 1988, 1129-1134.
229. W. P. Jencks and D. G. Oakenfull, *Journal of the American Chemical Society*, 1971, **93**, 178-188.
230. W. P. Jencks, D. G. Oakenfull and K. Salvesen, *Journal of the American Chemical Society*, 1971, **93**, 188-194.
231. J. F. Kirsch and W. P. Jencks, *Journal of the American Chemical Society*, 1964, **86**, 837-846.
232. A. Indelli, G. Nolan and E. S. Amis, *Journal of the American Chemical Society*, 1960, **82**, 3237-3238.

Appendix

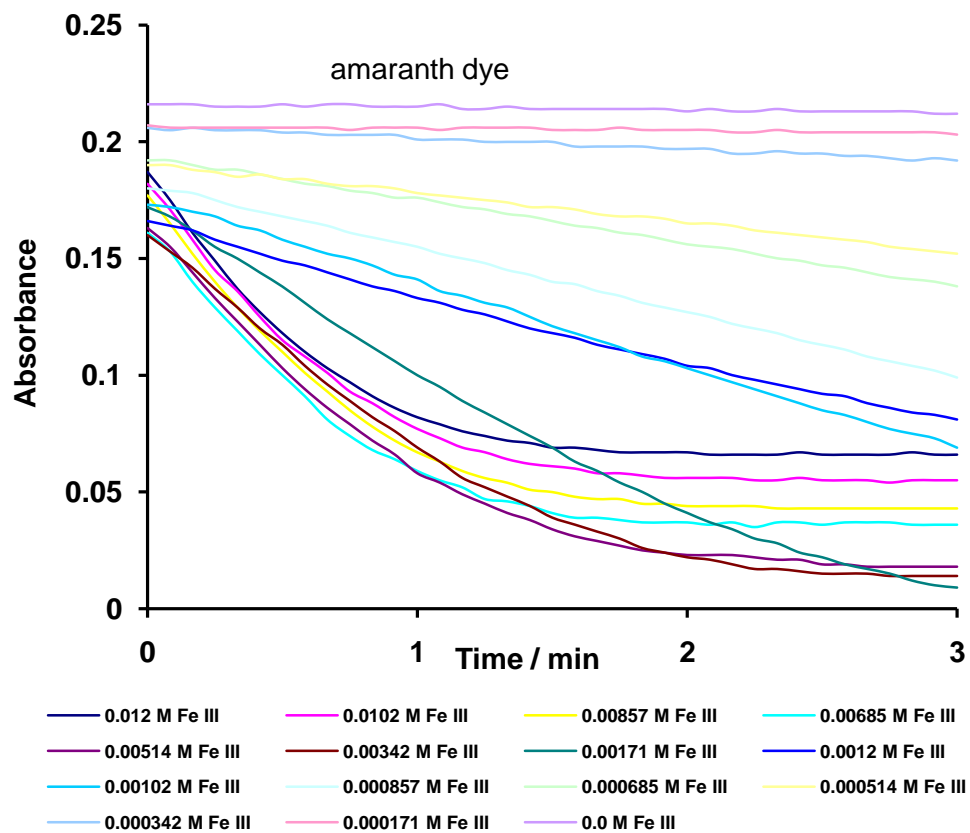


Figure A1.1:- Effect of Fe (III) concentrations on oxidation of Amaranth dye
Absorbance change with time, [PAA]= 2.05×10^{-2} mol dm⁻³, on absorbance of 1×10^{-5} M dye with different concentrations of Fe (III) as a catalyst, pH 2.09 , Temp 25⁰C

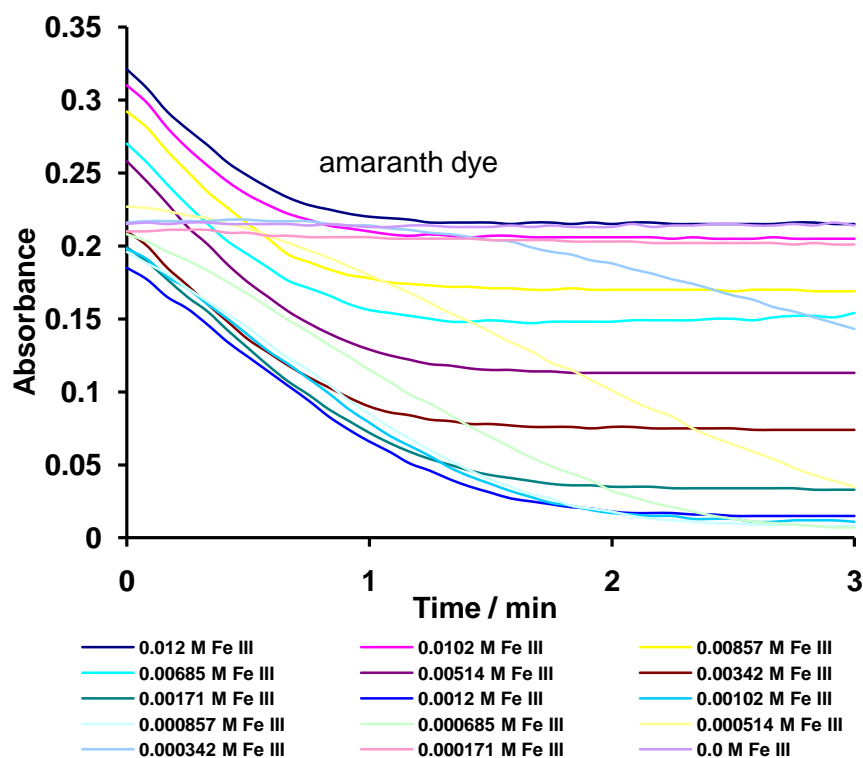


Figure A1.1 :- Effect of Fe (III) concentrations on oxidation of Amaranth dye Absorbance change with time, $2.05 \times 10^{-2} \text{ mol dm}^{-3}$ PAA, on absorbance of $1 \times 10^{-5} \text{ M}$ dye with different concentrations of Fe (III) as a catalyst, with $0.022 \text{ mol dm}^{-3}$ sodium acetate, pH 2.81 , Temp 25°C

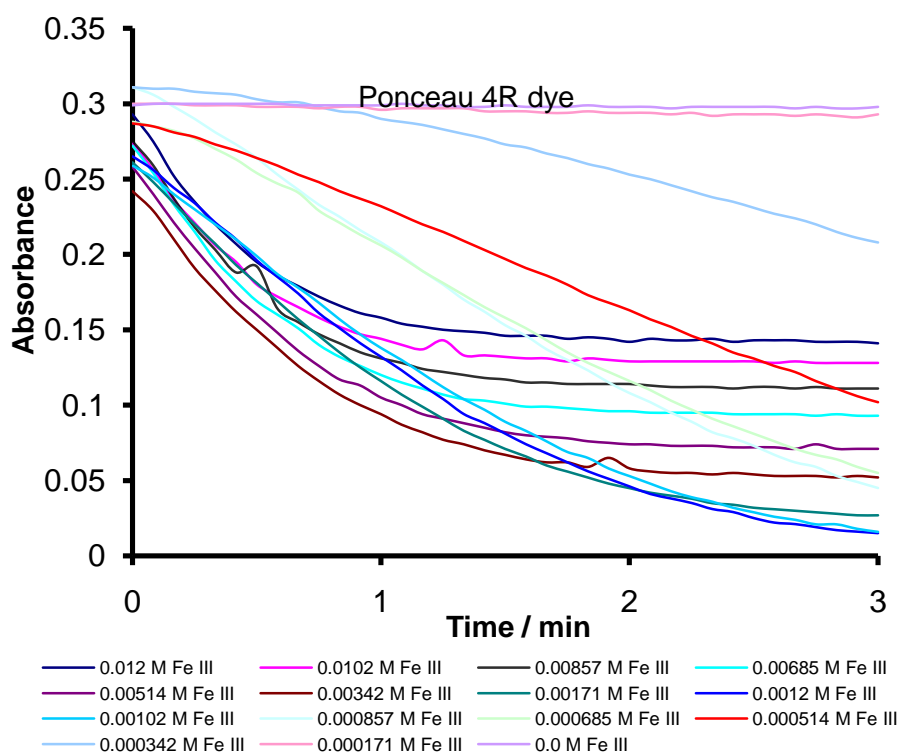


Figure A1.2:- Effect of Fe (III) concentrations on oxidation of Ponceau 4R dye Absorbance change with time, $2.05 \times 10^{-2} \text{ mol dm}^{-3}$ PAA, on absorbance of $1 \times 10^{-5} \text{ M}$ dye with different concentrations of Fe (III) as a catalyst, pH 2.29 , Temp 25°C

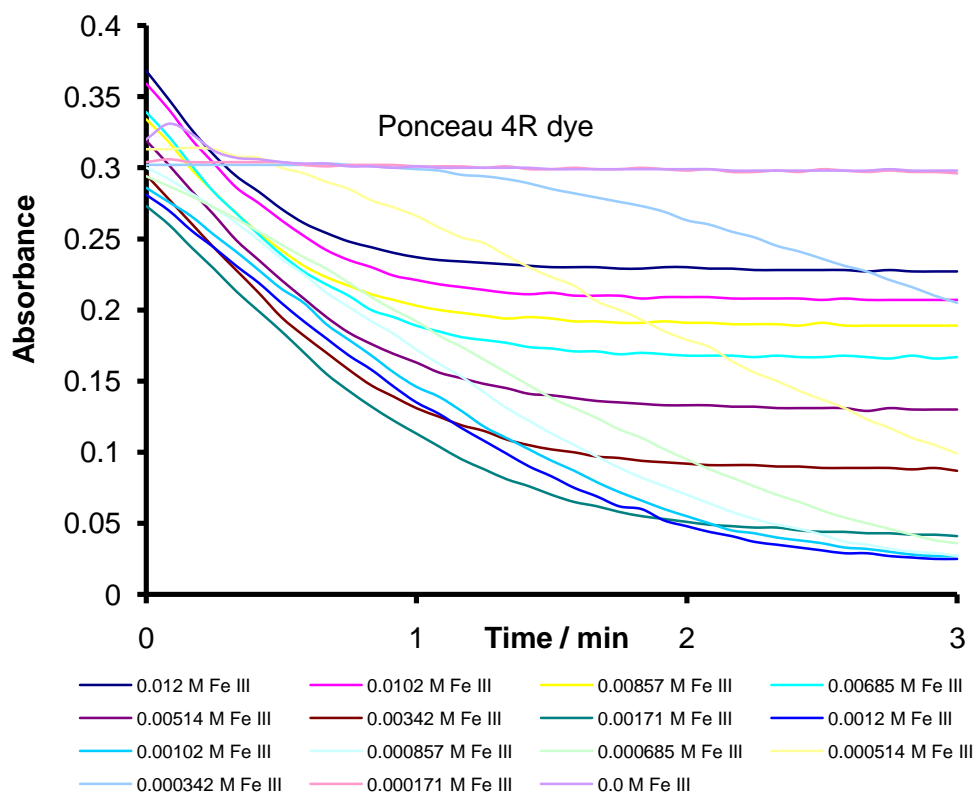


Figure A1.3 :- Effect of Fe (III) concentrations on oxidation of Ponceau 4R dye
 Absorbance change with time, $2.05 \times 10^{-2} \text{ mol dm}^{-3}$ PAA, on absorbance of $1 \times 10^{-5} \text{ M}$ dye
 with different concentrations of Fe (III) as a catalyst, pH 2.81 , Temp 25°C

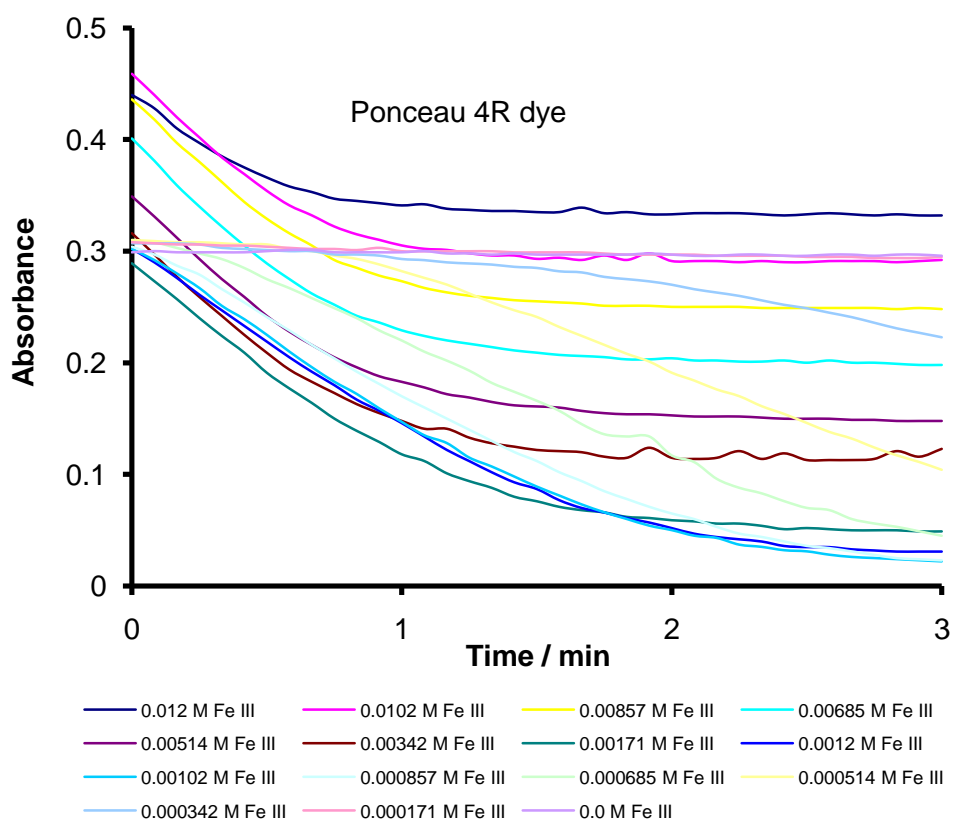


Figure A1.4 :- Effect of Fe (III) concentrations on oxidation of Ponceau 4R dye
 Absorbance change with time, $2.05 \times 10^{-2} \text{ mol dm}^{-3}$ PAA, on absorbance of $1 \times 10^{-5} \text{ M}$ dye
 with different concentrations of Fe (III) as a catalyst, , pH 3.10 , Temp 25°C

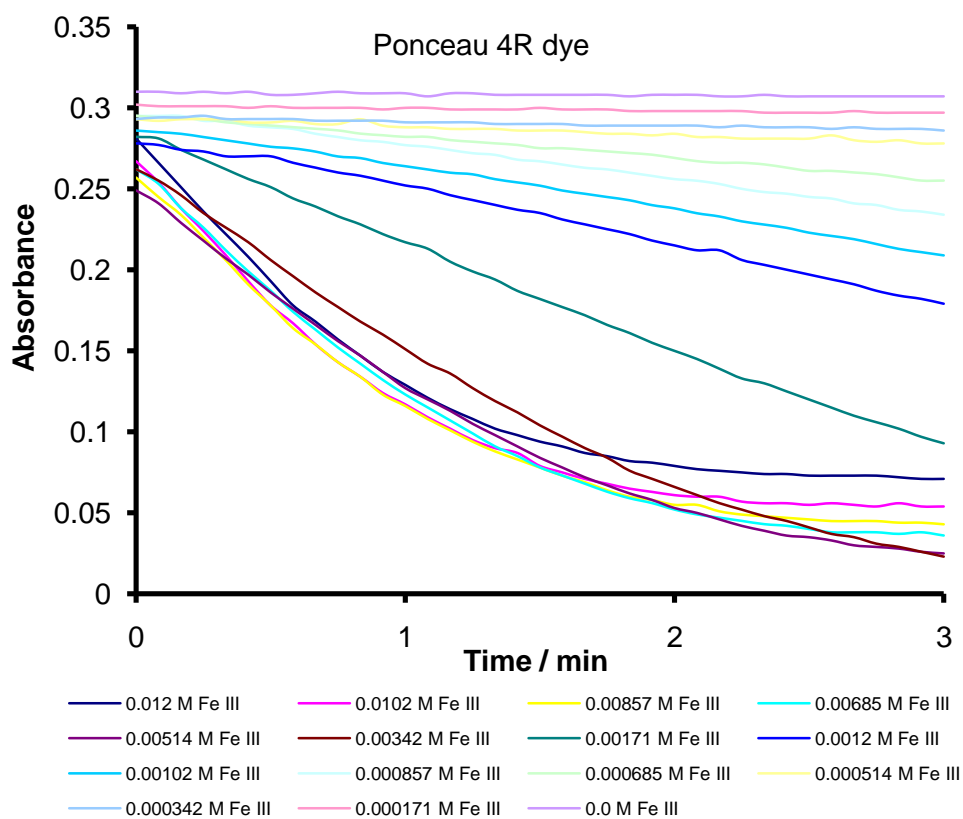


Figure A1.5:- Effect of Fe (III) concentrations on oxidation of Ponceau 4R dye
Absorbance change with time, $4.11 \times 10^{-2} \text{ mol dm}^{-3}$ PAA, on absorbance of $1 \times 10^{-5} \text{ M}$ dye
with different concentrations of Fe (III) as a catalyst, pH 1.48 , Temp 25°C

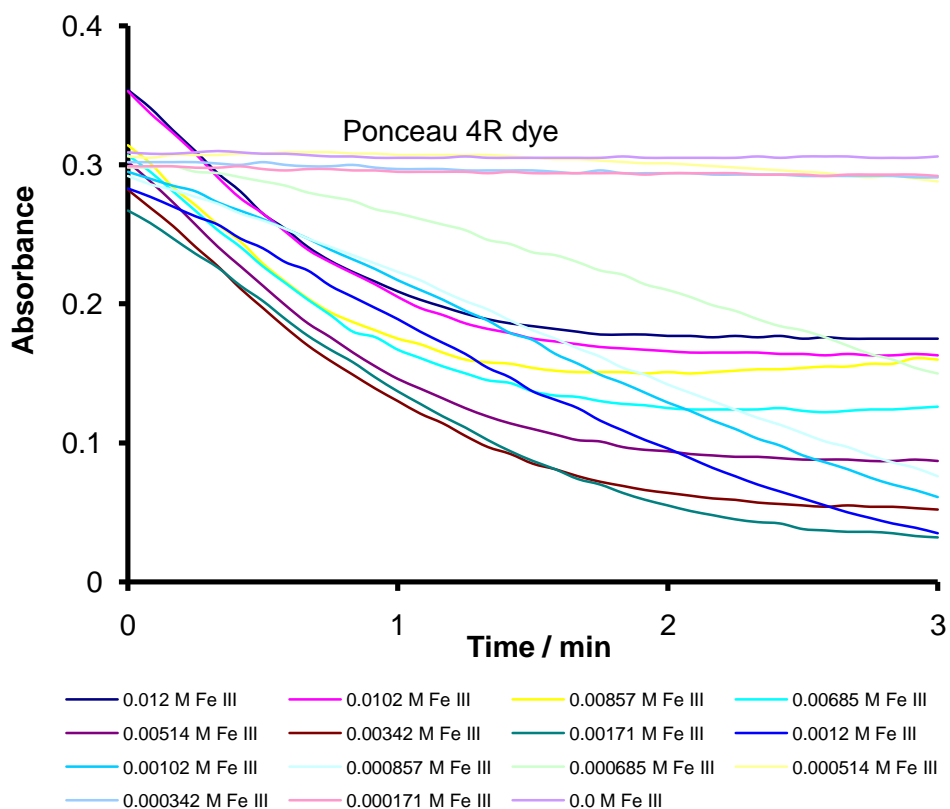


Figure A1.6:- Effect of Fe (III) concentrations on oxidation of Ponceau 4R dye
Absorbance change with time, $4.11 \times 10^{-2} \text{ mol dm}^{-3}$ PAA, on absorbance of $1 \times 10^{-5} \text{ M}$ dye
with different concentrations of Fe (III) as a catalyst, pH 1.88 , Temp 25°C

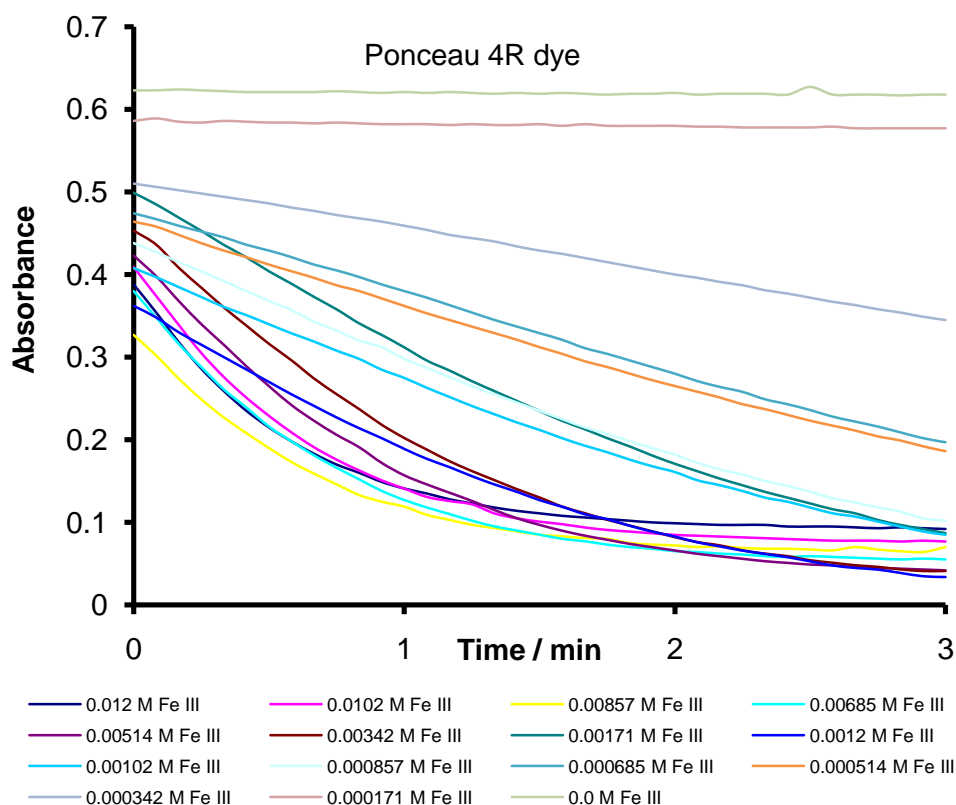


Figure A1.7:- Effect of Fe (III) concentrations on oxidation of Ponceau 4R dye Absorbance change with time, $2.05 \times 10^{-2} \text{ mol dm}^{-3}$ PAA, on absorbance of $2 \times 10^{-5} \text{ M}$ dye with different concentrations of Fe (III) as a catalyst, pH 2.09 , Temp 25°C

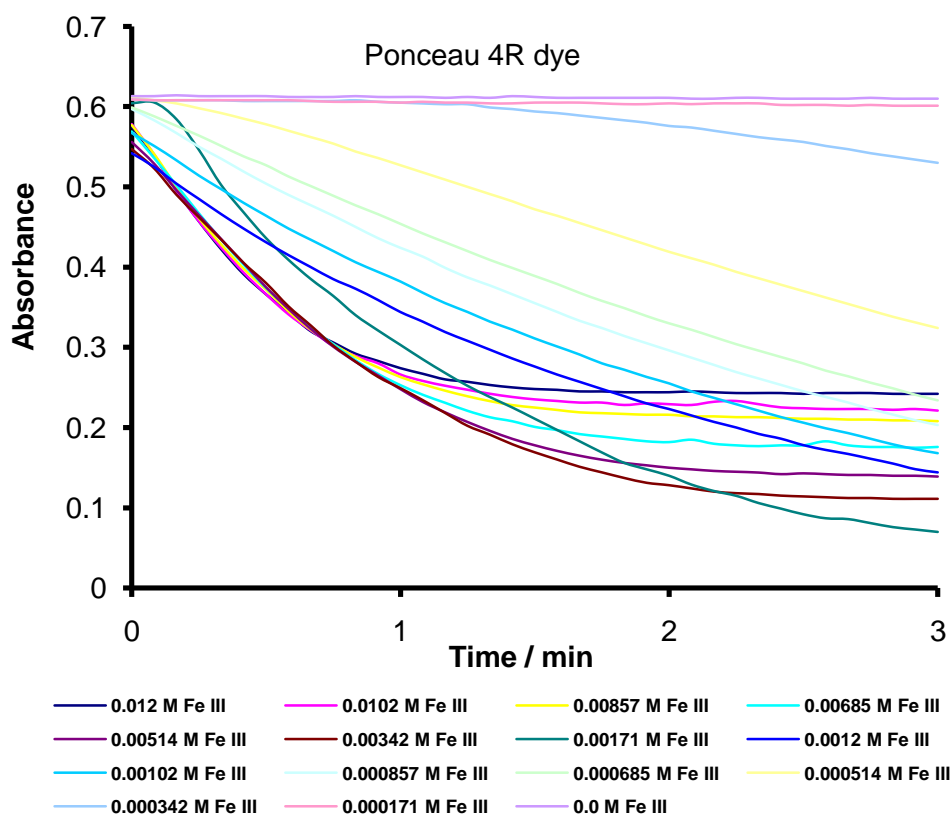


Figure A1.8:- Effect of Fe (III) concentrations on oxidation of Ponceau 4R dye Absorbance change with time, $2.05 \times 10^{-2} \text{ mol dm}^{-3}$ PAA, on absorbance of $2 \times 10^{-5} \text{ M}$ dye with different concentrations of Fe (III) as a catalyst, pH 2.81, Temp 25°C

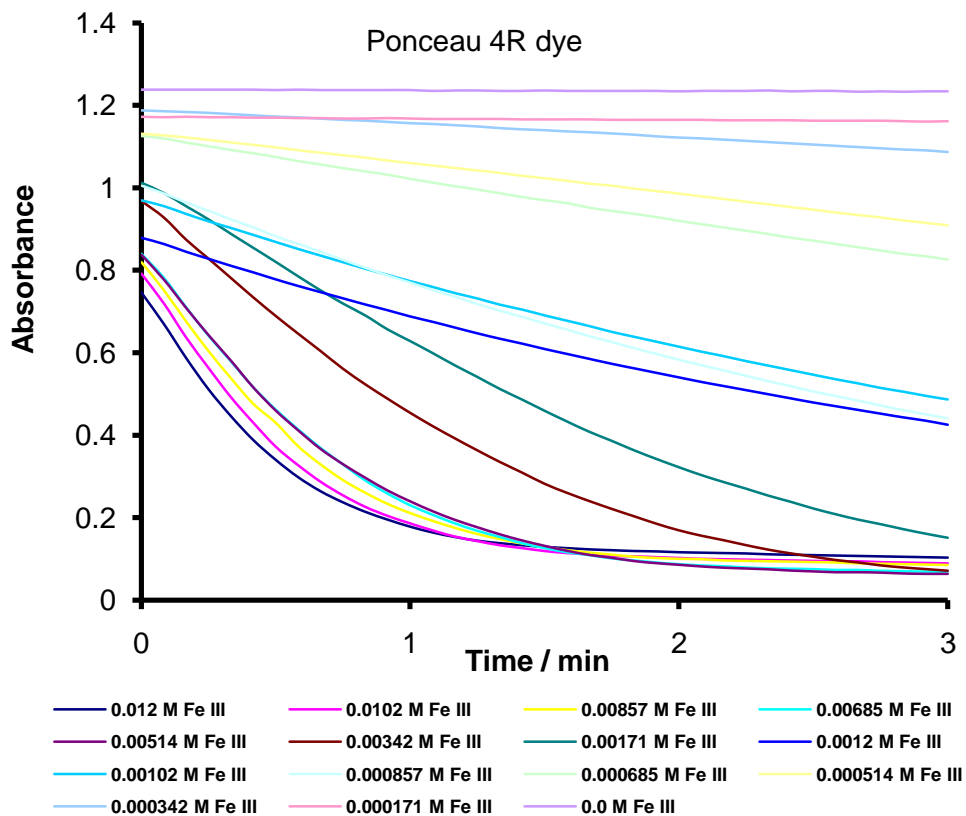


Figure A1.9:- Effect of Fe (III) concentrations on oxidation of Ponceau 4R dye Absorbance change with time, $2.05 \times 10^{-2} \text{ mol dm}^{-3}$ PAA, on absorbance of $4 \times 10^{-5} \text{ M}$ dye with different concentrations of Fe (III) as a catalyst, pH 2.09 , Temp 25°C

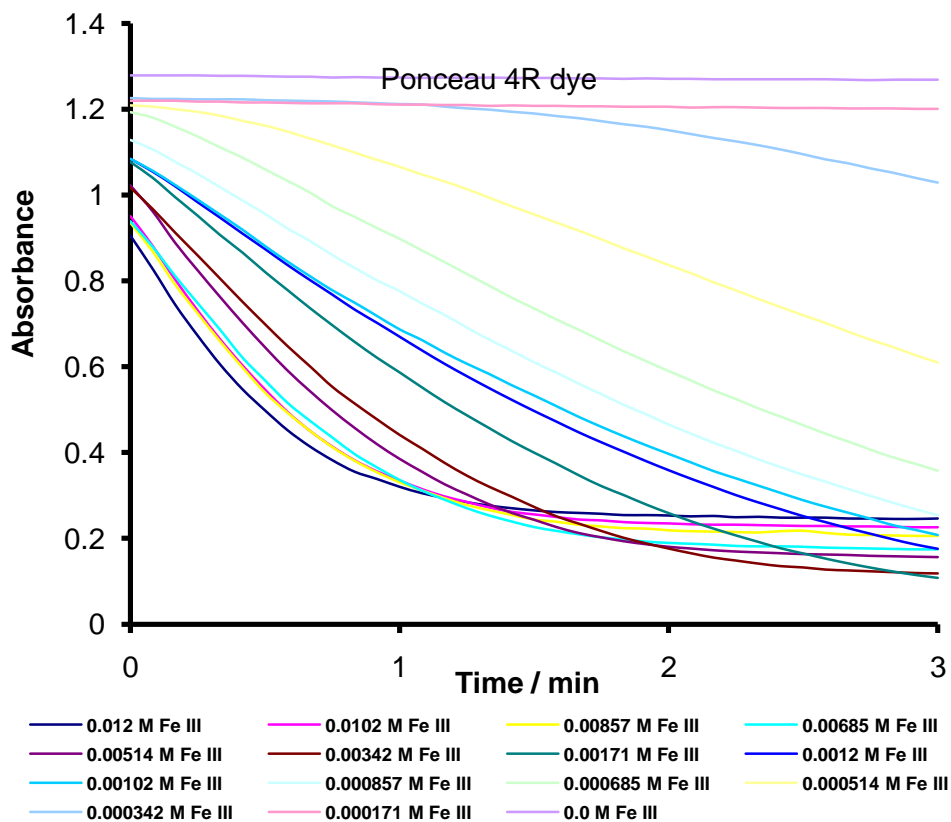


Figure A1.10:- Effect of Fe (III) concentrations on oxidation of Ponceau 4R dye Absorbance change with time, $2.05 \times 10^{-2} \text{ mol dm}^{-3}$ PAA, on absorbance of $4 \times 10^{-5} \text{ M}$ dye with different concentrations of Fe (III) as a catalyst, pH 2.81 , Temp 25°C

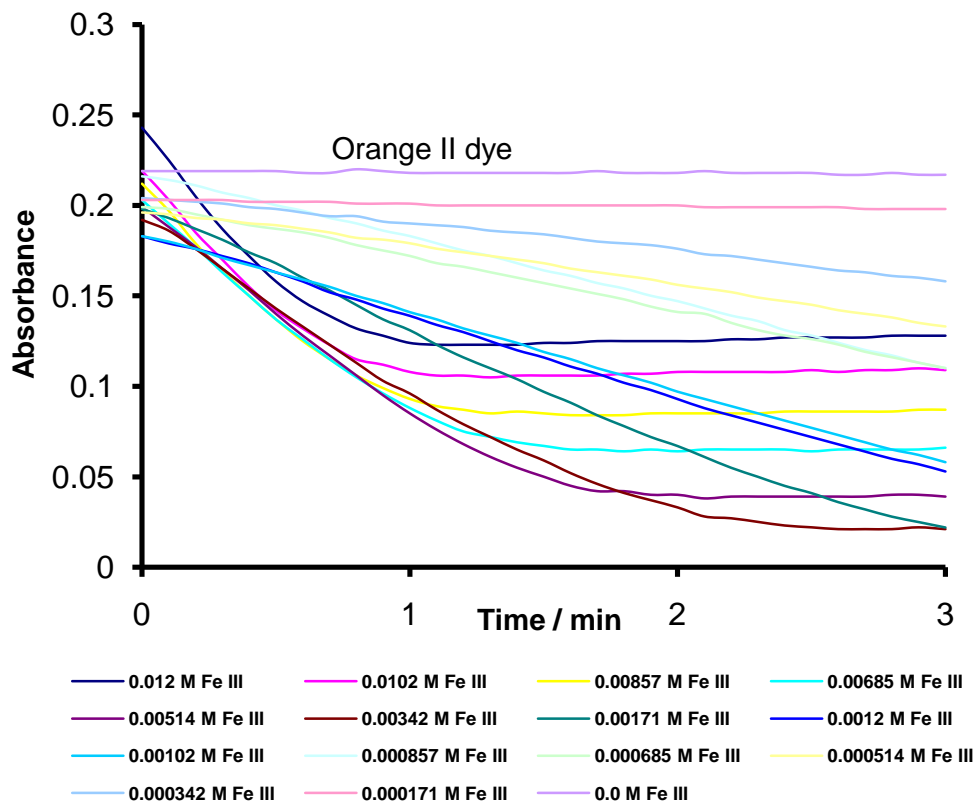


Figure A1.11:- Effect of Fe (III) concentrations on oxidation of Orange II dye
Absorbance change with time, $2.05 \times 10^{-2} \text{ mol dm}^{-3}$ PAA, on absorbance of $1 \times 10^{-5} \text{ M}$ dye
with different concentrations of Fe (III) as a catalyst, pH 2.09 , Temp 25°C

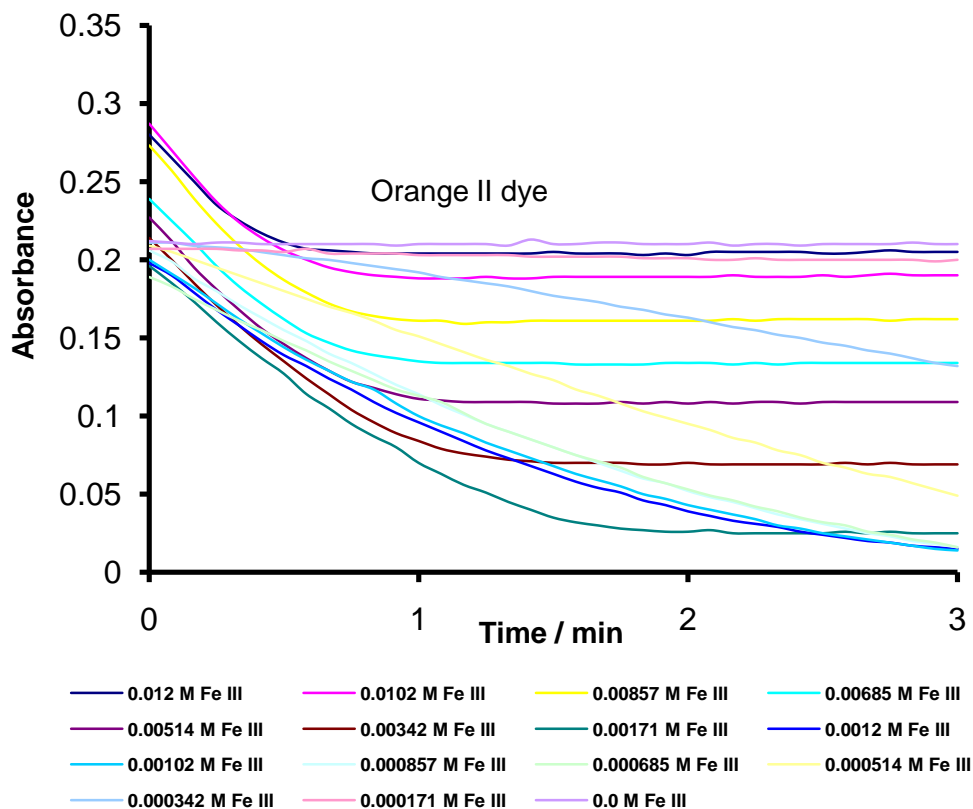


Figure A1.12:- Effect of Fe (III) concentrations on oxidation of Orange II dye
Absorbance change with time, $2.05 \times 10^{-2} \text{ mol dm}^{-3}$ PAA, on absorbance of $1 \times 10^{-5} \text{ M}$ dye
with different concentrations of Fe (III) as a catalyst, pH 2.29 , Temp 25°C

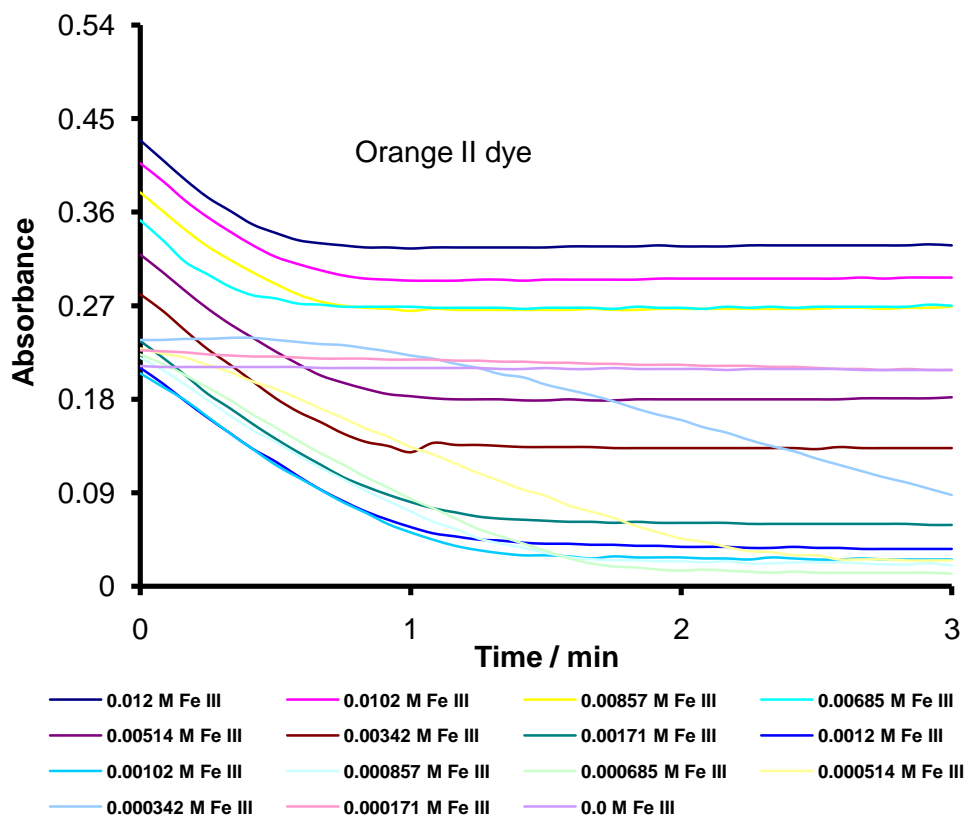


Figure A1.13:- Effect of Fe (III) concentrations on oxidation of Orange II dye
 Absorbance change with time, $2.05 \times 10^{-2} \text{ mol dm}^{-3}$ PAA, on absorbance of $1 \times 10^{-5} \text{ M}$ dye
 with different concentrations of Fe (III) as a catalyst, pH 2.81 , Temp 25°C

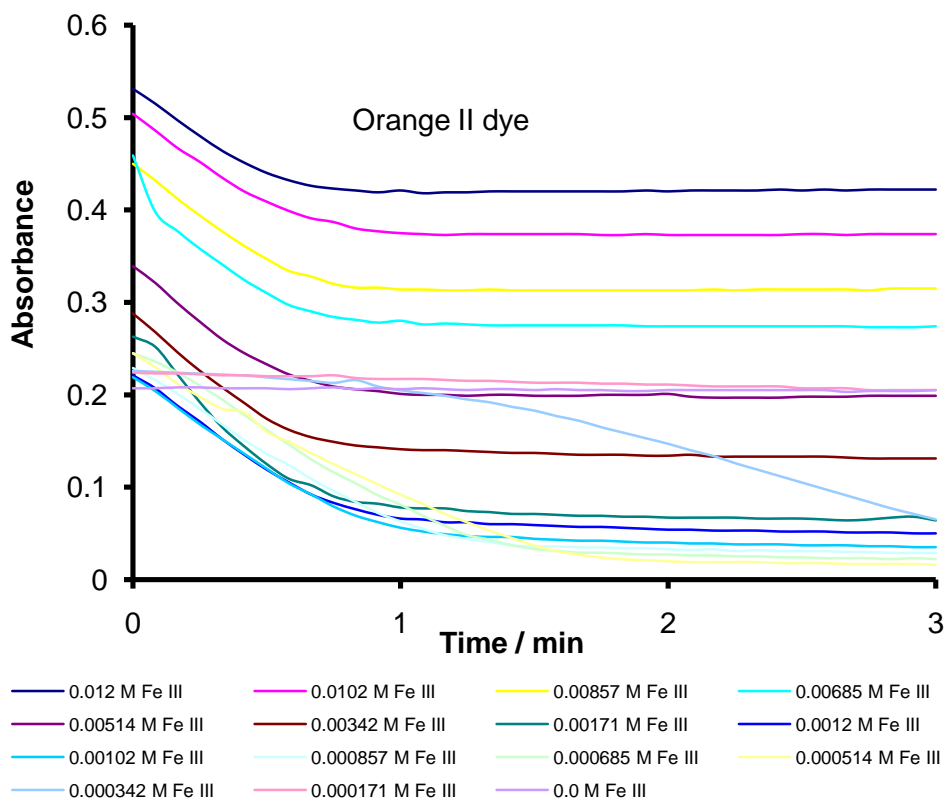


Figure A1.14:- Effect of Fe (III) concentrations on oxidation of Orange II dye
 Absorbance change with time, $2.05 \times 10^{-2} \text{ mol dm}^{-3}$ PAA, on absorbance of $1 \times 10^{-5} \text{ M}$ dye
 with different concentrations of Fe (III) as a catalyst, pH 3.10 , Temp 25°C

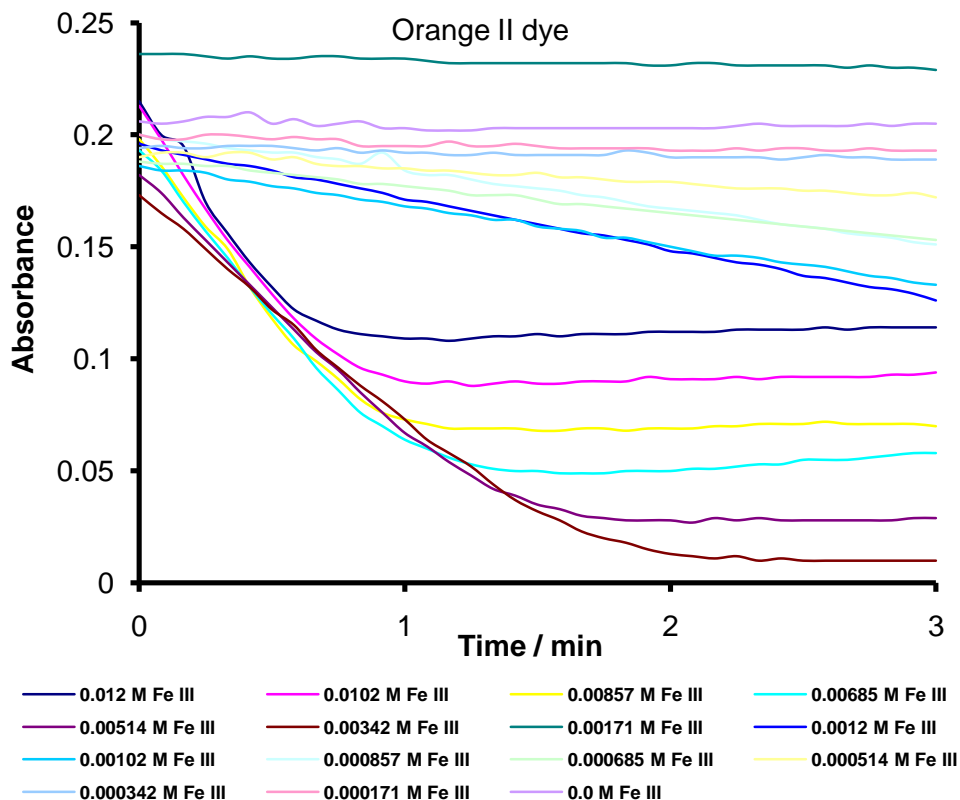


Figure A1.15:- Effect of Fe (III) concentrations on oxidation of Orange II dye Absorbance change with time, $4.11 \times 10^{-2} \text{ mol dm}^{-3}$ PAA, on absorbance of $1 \times 10^{-5} \text{ M}$ dye with different concentrations of Fe (III) as a catalyst, pH 1.48 , Temp 25°C

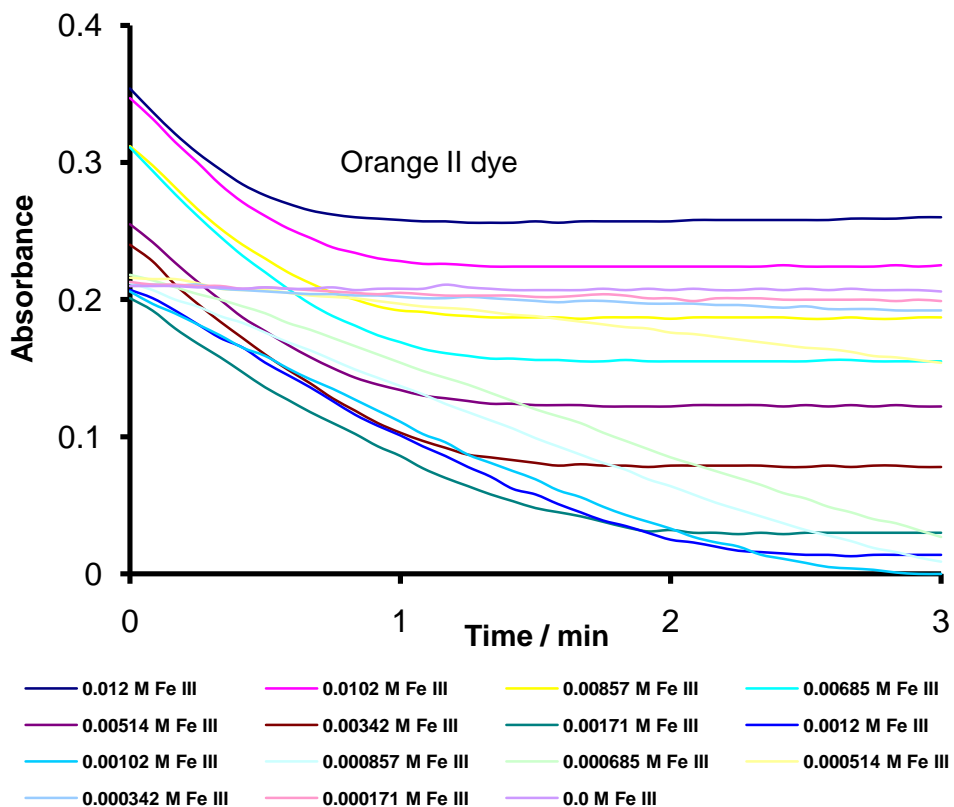


Figure A1.16:- Effect of Fe (III) concentrations on oxidation of Orange II dye Absorbance change with time, $4.11 \times 10^{-2} \text{ mol dm}^{-3}$ PAA, on absorbance of $1 \times 10^{-5} \text{ M}$ dye with different concentrations of Fe (III) as a catalyst, pH 1.88 , Temp 25°C

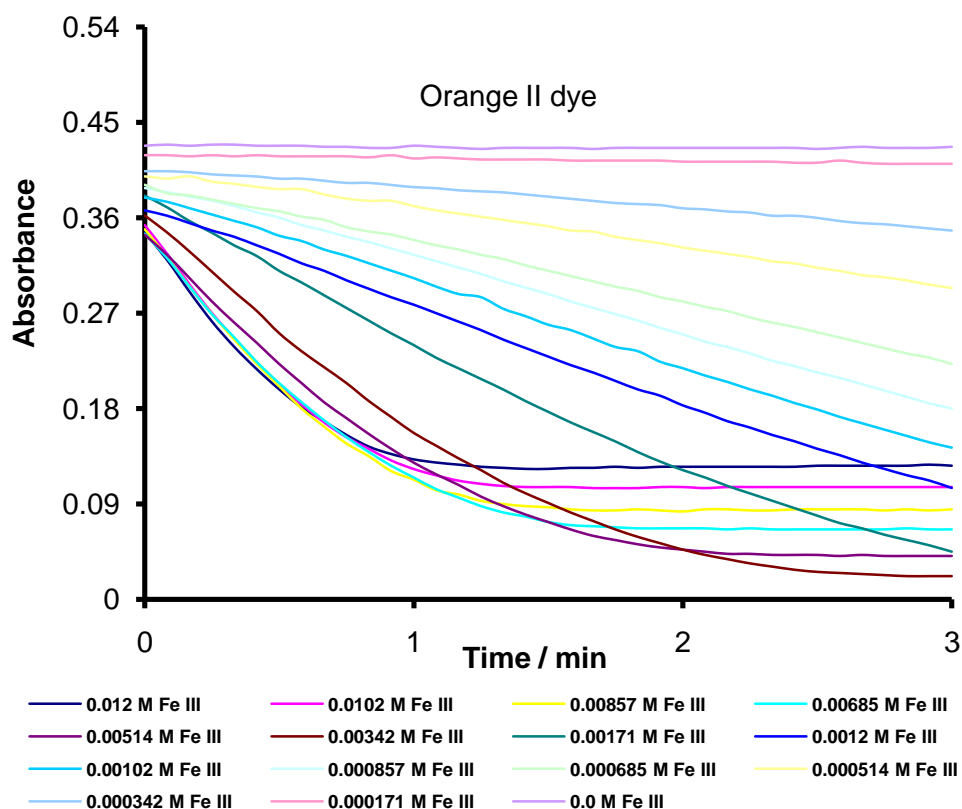


Figure A1.17:- Effect of Fe (III) concentrations on oxidation of Orange II dye
Absorbance change with time, $2.05 \times 10^{-2} \text{ mol dm}^{-3}$ PAA, on absorbance of $2 \times 10^{-5} \text{ M}$ dye
with different concentrations of Fe (III) as a catalyst, pH 2.09 , Temp 25°C

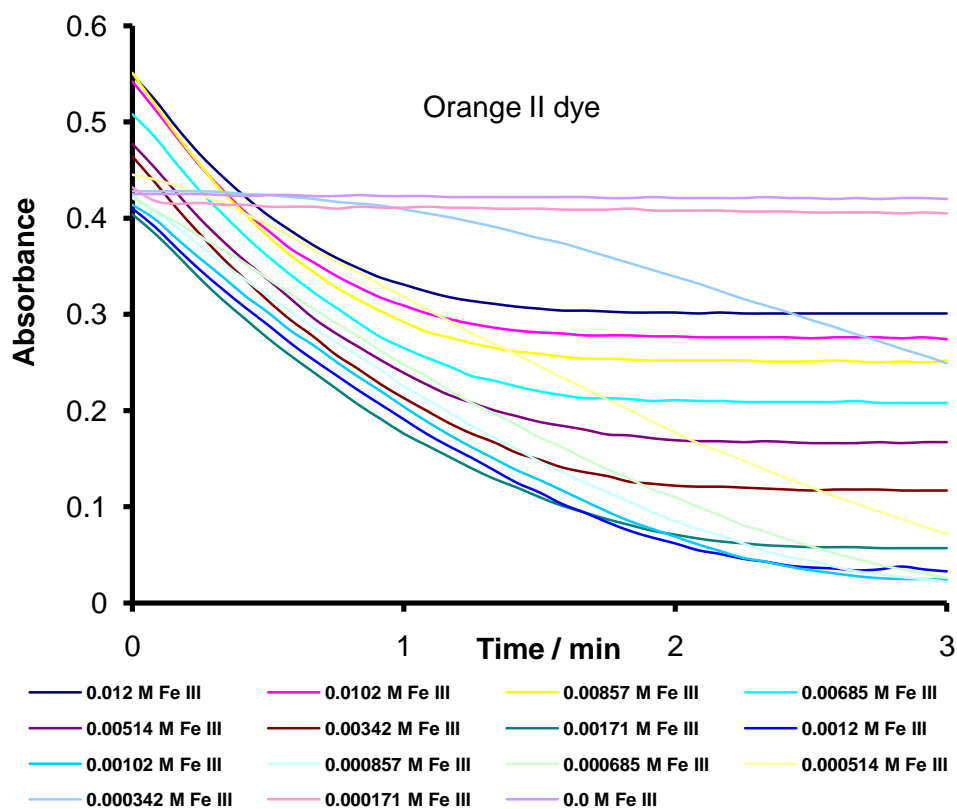


Figure A1.18 :- Effect of Fe (III) concentrations on oxidation of Orange II dye
Absorbance change with time, $2.05 \times 10^{-2} \text{ mol dm}^{-3}$ PAA, on absorbance of $2 \times 10^{-5} \text{ M}$ dye
with different concentrations of Fe (III) as a catalyst, pH 2.81 , Temp 25°C

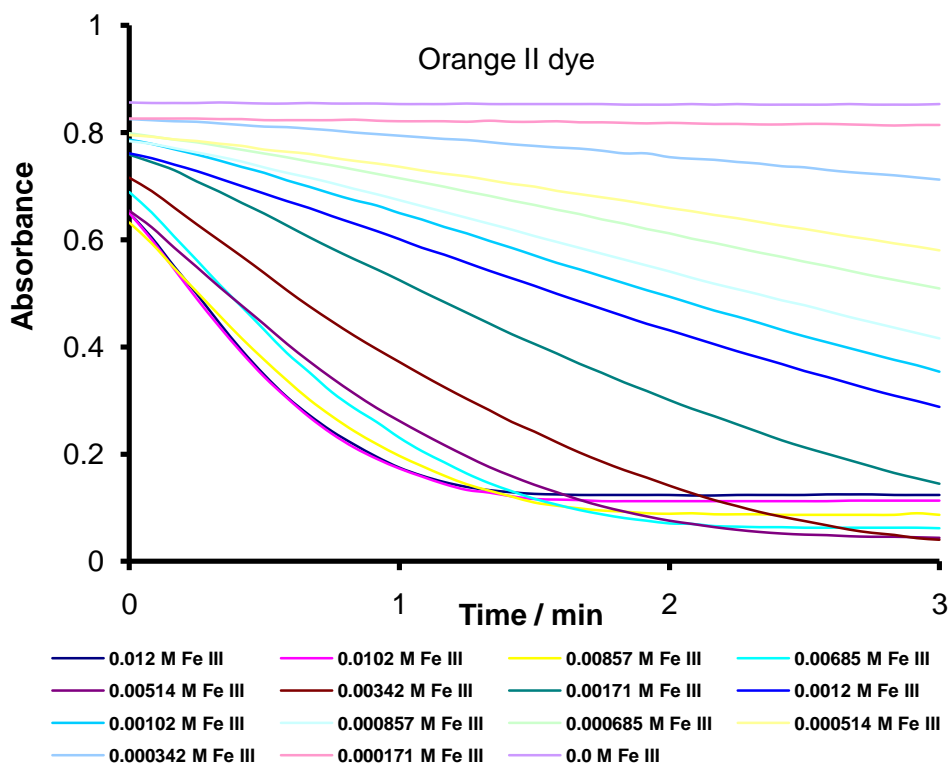


Figure A1.19:- Effect of Fe (III) concentrations on oxidation of Orange II dye
 Absorbance change with time, $2.05 \times 10^{-2} \text{ mol dm}^{-3}$ PAA, on absorbance of $4 \times 10^{-5} \text{ M}$ dye
 with different concentrations of Fe (III) as a catalyst, pH 2.09 , Temp 25°C

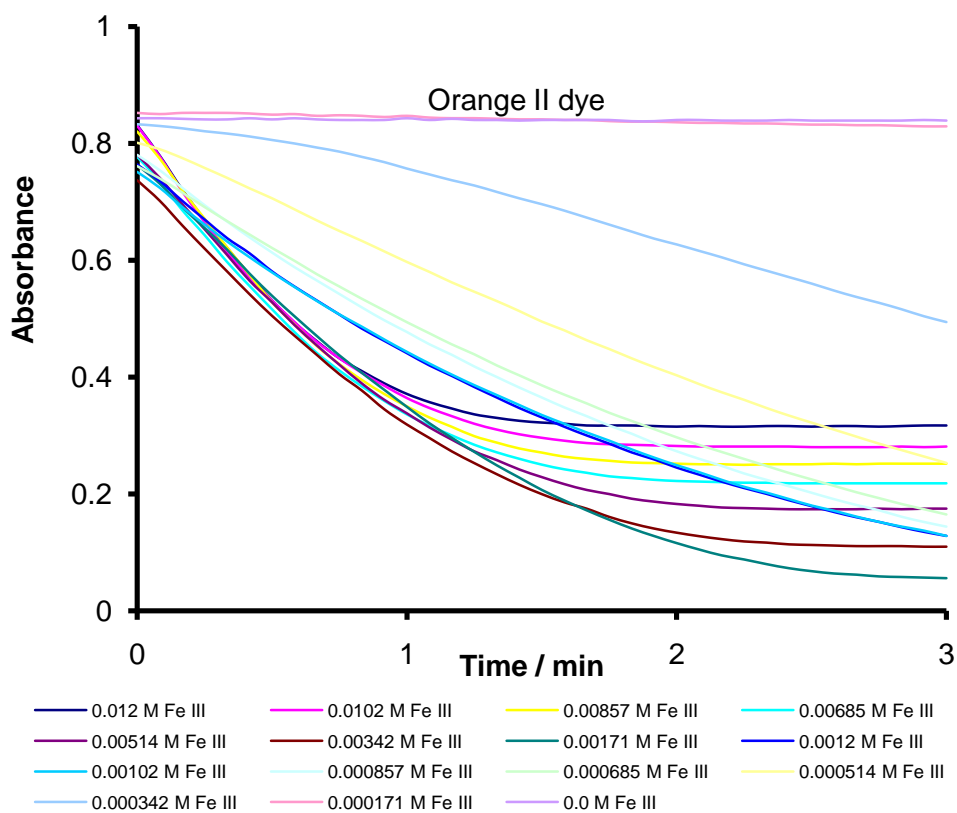


Figure A1.20:- Effect of Fe (III) concentrations on oxidation of Orange II dye
 Absorbance change with time, $2.05 \times 10^{-2} \text{ mol dm}^{-3}$ PAA, on absorbance of $4 \times 10^{-5} \text{ M}$ dye
 with different concentrations of Fe (III) as a catalyst, pH 2.81 , Temp 25°C

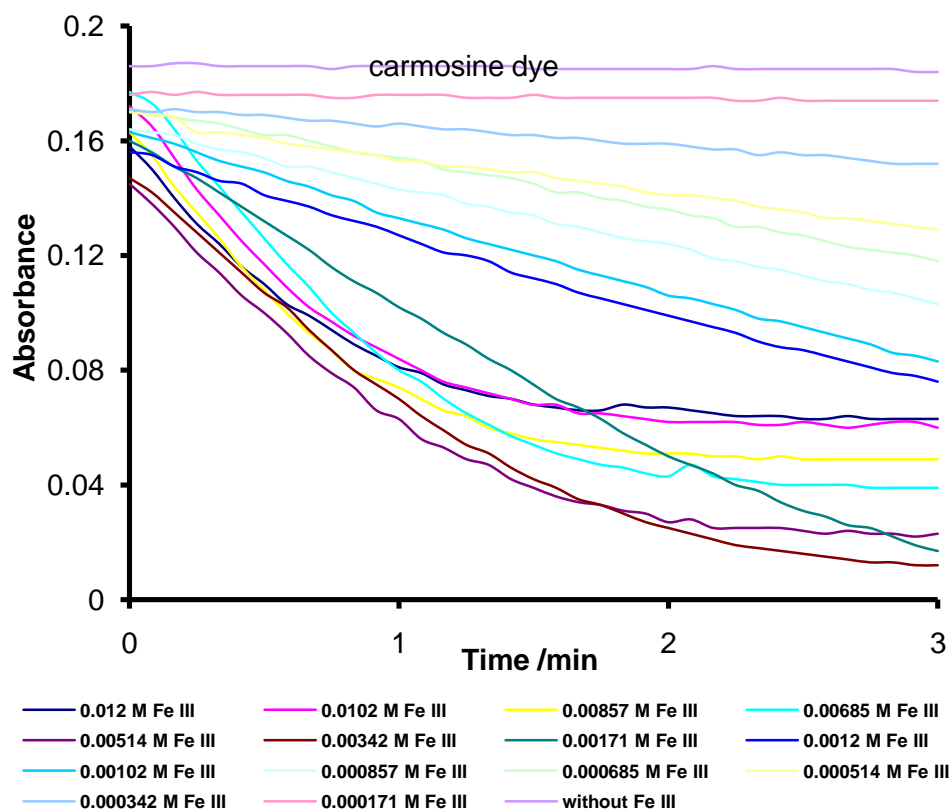


Figure A1.21:- Effect of Fe (III) concentrations on oxidation of Carmosine dye
Absorbance change with time, $2.05 \times 10^{-2} \text{ mol dm}^{-3}$ PAA, on absorbance of $1 \times 10^{-5} \text{ M}$ dye with different concentrations of Fe (III) as a catalyst, pH 2.09, Temp 25°C

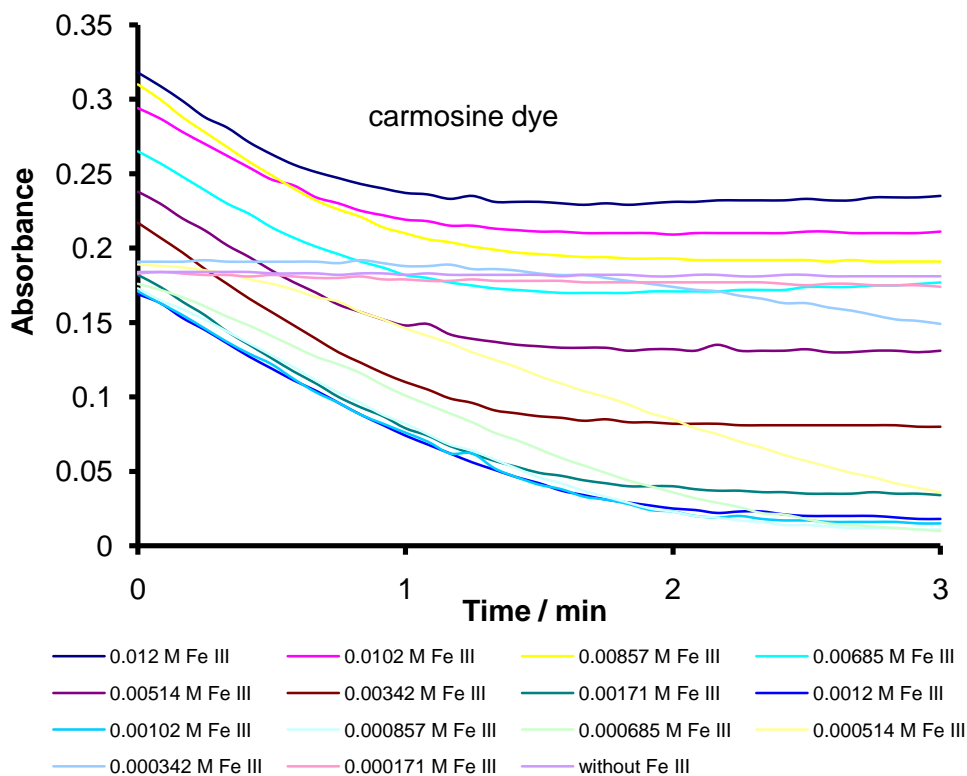


Figure A1.22:- Effect of Fe (III) concentrations on oxidation of Carmosine dye
Absorbance change with time, $2.05 \times 10^{-2} \text{ mol dm}^{-3}$ PAA, on absorbance of $1 \times 10^{-5} \text{ M}$ dye with different concentrations of Fe (III) as a catalyst, pH 2.81, Temp 25°C

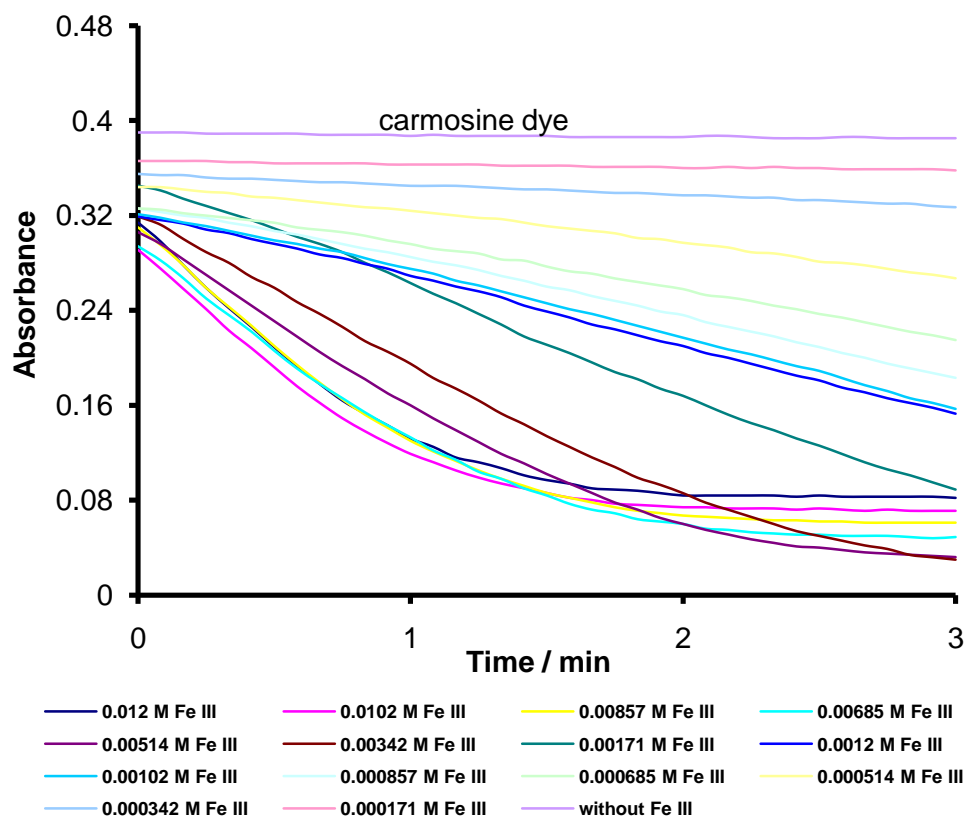


Figure A1.23:- Effect of Fe (III) concentrations on oxidation of Carmosine dye
Absorbance change with time, $2.05 \times 10^{-2} \text{ mol dm}^{-3}$ PAA, on absorbance of $2 \times 10^{-5} \text{ M}$ dye
with different concentrations of Fe (III) as a catalyst, pH 2.09, Temp 25°C

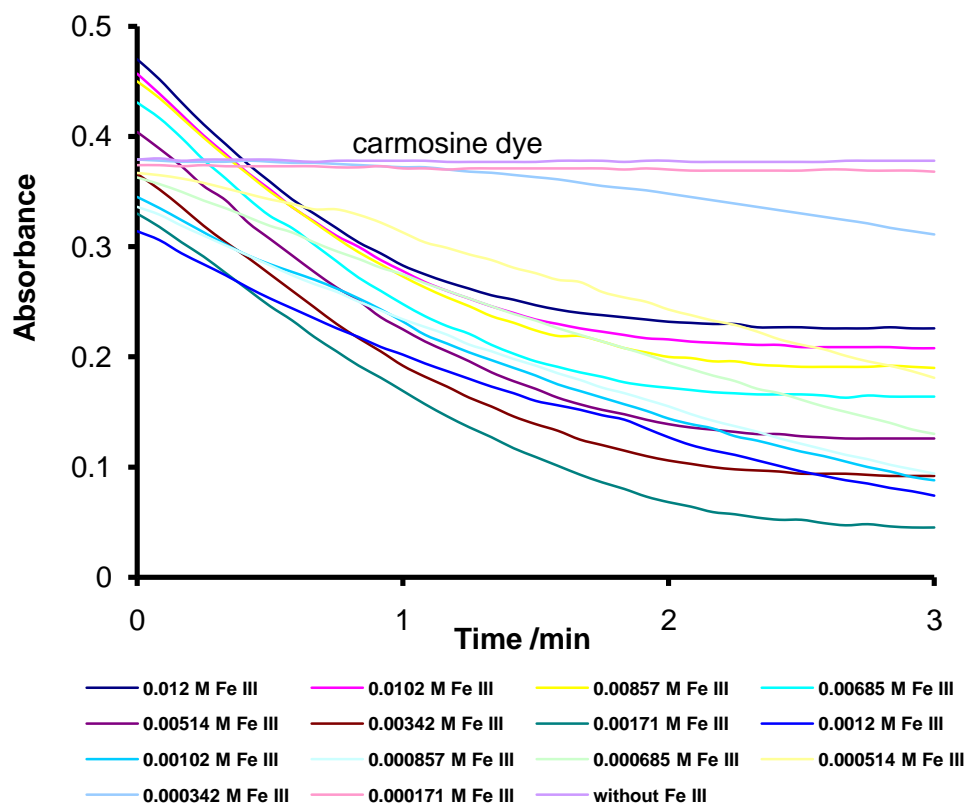


Figure A1.24:- Effect of Fe (III) concentrations on oxidation of Carmosine dye
Absorbance change with time, $2.05 \times 10^{-2} \text{ mol dm}^{-3}$ PAA, on absorbance of $1 \times 10^{-5} \text{ M}$ dye
with different concentrations of Fe (III) as a catalyst, pH 2.81, Temp 25°C

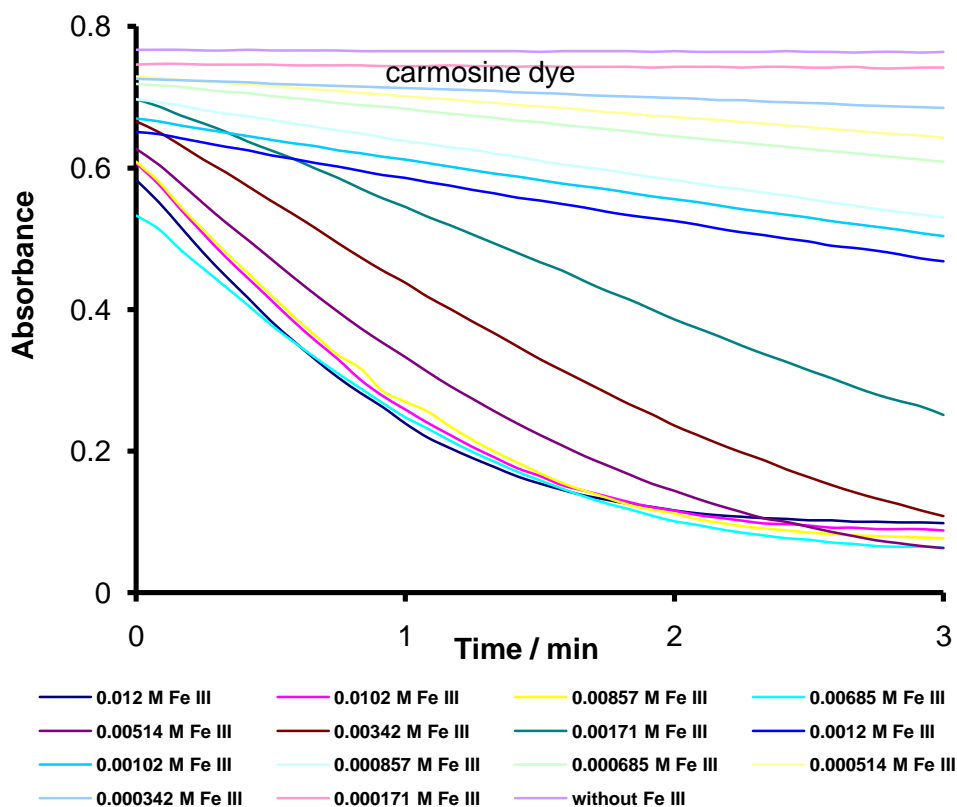


Figure A1.25:- Effect of Fe (III) concentrations on oxidation of Carmosine dye
Absorbance change with time, $2.05 \times 10^{-2} \text{ mol dm}^{-3}$ PAA, on absorbance of $4 \times 10^{-5} \text{ M}$ dye
with different concentrations of Fe (III) as a catalyst, pH 2.09, Temp 25°C

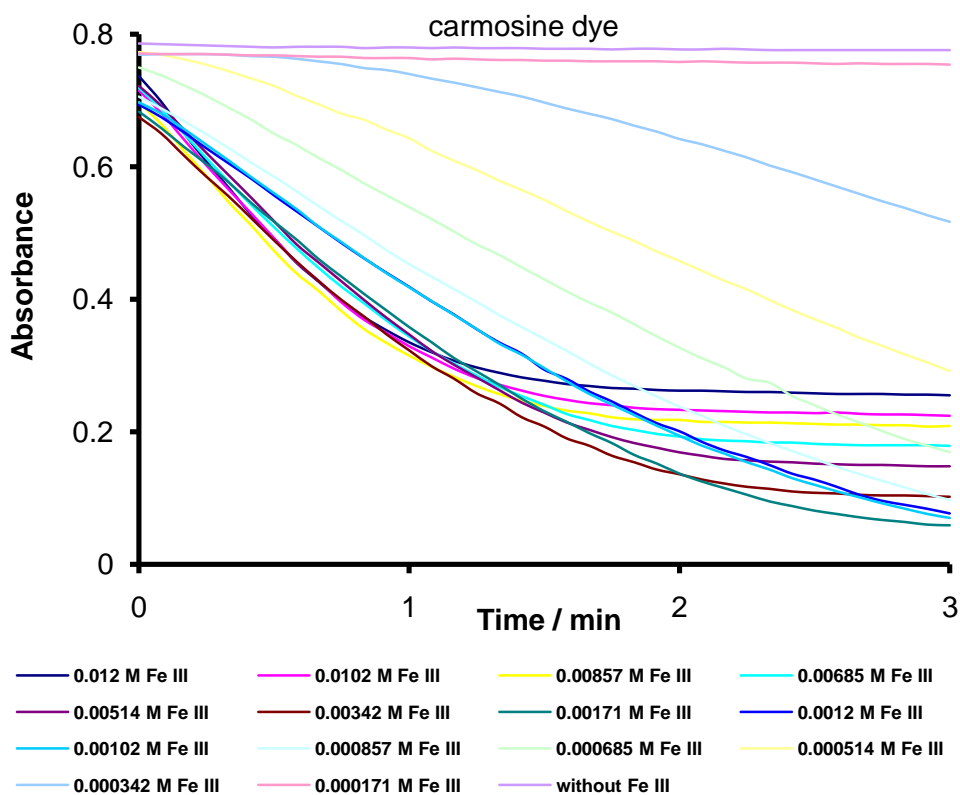


Figure A1.26:- Effect of Fe (III) concentrations on oxidation of Carmosine dye
Absorbance change with time, $2.05 \times 10^{-2} \text{ mol dm}^{-3}$ PAA, on absorbance of $4 \times 10^{-5} \text{ M}$ dye
with different concentrations of Fe (III) as a catalyst, pH 2.81, Temp 25°C

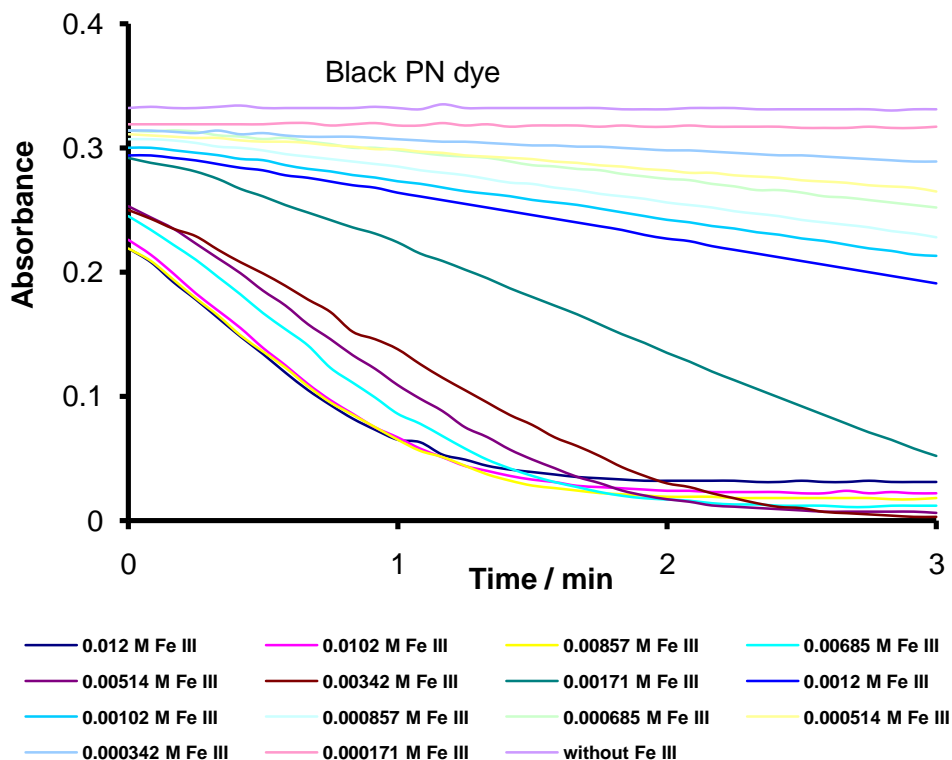


Figure A1.27:- Effect of Fe (III) concentrations on oxidation of Black PN dye
Absorbance change with time, $2.05 \times 10^{-2} \text{ mol dm}^{-3}$ PAA, on absorbance of $1 \times 10^{-5} \text{ M}$ dye
with different concentrations of Fe (III) as a catalyst, pH 2.09, Temp 25°C

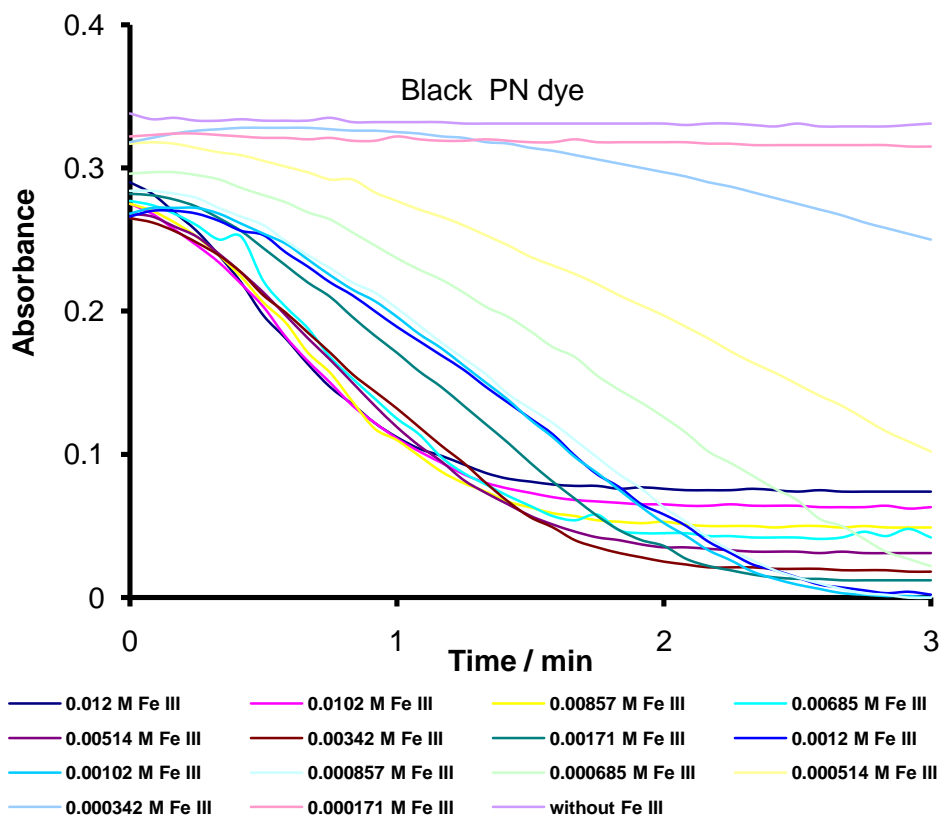


Figure A1.28:- Effect of Fe (III) concentrations on oxidation of Black PN dye
Absorbance change with time, $2.05 \times 10^{-2} \text{ mol dm}^{-3}$ PAA, on absorbance of $1 \times 10^{-5} \text{ M}$ dye
with different concentrations of Fe (III) as a catalyst, pH 2.81, Temp 25°C

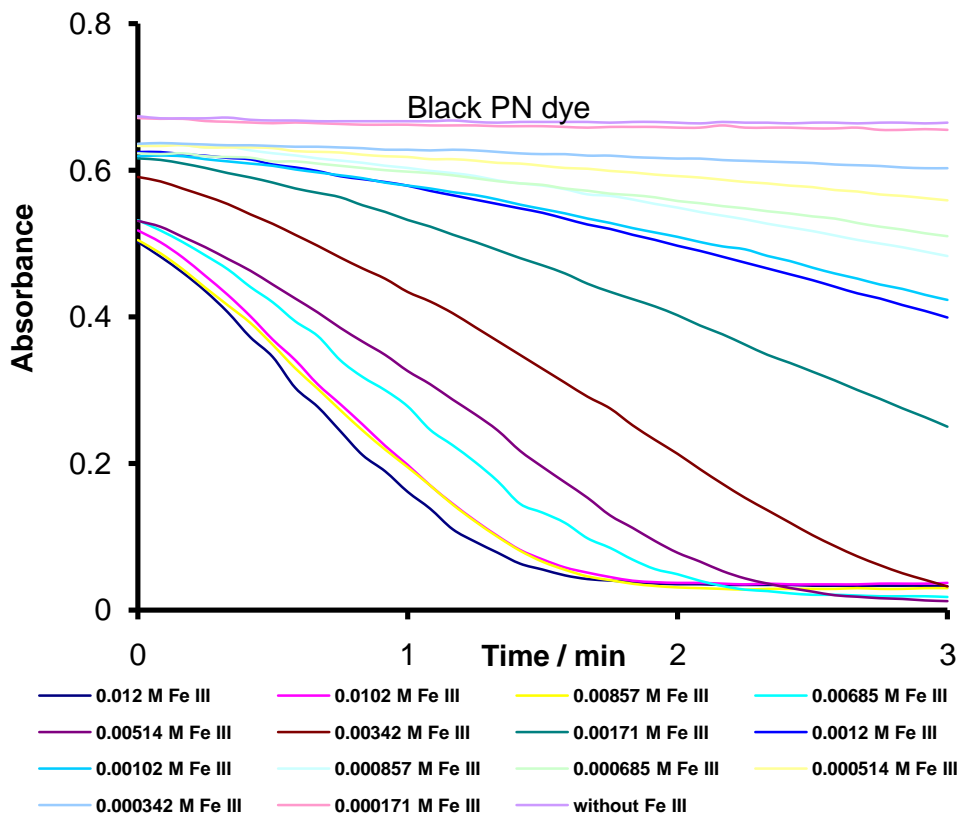


Figure A1.29:- Effect of Fe (III) concentrations on oxidation of Black PN dye
 Absorbance change with time, $2.05 \times 10^{-2} \text{ mol dm}^{-3}$ PAA, on absorbance of $2 \times 10^{-5} \text{ M}$ dye
 with different concentrations of Fe (III) as a catalyst, pH 2.09, Temp 25°C

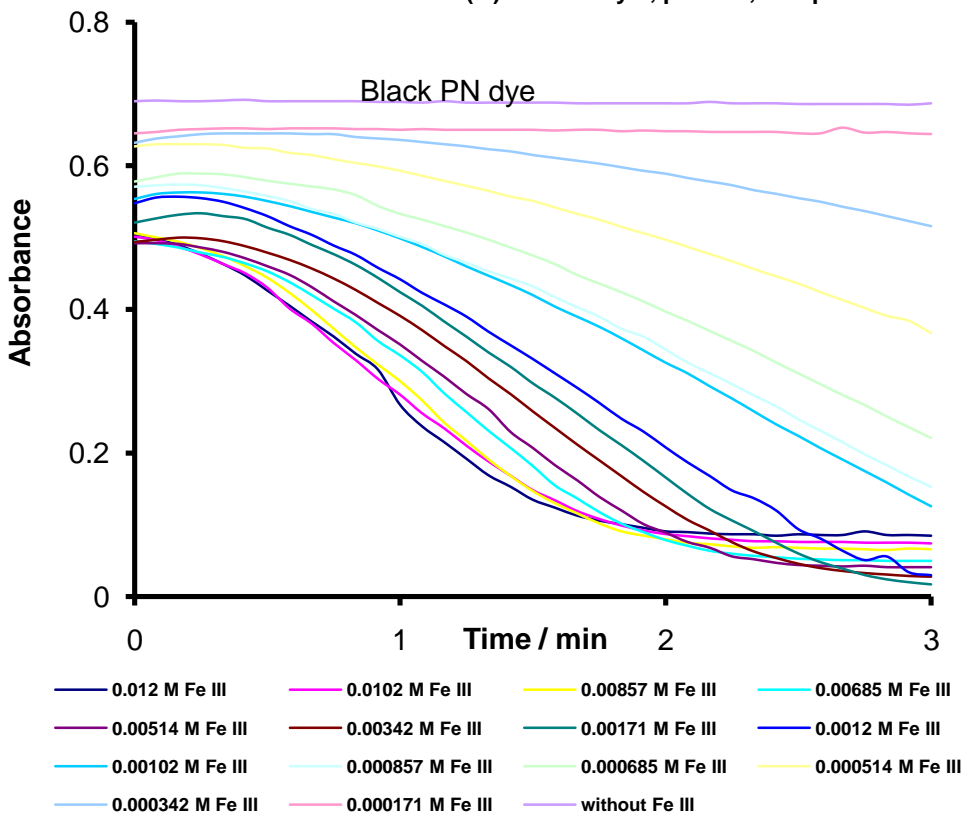


Figure A1.30:- Effect of Fe (III) concentrations on oxidation of Black PN dye
 Absorbance change with time, $2.05 \times 10^{-2} \text{ mol dm}^{-3}$ PAA, on absorbance of $2 \times 10^{-5} \text{ M}$ dye
 with different concentrations of Fe (III) as a catalyst, pH 2.81, Temp 25°C

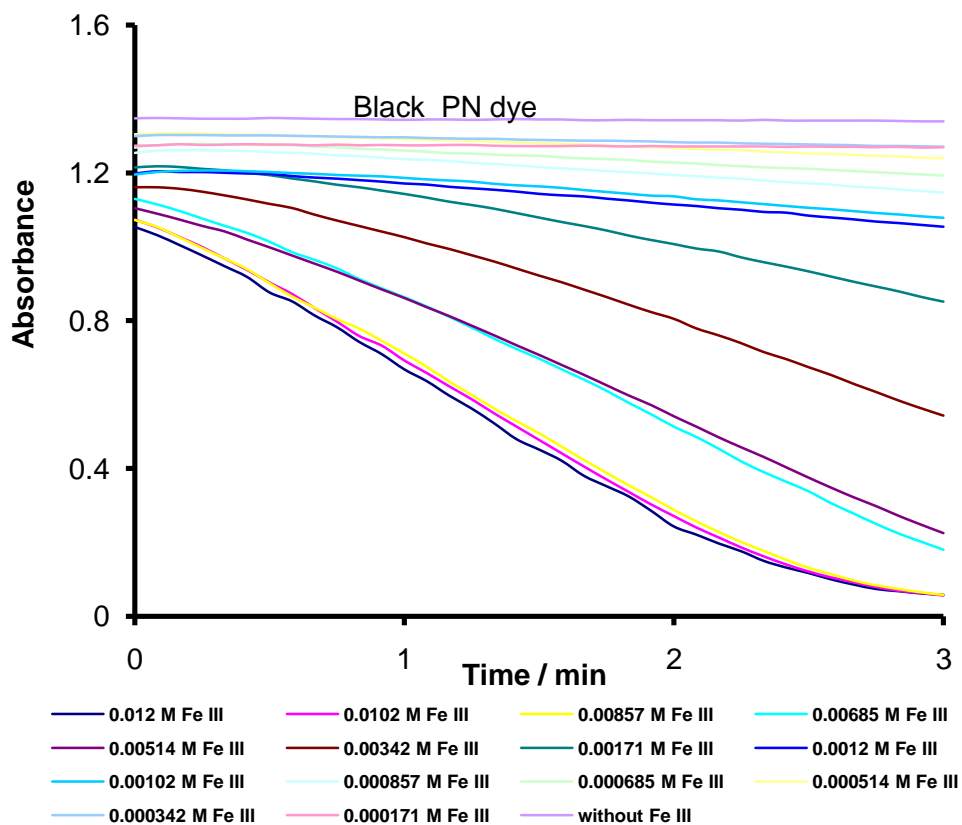


Figure A1.31:- Effect of Fe (III) concentrations on oxidation of Black PN dye
Absorbance change with time, $2.05 \times 10^{-2} \text{ mol dm}^{-3}$ PAA, on absorbance of $4 \times 10^{-5} \text{ M}$ dye
with different concentrations of Fe (III) as a catalyst, pH 2.09, Temp 25°C

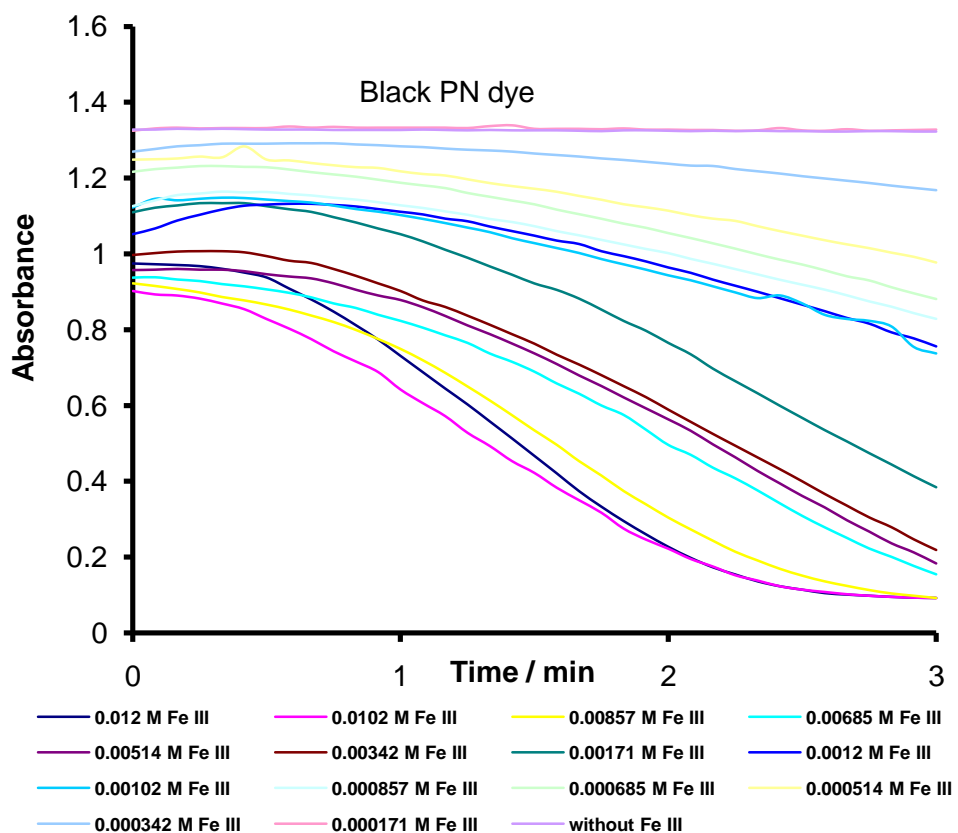


Figure A1.32:- Effect of Fe (III) concentrations on oxidation of Black PN dye
Absorbance change with time, $2.05 \times 10^{-2} \text{ mol dm}^{-3}$ PAA, on absorbance of $4 \times 10^{-5} \text{ M}$ dye
with different concentrations of Fe (III) as a catalyst, pH 2.81, Temp 25°C

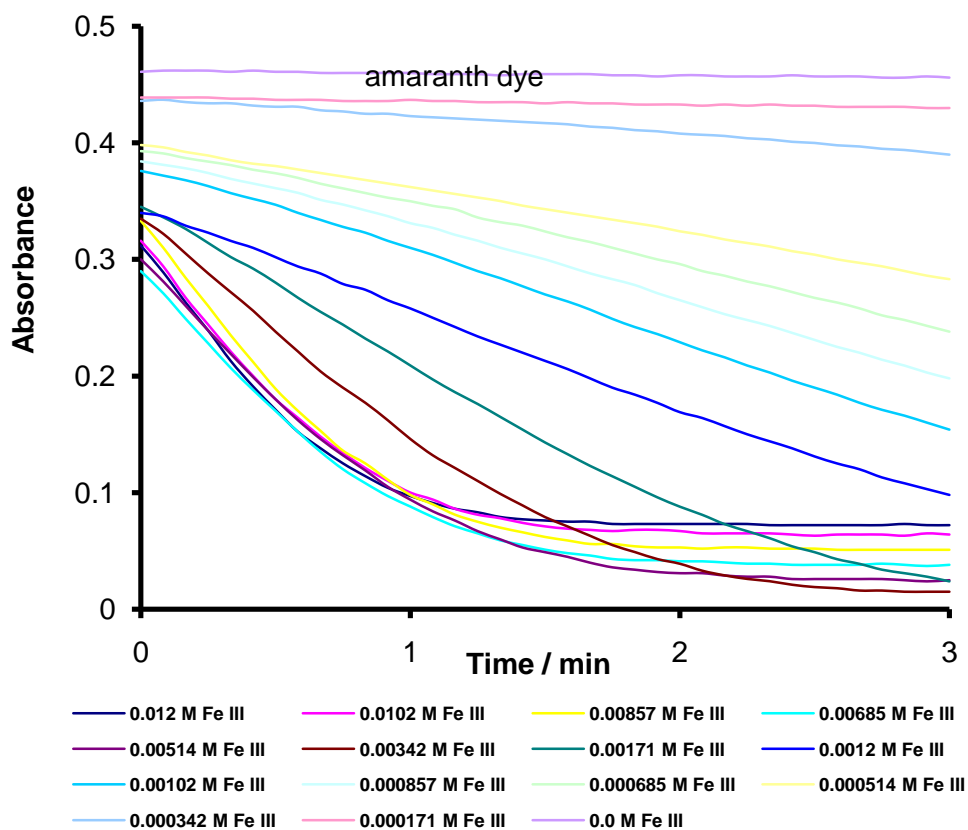


Figure A1.33:- Effect of Fe (III) concentrations on oxidation of Amaranth dye absorbance change with time, $2.05 \times 10^{-2} \text{ mol dm}^{-3}$ PAA, on absorbance of $2 \times 10^{-5} \text{ M}$ dye with different concentrations of Fe (III) as a catalyst, pH 2.09, Temp 25°C

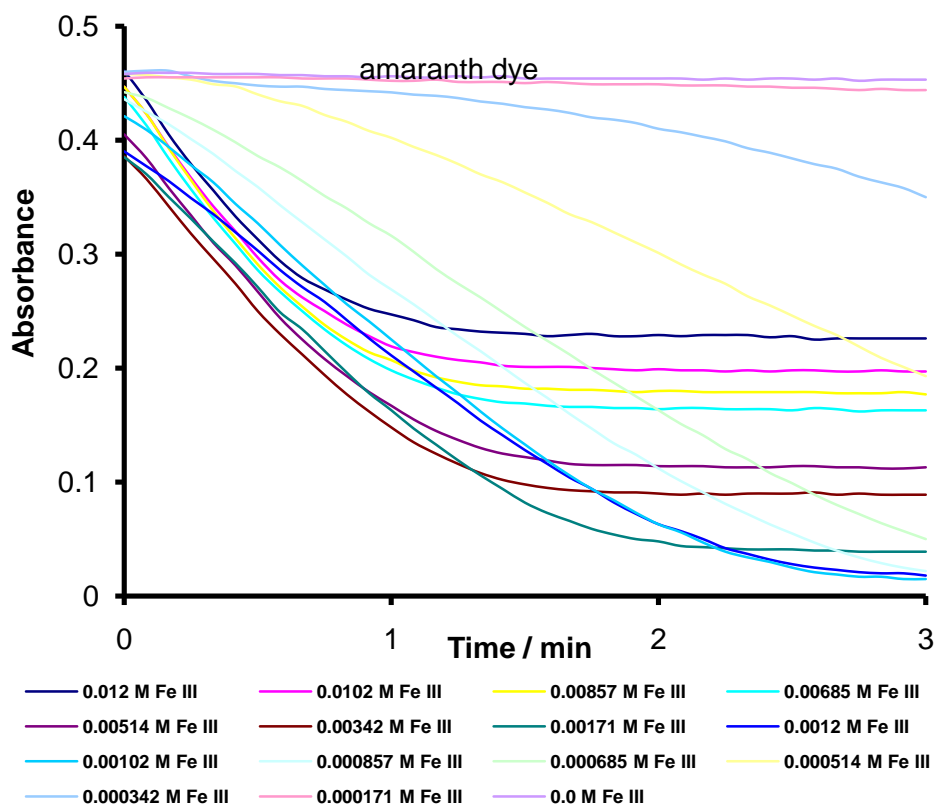


Figure A1.34:- Effect of Fe (III) concentrations on oxidation of Amaranth dye absorbance change with time, $2.05 \times 10^{-2} \text{ mol dm}^{-3}$ PAA, on absorbance of $2 \times 10^{-5} \text{ M}$ dye with different concentrations of Fe (III) as a catalyst, pH 2.81, Temp 25°C

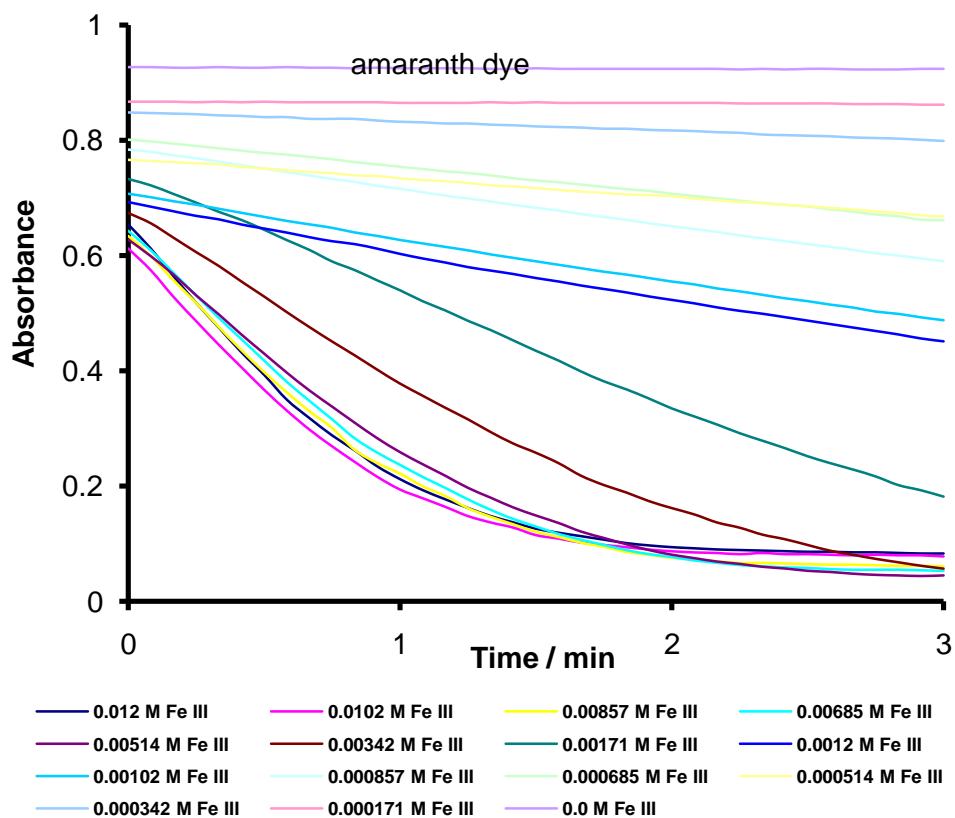


Figure A1.35:- Effect of Fe (III) concentrations on oxidation of Amaranth dye absorbance change with time, $2.05 \times 10^{-2} \text{ mol dm}^{-3}$ PAA, on absorbance of $4 \times 10^{-5} \text{ M}$ dye with different concentrations of Fe (III) as a catalyst, pH 2.09, Temp 25°C

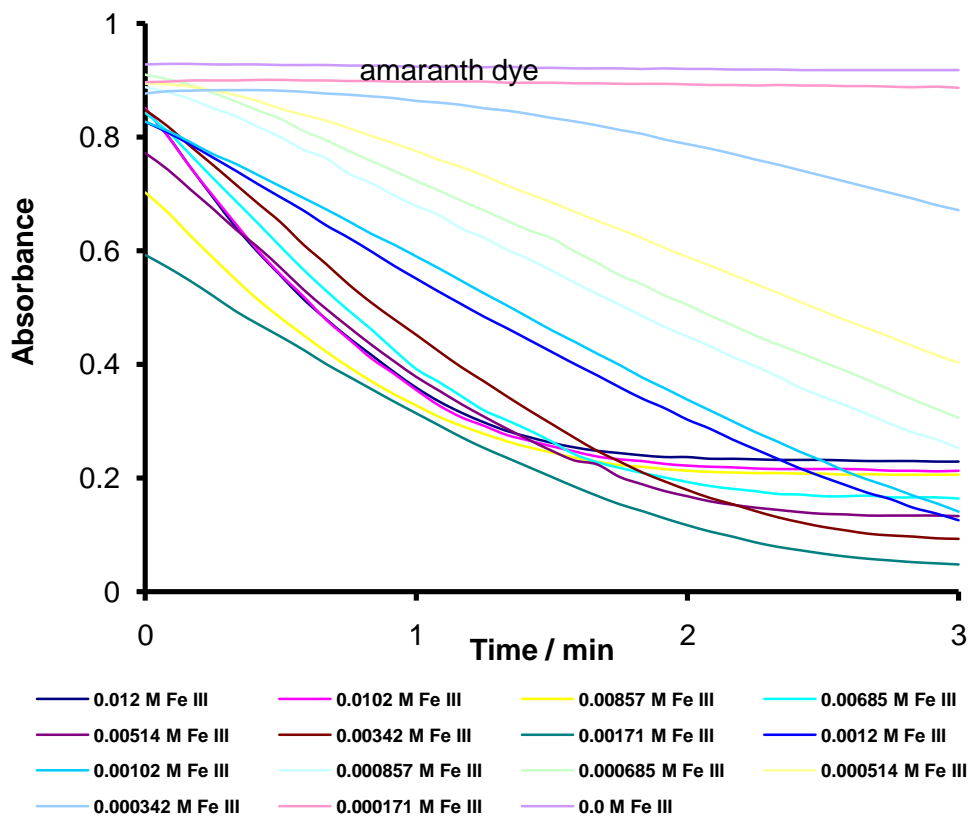


Figure A1.36:- Effect of Fe (III) concentrations on oxidation of Amaranth dye absorbance change with time, $2.05 \times 10^{-2} \text{ mol dm}^{-3}$ PAA, on absorbance of $4 \times 10^{-5} \text{ M}$ dye with different concentrations of Fe (III) as a catalyst, pH 2.81, Temp 25°C